GL01421

AREA
US
HtFlow

CHAPTER 13. HEAT FLOW FROM THE CRUST OF THE UNITED STATES

by

J. H. Sass, D. D. Blackwell, D. L. Blackstone, Jr.,

C. A. Brott, D. S. Chapman, J. K. Costain, E. R. Decker,

H. P. Heasler, A. H. Lachenbruch, L. A. Lawver, B. V. Marshall,

Paul Morgan, R. J. Munroe, J. L. Steele, and C. A. Swanberg

13.1 Introduction

13.1.1 Nomenclature and conventions. In a geologic context, the term heat flow usually means the vertical component of the heat being conducted through the outer kilometer or so of the earth's crust. It is defined as the product of two measurable quantities, temperature gradient and thermal conductivity and may be written

$$q_o \equiv K\frac{\partial T}{\partial z} \qquad (1)$$

where q_o is the surface heat flow, K the thermal conductivity, and $\partial T/\partial z$, the rate of increase of temperature T with depth z, z positive downwards.

13.1.2 Techniques of measurement. Although some of the most successful early heat-flow studies on continents involved temperature measurements in mines and tunnels having several hundred meters of vertical cover, the primary measurement, that of temperature, is most often made in near-vertical boreholes. Temperatures measured in the upper few tens of meters reflect not only the steady-state, one-dimensional conductive heat flow q_o, but thermal transients associated with seasonal and longer term climatic changes, convective motion of ground water, and perturbations to the thermal field resulting from complicated two or three dimensional near-surface structures. Experience has demonstrated that temperatures usually must be measured to depths on the order of 100 meters to achieve an acceptable signal-to-noise ratio for reliable determinations of regional heat flow. The temperature measurements are obtained using an electronic thermometer (most commonly a thermistor) connected to a surface readout by a multi-conductor electrical cable. The general principles of measurement and the basic systems are described adequately by Beck (1965), Roy and others (1968b), and Sass and others (1971b). The wheatstone bridges described in these papers have, however, largely given way to sophisticated digital meters which allow effectively continuous logging with real-time conversion of thermistor resistances to temperature and convenient data storage on magnetic tape or disk for off-line processing.

Thermal conductivities generally are measured in the laboratory (see Roy and others, chapter 12, this volume, for detailed descriptions). For most applications, in situ measurements are time consuming and costly, and the laboratory methods have been proved reliable except for very friable, porous materials whose physical character is altered substantially by the coring process. For core samples, variants of the needle probe originally described by Von Herzen and Maxwell (1959) or a type of steady-state divided-bar apparatus (see e.g., Birch, 1950) are used. The needle probe is most useful for soft sediments or friable rocks into which small-diameter (~1 mm) holes can be drilled, whereas the divided bar is preferable for rocks that can be machined into suitable cylindrical disk samples. The disk samples generally are a few centimeters in diameter and from 1 to 5 centimeters thick. The conductivity of the solid component of rocks (K_s) can be deduced from measurements on drill cuttings using either the needle probe or the divided bar (see Horai, 1971; Sass and others, 1971a). This quantity (K_s) can then be used to calculate heat flow if the porosity of the formation (ϕ) is very low ($K \cong K_s$)

or known ($K = F(K_s,\phi)$). There exist numerous models for estimating conductivity from mineral composition and porosity (see Beck, 1976; Roy and others, chapter 12, this volume), but it is always preferable to measure conductivity if suitable samples are available.

With present technology, it is easy to characterize the geothermal gradient over vertical distances of a few tens of meters to within 1%. For continuously cored holes, the conductivity (assuming lateral homogeneity at all depths) can be specified to about the same accuracy. Mostly, however, sampling problems and uncertainties concerning the three-dimensional conductivity structure limit the accuracy of conductivity estimates to about ±5% to 10% on the average and probably ±20% where drill cuttings are used and the porosity is uncertain. Thus, for the raw heat-flow datum obtained by applying equation 1 to data from a single borehole, the precision of the determination is limited by the difficulty in characterization of thermal conductivity (K) and is usually no better than ±10%.

To this ~10% must be added the uncertainties attributable to departures from one-dimensional, steady-state, conductive conditions, such as climatic history, topography, structure, and regional or local hydrology. A useful summary of these effects and their mathematical treatment is given by Jaeger (1965) and they are treated in detail in the heat-flow literature. We only wish to emphasize here that very few (if any) individual heat-flow data are precise to better than ±10% and that many internally consistent heat-flow values can be in error by ±50% or more because of unfavorable combinations of the factors listed above.

13.2 Scale and depth of heat-flow studies

13.2.1 Regional thermal regimes. Historically, heat flow on continents has been used as a constraint on models for chemical and physical processes occurring within the earth. Early measurements were concerned primarily with obtaining a number so as to constrain the total radioactivity in the outer few hundred kilometers of the earth and to make some estimates of temperature at depth. Later, as systematic differences in heat flow among various physiographic or tectonic units became apparent, these differences became an important factor in formulating models of the tectonic and thermal history of continents. For the holes drilled for mineral exploration (especially in high latitudes) used in most of the early heat-flow determinations, depths of 150 to 200 meters or more were considered essential to obtaining reasonably accurate determinations of regional heat flow. Recent studies where holes have been specifically sited as heat-flow test wells (that is, away from extreme topography, fault contacts, highly mineralized rocks, etc.) indicate that reliable values of regional heat flow can be obtained at depths of 100 meters or less where conditions are favorable. To completely specify the heat flow in a given region probably requires a grid of such holes with a horizontal spacing of a crustal thickness (25 to 30 km) or less. As will be seen on the maps of this chapter, this goal has been achieved over only a very small fraction of the continental United States, a region that has been studied more intensely than any except Japan and perhaps Western Europe.

13.2.2 Local studies related to geothermal energy. In regional heat-flow studies, great care is taken to avoid areas of hydrothermal convection, and values of heat flow within 5-10 km of hot springs or other surface hydrothermal manifestations are regarded as suspect from a regional point of view. Despite this, some local areas of very high heat flow have been discovered during regional heat-flow investigations. Probably the best documented of these "blind" geothermal areas is near Marysville, Montana (Blackwell and Baag, 1973; Blackwell and others, 1975). The chance discovery of these local anomalies serves as an incentive for increasing the density of regional heat-flow coverage, particularly in the more tectonically active regions. In the local studies whether of "blind" heat-flow anomalies or of the areas surrounding surface hydrothermal systems, the range of heat flow, scale, and philosophy of measurements are quite different from those employed in regional surveys. In regional studies, we are considering a restricted range of heat flow--say 25 to 100 mWm^{-2}--where uncertainties of 20% can be critically important to our interpretation. On the other hand, in geothermal areas the range of heat flow is much larger (0 to 1000 mWm^{-2} or more) and rough estimates of conductive flux are sufficient for calculations of energy loss and geothermal energy potential. Where the convective system closely approaches the surface, temperature measurements at depths of 1 to 10 meters can be used to delineate the boundaries of the system and provide crude estimates of heat flow (see Olmsted, 1977). Where conductive heat flows are 500 mWm^{-2} or less, however, it is preferable to make measurements at depths below which the effects of the seasonal variation of surface temperatures are not important (usually 15 meters or more). Usually, tens to hundreds of holes to depths on the order of 10 to 100 meters over tens to hundreds of square kilometers are required to map adequately the near-surface hydrothermal system associated with a potential geothermal resource. Within these rules of thumb, both the horizontal and vertical scales of local heat-flow surveys are dictated by the goals of the individual survey and by the near-surface structure and hydrology of the system under study.

13.3 Heat flow and near-surface radioactivity

13.3.1 Status of Observations. Near-surface rocks contain appreciable amounts of radioactive material, enough to account for a substantial fraction of the observed heat flow if it were distributed uniformly through the crust. This possibility has long been considered remote, strictly on geochemical and seismological grounds. Nevertheless, it seems reasonable to expect some relation between heat flow and radioactive heat production particularly for crystalline basement rocks whose formation probably involved partial melting and fractionation of radioelements over vertical distances of tens of kilometers. Many of the early papers on heat flow contain some reference to the radiogenic heat production of rocks; however, only in the decade since the discovery by Birch and others (1968) of a linear relation between heat flow and heat production for granites of the White Mountains of New Hampshire and its extension to other parts of the eastern United States, the Basin and Range province (Roy and others, 1968a), and the Sierra Nevada physiographic province (Roy and others, 1968a; Lachenbruch, 1968) has it become standard practice to measure radioactivity. As of mid-1977, combined heat flow - heat production information was available from only about 100 sites in the conterminous United States (Lachenbruch and Sass, 1977).

13.3.2 The concept of reduced heat flow and its empirical basis. The linear heat flow - heat production relation is expressed as

$$q_o = q_r + DA_o \qquad (2)$$

where q_r is the intercept or "reduced" heat flow, A_o is the radioactive heat production, and D is the slope of the line. The slope D has the dimensions of depth and can be identified with the thickness of a layer of variable radioactivity below which heat flow is constant and equal to q_r. The term "reduced heat flow" was first introduced by Roy and others (1972) in their discussion of U.S. heat-flow provinces.

A large number of vertical distributions of radioactivity will satisfy equation 2. In the simplest, D is the thickness of a surficial layer of constant radioactivity, (A_o). In general, however, the linear relation (2) can survive differential erosion only if heat production varies with depth z as $A_o \exp(-z/d)$ (Lachenbruch, 1968, 1970). There is some experimental evidence for a decrease in radioactivity with depth (Lachenbruch and Bunker, 1971; Swanberg, 1972) within intrusive complexes, but the scatter in the data precludes defining an unambiguous model.

The presently available q_o-A_o data are shown in Figure 13.1 together with the lines originally defined by Roy and others (1968a).

13.3.3 Heat-flow provinces. The linear heat-flow relation (equation 2) serves as the basis for defining heat-flow provinces. The original three provinces were those defined on the basis of the lines shown in Figure 13.1 (Roy and others, 1968a, 1972) but the concept has since been extended to other continents (Table 1). The table illustrates the variation in the parameters q_r and D among the heat-flow provinces defined to date. Most values of D range from 7 to 11 10 km whereas q_r varies by nearly a factor of four. Pollack and Chapman (1977) have noted that there is also a linear relation between q_o and q_r such that the reduced heat flow q_r is, on the average, about 60% of the surface heat flux q_o.

The scatter in the q_o versus A_o points for the Basin and Range province prompts a re-examination of the definition of a "heat-flow province." If we assume that the scatter results from perturbations to some steady or average condition and also assume a value for D, the characteristic depth, we may rewrite equation 2 as $q_r = q_o - DA_o$, calculate individual reduced heat flows, and define our heat-flow province on the basis of the average q_r. This was done by Lachenbruch and Sass (1977) for the Basin and Range province using the value of D (10 km) established empirically for the neighboring Sierra Nevada (Figure 13.5). Blackwell (1978) noted that the q_o - A_o data from provinces with volcanic and tectonic ages greater than 17 m.y. tend to have less scatter and to lie close to the line (B&R, Figure 13.1) originally defined by Roy and others (1968a).

TABLE 13.1. Average surface heat flow (q_o), reduced heat flow (q_r), and characteristic depth (D) for several continental heat-flow provinces[a]

Continent Province	q_o (mWm^{-2})	q_r (mWm^{-2})	D (km)
North America			
Basin and Range	92	59	9.4
Sierra Nevada	39	17	10.1
Eastern USA	57	33	7.5
Canadian Shield	39	{22 34	12.3 7.1
Europe			
Baltic Shield	36	22	8.5
Ukranian Shield	36	25	7.1
Africa			
Niger	20	11	8
Zambia	67	40	(11)[b]
Asia			
Indian Shield	64	{39 33	14.8 7.5
Australia			
Western Shield	39	26	4.5
Central Shield	83	27	11.1
Eastern Australia	72	57	(11.1)[b]

[a]Data from Pollack and Chapman, 1977; Rao and Jessop, 1975; Rao and others, 1976; Kutas, 1977, and Sass and Lachenbruch, 1979b.

[b]Value of D assumed for calculation of q_r.

13.4 Heat flow and convective processes

There are some spectacular, if isolated, examples of convection, both magmatic and hydrothermal, at such places as Yellowstone Park, The Geysers of northern California, and the Cascade ranges of Oregon-Washington (see Figure 13.5). Figure 13.1 provides evidence that convective processes may be more widespread than suggested by the obvious surface manifestations. The single point lying off the Sierra Nevada q_o-A_o line (DP) is located within a few kilometers of the rim of the Long Valley caldera (LV, Figure 13.5), the site of Holocene volcanism and contemporary hydrothermal activity.

It is probable that much of the scatter about the original Basin and Range province line can also be attributed to convective processes related to extensional tectonics in the last 15-20 m.y. Figure 13.2 presents one-dimensional, conductive, steady-state geotherms for a simple model in which the radioactive heat generation (A_o) decays exponentially with depth from an average surface value ($\sim 2\ \mu Wm^{-3}$) with a decrement D of 10 km (cf. Table 1) and thermal conductivity (K) is constant ($\sim 2.5\ Wm^{-1}\ K^{-1}$). Also shown on Figure 13.2 are some pressure-melting relations for intermediate crustal rocks and basalt (from Wyllie, 1971). The ordinate scale in addition to depth has approximate conductive time constants τ in m.y. governing the surface response to transient thermal processes at various depths. From the relation between melting curves and conductive geotherms, it is clear that heat transfer must be (or have been) more efficient than is allowed by plausible steady-state conductive models. Thermal regimes like that for the Battle Mountain high must be maintained by some combination of quasi steady-state convection in the lower crust and conductive decay of the transients associated with

?

is mentioned in text? ref?

earlier convective episodes (see Lachenbruch and Sass, 1977, 1978; Lachenbruch, 1978; Blackwell, 1978). High mean values of q_o relative to A_o for areas like the Battle Mountain high probably reflect magmatic or solid state convection in the lower crust during the late Tertiary possibly extending into the Quaternary. Much of the large scatter evident in the q_o-A_o relation for the Basin and Range as a whole can be attributed to hydrothermal convection in the upper crust.

Heat-flow studies near many of the hundreds of areas of natural discharge in the United States and Mexico confirm that these are associated with shallow hydrothermal convection systems, some maintained by magma chambers, and others that could be maintained entirely by deep circulation in a region of high heat flow.

In the maps and discussions that follow, we discuss heat flow both in terms of SI units (mWm^{-2}) and the traditional heat-flow units (1 HFU = 41.8 mWm^{-2}). Owing to space limitations, we are unable to present a comprehensive list of all published heat-flow sources. For references to some of the older publications and some "grey literature" (theses, open files, etc.) the reader is referred to Sass and Lachenbruch (1979a) and the publications cited herein for the region of particular interest.

13.5 Heat-flow map of the conterminous United States and adjoining region of Canada and Mexico

In this section we present four maps (Figures 13.3 to 13.6) illustrating the gross heat-flow field in relation to the major physiographic boundaries. At the scale of these maps, we have had to generalize control where data density is high (Figure 13.3). Heat-flow contours for the entire United States are shown in Figure 13.4 and the heat-flow provinces defined for the western United States in Figure 13.5. The contours shown in Figures 13.4 and 13.5 represent a consensus among the various collaborators whereby each worker was responsible for contouring the area depicted in his regional map. In areas of overlap or of conflicting interpretations, the final contouring was done by the first author (JHS). Figure 13.6 shows the published reduced heat flows (equation 2). The general features of the heat-flow field remain unchanged from earlier published heat-flow maps. Heat flow is still high in the west--relative to the east (Figure 13.4). However, there are sizable areas of low-to-normal heat flow in the tectonically active western U.S. and some recently discovered areas of higher-than-average heat flow in the east (see discussions by Costain in Sections 13.12 and 13.13).

13.6 Regional heat-flow maps

Figure 13.7 is an index showing the areas covered in the regional maps presented in this chapter. The philosophy of the following sections is to present page-sized maps showing detailed control (although once again some generalization is necessary where coverage is very dense) and the relevant gross geologic units and structure. These have been generalized by the individual compilers from the 1:2,500,000 Geologic Map of the United States (King and Beikman, 1974). More up-to-date geologic information was added by individual contributors when they deemed it necessary. Even though the regional maps focus on smaller units than can be presented on the scale of the preceding section, the reader is urged to consult the source publications when attempting to use data from an individual locality.

13.7 Heat Flow in the Pacific Northwest by D. D. Blackwell, J. L. Steele, and Charles A. Brott (Southern Methodist University, Dallas, Texas)

13.7.1 Introduction. Heat-flow investigations began in the Pacific Northwest in the late 1960's and were initially discussed by Blackwell (1969). Since then, the intensity of study has increased due to the interest in the tectonics of the region and in the possible utilization of areas of high heat flow and high temperature as geothermal energy resources. Subsequent papers dealing with various aspects of heat flow in the Pacific Northwest have been published (Sass and others, 1971b; Blackwell and Robertson, 1973; Blackwell, 1974; Blackwell and Baag, 1973; Bowen and others, 1976, 1977; Morgan and others, 1977; Sass and Sammel, 1976; Sass and others, 1976; Brott and others, 1976, 1978; Schuster and others, 1978; Blackwell, 1978). The most comprehensive papers are a study of heat flow in the state of Oregon (Blackwell and others, 1978) and a report in preparation on Idaho by Brott and Blackwell. The correlations of heat flow with the physiography, tectonics, and volcanic history of the Pacific Northwest are many and complex and can only be briefly summarized here. For more details, readers are referred to the papers referenced. In a general overall sense, the heat-flow values correlate with certain physiographic provinces, primarily because the physiographic provinces are tectonically controlled. Therefore, in order to systematize the discussion of the distribution of heat flow in the Pacific Northwest, selected physiographic provinces are shown in Figure 13.8.

Available heat-flow data in the Pacific Northwest, amounting to more than 600 heat-flow values are shown in Figure 13.8. Division of heat-flow values is similar to that shown in the other figures. In addition, symbols are shown for heat-flow values less than zero, and for areas (as opposed to individual sites) where heat-flow values are greater than 2.5 HFU (103 mW/m^2). Some large areas of the Pacific Northwest have heat-flow values of 0 or less in holes 150-300 m deep. These low values are related to large-scale motions of water in aquifers and are especially characteristic of the recharge regions of the Snake Plain aquifer (Brott and others, 1976). The heat flow from the interior of the earth below these regions is certainly not zero, but at the depth of conventional heat-flow measurement, the heat flow is zero over large areas. The difference between the actual measured "surface" heat flow and the estimated overall energy loss is discussed by Blackwell (1978). Similarly, there are many hydrothermal convective systems where heat-flow values in excess of 2.5 HFU are observed over relatively large geographic areas (at least several km^2). In cases where heat-flow data have been published or are available outlining such anomalies, the locations have been shown by a separate symbol in Figure 13.8. Of course, many other such anomalies exist which have not yet been outlined by published drilling results and so the areas shown are by no means exclusive. The heat flow in the individual provinces or groups of provinces will be discussed briefly.

13.7.2 Coast Ranges--Willamette Valley, Puget Lowland--Klamath Mountains--Western Cascade Range. This group of provinces in western Washington and Oregon represents the area of most homogeneous heat flow in the entire Pacific Northwest. In the recent study of the heat flow of Oregon (Blackwell and others, 1978), a mean value of 1.00±.003 HFU was found for these coastal provinces (60 measurements). In this area, evidence of convective heat transfer either in local groundwater systems or in large-scale hydrothermal systems in general does not exist and predominant heat transfer mechanism is conduction. This group of provinces represents the region of lowest heat flow in the Pacific Northwest.

13.7.3 Great Plains. The region of next lowest heat flow is the Great Plains province which is the easternmost province. Heat-flow data are relatively sparse for this area, the heat flow generally being on the order of 1 to 1.5 HFU. Additional heat-flow determinations are necessary before the complete heat-flow pattern in this province is known; however, the heat flow does appear to be near the continental average.

13.7.4 Middle Rocky Mountains. Heat flow in the Middle Rocky Mountain province is also not very well determined. A few scattered points are generally of approximately normal values. For example, heat flow of the Beartooth Plateau ranges from 1.2 to 1.5 HFU. The Middle Rocky Mountains province in Idaho, which includes part of the overthrust belt and abuts the eastern edge of the Basin and Range province may have high heat flow; however, no data exist at the present time for this particular area.

13.7.5 Northern Rocky Mountains--Blue Mountains. All the remainder of the Pacific Northwest has high heat flow with the values, however, varying depending on the detailed tectonics of the region. The area of most homogeneous heat flow includes the Northern Rocky Mountains and Blue Mountains provinces. These provinces include predominately Mesozoic volcanic arc terranes with widespread granitic plutons. In general, these provinces have not been as extensively affected by late Cenozoic volcanic and tectonic events as the remainder of the intermountain provinces, although some faulting and some volcanism does extend into the late Cenozoic era. Mean heat flow for these provinces is approximately 1.8 HFU. Heat flow - heat production correlations suggest that the mantle heat flow in these provinces is approximately 1.4 HFU, approximately equal to the Basin and Range province mantle heat flow as originally defined by Roy and others (1968a, 1972). Heat flow in these provinces generally is conductive although there is some heat transfer by convection; in particular, there are several geothermal systems along the Intermountain Seismic Belt in Montana and in the Blue Mountains of Oregon. Large-scale and very hot geothermal systems generally do not occur in these provinces.

13.7.6 Columbia Basin. The Columbia Basin is an area of mid- to late-Cenozoic flood basalt volcanism. Mean heat flow seems to vary with position in the Columbia Basin ranging from approximately 1.4 HFU in the southern part of the basin up to values of 1.6 to 1.7 HFU in the northern part of the basin. This variation in heat flow probably reflects a variation in the crustal section underlying the basin. The mantle heat flow in this province is on the order of 1.2 to 1.4 HFU, again, typical of the Basin and Range mantle heat flow as defined by Roy and others (1968a, 1972). There is very little apparent residual thermal effect associated with the extensive basaltic volcanism occurring between 8 and 14 m.y. ago. This small thermal signature is characteristic of basaltic volcanic terrains where relatively little of the heat is transmitted to the crust and most of the energy comes directly to the surface as volcanic rocks. Within this province, there is extensive modification of the regional heat flow by local groundwater motion, however, due to interborehole connection of various aquifers. Unaffected single boreholes in the region are the exception. The aquifer systems are as extensive and complex as the Snake River Plain aquifer.

13.7.7 Southern Idaho Batholith. The geology of the southern Idaho batholith compares to the geology of the Blue Mountains and the Northern Rocky Mountains. However, the heat flow appears to be somewhat higher and/or the mechanisms of heat transfer significantly different from that in the other two provinces. There are extensive low to moderate temperature geothermal systems associated with major linear physiographic features cutting the granitic rocks of the Idaho batholith. Almost continuous chains of hot springs occur along several of the major rivers with evidence for widespread convective systems away from the valleys as well. On the other hand, the regional heat flow appears to be similar to or only slightly higher than the Northern Rocky Mountains and Blue Mountains (approximately 2.0 HFU). Therefore, in general, the high degree of modification of the regional heat flow by hydrothermal convection must be related to the hydraulic properties of the crust rather than to a difference in regional heat flow. This province illustrates that groundwater convection is as likely to occur, given appropriate tectonic settings, in granitic rocks, as in rocks which are conventionally thought to be more porous and permeable.

13.7.8 Young Volcanic and Tectonic Provinces. The remainder of the provinces in the Pacific Northwest are characterized by late Cenozoic volcanic and/or tectonic activity. In general, the patterns of heat flow in these provinces are much more complex than in the provinces previously discussed, with the exception of the southern Idaho batholith. Heat-flow values may range from 0 to over 5 HFU at heat-flow sites less than 1 km apart. The extreme variation of heat flow is related to the laterally complex hydrology, structure (and thermal conductivity) and tectonic history of individual areas. The numerous hydrothermal systems may or may not be related to specific upper or mid-crustal geothermal anomalies such as magma chambers; in many cases they may be driven by high heat flow related to lower crustal thermal events or the highly fractured nature of the crust. Conventional heat-flow studies which emphasize measurements in granitic rocks cannot be applied to these provinces. Even in areas where granitic rocks crop out, exposures are generally small, and the results are of dubious regional significance. Only extensive numbers of measurements in a variety of hydrologic, physiographic, and structural settings are suitable for complete analysis of the heat-flow distribution. Complete enough studies have not been carried out, in general, to evaluate the complete controls on the heat flow in these provinces. The predominant effects are certainly local and regional hydrology, local and regional structural affects, and lateral variations in crustal temperatures. Nonetheless, each individual province is somewhat different, and we will discuss this area in terms of groups of provinces.

13.7.9 Oregon High Cascade Range--Washington Cascade Range. The High Cascade Range of Oregon is that part of the Cascade Range characterized by Pliocene and younger volcanic activity. Extensive heat-flow measurements are available in the northern part of this province and on the boundary between this province and the Western Cascade Range province in Oregon. Data are relatively sparse in the Washington Cascade Range and the two provinces have been lumped together because of the volcanic similarity rather than because of any known heat flow similarity. There is a major heat-flow transition associated approximately with the western boundary of the High Cascade Range where heat flow drops from an average value of 2.5 HFU at the border of the High Cascade Range to regional values of 1 HFU in the coastal provinces, including the Western Cascade Range. Heat-flow data in the High Cascade range itself, are sparse, but based on the data on its western margin, regional heat flow is expected to be in excess of 2.5 HFU. To the north, this value of heat flow seems to decrease so that in the area of Mount Hood the regional heat flow is slighly below 2 HFU, although there are still some areas of slightly higher heat flow, associated closely with the Mount Hood volcano. Farther to the north, in the southern Washington Cascade Range, heat flow appears to drop even lower, to values of 1.5 to 1.8 HFU. North of latitude 46°30', however, there are not enough heat-flow data in the Washington Cascade Range to evaluate the regional heat-flow picture.

The decrease in heat flow from south to north can be associated in part with the diminution of intensity of Pliocene and Quaternary volcanism into southern Washington. North of 46°30', little or no Quaternary volcanism has occurred, except that immediately associated with the straticone volcanos. South of this latitude, volcanism is much more extensive away from the straticone volcanos, and south of approximate latitude 45°, the High Cascade Range surface rocks are all Pliocene and Quaternary volcanos.

13.7.10 Basin and Range province. The part of the Basin and Range province in the Pacific Northwest is very small, occupying part of south-central Oregon and part of southeastern Idaho. Data are very sparse from southeastern Idaho, and the regional heat-flow pattern in that part of the Basin and Range province is not yet known. There are some data in the Oregon part of the Basin and Range province, but the extreme variation of heat-flow measurements does not allow a complete analysis of the controls on heat flow in that province. For a much more detailed discussion, see Blackwell and others (1978) who found the regional heat flow to be 2.1±0.2 HFU (61 measurements).

13.7.11 Oregon High Lava Plains. The High Lava Plains represent the northern portion of the Basin and Range province and may function as a transfer fault zone taking up the lateral strain of the Basin and Range against the Blue Mountains (Lawrence, 1976). Heat-flow values in the High Lava Plains tend to be less scattered than in the Basin and Range province, and average 2.2±0.1 HFU (Blackwell and others, 1978). Several major geothermal anomalies exist in that province. At the extreme western end of the province near the town of Bend, extensive young subhorizontal basalt flows are characterized by large-scale groundwater regime which results in low or negative heat-flow values to fairly great depths and the regional heat flow in this part of the province is undetermined.

13.7.12 Owyhee Upland. The Owyhee Upland represents the western margin of the Snake River Plain and the northern margin of the Basin and Range province, with some characteristics of both. Late Cenozoic volcanism in this province has been extensive. In general, heat flow appears to be high in the area, the average for the Oregon portion of the province being 2.5±0.3 HFU (15 measurements, Blackwell and others, 1978). Extensive geothermal systems are present on the northern margin of the province where it abuts the Snake River Plain.

13.7.13 Western Snake River Plain. The western Snake River Plain represents the older part of the Snake River Plain where volcanism was initiated between 12 and 20 m.y. ago. Basaltic volcanism has extended up until fairly recent times. Silicic volcanism ended in excess of 10 m.y. ago. The heat-flow pattern in this province is quite complicated. Extensive geothermal systems and areas of heat flow greater than 2.5 HFU are interspersed with areas of heat flow between 1.2 and 1.8 HFU (for more details, see Brott and others, 1976, 1978). The overall heat flow of the province is on the order of 2 to 2.5 HFU.

13.7.14 Eastern Snake River Plain. The eastern Snake River Plain represents the younger part of the Snake River Plain feature with silicic volcanism generally occurring between 12 and 2 m.y. ago. The surface rocks of the eastern Snake River Plain are composed of extensive subhorizontal basalt flows. A major aquifer exists in these basalt flows from Island Park at the east edge of the province to Thousand Springs at the west edge of the province. Lateral flow of water in this aquifer masks the regional heat flow over an area approximately 200 km long by 50 km wide. This area is characterized by heat-flow values of less than 1.5 HFU. Based on the volcanic history and a proposed relationship between heat flow and elevation (Brott and others, 1978), the regional heat flow in this part of the Snake River Plain is expected to be between 2.5 and 3.5 HFU. Several deep holes have recently been drilled in this province which give values consistent with this expected high regional heat flow. Extensive geothermal systems are present along the margins of the aquifer related either to water circulation from the margins, to leakage of warm water from under the aquifer, or to some other causes.

13.7.15 Island Park--Yellowstone National Park. This province represents the area of youngest volcanism associated with the propagating Snake River Plain "hotspot." Extensive silicic volcanism in the Island Park area occurred as recently as 1.2 m.y. ago. The Island Park caldera has since been filled by basalt flows and appears to be in the waning phases of its activity. The Yellowstone Park caldera system, however, remains extraordinarily active. Based on geochemical analyses, the regional heat flow of the Yellowstone caldera is approximately 50 HFU (Fournier and others, 1976). Heat-flow measurements in Yellowstone Lake, which occupies part of the Yellowstone caldera, document conductive heat flow ranging from 16 to 40 HFU over the part of the lake inside the caldera ring fractures. These values are consistent with the measured convective heat-flow loss for the caldera. The area occupied by the caldera is 2,500 km^2, so a very significant area has this extremely high heat flow. In fact, the heat-flow loss from the Yellowstone system comprises approximately 5% of the total energy loss by heat from the interior of the earth in the Pacific Northwest.

13.7.16 Origins of heat-flow patterns. The heat-flow pattern along the west coast very evidently owes its origin to the process of subduction, presently or very recently active along the Pacific coast. The characteristic couple of low heat flow juxtaposed with high heat flow in association with a volcanic arc is characteristic of subduction zones all over the world. This pattern gives some indication of the nature of the subduction process and of the variation of the process with time. For example, a mid-Cenozoic volcanic arc was centered on the Western Cascade Range. At the present time, however, the volcanic arc has migrated eastward to the location of the High Cascade Range and the heat flow in the Western Cascade Range has been dropped from values as high as 2.5 HFU to a low value of 1.0 HFU.

The remainder of the interior mountain provinces of the Pacific Northwest have generally high heat flow compared to the continental average, with the youngest volcanic and tectonic provinces having the highest heat flow. The whole broad zone of high heat flow has been referred to as the Cordilleran Thermal Anomaly Zone (Blackwell, 1969) because it is characteristic of the Cordilleran Mountain Belt from north to south as far as it has been investigated (central-western Canada to the trans-Mexico volcanic belt). The most reasonable explanation for this broad belt of high heat flow is that it is related to a process of subduction and that the broad high relates in general to a process of back-arc volcanism and possible rifting which has occurred over the past 150 m.y. The details of the process and the details of the way such an important individual feature as the Snake River Plain/Yellowstone Park "hot spot" can be related to this overall explanation are not yet clear. Whether the detailed local variation of volcanic and tectonic history relates to changes in the stress state of the block due to changes in the subduction zone pattern, whether it relates to changes in the nature, depth, speed, etc., of the sinking block, whether it relates to inhomogeneities in the upper mantle or to many other possibilities, remains unclear at this time.

13.8 Heat Flow in Northern and Central California by J. H. Sass, A. H. Lachenbruch, R. J. Munroe, and B. V. Marshall (U.S. Geological Survey, Menlo Park, California)

13.8.1 Introduction. The gross tectonic features of central and northern California are illustrated in Figure 13.9. Within this region, the heat-flow pattern is quite systematic, and the various physiographic units have characteristic heat flows.

13.8.2 Klamath Mountains. There are at present seven heat-flow points in the Klamath Mountain province (Sass and others, 1976; Blackwell and others, 1978). Only one point is shown in Figure 13.9; however, with reference to Figure 13.8 and the discussion by Blackwell and others in Section 13.7.2, we see that the Klamaths are characterized by the low-to-normal heat flow also characteristic of the Pacific Northwest Coast Ranges and that it is probably attributable to the same cause (thermal sinks associated with subduction).

13.8.3 California Coast Ranges. This region generally has high heat flow (Figure 13.9) which can be explained in terms of a hot lithosphere, mechanical heat generation in the upper 10 to 15 km of an ~100 km wide zone of slip associated with the San Andreas fault system (SAF, Figure 13.9) or some combination of the two. There is no peaked heat-flow anomaly coinciding with the main trace of the San Andreas fault, an observation that may impose significant constraints on the magnitude and distribution of shear stresses within the fault zone (Henyey, 1968; Brune and others, 1969; Henyey and Wasserburg, 1971; Lachenbruch and Sass, 1973, and 1979, in preparation). Preliminary results from recent drilling (Lachenbruch and Sass, in preparation) indicate a systematic increase in heat flow from the low value at EUR (Figure 13.9) to values more characteristic of the Coast Ranges over a distance of ~200 km SSW along the San Andreas fault system. This increase may reflect thermal transients related to the duration of slip on the younger parts of the San Andreas and associated faults.

13.8.3 Great Central Valley. Although heat-flow data are scarce, this region seems generally to have low heat flow, an observation confirmed by numerous temperature gradient data (AAPG-USGS, 1976; USGS, unpublished data). Thus far, no evidence has been found for the heat-flow anomalies suggested by the interpretive studies of silica geothermometry by Swanberg and Morgan (1978) (see also Section 13.15 and Figure 13.18, this chapter).

13.8.5 Sierra Nevada. Subsequent to the discovery of high heat flow in the Front Range, Colorado (Birch, 1950), it was expected that the Sierra Nevada, with their thick granitic root, would also be a region of high heat flow. In fact, Clark's (1957) original low value at Grass Valley, California, was met with skepticism and was generally ignored in models involving the thermal state of the Sierra Nevada province. Later detailed work by Roy and others (1968a, b, 1972), Lachenbruch (1968, 1970), and Sass and others (1971b) confirmed Clark's initial estimate and established that the Sierra Nevada is a province not only of low heat flow, but of uniform and exceptionally low reduced heat flow (see Figures 13.1 and 13.6). It has also been noted (Sass and others, 1971b; Roy and others, 1968b; 1972; Henyey and Lee, 1976) that the transition on the east between low heat flow and the higher values characteristic of the Northern Great Basin occurs abruptly over a horizontal distance of few tens of kilometers. The most widely accepted explanation for these observations involves the heat sink associated with subduction, ending in the late Cenozoic era, beneath the Sierra Nevada juxtaposed with shallow heat sources (most likely the result of both the transient and steady-state effects of extension and intrusion of magma into the upper lithosphere) in the Northern Great Basin (Roy and others, 1972; Blackwell, 1978; Lachenbruch and Sass, 1978).

13.9 Heat flow in Southern California, Southern Nevada, and Arizona, by J. H. Sass, A. H. Lachenbruch, R. J. Munroe, and B. V. Marshall (U.S. Geological Survey, Menlo Park, California)

13.9.1 Introduction. The southwestern part of the continental United States contains a large variety of physiographic and tectonic units and, not surprisingly, heat flow is also quite variable (Figure 13.10). As with Central and Northern California, however, there are systematic spatial variations of heat flow, albeit not as dramatically identified with individual physiographic units as in the previous section (Figure 13.9). Almost the entire region including Northern Mexico (Smith, 1974; Smith and Jones, 1979; Smith and others, 1979) and the Southern California borderland offshore (Lee and Henyey, 1975) is characterized by higher-than-normal heat flow.

13.9.2 Transverse Ranges. West of the San Andreas fault, we have virtually no heat-flow data in the Transverse ranges (Figure 13.10). This constitutes an important and conspicuous gap in the data. We might expect measurable differences in heat flow in this region because of the component of thrust in the San Andreas and associated fault systems as contrasted with the northern Coast ranges where the tectonic deformation is entirely by right-lateral strike slip.

13.9.3 The Mojave Block. This subregion of the Basin and Range province is a granitic bedrock terrane within which tectonic deformation is primarily by thrusting and strike-slip faulting as contrasted with the normal faulting characteristic of most of the province. Outside of some rather small areas of conspicuous hydrothermal activity, the Mojave Block has uniform heat flow averaging about 1.6 HFU (70 mWm^{-2}) significantly lower than the mean of about 2 HFU ($\sim$80 mWm^{-2}) for the Basin and Range as a whole (Lachenbruch and others, 1978). As in the north, no peaked heat-flow anomaly is associated with the San Andreas fault.

13.9.3 Southern California Batholith. This block, forming the northern tip of the Peninsular ranges, has low-to-normal heat flow in contrast to most of the region depicted in Figure 13.10. The low heat flow extends southward into Baja California (Roy and others, 1972; Smith, 1974; Smith and Jones, 1979), and is generally attributed to the lingering aftereffects of late Cenozoic subduction (Roy and others, 1972; Smith, 1974).

13.9.3 Southern Basin and Range province. North and east of the Mojave Block, the Basin and Range province has about the same range and mean heat flow as the remainder of the Basin and Range (excluding the Battle Mountain high and Eureka low, Figure 13.5). There are some scattered low-to-normal heat flows (open symbols, Figure 13.10), as well as some very high values (asterisks, Figure 13.10) both in granitic basement rocks and in the sedimentary basins. These extreme values seem, in most instances, to be associated with local, fault-controlled hydrothermal convection systems.

13.9.5 Colorado Plateau. Reiter and Shearer (1979) recently have published several heat-flow data which result in a major modification to the 1.5 HFU (~60 mWm^{-2}) contour (compare Figures 13.4 and 13.5 with earlier versions; e.g., Figure 2, Lachenbruch and Sass, 1977, and Figure 9-1b, Lachenbruch and Sass, 1978). It now appears that the southeastern Colorado Plateau has high heat flow and is indistinguishable thermally from the southern Basin and Range province.

13.10 Heat Flow and Generalized Geology in Eastern Arizona, the Rio Grande Rift, the Southern Rocky Mountains, and the Northern and Central Rocky Mountains by E. R. Decker, H. P. Heasler, and D. L. Blackstone, Jr. (University of Wyoming, Laramie, Wyoming)

The data are shown together with generalized geology in Figures 13.11 and 13.12. Principal sources of data are: Birch, 1950; Decker and Birch, 1974; Decker and Smithson, 1975; Decker and others, 1979; Edwards and others, 1977; Reiter and others, 1975, 1978; Roy and others, 1968b; Sass and others, 1971b; and Warren and others, 1969.

A geologic synthesis by Chapin (1971) outlines the Rio Grande Rift as a zone extending from extreme southern New Mexico to the Leadville area in Colorado. More recently, Tweto (1977) implies that the Rift extends well into northern Colorado, and perhaps into southern Wyoming. In our compilation (Figure 13.11), Chapin's commonly accepted north-south outline of the Rift is followed; consequently, the central part of the Rift is coincident with the Rio Grande River in New Mexico, and the San Luis Basin and northern Arkansas River Valley in Colorado. We defer attempts to delineate a more northerly extension of the Rift, except to note that two unusually high estimated heat flows are consistent with late Tertiary volcanism, faulting, and perhaps rifting in the Southern Rocky Mountains in the North Park area near the Colorado-Wyoming border (Tweto, 1977; Blackstone, 1975; Decker and others, 1979).

The map of the Central and Northern Rocky Mountains (Figure 13.12) also shows generalized geology and thermal data for the Southern Rockies in Wyoming because the Laramie Mountains and eastern Wyoming Basin appear to form a province of continuous low-to-normal heat flow (Decker and others, 1979). Both maps can be used to study the width of the heat-flow transition between the Laramie Mountains and the Colorado Front Range.

A similar rationale was followed during compilation of both maps. Briefly, faulting and Cenozoic volcanism are outlined in considerable detail because anomalous flux (high or low) often is associated with extensive faulting, tectonic extension, and geologically young volcanic or caldera-forming activity. The large outcrops of the Precambrian basement, the Mesozoic batholiths, and the Tertiary intrusions are also depicted since their locations relative to existing heat-flow sites can provide information on the distance to bedrock radioactivity samples, and because drilling in many of these areas could lead to a more complete understanding of heat flow and radioactivity. Additionally, many of the heat-flow sites in Idaho and Montana are in or near the Idaho and Boulder batholiths, respectively, but in contrast several of those in Arizona, Colorado, and New Mexico are in small Tertiary stocks or laccoliths. Finally, to indicate the centers of the major sedimentary basins, the general outlines of the larger areas of Tertiary sediments are indicated on each map.

13.11 Heat Flow and the Major Tectonic Units of Utah by D. S. Chapman (University of Utah, Salt Lake City, Utah)

The state of Utah includes large segments of three major physiographic provinces (Fenneman, 1928): Basin and Range (BR), Colorado Plateau (CP), and Middle Rocky Mountains (MRM) as shown in Figure 13.13. A further physiographic subdivision has been proposed by Stokes (1977), but we utilize only his concept of a BR-CP Transition province (Figure 13.13), which in geographic, geologic and geophysical aspects is transitional in nature between the BR and CP. Topographic forms in the transition include both flat-topped plateaus and sharp crested ranges separated by alluvial valleys. Long parallel normal faults typical of BR structure are found within the plateaus. The transition zone is seismically active (Smith and Arabasz, 1979), has anomalously low upper mantle velocities, possibly an upper crustal low velocity zone, and lies over a mantle upwarp (Smith and Braile, 1975).

Heat-flow results from Utah (Figure 13.13) illustrate the contrasting thermal regimes of the BR and CP physiographic provinces. Most data from Utah have been obtained during the past three years (Chapman and others, in preparation). Other data sources include: Costain and Wright (1973); Roy and others (1968b); Sass and others (1971b). Heat flow in the BR is generally greater than 75 mWm^{-2}, with a zone of scattered but very high values running north-south between 37°N and 40°N at the eastern extremity of the BR. Within this zone are located several KGRA's (Known Geothermal Resources Areas) although no data from any KGRA is included in Figure 13.13. Heat flow from the Utah CP is below 65 mWm^{-2} except for one site which is in proximity to recent volcanic features.

The mean heat flow for nine Utah CP sites east of 112°W longitude is 49 ± 9 (s.d.) $mW\ m^{-2}$. In contrast, the mean heat flow for 52 BR sites is

101 ± 27 (s.d.) mW m^{-2}. Both the mean heat flow and the standard deviations in the distribution of heat-flow values for the BR are more than double those of the CP. Although sites where hydrologic disturbances in or near the drill holes, as inferred from temperature-depth profiles, have been excluded from these data, the likely cause of the large scatter in our Basin and Range heat-flow values is water movement due to hydrothermal or forced convection on a scale of several kilometers in a pervasively faulted upper crust. If three BR sites where heat flow is less than 60 mW m^{-2} are excluded as probable regional groundwater recharge areas and twelve BR sites where heat flow exceeds 120 mW m^{-2} are excluded because of inferred large-scale fluid or solid-state convection, then the mean BR heat flow becomes 92 ± 12 (s.d.) mW m^{-2}. Exclusion of the extreme BR data does not significantly alter the mean but more than halves the standard deviation.

Although recent work provides useful constraints for the mean BR and CP values, the nature of the transition is not yet well constrained. High heat-flow values are observed to the eastern edge of the BR, variable heat flow is observed at the few sites in the transition province and low heat-flow values have been measured across 200 km of the CP. On the basis of these broadly spaced measurements, the heat-flow transition is thought to occur somewhat east of the Wasatch Line and is no broader than 100 km. Preliminary new results based on measured thermal gradients and assumed thermal conductivities suggest that the transition may occur within a lateral distance of less than 30 km. Such a sharp transition over a short lateral distance is to be expected if the heat sources causing elevated BR heat flow are at the base of, or within the crust rather than at the base of the lithosphere as would be the case if the heat-flow provinces had their roots in the asthenosphere.

13.12 Heat Flow and Generalized Geology in the Southeastern United States by John K. Costain (Virginia Polytechnic Institute and State University, Blacksburg, Virginia)

The southeastern United States can be divided into several geologic belts (Figure 13.14). A summary of the major subdivisions of the southern Appalachians is given by Hatcher and Butler (1979). A few of the belts or parts of them can be correlated with those in the northeastern U.S.; e.g., Valley and Ridge province, metamorphic and plutonic rocks of Precambrian age (Blue Ridge), and possibly the Carolina Slate Belt with the Avalonian Platform.

New heat-flow values are now available in the southeastern U.S. (Costain and others, 1979a, 1979b; Smith and Griffin, 1977; Smith and others, 1978). Like the tectonically stable northeast U.S., high heat flows are found to be associated with higher concentrations of U, Th, and K in crustal igneous rocks, primarily granites. In the southeast, no young granites like the Conway Granite (White Mountain Plutonic Series) occur, unless they are concealed beneath the unconsolidated sedimentary wedge of the Atlantic Coastal Plain. The highest (65-75 mW/m^2) heat-flow values are associated with unmetamorphosed (270-330 m.y.) granite plutons. These are the youngest granites known to date in the southeast.

The Cumberland Plateau begins in southern Kentucky and extends to the Gulf Coastal Plain and Valley and Ridge province. It is underlain by nearly horizontal shales and sandstones, and to the north is called the Alleghany Plateau. The heat flow is normal (60 mW/m^2).

The Valley and Ridge province is composed primarily of unmetamorphosed thrusted and folded sedimentary rocks of Paleozoic age. The Cumberland

Plateau and Valley and Ridge make up the foreland thrust belt of the southern Appalachian orogen. In the southern Appalachian foreland, rocks ranging in age from Cambrian to Pennsylvanian form a wedge-shaped sequence that thickens markedly from west to east. This sedimentary wedge rests on Grenville basement. Deformation of the foreland Cumberland Plateau and Valley and Ridge was principally Alleghanian, and decreases westward to zero. The Pine Mountain thrust sheet (Virginia-Tennessee-Kentucky) is the classic example of thin-skinned deformation. Overthrusting in the Valley and Ridge province is of the thin-skin bedding type (Harris, 1976). The heat flow in the Valley and Ridge province seems to be somewhat lower than the Cumberland Plateau, averaging about 50 mW/m^2, but only a few values are known.

The Blue Ridge province extends from Pennsylvania to Alabama and reaches its greatest width in the Tennessee-Carolinas-Georgia part of the southern Appalachians. The province is bordered on the west by the Blue Ridge thrust. Grenville (1.-1.2 m.y.) basement is exposed in the western part of the Blue Ridge which is made up of relatively unmetamorphosed to moderately metamorphosed Late Precambrian and Cambrian sedimentary and volcanic rocks. Paleozoic metamorphism in the Blue Ridge increases from zero along the western edge to granulite facies in the central Blue Ridge near the North Carolina-Georgia border (Hatcher and others, 1979). Ultramafic rocks crop out in the central to eastern Blue Ridge, but it is not certain whether these are intrusive or have been tectonically emplaced. Heat-flow values in the Blue Ridge province are the lowest of any in the Appalachian Mountain System. New data have modified the generalized heat-flow map of Sass and others (1976) in the southeast U.S., but lower heat flow still seems to be indicated at least along parts of the Blue Ridge.

The Blue Ridge province is separated from the Piedmont by the Brevard fault zone, a zone now believed to be nothing more than a splay from a master sole thrust beneath the Blue Ridge and Piedmont (Clark and others, 1978; Cook and others, 1979). This is of major significance since it implies for the first time that large portions of the southern Appalachian orogen, including the Piedmont, are also allocthonous, and, like the northeast U.S., thick slices of continental crust have been transported westward.

Hundreds of plutons intrude the rocks of the Blue Ridge and Piedmont. Plutons of Paleozoic age in the Blue Ridge and Piedmont generally fall into three age groups: 595-520 m.y., 440-385 m.y., and 270-330 m.y. (Wright and others, 1975; Fullagar and Butler, 1979). Most of the younger plutons are granitic. There is a suggestion of younging of Paleozoic plutons from west to east across the Piedmont.

Some of the highest (70 mWm^2) heat-flow values found to date in the southeast U.S. are in post-metamorphic granite plutons in and near the part of the Piedmont called the Carolina Slate Belt. These are the youngest (270-330 m.y.) granites discovered to date in the Piedmont. The Carolina Slate Belt is composed of low-grade (biotite and chlorite zones) metavolcanic and metasedimentary rocks. The belt is outlined on Figure 13.14 because of the occurrence of higher heat-flow values; it is part of the Piedmont.

Southeast of the Piedmont, a seaward-thickening wedge of unconsolidated sediments beneath the Atlantic Coastal Plain extends from New York to Florida. The sediments are Cretaceous and younger in age. At Cape Hatteras in North Carolina, sediment thickness is about 3 km. Presumably, rocks similar to those exposed in the Piedmont occur in the basement beneath the Atlantic Coastal Plain, but the nature and configuration of belt boundaries is unknown at present. High heat-flow values at sites on the Atlantic Coastal

Plain in Virginia and North Carolina are probably associated with radiogenic heat-producing granites in the basement.

13.13 Heat Flow and Generalized Geology in the Northeastern United States by John K. Costain (Virginia Polytechnic Institute and State University, Blacksburg, Virginia)

Variations in heat flow in the eastern U.S. are caused primarily by differences in concentrations of radiogenic heat-producing elements (uranium, thorium, and potassium) in igneous and metamorphic rocks in the upper crust of the earth. U and Th each contribute about 40%-45% of the total radiogenic heat produced. The remaining 10%-20% comes from potassium (Birch, 1954). In igneous rocks, young unmetamorphosed granite plutons and batholiths can be expected to contain the highest concentrations of U and Th. In the northeast U.S. the genesis, age, and mode of emplacement of many of the granites have been studied in detail (Page, 1968; Chapman, 1968; Thompson and Norton, 1968; Nielson and others, 1976). The occurrence of granite concealed beneath sedimentary, metasedimentary, or volcanic rocks can sometimes be inferred from geophysical data. A knowledge of the chemistry (U, Th, K) and geographic distribution of granitic rocks in the basement and upper crust can explain most known variations in heat flow in the eastern U.S.; however, large-scale overthrusting of continental crust may preclude a simple interpretation of heat-flow data in parts of the Appalachian system. The following discussion of the major geologic subdivisions of the northeast U.S. indicates, where known, the correlation between the occurrence of granite and high heat flow. The number of published heat-flow values (Figure 13.15) is small for the size of the area under consideration.

The Appalachian Mountain System in New England can be divided into five lithotectonic units (Osberg and Skehan, 1979):

1) Avalonian platform or Coastal Belt,

2) Merrimack trough,

3) Connecticut Valley-Gaspe trough,

4) Foreland, and

5) Berkshire and Taconic allochthons.

Upper Precambrian to (?) Ordovician volcanic rocks of the Avalonian Platform are intruded by approximately contemporaneous granite batholiths (550-650 m.y.). The granites intrude mafic and felsic volcanic and volcaniclastic rocks and mafic plutons. The Paleozoic rocks are relatively undeformed and only slightly metamorphosed. This sequence of rocks is correlative with the low-grade Carolina Slate Belt in the southeastern U.S. Heat-flow values in the range of 50-75 mW/m^2 have been reported from the Avalonian Platform, and are about the same as those determined in the Carolina Slate Belt.

The basement beneath the Connecticut Valley and Gaspe and Merrimack troughs is made up of gneiss and interlayered amphibolites. Ages range from 450-600 m.y. Heat flow is in the range 35-60 mW/m^2.

Grenville basement (1 b.y.o.) beneath the Foreland sequence contains para- and ortho-gneiss, schist, and calcsilicate granulite. The overlying foreland section is a shelf facies of Cambrian and Lower Ordovician rocks including basal conglomerate, quartzite, and carbonate. Heat-flow values are in the range 36-48 mW/m^2.

The Berkshire massif is composed of overthrust slices or slabs of continental crust (1 b.y.o.) that were thrust westward over a carbonate-shelf sequence of Cambrian and Ordovician age (Ratcliffe and Hatch, 1979). This massif is part of the long chain of Precambrian metamorphic and plutonic rocks that extends from Newfoundland to Georgia (see, e.g., King, 1967). The section in the Berkshire allocthon is similar to that of the foreland.

Grenville basement contains para- and ortho-gneiss and schist, and unconformably underlies a clastic sequence of either Eocambrian or earliest Cambrian age. A shelf facies of quartzite and carbonates overlies the clastic sequence. The allocthon consists of imbricate slices thrust westward over the foreland in Middle to Upper Ordovician time. The Taconic allocthon is made up of six slices of Cambro-Ordovician shales, sandstones, minor carbonates, and minor volcanics. The slices are unrooted and internal structures indicate a westward direction of transport. Low heat-flow values seem to occur in or near allocthonous metamorphic and plutonic rocks of later Precambrian age; a low value has also been determined by Perry and others (1979) in the overthrust Precambrian rocks of the Blue Ridge in the southeastern U.S.

The most conspicuous heat-flow anomalies in the eastern U.S. are the high values associated with granite plutons in New Hampshire. The highest heat-flow values (92 mW/m^2) are in the Conway Granite (White Mountain Magma Series). Billings and Keevil (1946) described unusually high radioactivity in the Conway Granite. Birch and others (1968) noted the strong correlation between surface heat flow and local bedrock radioactivity at heat-flow sites in the White Mountain and New Hampshire Magma Series in New Hampshire, the Cambridge Argillite in Massachusetts, and gneiss and anorthosite in New York and Vermont; the linear correlation between heat flow and heat production discussed in this chapter was discovered by Birch and others (1968) from heat-flow sites in these rocks, and led to the definition of continental heat-flow provinces by Roy and others (1968a, 1972). On the basis of data available to date, including many new heat-flow values (Costain and others, 1979a), the entire eastern U.S. remains a single heat-flow province as originally suggested by Roy and others (1968a).

Initial variations in concentrations of uranium and thorium at the time of granite emplacement depend on composition of the source rock (Whitney, and Stormer, 1978), but heat flow in the eastern United States will also be influenced by metamorphic redistribution of uranium and thorium.

Concentrations of uranium and thorium in the (unmetamorphosed) Conway Granite are exceptionally high, averaging three or four times that of the average granite and about twice that of granites of the New Hampshire Magma Series (Birch and others, 1968). The areal exposure of these rocks, and presumably, therefore, the volume of granite produced, is much less than that of the New Hampshire Series. A similar relationship between volume of granite and magnitude of heat flow is found in granite plutons and batholiths in the southeastern U.S.

Birch and others (1968) reported horizontal gradients in heat flow of up to 1 mW/m^2 per km between granites of the New Hampshire and White Mountain Magma Series. Because of the close association of crustal concentrations of U and Th with heat flow, other local differences in heat flow can be expected as the data base in the northeast U.S. improves.

In parts of New Jersey, Delaware, and Maryland, the wedge of unconsolidated sediments beneath the Atlantic Coastal Plain conceals the basement rocks. Along the New Jersey coast the depth to basement varies from about 335 m (Fort Monmouth) to 1900 m (Cape May). Only a few samples of basement rock have been obtained from deep drilling and the nature of the basement must be inferred from geophysical data. A heat-flow value of 59 mW/m^2 at Sea Girt, N. J., is coincident with a negative Bouguer gravity anomaly, and is higher than values (45 mW/m^2 north and south of Sea Girt. Because granites have a lower density than most host rocks into which they are intruded, this implies an expected correlation between high heat flow and negative Bouguer gravity anomalies (Costain and others, 1979b).

Heat flow is low at sites in Precambrian anorthosites of the Adirondack massif in New York. Values from this region were used to develop the linear relation between heat flow and heat generation.

Heat flow is normal (60 mW/m^2) in the rest of New York and Pennsylvania, although the density of heat-flow sites is low. South of the Adirondacks in western Pennsylvania and New York, Paleozoic platform deposits increase in thickness to about 7 km and overlie basement rocks of Precambrian age. Southern Pennsylvania is characterized by folded miogeosynclinal sediments of early to late Paleozoic age (Appalachian foldbelt). Locally higher values of heat flow might be the result of an increase in heat production in basement rocks (Diment and others, 1972).

13.14 Heat Flow in Alaska by L. A. Lawver, A. H. Lachenbruch, and R. J. Munroe (U.S. Geological Survey, Menlo Park, California)

Thermal-gradient measurements in Alaska were made as early as 1948 in wells in the South Barrow gasfield near Point Barrow. In spite of extensive drilling in association with mining and oil exploration in Alaska since then, little is known from a geothermal standpoint due to logistic difficulties in obtaining data and the vast size of the state. A much greater amount of effort and money is required to get a heat-flow value in Alaska than in most other areas in the United States. Thermal-gradient measurements have been made in numerous holes in the Naval Petroleum Reserve (now the NPRA or National Petroleum Reserve in Alaska) as part of permafrost studies. Until the drilling for oil at Prudhoe Bay commenced in the sixties where a number of thermal gradients were obtained, the only thermal-gradient measurements made were holes of opportunity, usually in the NPRA region including holes drilled at Cape Thompson as part of Project Chariot and at the Lisburne site just north of the Brooks Range for acoustical experiments. Outside the NPRA, the only early heat-flow measurements were made at Eielson Air Force Base just east of Fairbanks, and on Amchitka Island in holes drilled in conjunction with underground nuclear tests. In recent years, other heat-flow values have been obtained through the courtesy of various private corporations engaged in mineral exploration.

While some of the values shown in Figure 13.16 are quite reliable, such as the Eielson Air Force Base hole near Fairbanks (temperature measurements every 3 m to 3 km, 21 conductivity values and 85 heat-generation measurements) most of the values are somewhat tenuous. Limited conductivity samples, few, if any, heat-generation measurements, inadequate hole depth, and uncertain climatic (glacial) history all tend to affect the reliability of most of the Alaskan heat-flow measurements. In addition, none of the values have been corrected for topography. The North Slope values do not need topographic correction but may need corrections for lateral variations in surface temperature when they are near glaciers or large bodies of water (or have been in the recent past). Even so, it is believed that few of the values will have corrections large enough to move them out of the rather broad categories they are now in (Figure 13.16).

The values on Amchitka Island were published by Sass and Munroe (1970). The thermal gradients from Cape Thompson, Point Barrow, Cape Simpson (near Barrow) and Prudhoe Bay were discussed in some or all of the following papers: Lachenbruch and Brewer (1959); Lachenbruch and others (1962); Lachenbruch and Marshall (1969); Gold and Lachenbruch (1973). The values shown in Figure 13.16 are too few in number to make any but the most general comments about regional heat flow in Alaska. Alaska is an extremely complex tectonic region with active plate subduction, active volcanic ranges, major strike-slip faults and Precambrian sedimentary regions with almost all geology in between represented somewhere in the state. Perhaps the biggest surprise in Alaskan heat flow is the lack of very low values with a general average (so far) well above that for old continental regions. Not surprising are the fairly high heat-flow values found near Mt. Wrangell in south-central Alaska, on the Alaskan Peninsula in the Aleutian Range, in and near the Alaska Range in central Alaska, and in southeast Alaska. As we obtain more heat-flow values, a clearer picture of the thermal regime of Alaska is expected to emerge.

13.15 Heat-Flow Map of the United States based on Silica Geothermometry by C. A. Swanberg and Paul Morgan (New Mexico State University, Las Cruces, New Mexico)

13.15.1 Introduction. The silica heat-flow interpretation technique is based on the temperature dependence of quartz solubility in water (the silica geothermometer of Fournier and Rowe, 1966), and the empirical linear relation between temperatures based on the silica geothermometer and regional heat flow (Swanberg and Morgan, 1978). The silica geothermometer can be expressed quantitively according to the equation of Truesdell (1975),

$$TSiO_2 = \frac{1314}{5.205 - \log_{10} SiO_2} - 273.15 \qquad (3)$$

where $TSiO_2$ is the silica geotemperature in degrees Celcius and dissolved silica is expressed in parts per million. The linear relation between silica geotemperatures and regional heat flow can be expressed quantitively according to the empirical equation of Swanberg and Morgan (1978)

$$TSiO_2 = mq + b \qquad (4)$$

where q is regional heat flow in mWm^{-2} and m and b are constants determined to be 670 $°Cm^2W^{-1}$ and 13.2°C, respectively. The physical significance of "b" is the mean annual air temperature and the slope "m" is related to the minimum average depth to which groundwaters may circulate. This minimum depth is estimated to be between 1.4 and 2.0 km depending upon rock type. A full description of equations (3) and (4), the assumptions upon which they are based and the condition under which they may be applied are presented by Truesdell (1975) and by Swanberg and Morgan (1978, 1980).

Equation (4) was originally derived by averaging 2000-10,000 values of $TSiO_2$ for each tectonic province in the United States for which regional heat flow was well known (Swanberg and Morgan, 1978). This regression is reproduced in Figure 13.17a. More recently, Swanberg and Morgan (1980) redeveloped equation (4) by plotting average values of $TSiO_2$ against heat flow for 1° x 1° blocks using only those blocks for which both $TSiO_2$ and heat flow were well defined. Heat flow was considered to be well defined if at least three points were available and the standard deviation was less than 20% of the mean. Values of $TSiO_2$ were considered to be well defined if at least 100 points were available and the standard deviation was less than 20°C. This regression is reproduced in Figure 13.17. The second regression is not sufficiently different from the first to justify changing the values of the constants m and b, and our preferred regression is

$TSiO_2 = mq + b$, where

$m = 670 \pm 67°Cm^2W^{-1}$ and

$b = 13.2 \pm 5.1°C$.

This second regression permits us to average a manageable number of silica values (50-100) to estimate regional heat flow over a fairly small region (1° x 1° = $\sim 10^4$ km^2); moreover, it permits us to assign error estimates to the resulting heat flow. Thus, heat flow can be determined to $\pm 7.5 + 0.067q$ mWm^{-2} of whatever value would be obtained if three traditional heat-flow determinations existed, and they were in good agreement. Over the range of typical heat-flow values (40-120 mWm^{-2}), these errors correspond to 11.5 and 19.5 mWm^{-2}. This variation is about the same as typically observed among standard heat-flow determinations (Section 13.1.2) covering a comparable area; thus, it appears that the silica heat-flow method is working as well as the traditional approach.

13.15.2 Preparation of Figure 13.18. Figure 13.18 is a heat-flow map of the United States prepared by using equations (3) and (4) to convert ground-water silica concentrations to heat flow and averaging the results for each 1° x 1° block. These averages were then plotted at the center of each block and contoured. The silica data was taken from the USGS WATSTORE file and supplemented by State data in areas where the WATSTORE coverage was sparse. Roughly 200,000 silica-heat flow determinations were used in preparing Figure 13.18.

Our basic approach in preparing Figure 13.18 has been the contouring of 1° x 1° averages, but we have allowed ourselves the following modifications:

1) In areas where heat flow changes rapidly such as near province boundaries, we have positioned the contours on the basis of individual points rather than by placing the average silica heat-flow value at the center of the 1° x 1° block.

2) The contours have been adjusted slightly so that wherever reasonable, Quaternary volcanic rocks and major geothermal areas fall on the high side of the closest contour.

3) The contours have been adjusted to be as consistent as possible with traditional heat-flow values.

4) Several blocks contain clusters of points (geothermal areas) where the predicted heat flow is substantially higher than that predicted by the average value for the block. Several of these clusters have been delineated, particularly when supported by traditional heat-flow values.

13.14.3 Interpretation. In general, the heat-flow contours based upon the silica method are similar to those based on traditional methods except that the abundance of silica data has made it possible to more accurately locate the contours between widely scattered heat-flow sites and also coverage is provided in those areas where traditional data are lacking.

Most of the eastern United States exhibits normal heat flow (<60 mWm^{-2}). Notable exceptions include elevated heat flow throughout much of the Mississippi Embayment including the New Madrid Seismic Zone (Swanberg and others, 1979) and high heat flow (>85 mWm^{-2}) associated with that portion of south Texas, where the geopressured regions are closest to the surface (White and Williams, 1975). Other elevated regions include those portions of the Atlantic Coast Province which are underlain by highly radioactive plutons (Costain and others, 1977), and along the boundary between the Piedmont and Atlantic Coast provinces. Also, the silica data suggest the presence of a major midcontinent heat flow high (the "Ogallala High") extending north from the high plains of west Texas to the Canadian border. The existence of this anomaly is consistent with the sparse heat-flow data summarized by Sass and others (1976) and the unpublished heat-flow data from Nebraska (W. D. Gosnold, personal communication, 1979).

Normal heat flow is also observed throughout much of the area extending north from the Colorado Plateau through the Middle Rocky Mountains and Wyoming Basin to the plains of eastern Montana. Several subareas of elevated heat flow have been delineated on the heat-flow map (Figure 13.18).

The highest heat-flow regions are the Rio Grande Rift of central Colorado and New Mexico and the "Battle Mountain high" of Nevada and southern Idaho. Very low heat flow is associated with the Sierra Nevada, Klamath Mountains, the Oregon Coast Ranges, and the Olympic Mountains of Washington.

<u>13.15.4 Summary</u>. An empirical relation has been developed between regional heat flow and the silica content of groundwater. Using this relation, 200,000 silica values have been converted to heat flow and the results contoured to yield a new heat-flow map of the United States. This new

heat-flow map is generally similar to maps prepared by the traditional borehole techniques (compare Figures 13.4 and 13.18) except that more detail is provided and new estimates of regional heat flow are provided for areas where traditional data are non-existent. Where the data derived from silica geothermometry indicate strong constraints on thermotectonic models, they provide a focus for the planning of additional borehole heat-flow measurements.

13.15.5 Acknowledgments. We thank J. K. Costain, J. H. Sass, W. D. Gosnold, D. S. Chapman, and D. D. Blackwell, for providing unpublished heat-flow estimates. The work was supported in part by U.S. Geological Survey grant 14-08-0001-G-406.

References

American Association of Petroleum Geologists-U.S. Geological Survey, Geothermal gradient map of North America, scale 1:5,000,000, U.S. Geological Survey, Reston, Virginia, 1976.

Beck, A. E., Techniques of measuring heat flow on land, in _Terrestrial Heat Flow_, _Geophys. Monogr. Ser._, vol. 8, edited by W. H. K. Lee, pp. 24-57, AGU, Washington, D. C., 1965.

Beck, A. E., An improved method of computing the thermal conductivity of fluid-filled sedimentary rocks, _Geophysics_, _41_, 133-144, 1976.

Billings, M. P., and N. B. Keevil, Petrography and radioactivity of four Paleozoic magma series in New Hampshire, _Geol. Soc. Amer. Bull._, _57_, 797-828, 1946.

Birch, Francis, Flow of heat in the Front Range, Colorado, _Geol. Soc. Amer. Bull._, _61_, 567-630, 1950.

Birch, Francis, Heat from radioactivity, in _Nuclear Geology_, edited by H. Faul, pp. 148-174, Wiley, New York, 1954.

Birch, Francis, R. F. Roy, and E. R. Decker, Heat flow and thermal history in New England and New York, in _Studies of Appalachian Geology: Northern and Maritime_, edited by E-an Zen, W. S. White, J. B. Hadley, and J. B. Thompson, Jr., pp. 437-451, Interscience, New York, 1968.

Blackstone, D. L., Jr., Late Cretaceous and Cenozoic history of Laramie Basin region, southeast Wyoming, in _Cenozoic History of the Southern Rocky Mountains_, _Mem. 144_, edited by B. F. Curtis, pp. 249-279, Geological Society of America, Boulder, Colorado, 1975.

Blackwell, D. D., Heat flow determinations in the northwestern United States, _J. Geophys. Res._, _74_, 992-1007, 1969.

Blackwell, D. D., Terrestrial heat flow and its implications on the location of geothermal reservoirs in Washington, in Washington Div. Mines Geol. Inform. Circ. 50, 21-33, 1974.

Blackwell, D. D., Heat flow and energy loss in the western United States, in Cenozoic Tectonics and Regional Geophysics of the Western Cordillera, Mem. 152, pp. 209-250, Geological Society of America, Boulder, Colorado, 1978.

Blackwell, D. D., and D. Baag, Heat flow in a blind geothermal area near Marysville, Montana, Geophysics, 38, 941-956, 1973.

Blackwell, D. D., M. J. Holdaway, P. Morgan, D. Petefish, T. Rape, J. L. Steele, D. Thorstenson, and A. F. Waibel, Results and analysis of exploration and deep drilling at Marysville geothermal area, in The Marysville, Montana, Geothermal Project, Final Report, pp. E.1-E.116, Battelle Pacific Northwest Laboratories, Richland, Washington, 1975.

Blackwell, D. D., D. A. Hull, R. G. Bowen, and J. L. Steele, Heat flow of Oregon, Oreg. Dep. Geol. Mineral. Ind. Spec. Pap., 4, 42 pp., 1978.

Blackwell, D. D., and E. C. Robertson, Thermal studies of the Boulder batholith and vicinity, Montana, Soc. Econ. Geologists Guidebook, Butte Field Meeting, August 18-21, D-1 - D-8, 1973.

Bowen, R. G., D. D. Blackwell, D. A. Hull, and N. V. Peterson, Progress report on heat-flow study of the Brothers fault zone, central Oregon, Ore Bin, 38, 39-46, 1976.

Bowen, R. G., D. D. Blackwell, and D. A. Hull, Geothermal exploration studies in Oregon, Oreg. Dep. Geol. Miner. Ind. Misc. Pap., 19, 50 pp., 1977.

Brott, C. A., D. D. Blackwell, and J. C. Mitchell, Heat flow study of the Snake River Plain region, Idaho, in Geothermal investigations in Idaho, Water Inform. Bull., 30, pt. 8, 195 pp., Idaho Department of Water Resources, 1976.

Brott, C. A., D. D. Blackwell, and J. C. Mitchell, Tectonic implications of the heat flow of the western Snake River Plain, Geol. Soc. Amer. Bull., 89, 1697-1707, 1978.

Brune, J. N., T. L. Henyey, and R. F. Roy, Heat flow, stress, and rate of slip along the San Andreas fault, California, J. Geophys. Res., 74, 3821-3827, 1969.

Chapin, C. E., The Rio Grande rift, 1, Modifications and additions, Guidebook to the San Luis Basin, New Mex. Geol. Soc. Field Conf. Guideb., 22nd, 191-201, 1971.

Chapman, C. A., A comparison of the Maine coastal plutons and the magmatic central complexes of New Hampshire, in Studies of Appalachian Geology: Northern and Maritime, edited by E-an Zen, W. S. White, J. B. Hadley, and J. B. Thompson, Jr., pp. 385-396, Interscience, New York, 1968.

Clark, H. B., J. K. Costain, and L. Glover, III, Structural and seismic reflection studies of the Brevard ductile deformation zone near Rosman, North Carolina: Am. J. Sci., 278, 419-441, 1978.

Clark, S. P., Jr., Heat flow at Grass Valley, California, Trans., Am. Geophys. Union, 38, 239-244, 1957.

Cook, F. A., D. S. Albaugh, L. D. Brown, S. Kaufman, J. E. Oliver, and R. D. Hatcher, Jr., Thin-skinned tectonics in the crystalline southern Appalachians; COCORP seismic reflection profiling of the Blue Ridge and Piedmont, Geology, in press, 1979.

Costain, J. K., L. Glover, III, and A. K. Sinha, Evaluation and targeting of geothermal energy resources in the southeastern United States, Virginia Poly. Tech. Prog. Rep. VP1-SU-5103-3, Blacksburg, Virginia, 1977.

Costain, J. K., L. Glover, III, and A. K. Sinha, Evaluation and targeting of geothermal energy resources in the southeastern United States, Prog. Rep. VPI&SU-5648-5, to the Department of Energy, Contract ET-78-C-05-5648, 1979a.

Costain, J. K., L. Glover, III, and A. K. Sinha, Low-temperature geothermal resources in the eastern United States, Eos Trans. AGU, in press, 1979b.

Costain, J. K., and P. M. Wright, Heat flow at Spor Mountain, Jordan Valley, Bingham, and La Sal, Utah, J. Geophys. Res., 78, 8687-8698, 1973.

Decker, E. R., K. H. Baker, G. J. Bucher, and H. P. Heasler, Preliminary heat flow and radioactivity studies in Wyoming, J. Geophys. Res., in press, 1979.

Decker, E. R., and Francis Birch, Basic heat flow data from Colorado, Minnesota, New Mexico, and Texas, U.S. Geol. Surv. Open-File Rep. 74-9, 5-1 - 5-59, 1974.

Decker, E. R., and S. B. Smithson, Heat flow and gravity interpretation across the Rio Grande Rift in southern New Mexico and west Texas, J. Geophys. Res., 80, 2542-2552, 1975.

Diment, W. H., T. C. Urban, and F. A. Revetta, Some geophysical anomalies in the eastern United States, in The Nature of the Solid Earth, edited by E. C. Robertson, pp. 544-572, McGraw-Hill, New York, 1972.

Edwards, C. L., M. A. Reiter, Charles Shearer, and W. Young, Terrestrial heat flow and crustal radioactivity in northeastern New Mexico and southeastern Colorado, Geol. Soc. Amer. Bull., 89, 1341-1350, 1977.

Fenneman, N. M., Physiographic division of the United States, Ann. Ass. Amer. Geogr., 18, 261-353, 1928.

Fournier, R. O., and J. J. Rowe, Estimation of underground temperatures from the silica content of water from hot springs and wet steam wells, Am. J. Sci., 264, 685-697, 1966.

Fournier, R. O., D. E. White, and A. H. Truesdell, Convective heat flow in Yellowstone National Park, in Proceedings of the Second United Nations Symposium on the Development and Use of Geothermal Resources, pp. 731-739, U.S. Government Printing Office, Washington, D. C., 1976.

Fullagar, P. D., and J. R. Butler, 325-265 m.y.-old granitic plutons in the Piedmont of the southeastern Appalachians, Am. J. Sci., 279, 161-185, 1979.

Gold, L. W., and A. H. Lachenbruch, Thermal conditions in permafrost--A review of North American literature, in Permafrost, North American Contribution, Second Internat. Conf., Yakutsk, USSR, July 1973, pp. 3-25, Natl. Acad. Sci., Washington, D. C., 1973.

Hart, S. R., J. S. Steinhart, and T. J. Smith, Heat flow, Yearbook Carnegie Institute, 67, Washington, D. C., 360-367, 1968.

Harris, L. D., Thin-skinned tectonics and potential hydrocarbon traps - illustrated by a seismic profile in the Valley and Ridge province of Tennessee, J. Res., U.S. Geol. Surv., 4, 379-386, 1976.

Hatcher, R. D., and J. R. Butler, Guidebook for the Southern Appalachian Field Trip in the Carolinas, Tennessee, and northeastern Georgia, North Carolina Geological Survey, Raleigh, 1979.

Hatcher, R. D., Jr., L. L. Acker, J. G. Bryan, and S. C. Godfrey, The Hayesville thrust of the central Blue Ridge of North Carolina and nearby Georgia a pre-metamorphic, polydeformed thrust and cryptic suture within the Blue Ridge thrust sheet (abstract), Geol. Soc. Amer. Abstr. Programs, 11, 181, 1979.

Henyey, T. L., Heat flow near major strike-slip faults in central and southern California, Ph.D. thesis, California Institute of Technology, Pasadena, 1968.

Henyey, T. L., and T. C. Lee, Heat flow in Lake Tahoe, California-Nevada, and the Sierra Nevada - Basin and Range transition, Geol. Soc. Amer. Bull., 87, 1179-1187, 1976.

Henyey, T. L., and G. J. Wasserburg, Heat flow near major strike-slip faults in California, J. Geophys. Res., 76, 7924-7946, 1971.

Horai, Ki-iti, Thermal conductivity of rock-forming minerals, J. Geophys. Res., 76, 1278-1308, 1971.

Jaeger, J. C., Application of the theory of heat conduction to geothermal measurements, in Terrestrial Heat Flow, Geophys. Monogr. Ser., vol. 8, edited by W. H. K. Lee, pp. 7-23, AGU, Washington, D. C., 1965.

King, P. B., Map of tectonic features of conterminous U.S., U.S. Geol. Surv., Natl. Atlas, Sheet 70, 1967.

King, P. B., and H. M. Beikman, Geologic map of the United States, scale 1:2,500,000, U.S. Geol. Surv., 1974.

Kutas, R. I., Investigation of heat flow in the territory of the Ukraine, Tectonophysics, 41, 139-145, 1977.

Lachenbruch, A. H., Preliminary geothermal model of the Sierra Nevada, J. Geophys. Res., 73, 6977-6989, 1968.

Lachenbruch, A. H., Crustal temperature and heat production: Implications of the linear heat-flow relation, J. Geophys. Res., 75, 3291-3300, 1970.

Lachenbruch, A. H., Heat flow in the Basin and Range Province and thermal effects of tectonic extension, Pure Appl. Geophys., 117, 34-50, 1978.

Lachenbruch, A. H., and M. C. Brewer, Dissipation of the temperature effect of drilling a well in Arctic Alaska, U.S. Geol. Surv. Bull., 1083-C, 73-109, 1959.

Lachenbruch, A. H., M. C. Brewer, G. W. Greene, and B. V. Marshall, Temperatures in permafrost, in Temperature--Its Measurement and Control in Science and Industry, pp. 791-803, Reinhold, New York, 1962.

Lachenbruch, A. H., and C. M. Bunker, Vertical gradients of heat production in the continental crust, 2, Some estimates from borehole data, J. Geophys. Res., 76, 3852-3860, 1971.

Lachenbruch, A. H., and B. V. Marshall, Heat flow in the Arctic, Arctic, 22, 300-311, 1969.

Lachenbruch, A. H., and J. H. Sass, Thermo-mechanical aspects of the San Andreas fault system, in Proceedings of the Conference on the Tectonic Problems of the San Andreas Fault, pp. 192-205, Stanford University Press, 1973.

Lachenbruch, A. H., and J. H. Sass, Heat flow in the United States and the thermal regime of the crust, in The Earth's Crust--Its Nature and Physical Properties, Geophys. Monogr. Ser., vol. 20, edited by J. G. Heacock, pp. 626-675, AGU, Washington, D. C., 1977.

Lachenbruch, A. H., and J. H. Sass, Models of an extending lithosphere and heat flow in the Basin and Range province, in Cenozoic Tectonics and Regional Geophysics of the Western Cordillera, Mem. 152, edited by R. B. Smith and G. P. Eaton, pp. 209-250, Geological Society of America, Boulder, Colo., 1978.

Lachenbruch, A. H., J. H. Sass, and S. P. Galanis, Jr., New heat-flow results from southern California (abstract), Eos Trans. AGU, 59, 1051, 1978.

Lawrence, R. D., Strike-slip faulting terminates the Basin and Range province in Oregon, Geol. Soc. Amer. Bull., 87, 846-850, 1976.

Lee, Tien-Chang, and T. L. Henyey, Heat flow through the southern California borderland, J. Geophys. Res., 80, 3733-3743, 1975.

Morgan, Paul, D. D. Blackwell, R. E. Spafford, and R. B. Smith, Heat flow measurements in Yellowstone Lake and thermal structure of the Yellowstone caldera, J. Geophys. Res., 82, 3719-3732, 1977.

Nielson, D. L., R. G. Clark, J. B. Lyons, E. J. Englund, and D. J. Borns, Gravity models and mode of emplacement of the New Hampshire plutonic series, in Studies of New England Geology, Mem. 146, edited by P. C. Lyons and A. H. Brownlow, pp. 301-318, Geological Society of America, Boulder, Colorado, 1976.

Olmsted, F. H., Use of temperature surveys at a depth of 1 meter in geothermal exploration in Nevada, U.S. Geol. Surv. Prof. Pap. 1044-B, 25 pp., 1977.

Osberg, P. H., and J. W. Skehan, S. J., The Caledonides in the U.S.A., in Geological excursions in the northeast Appalachians, edited by J. W. Skehan and P. H. Osberg, 250 pp., Contributions to the Internat. Geol. Correlation Program (IGCP), Proj 27 - Caledonide Orogen, Weston Observatory, Boston College, 1979.

Page, L. R., Devonian plutonic rocks in New England, in Studies of Appalachian Geology: Northern and Maritime, edited by E-an Zen, W. S. White, J. B. Hadley, and J. B. Thompson, Jr., pp. 371-383, Interscience, New York, 1968.

Perry, L. D., J. K. Costain, and P. A. Geiser, Heat flow in western Virginia and a model for the origin of thermal springs in the folded Appalachians, J. Geophys. Res., in press, 1979.

Pollack, H. N., and D. S. Chapman, On the regional variation of heat flow, geotherms and lithospheric thickness, Tectonophysics, 38, 279-296, 1977.

Rao, R. U. M., and A. M. Jessop, A comparison of the thermal characters of shields, Can. J. Earth Sci., 12, 347-360, 1975.

Rao, R. U. M., G. V. Rao, and H. Narain, Radioactive heat generation and heat flow in the Indian Shield, Earth Planet. Sci. Lett., 30, 57-64, 1976.

Ratcliffe, N. M., and N. L. Hatch, Jr., A traverse across the Taconide zone in the area of the Berkshire massif, western Massachusetts, in The Caledonides in the U.S.A.: Geologic Excursions in the Northeast Appalachians, edited by J. W. Skehan, S. J., and P. H. Osberg, pp. 175-200, Weston Observatory, Boston College, 1979.

Reiter, M. A., C. L. Edwards, H. Hartman, and C. Weidman, Terrestrial heat flow along the Rio Grande Rift, New Mexico and southern Colorado, Geol. Soc. Am. Bull., 86, 811-818, 1975.

Reiter, M. A., and Charles Shearer, Terrestrial heat flow in eastern Arizona, a first report, J. Geophys. Res., 1979, in press.

Reiter, M. A., Charles Shearer, and C. L. Edwards, Geothermal anomalies along the Rio Grande Rift in New Mexico, Geology, 6, 85-88, 1978.

Roy, R. F., D. D. Blackwell, and Francis Birch, Heat generation of plutonic rocks and continental heat flow provinces, Earth Planet. Sci. Lett., 5, 1-12, 1968a.

Roy, R. F., E. R. Decker, D. D. Blackwell, and Francis Birch, Heat flow in the United States, J. Geophys. Res., 73, 5207-5221, 1968b.

Roy, R. F., D. D. Blackwell, and E. R. Decker, Continental heat flow, in The Nature of the Solid Earth, edited by E. C. Robertson, pp. 506-543, McGraw-Hill, New York, 1972.

Sass, J. H., W. H. Diment, A. H. Lachenbruch, B. V. Marshall, R. J. Munroe, T. H. Moses, Jr., and T. C. Urban, A heat-flow contour map of the conterminous United States, U.S. Geol. Surv. Open-File Rep. 76-756, 24 pp., 1976.

Sass, J. H., and A. H. Lachenbruch, Heat flow and conduction-dominated thermal regimes, in Assessment of Geothermal Resources of the United States, 1978, edited by L. J. P. Muffler, pp. 8-11, U.S. Geol. Surv. Circ. 790, 1979a.

Sass, J. H., and A. H. Lachenbruch, Thermal regime of the Australian continental crust, in The Earth, Its Origin, Structure, and Evolution, edited by M. W. McElhinny, pp. 301-351, Academic Press, London, 1979b.

Sass, J. H., A. H. Lachenbruch, and R. J. Munroe, Thermal conductivity of rocks from measurements on fragments and its application to heat-flow determinations, J. Geophys. Res., 76, 3391-3401, 1971a.

Sass, J. H., A. H. Lachenbruch, R. J. Munroe, G. W. Greene, and T. H. Moses, Jr., Heat flow in the western United States, J. Geophys. Res., 76, 6376-6413, 1971b.

Sass, J. H., and R. J. Munroe, Heat flow from deep boreholes on two island arcs, J. Geophys. Res., 75, 4387-4395, 1970.

Sass, J. H., and E. A. Sammel, Heat flow data and their relation to observed geothermal phenomena near Klamath Falls, Oregon, J. Geophys. Res., 81, 4863-4868, 1976.

Scattolini, Richard, Heat flow and heat production studies in North Dakota, Ph.D. thesis, University of North Dakota, Grand Forks, 1978.

Schuster, J. E., D. D. Blackwell, P. E. Hammond, and M. T. Huntting, Heat flow studies in the Steamboat Mountain - Lemei Rock area, Skamania County, Washington, Div. Geol. Earth Resour. Inf. Circ. 62, Washington State, 56 pp, 1978.

Smith, D. L., Heat flow, radioactive heat generation, and theoretical tectonics for northern Mexico, Earth Planet. Sci. Lett., 23, 43-52, 1974.

Smith, D. L., R. G. Gregory, and M. J. Garvey, A thermal reconnaissance of Georgia: Heat flow and radioactive heat generation, Georgia Geol. Surv. Bull., 93, 93-104, 1978.

Smith, D. L., and G. M. Griffin, editors, The geothermal nature of the Floridan Plateau, Florida Dep. Nat. Resour. Spec. Pub. 21, 161 pp., Bureau of Geology, Division of Resource Management, 1977.

Smith, D. L., and R. L. Jones, Thermal anomaly in northern Mexico: An extension of the Rio Grande Rift?, in Rio Grande Rift Tectonics and Magmatism, edited by R. E. Riecker, pp. 269-278, AGU, Washington, D. C., 1979.

Smith, D. L., C. E. Nuckels, R. L. Jones, and G. A. Cook, Distribution of heat flow and radioactive heat generation in northern Mexico, J. Geophys. Res., 84, 2371-2379, 1979.

Smith, R. B., and W. J. Arabasz, Seismicity, tectonics and crustal structure in Utah: Important aspects from new data, in Earthquake Studies in Utah 1850 to 1978, edited by W. J. Arabasz, R. B. Smith, and W. D. Richins, 552 pp., University of Utah Press, 1979.

Smith, R. B., and L. W. Braile, Upper crustal low-velocity layers: Possible effect of high temperatures over a mantle upwarp at the Basin Range - Colorado Plateau transition, Earth Planet. Sci. Lett., 28, 197-204, 1975.

Stokes, W., Subdivision of the major physiographic provinces in Utah, _Utah Geol._, _4_, 1-17, 1977.

Swanberg, C. A., Vertical distribution of heat generation in the Idaho batholith, _J. Geophys. Res._, _77_, 2508-2513, 1972.

Swanberg, C. A., B. J. Mitchell, R. L. Lohse, and D. D. Blackwell, Heat flow in the Upper Mississippi Embayment, _Geol. Soc. Amer. Spec. Pap._, in press, 1979.

Swanberg, C. A., and P. Morgan, The linear relation between temperatures based on the silica content of groundwater and regional heat flow: A new heat flow map of the United States, _Pure Appl. Geophys._, _117_, 227-241, 1978.

Swanberg, C. A., and P. Morgan, The silica heat flow interpretation techniques: Assumptions and applications, _J. Geophys. Res._, in press, 1980.

Thompson, J. B., Jr., and S. A. Norton, Paleozoic regional metamorphism in New England and adjacent areas, in _Studies of Appalachian Geology: Northern and Maritime_, edited by E-an Zen, W. S. White, J. B. Hadley, and J. B. Thompson, Jr., pp. 319-327, Interscience, New York, 1968.

Truesdell, A. H., Summary of Section III, Geochemical techniques in exploration, in _Proceedings of the Second United Nations Symposium on the Development and Use of Geothermal Resources_, pp. liii-lxxix, U.S. Government Printing Office, Washington, D. C., 1976.

Tweto, O., Tectonic map of the Rio Grande rift system in Colorado, _U.S. Geol. Surv. Open-File Rep. 77-750_, Denver, Colorado, 1977.

Von Herzen, R. P., and A. E. Maxwell, The measurement of thermal conductivity of deep sea sediments by a needle probe method, _J. Geophys. Res._, _64_, 1557-1563, 1953.

Warren, R. E., J. G. Sclater, Victor Vacquier, and R. F. Roy, A comparison of terrestrial heat flow and transient geomagnetic fluctuations in the southwestern United States, Geophysics, 34, 463-478, 1969.

White, D. E., and D. L. Williams, (editors), Assessment of geothermal resources of the United States-1975, U.S. Geol. Surv. Circ. 726, 155 pp., 1975.

Whitney, J. A., and J. C. Stormer, Jr., Rare earth distribution and fractionation within post-metamorphic granites of the southern Appalachian Piedmont, Eos Trans. AGU, 59, 393, 1978.

Wright, J. E., A. K. Sinha, and L. Glover, III, Age of zircons from the Petersburg Granite, Virginia; with comments on belts of plutons in the Piedmont, Am. J. Sci., 275, 848-856, 1975.

Wyllie, P. J., Experimental limits for melting in the earth's crust and upper mantle, in The Structure and Physical Properties of the Earth's Crust, Geophys. Monogr., Ser., vol. 14, edited by J. G. Heacock, pp. 279-301, AGU, Washington, D. C., 1971.

Figure captions

Figure 13.1. Heat flow versus heat production for the three heat-flow provinces defined by Roy and others (1968a) (from Lachenbruch and Sass, 1978).

Figure 13.2. Generalized steady-state conductive temperature profiles for various heat-flow provinces in the United States (from Lachenbruch and Sass, 1977). Surface heat flow and reduced heat flow are shown at the bottom of each curve. Melting relations are adapted from Wyllie (1971).

Figure 13.3 Heat-flow map of the United States and adjoining regions of Canada and Mexico. Additional control from North Dakota is from Scattolini (1978); from Lake Superior, Hart and others (1968).

Figure 13.4. Heat-flow contours (HFU) in the United States (after Lachenbruch and Sass, 1977, with modifications based on the new data presented in Sections 13.7 through 13.14). Compare with Figure 13.18.

Figure 13.5. Map of the western United States showing heat-flow contours (HFU), heat-flow provinces, and major physiographic divisions. SRP, Snake River Plain; BMH, Battle Mountain high; EL Eureka Low; RGR, Rio Grande Rift Zone; Y, Yellowstone; LV, Long Valley.

Figure 13.6. Reduced heat flow (q_r, equation 2) and major physiographic divisions of the United States and adjoining regions of Canada and Mexico.

Figure 13.7. Index map for regional heat-flow maps. The number refers to the corresponding figure in the following sections (e.g., 8 refers to Figure 13.8).

Figure 13.8. Heat-flow and physiographic-tectonic provinces in the Pacific Northwest. Compiled by D. D. Blackwell, J. L. Steele, and C. A. Brott.

Figure 13.9. Heat-flow and physiographic-tectonic provinces in northern and central California. Compiled by J. H. Sass, A. H. Lachenbruch, R. J. Munroe, and B. V. Marshall. TR, Transverse Ranges; MB, Mojave Block; EUR, Eureka; SAF, San Andreas fault.

Figure 13.10. Heat-flow and physiographic-tectonic provinces of southern California, southern Nevada, and Arizona. Compiled by J. H. Sass, A. H. Lachenbruch, R. J. Munroe, and B. V. Marshall. MB is Mojave Block.

Figure 13.11. Heat flow and generalized geology for eastern Arizona, the Rio Grande Rift, and the southern Rocky Mountains. Generalized geology essentially after King and Beikman (1974). Compiled by E. R. Decker, H. P. Heasler, and D. L. Blackstone, Jr.

Figure 13.12. Heat flow and generalized geology for the central and northern Rocky Mountains. Generalized geology essentially after King and Beikman (1974). Compiled by E. R. Decker, H. P. Heasler, and D. L. Blackstone, Jr.

Figure 13.13. Heat-flow map of Utah showing the major physiographic-tectonic units. Compiled by D. S. Chapman, J. Bodell, M. Clement, and R. Darling.

Figure 13.14. Heat flow and generalized geology in the southeastern United States. Compiled by J. K. Costain.

Figure 13.15. Heat flow and generalized geology in the northeastern United States. Compiled by J. K. Costain.

Figure 13.16. Heat flow and major structures of Alaska. Compiled by L. A. Lawver, A. H. Lachenbruch, and R. J. Munroe.

Figure 13.17. Plot of $TSiO_2$ against regional heat flow for a) the major tectonic provinces of the United States for which heat flow is well known, and b) 1° x 1° blocks for which $TSiO_2$ and q are both well defined (see text). The abbreviations are national mean air temperature (NMAT), eastern United States (EUS), Colorado Plateau (CP), Basin and Range (BR), Rio Grande Rift (RGR), and Battle Mountain high (BMH).

Figure 13.18. Heat-flow map of the United States based on silica geothermometry. Compiled by C. A. Swanberg and Paul Morgan. Contours are in heat-flow units, 1 HFU = 10^{-6} cal/cm² sec = 41.8 mWm^{-2}. Compare with Figure 13.4.

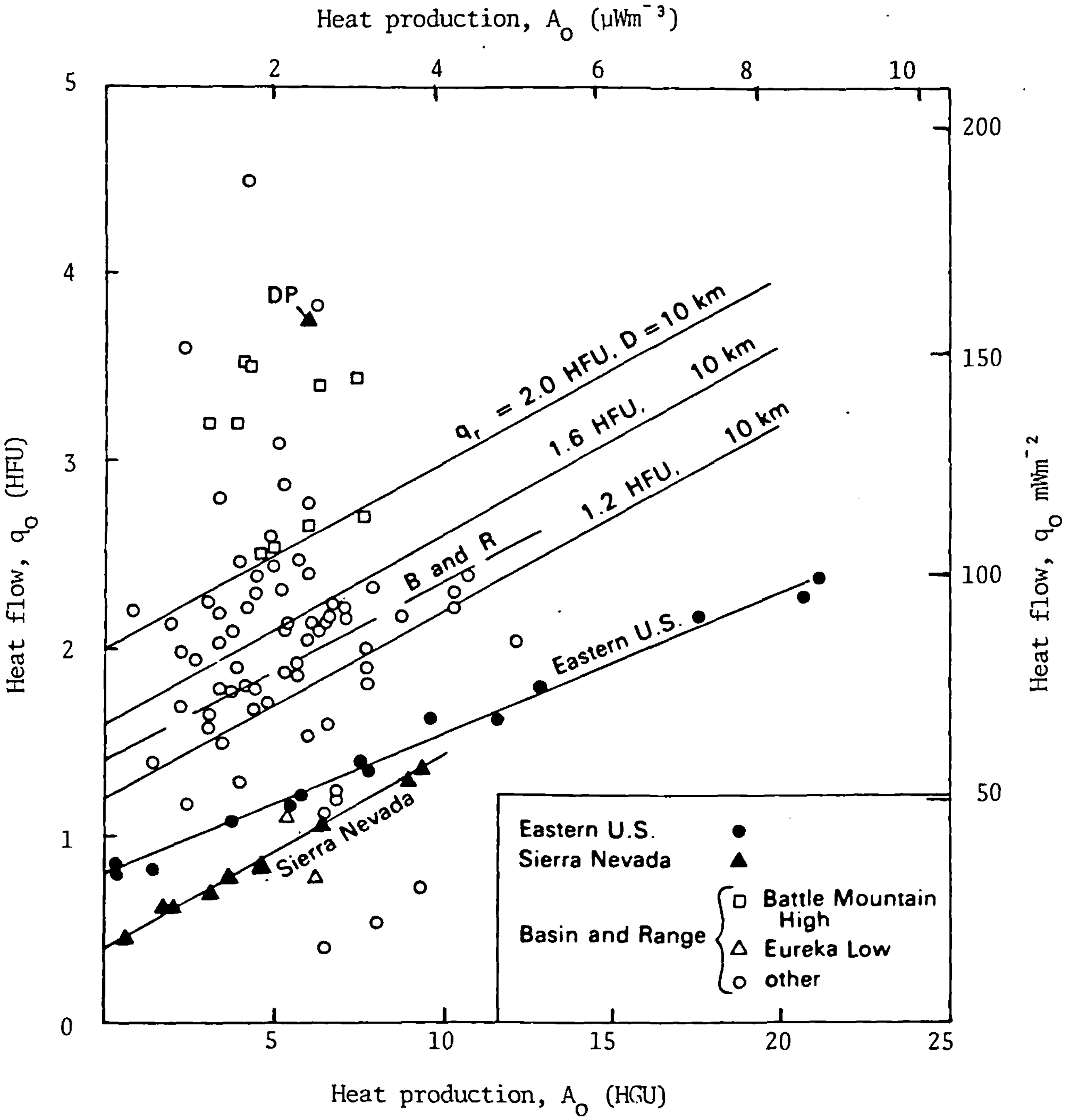

Heat production, A_o (μWm^{-3})
2
4
6
8
10
5
4
3
2
1
0
200
150
100
50
DP
q_r = 2.0 HFU. D = 10 km
1.6 HFU. 10 km
1.2 HFU. 10 km
B and R
Eastern U.S.
Sierra Nevada
Eastern U.S.
Sierra Nevada
Basin and Range
Battle Mountain High
Eureka Low
other
Heat flow, q_o (HFU)
Heat flow, q_o mWm^{-2}
5
10
15
20
25
Heat production, A_o (HGU)

Figure 13.1

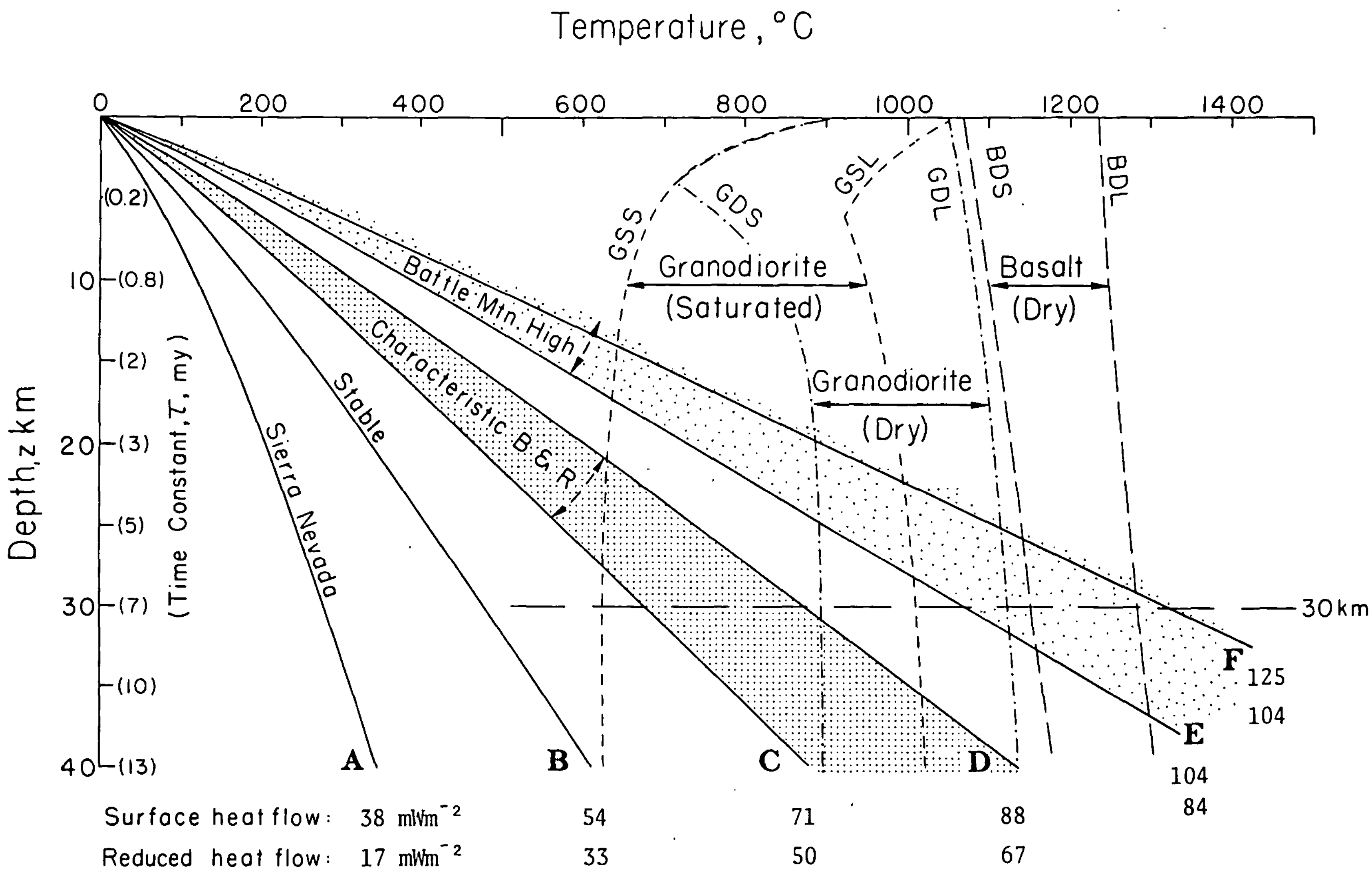

Temperature, °C
0
200
400
600
800
1000
1200
1400
Depth, z km
(Time Constant, τ, my)
10
20
30
40
(0.2)
(0.8)
(2)
(3)
(5)
(7)
(10)
(13)
Sierra Nevada
Stable
Characteristic B & R
Battle Mtn. High
GSS
GDS
GSL
GDL
BDS
BDL
Granodiorite
(Saturated)
Granodiorite
(Dry)
Basalt
(Dry)
30km
A
B
C
D
E
F
125
104
104
84
Surface heat flow: 38 mWm⁻² 54 71 88
Reduced heat flow: 17 mWm⁻² 33 50 67

Figure 13.2

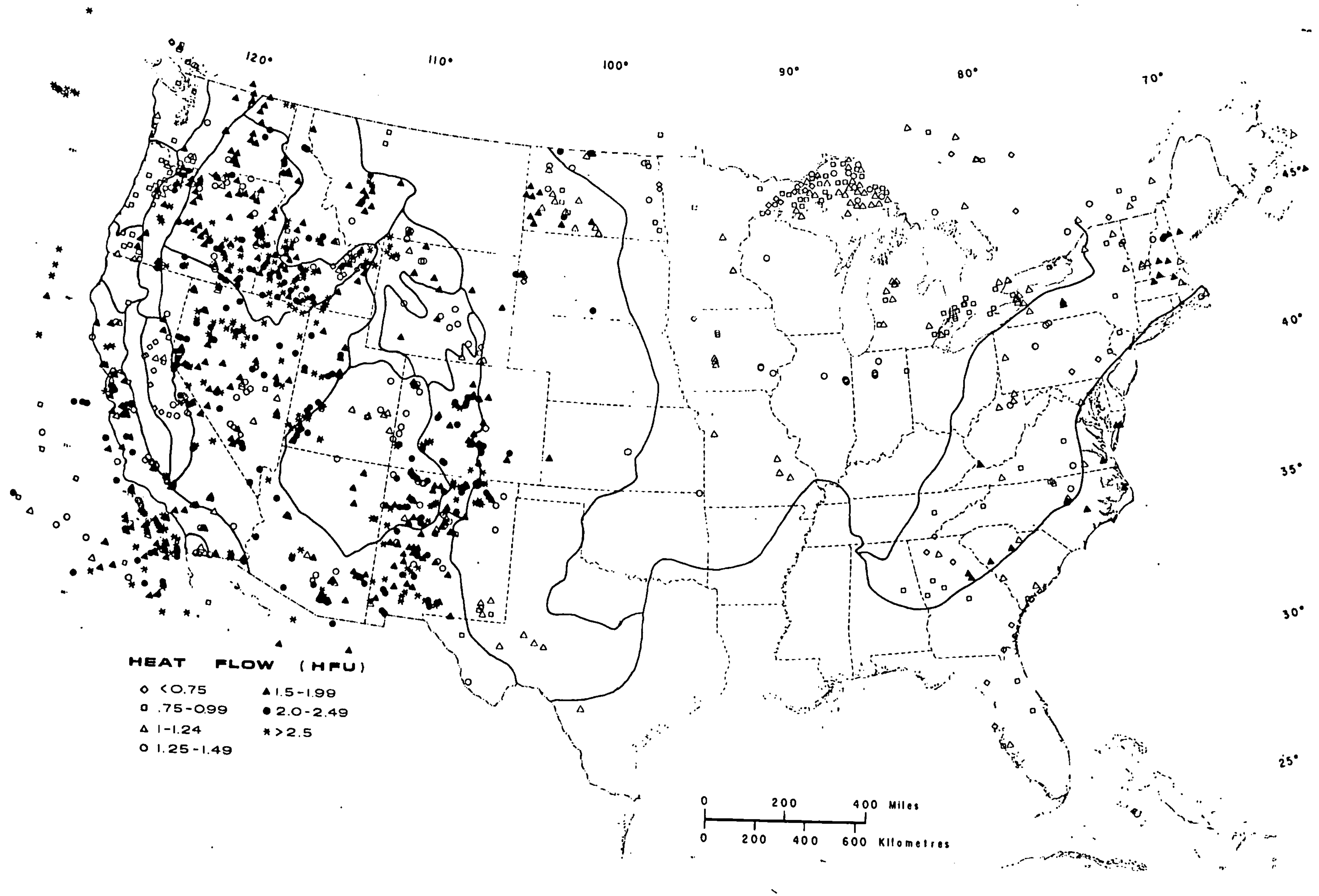
120°
110°
100°
90°
80°
70°
45°
40°
35°
30°
25°
HEAT FLOW (HFU)
<0.75
.75-0.99
1-1.24
1.25-1.49
1.5-1.99
2.0-2.49
>2.5
0 200 400 Miles
0 200 400 600 Kilometres

Figure 13.3

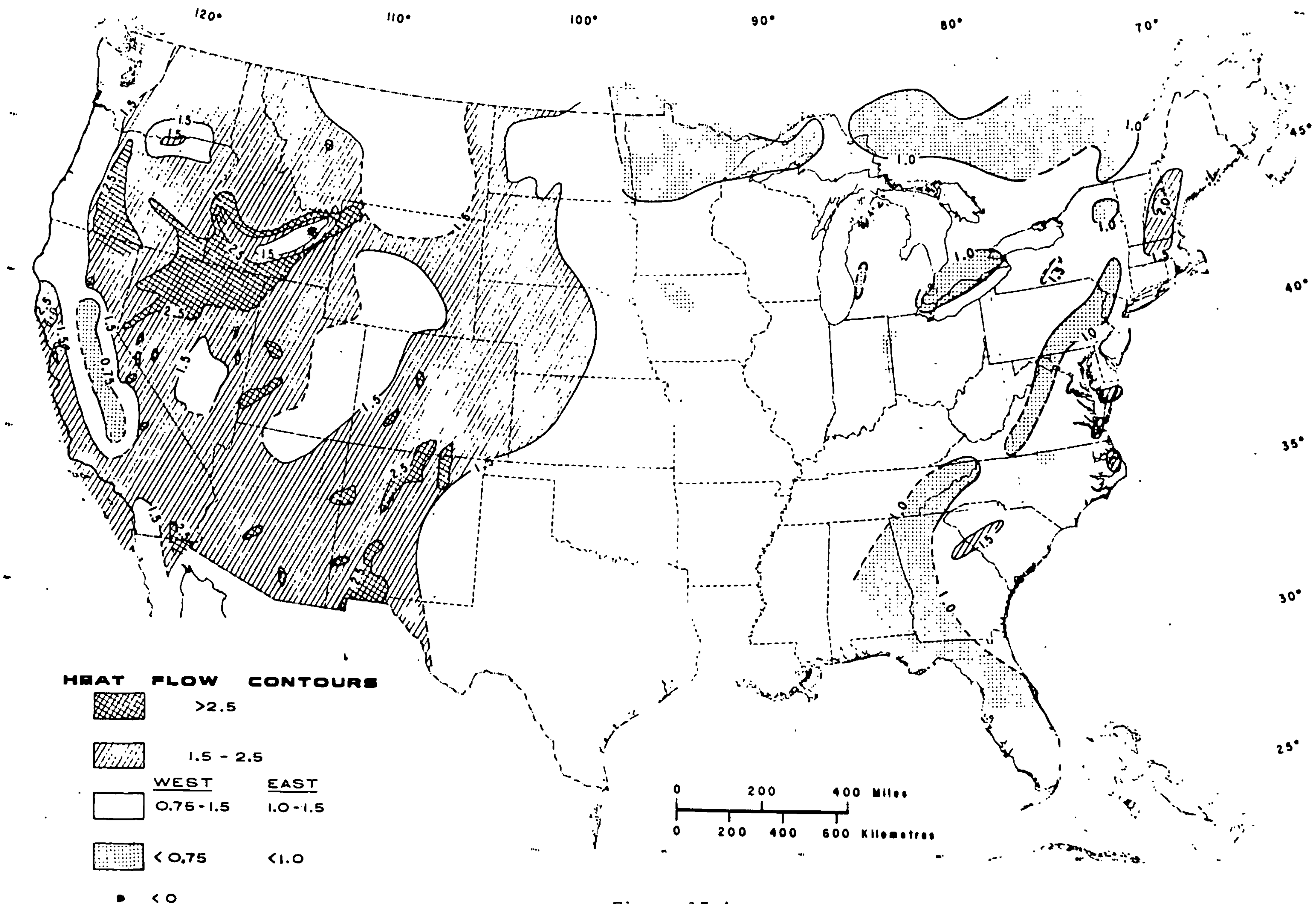
120°
110°
100°
90°
80°
70°
45°
40°
35°
30°
25°
HEAT FLOW CONTOURS
>2.5
1.5 - 2.5
WEST
EAST
0.75-1.5
1.0-1.5
< 0.75
<1.0
< 0
0 200 400 Miles
0 200 400 600 Kilometres

Figure 13.4

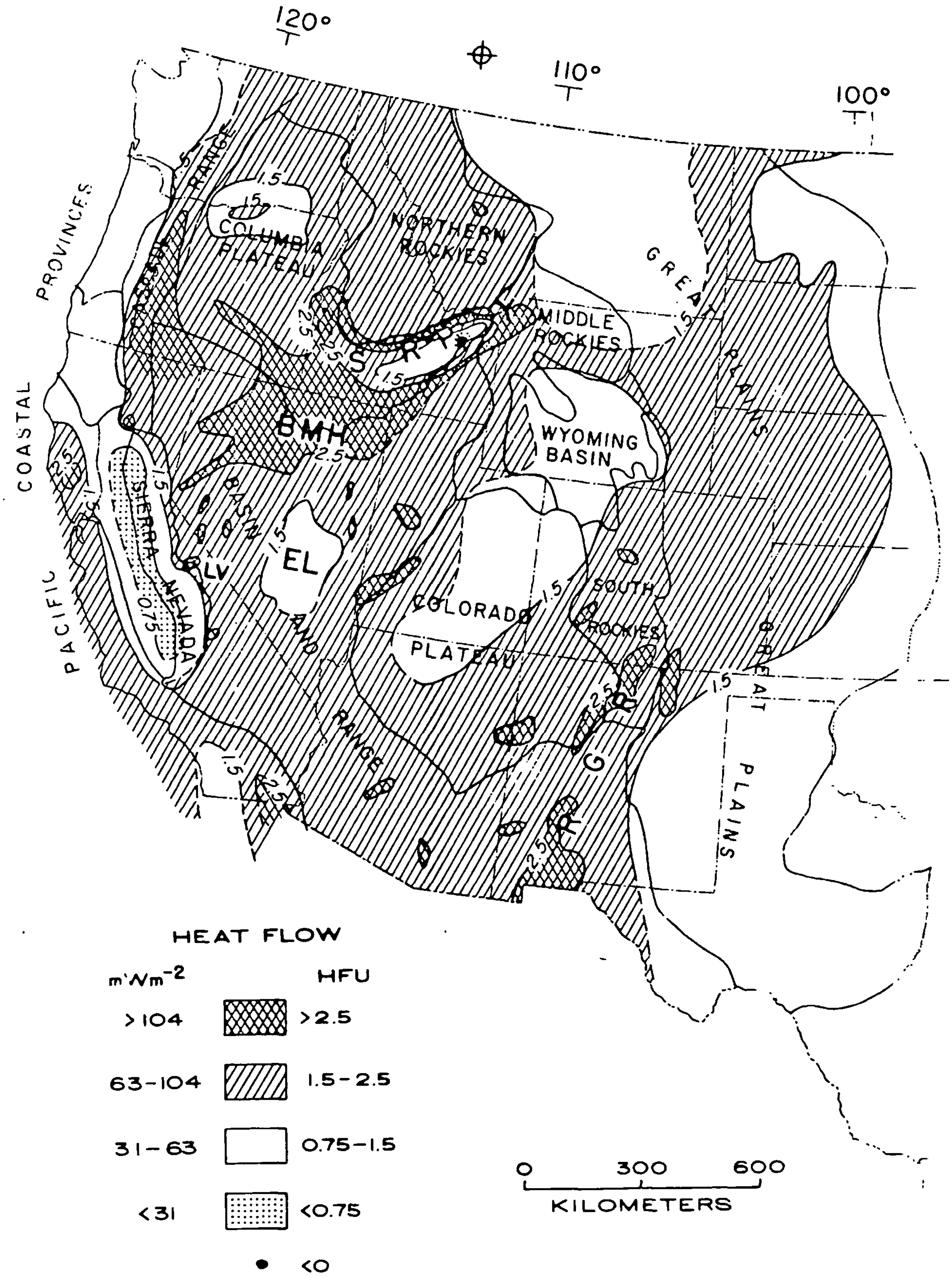

120°
110°
100°
COASTAL
PROVINCES
PACIFIC
COLUMBIA
PLATEAU
NORTHERN
ROCKIES
MIDDLE
ROCKIES
WYOMING
BASIN
GREAT
PLAINS
SIERRA
NEVADA
BMH
EL
LV
COLORADO
PLATEAU
SOUTH
ROCKIES
RANGE
HEAT FLOW
mWm-2
HFU
>104
>2.5
63-104
1.5-2.5
31-63
0.75-1.5
<31
<0.75
<0
0
300
600
KILOMETERS

Figure 13.5

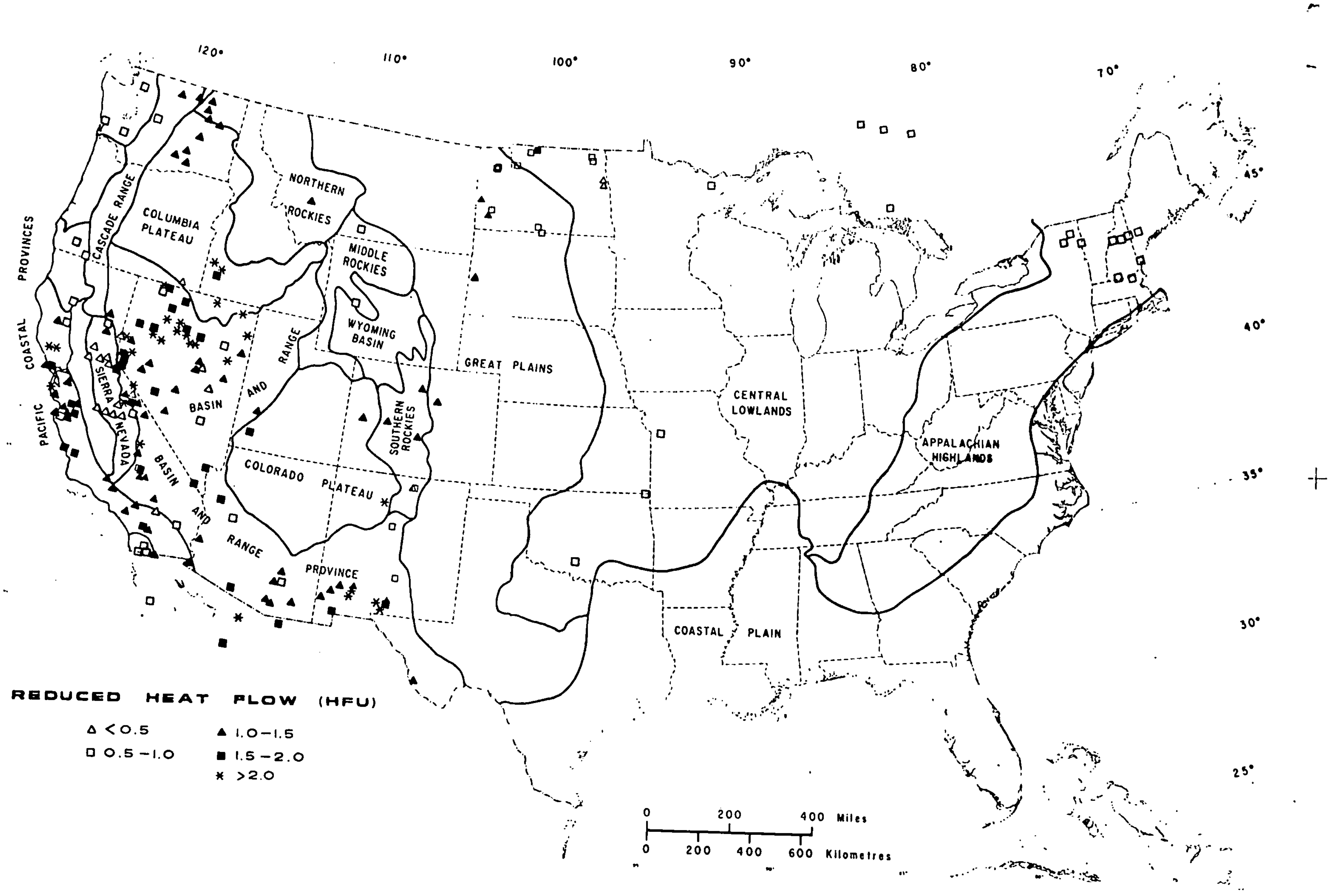

120°
110°
100°
90°
80°
70°
45°
40°
35°
30°
25°
CASCADE RANGE
COLUMBIA PLATEAU
NORTHERN ROCKIES
MIDDLE ROCKIES
WYOMING BASIN
GREAT PLAINS
CENTRAL LOWLANDS
APPALACHIAN HIGHLANDS
COASTAL PLAIN
PACIFIC COASTAL PROVINCES
SIERRA NEVADA
BASIN AND RANGE
BASIN AND RANGE PROVINCE
COLORADO PLATEAU
SOUTHERN ROCKIES
REDUCED HEAT FLOW (HFU)
△ <0.5
□ 0.5 – 1.0
▲ 1.0 – 1.5
■ 1.5 – 2.0
✱ >2.0
0 200 400 Miles
0 200 400 600 Kilometres

Figure 13.6

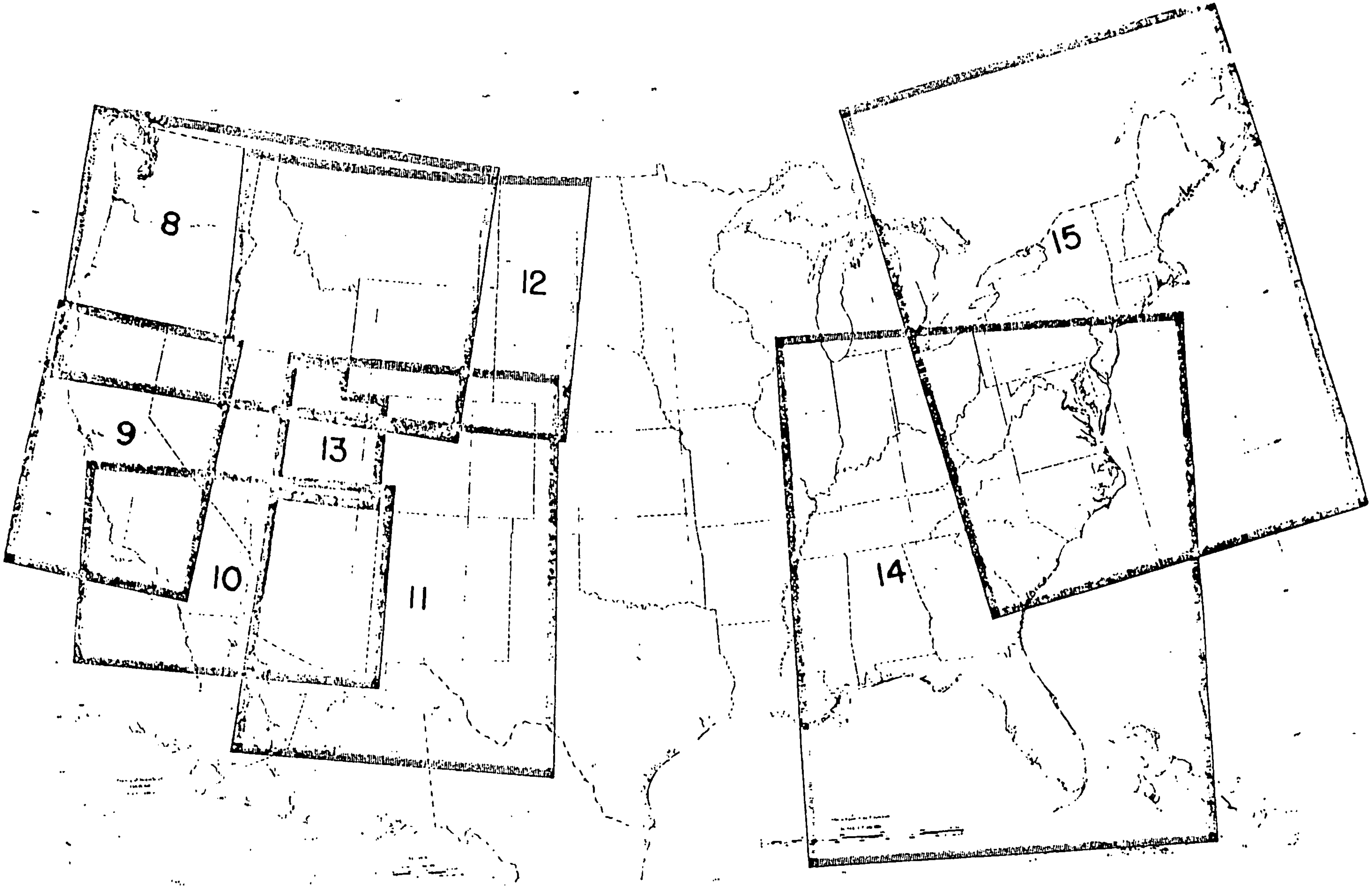

Figure 13.7

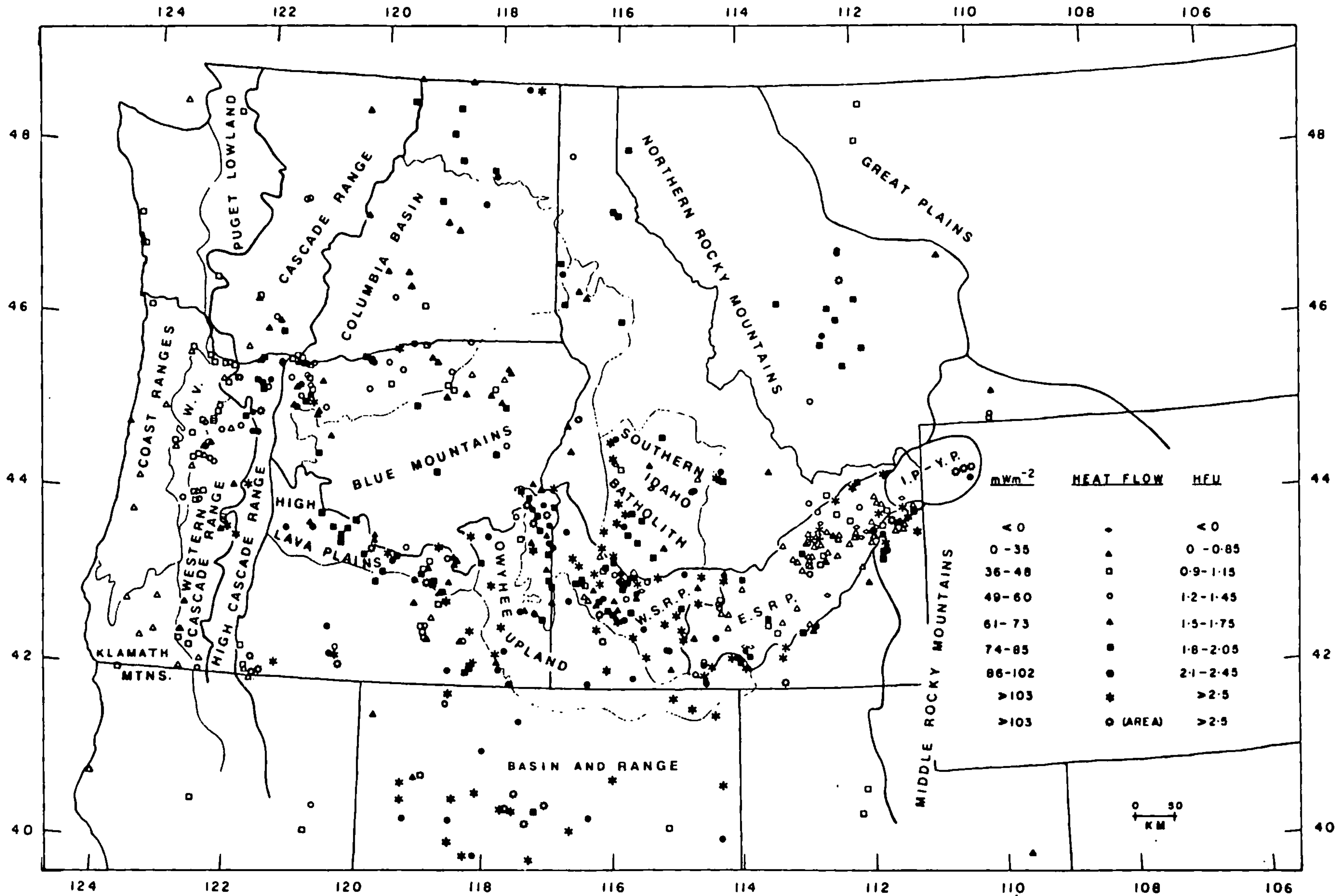

PUGET LOWLAND
CASCADE RANGE
COLUMBIA BASIN
NORTHERN ROCKY MOUNTAINS
GREAT PLAINS
COAST RANGES
W.V.
WESTERN CASCADE RANGE
HIGH CASCADE RANGE
HIGH LAVA PLAINS
BLUE MOUNTAINS
SOUTHERN IDAHO BATHOLITH
OWYHEE UPLAND
W.S.R.P.
E.S.R.P.
I.P.-Y.P.
MIDDLE ROCKY MOUNTAINS
KLAMATH MTNS.
BASIN AND RANGE
mWm-2
HEAT FLOW
HFU
<0
0-35
36-48
49-60
61-73
74-85
86-102
>103
>103
(AREA)
<0
0-0.85
0.9-1.15
1.2-1.45
1.5-1.75
1.8-2.05
2.1-2.45
>2.5
>2.5
0 50
KM

Figure 13.8

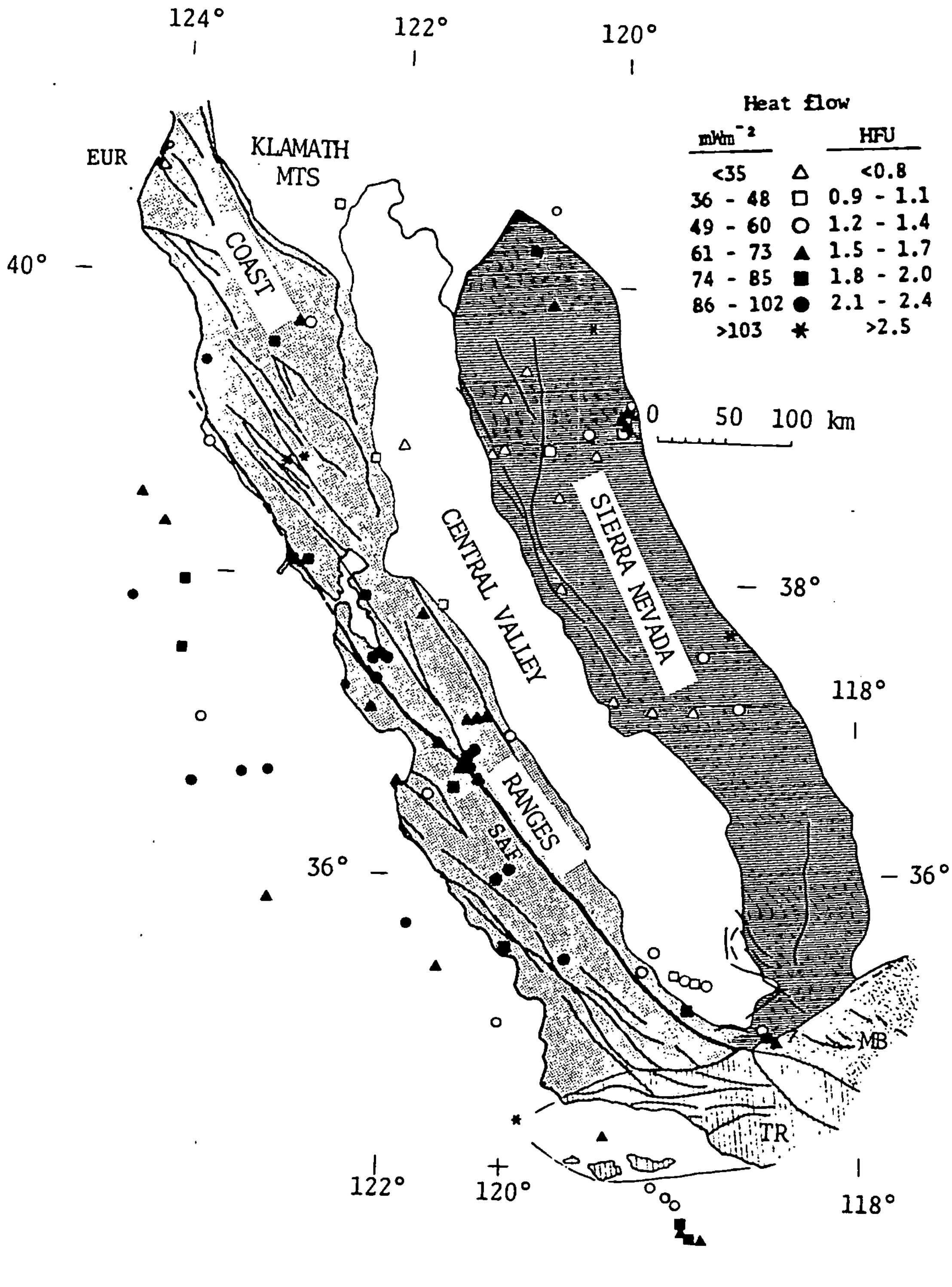
124°
122°
120°
Heat flow
mWm⁻²
HFU
<35
<0.8
36 - 48
0.9 - 1.1
49 - 60
1.2 - 1.4
61 - 73
1.5 - 1.7
74 - 85
1.8 - 2.0
86 - 102
2.1 - 2.4
>103
>2.5
EUR
KLAMATH MTS
40°
COAST
0 50 100 km
CENTRAL VALLEY
SIERRA NEVADA
38°
118°
RANGES
SAF
36°
36°
MB
TR
122°
120°
118°

Figure 13.9

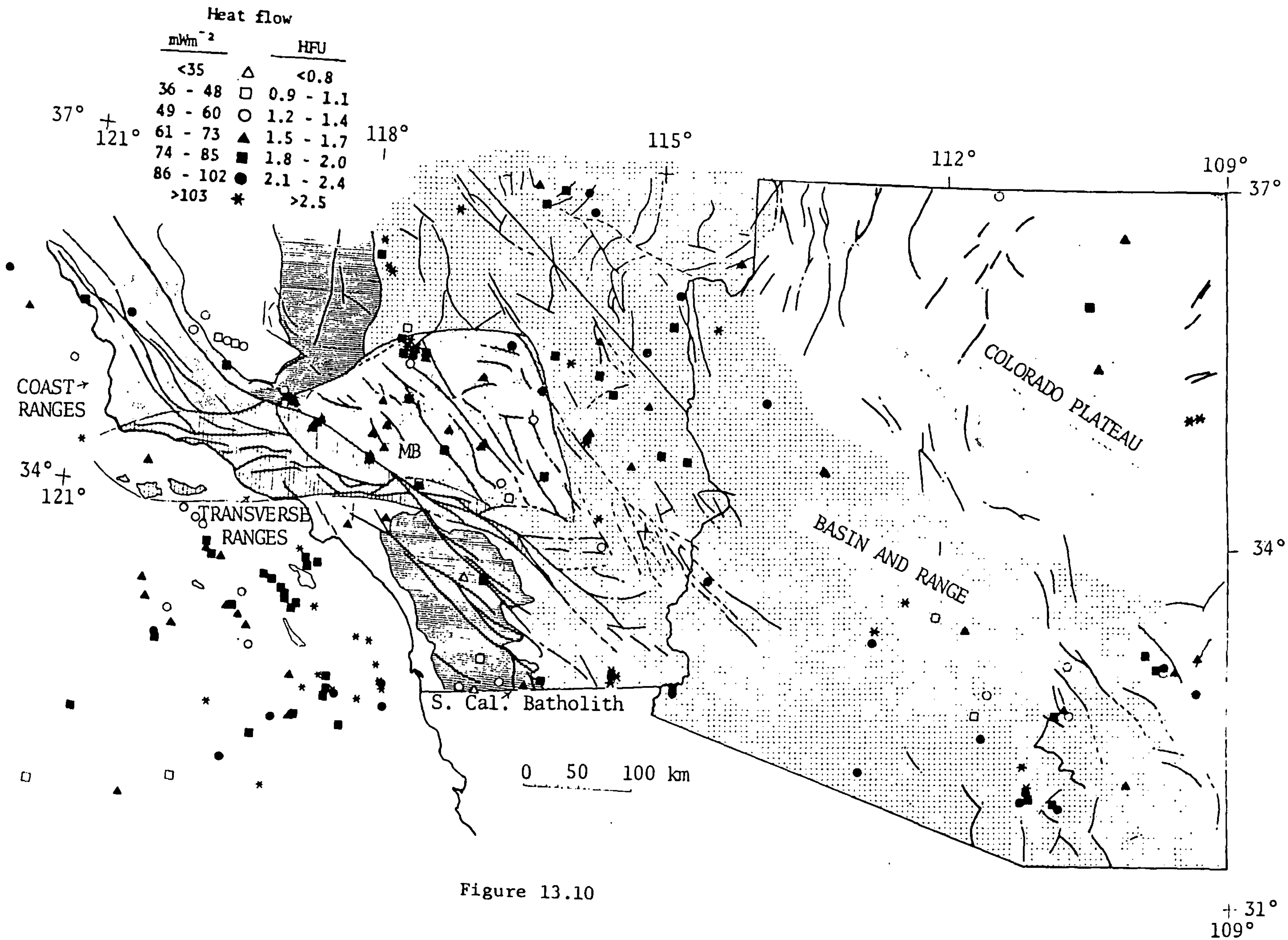
Heat flow
mWm⁻²
HFU
<35 <0.8
36 - 48 0.9 - 1.1
49 - 60 1.2 - 1.4
61 - 73 1.5 - 1.7
74 - 85 1.8 - 2.0
86 - 102 2.1 - 2.4
>103 >2.5
37°
121°
118°
115°
112°
109°
37°
COAST RANGES
34°
121°
TRANSVERSE RANGES
MB
S. Cal. Batholith
COLORADO PLATEAU
BASIN AND RANGE
34°
0 50 100 km
31°
109°

Figure 13.10

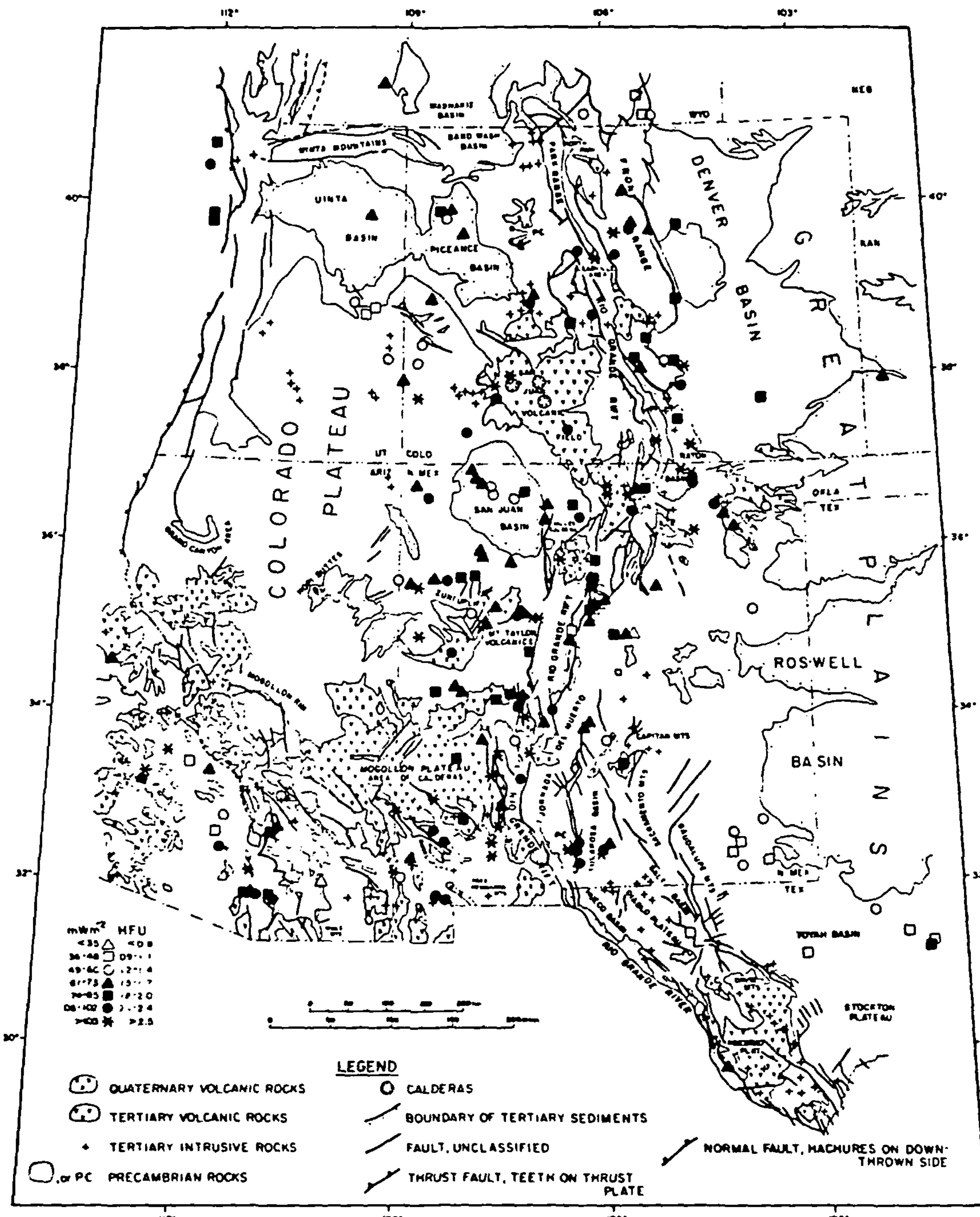
COLORADO PLATEAU
DENVER BASIN
GREAT PLAINS
ROSWELL BASIN
UINTA BASIN
PICEANCE BASIN
SAN JUAN BASIN
RIO GRANDE RIFT
MOGOLLON PLATEAU AREA OF CALDERAS
RIO GRANDE RIVER
STOCKTON PLATEAU
mWm^{-2} HFU
LEGEND
QUATERNARY VOLCANIC ROCKS
TERTIARY VOLCANIC ROCKS
TERTIARY INTRUSIVE ROCKS
,or PC PRECAMBRIAN ROCKS
CALDERAS
BOUNDARY OF TERTIARY SEDIMENTS
FAULT, UNCLASSIFIED
THRUST FAULT, TEETH ON THRUST PLATE
NORMAL FAULT, HACHURES ON DOWNTHROWN SIDE

Figure 13.11

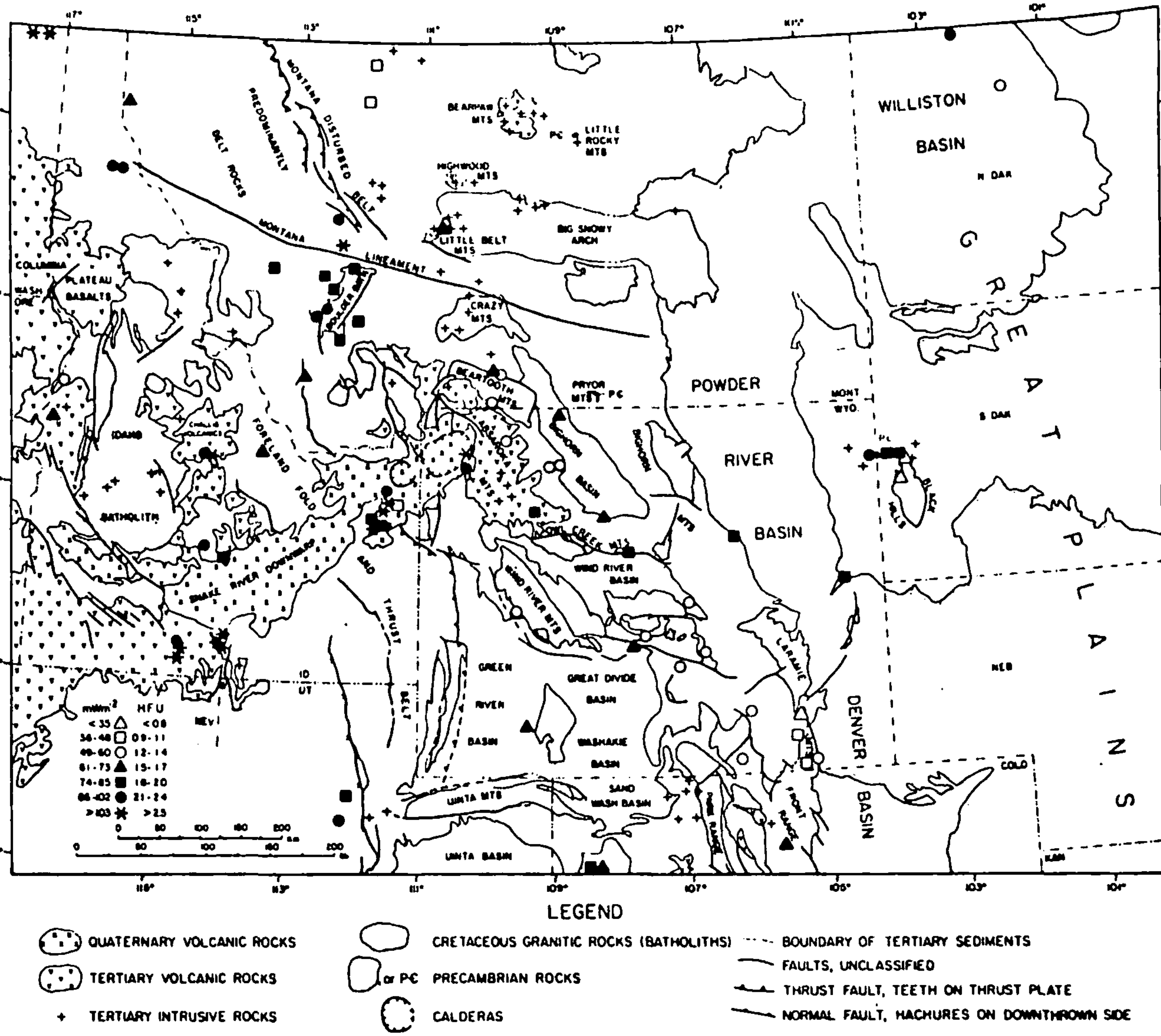
WILLISTON
BASIN
GREAT PLAINS
POWDER
RIVER
BASIN
DENVER
BASIN
MONTANA LINEAMENT
LEGEND
QUATERNARY VOLCANIC ROCKS
TERTIARY VOLCANIC ROCKS
TERTIARY INTRUSIVE ROCKS
CRETACEOUS GRANITIC ROCKS (BATHOLITHS)
or PC PRECAMBRIAN ROCKS
CALDERAS
BOUNDARY OF TERTIARY SEDIMENTS
FAULTS, UNCLASSIFIED
THRUST FAULT, TEETH ON THRUST PLATE
NORMAL FAULT, HACHURES ON DOWNTHROWN SIDE

Figure 13.12

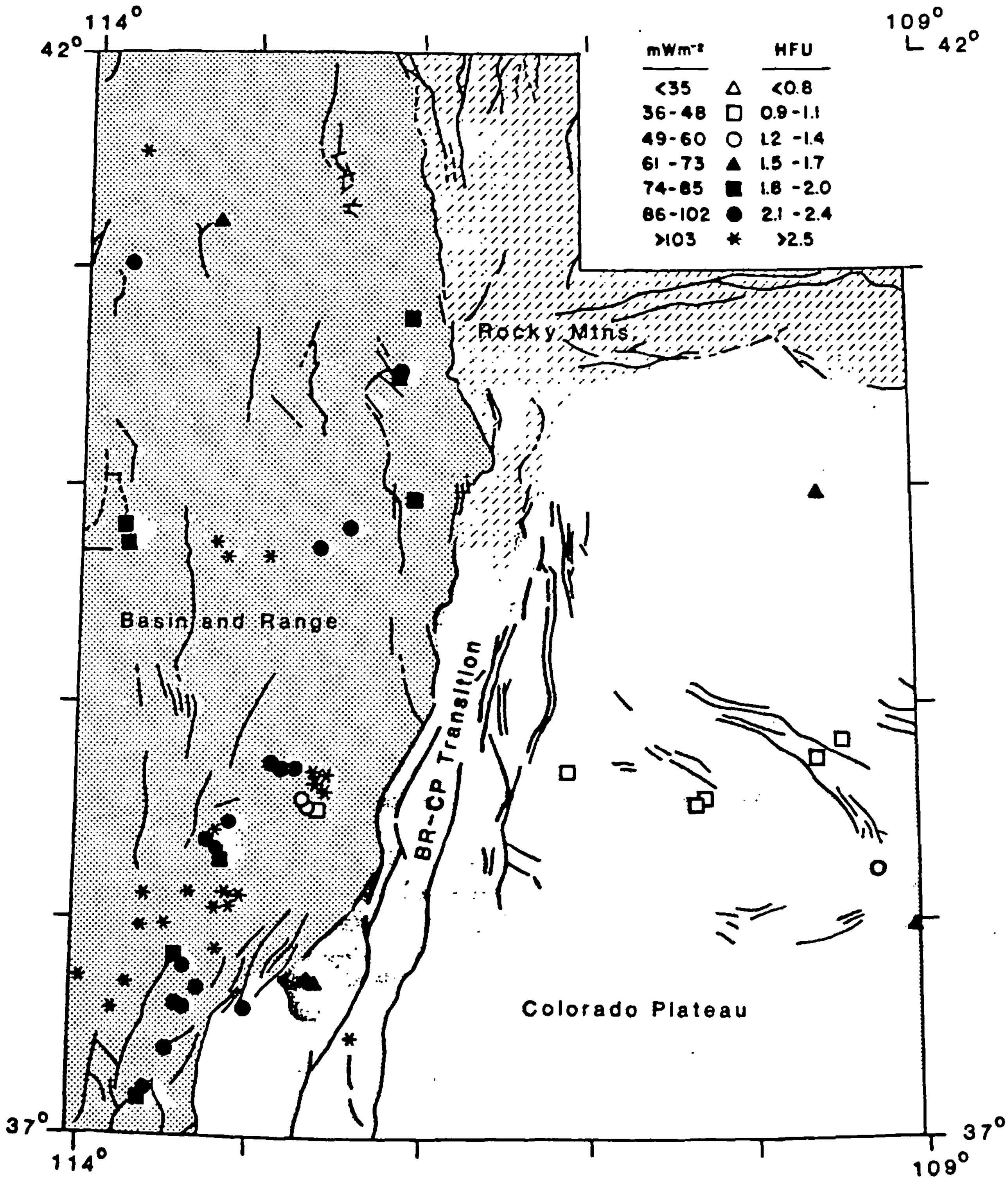

114°
42°
109°
42°
mWm⁻²
HFU
<35
<0.8
36-48
0.9-1.1
49-60
1.2 -1.4
61 -73
1.5 -1.7
74-85
1.8 -2.0
86-102
2.1 -2.4
>103
>2.5
Rocky Mtns.
Basin and Range
BR-CP Transition
Colorado Plateau
37°
114°
37°
109°

Figure 13.13

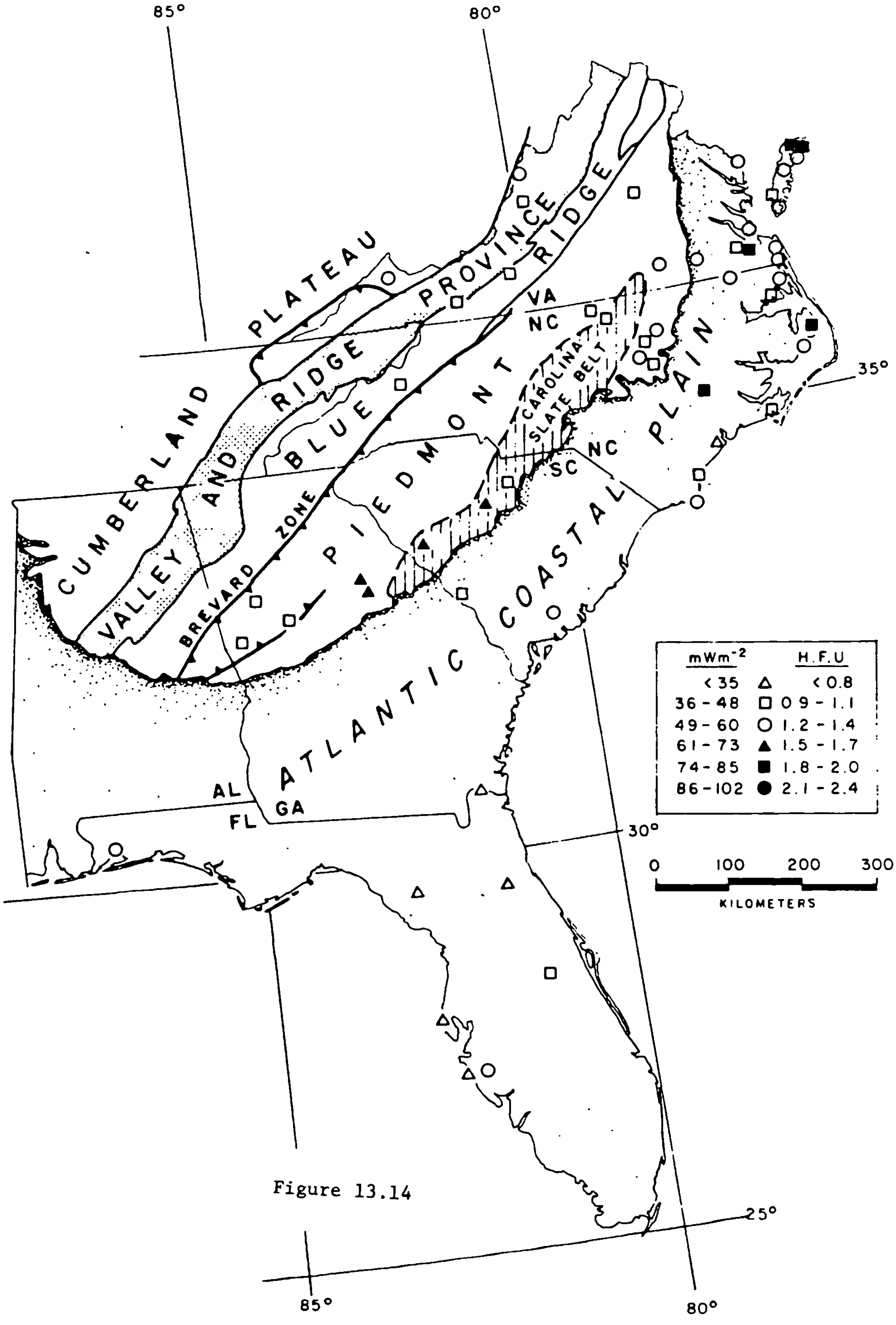
85°
80°
CUMBERLAND PLATEAU
VALLEY AND RIDGE PROVINCE
BLUE RIDGE
BREVARD ZONE
PIEDMONT
CAROLINA SLATE BELT
ATLANTIC COASTAL PLAIN
VA
NC
SC
AL
GA
FL
35°
30°
25°
mWm⁻²
H.F.U
< 35
< 0.8
36 - 48
0.9 - 1.1
49 - 60
1.2 - 1.4
61 - 73
1.5 - 1.7
74 - 85
1.8 - 2.0
86 - 102
2.1 - 2.4
0 100 200 300
KILOMETERS

Figure 13.14

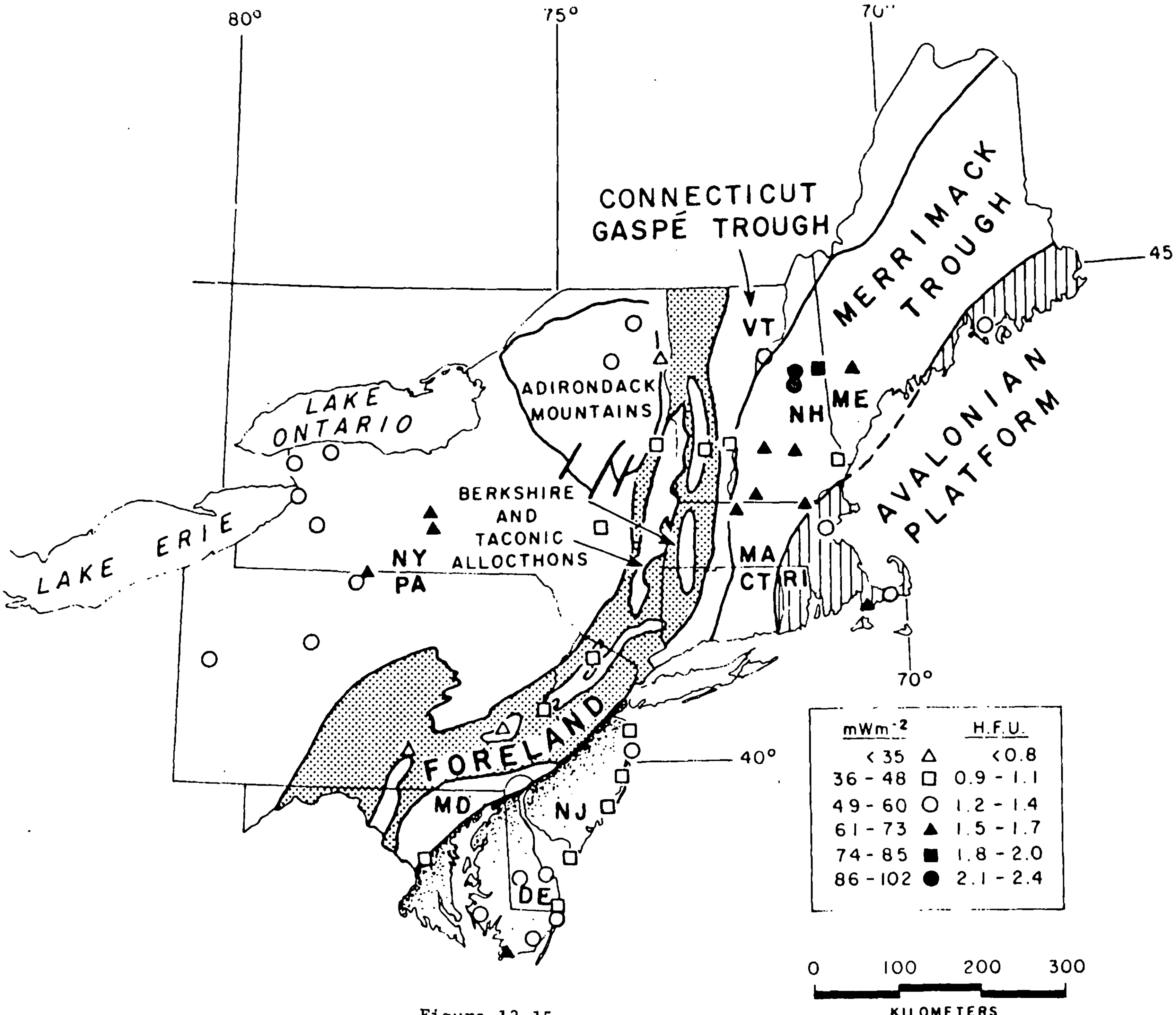

80°
75°
70°
45°
70°
40°
CONNECTICUT
GASPÉ TROUGH
MERRIMACK
TROUGH
AVALONIAN
PLATFORM
ADIRONDACK
MOUNTAINS
LAKE
ONTARIO
LAKE ERIE
BERKSHIRE
AND
TACONIC
ALLOCTHONS
FORELAND
VT
NH
ME
NY
PA
MA
CT
RI
MD
NJ
DE
mWm⁻²
H.F.U.
< 35
< 0.8
36 - 48
0.9 - 1.1
49 - 60
1.2 - 1.4
61 - 73
1.5 - 1.7
74 - 85
1.8 - 2.0
86 - 102
2.1 - 2.4
0
100
200
300
KILOMETERS

Figure 13.15

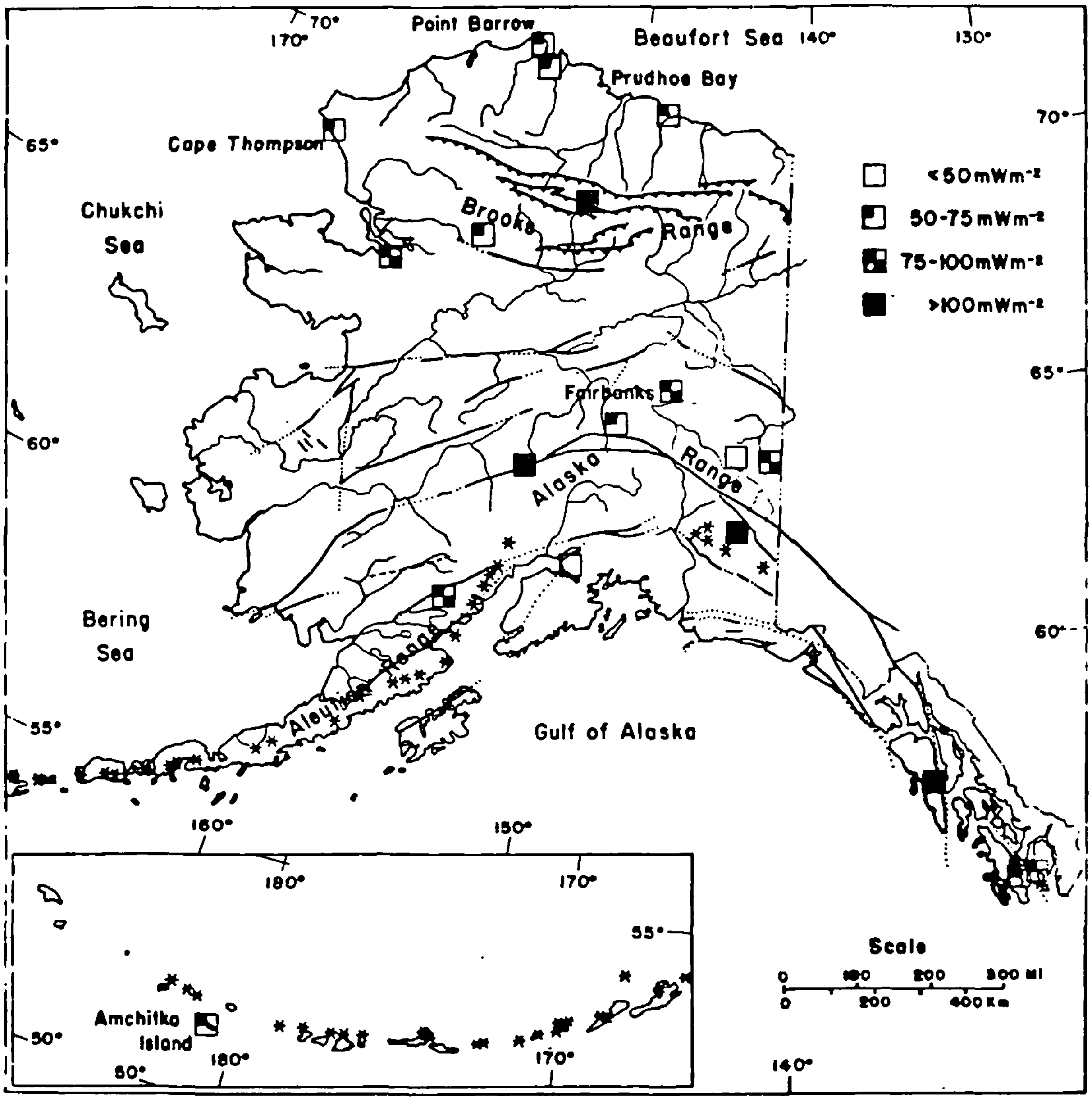

Point Barrow
Beaufort Sea
Prudhoe Bay
Cape Thompson
Chukchi Sea
Brooks Range
Fairbanks
Alaska Range
Bering Sea
Aleutian Range
Gulf of Alaska
<50mWm-2
50-75mWm-2
75-100mWm-2
>100mWm-2
Amchitka Island
Scale
0 100 200 300 MI
0 200 400 Km

Figure 13.16

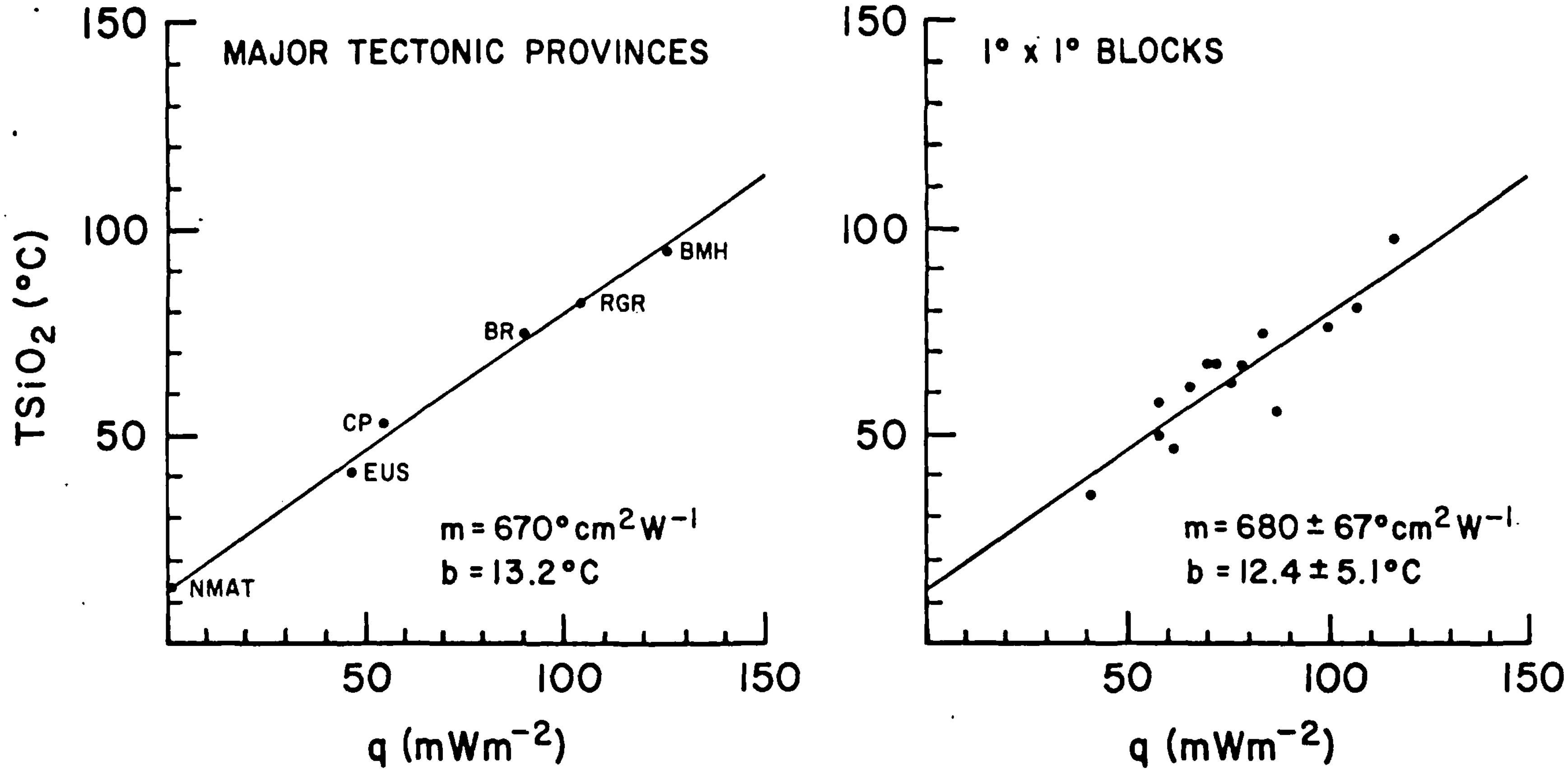

150
100
50
TSiO2 (°C)
MAJOR TECTONIC PROVINCES
BMH
RGR
BR
CP
EUS
NMAT
m = 670° cm2 W-1
b = 13.2°C
50
100
150
q (mWm-2)
150
100
50
1° x 1° BLOCKS
m = 680 ± 67° cm2 W-1
b = 12.4 ± 5.1°C
50
100
150
q (mWm-2)

Figure 13.17

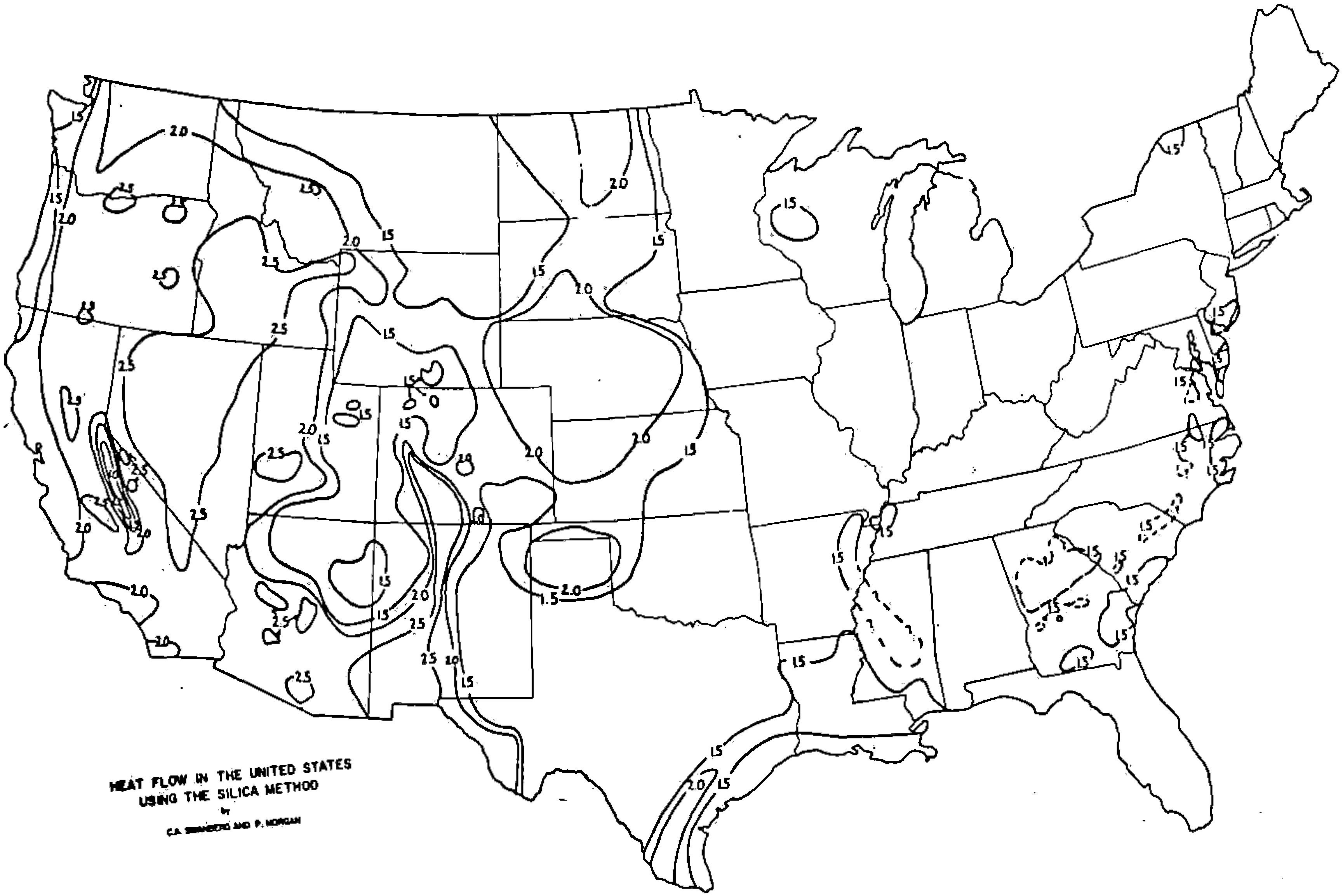

Figure 13.18

FROM, 1977, HEACOCK, JOHN G., (ed.), THE EARTH'S CRUST — ITS NATURE AND PHYSICAL PROPERTIES, AMER. GEOPHY. UNION MONOGRAPH 20, p 626-675

AREA US HF FLOW

HEAT FLOW IN THE UNITED STATES AND THE THERMAL REGIME OF THE CRUST

Arthur H. Lachenbruch and J. H. Sass

U.S. Geological Survey
Menlo Park, California 94025

Abstract. A contour map of heat flow based on 625 observations now available in the conterminous United States shows new detail. Subprovinces of exceptionally high heat flow (>2.5 HFU (1 HFU = 10^{-6} cal/cm^2 s)) in the western states are beginning to emerge as regional features, but their boundaries are still largely unknown. The 'Battle Mountain High,' previously described in north central Nevada, probably extends northeastward to Utah and Idaho and westward almost to California. With the eastern Snake River Plain, a region that probably has large convective loss, it could form a zone of exceptionally high heat loss that extends almost continuously for 1000 km from the vicinity of Steamboat Springs near Reno, Nevada, to Yellowstone Park in Wyoming and possibly northward into the Idaho batholith. A sinuous high heat flow subprovince of comparable length is emerging in the Rio Grande Trough in New Mexico and southern Colorado. The linear relation between surface heat flow and radioactive heat production, so successful in the Sierra Nevada and eastern United States provinces, does not apply in the Basin and Range province. There the variations in heat flow caused by hydrothermal and magmatic convection are probably greater by a factor of 3 or 4 than those caused by crustal radioactivity, and heat flux into the lower crust is not uniform; it is probably controlled by the mass flux of intruding magma. Regional variations in this mass flux, probably associated with crustal spreading, can account for the high heat flow subprovinces, and more local anomalies and silicic volcanic centers as well. Although convective processes cause a large dispersion of heat flow in the Basin and Range province, modal values of reduced heat flow can be used to construct generalized crustal temperature profiles for comparison with profiles for more stable areas and with melting relations for crustal rocks. Theoretical profiles are consistent with the widespread magmatic manifestations observed in the Basin and Range province. Laterally extensive silicic partial melts are possible at midcrustal levels in 'hot' subprovinces like the Battle Mountain High. Effects of hydrologic convection (whether driven by thermal density differences or regional piezometric conditions) are important to an understanding of regional heat flow, especially in tectonically active areas. The 'Eureka Low,' a conspicuous subprovince (~3 x 10^4 km^2) with anomalously low heat flow in southern Nevada, is probably caused by interbasin flow in deep aquifers fed by downward percolation of a small fraction of the annual precipitation. Heat flow observations in such areas provide useful information on regional hydrologic patterns.

Introduction

The net outward flow of heat across the earth's surface is a fundamental term in the energy balance of processes within the earth. Consequently, measurements of this quantity not only contain information about the state of the earth but also about processes associated with the generation, transport, and storage of heat within it. The number of heat flow data has increased tenfold in the last decade, and this has led to a more complete understanding of regional variation of heat flow and its causes. The observations often can be interpreted in terms of very simple, internally consistent models that give useful insights into processes of the lithosphere beneath both oceans and continents [see e.g., Birch et al., 1968; Roy et al., 1968a, b, 1972; Lachenbruch, 1970; Sclater and Francheteau, 1970]. This paper summarizes the data available on regional heat flow in the conterminous United States and discusses some of their implications for the thermal regime and processes within the crust.

A Heat Flow Map

The heat flow data available to us as of June 1976 are presented as coded symbols in Figure 1, and a contoured interpretation of them is shown as Figure 2. The heat flow unit (HFU) is 10^{-6} cal/cm^2 s (41.8 mW/m^2). For continuity, we have included in Figure 1 heat flows measured in the Pacific Ocean near the coast; however, we have made no attempt to contour them. The 625 points from the conterminous United States include published results from many laboratories and 130 or so recent determinations in preparation for formal publication by the U.S. Geological Survey (USGS) (see Diment et al. [1975] and Sass et al. [1976a] for a complete bibliography of published values). Most of the published data are supported by tabulations of thermal gradient and conductivity, but a few of the points have been taken only from published graphs or maps. The quality of the data is quite variable, as many of the determinations were made in holes drilled for purposes other than heat flow measurement; some were made in shallow holes drilled primarily for geothermal energy prospecting, and some in holes (usually in crystalline rock) drilled for scientific studies of regional heat flow. The best and the worst determinations are generally from holes drilled for other purposes; the best because such holes may be drilled to much greater depths than can be justified by limited research budgets and the worst because such holes are sometimes sited poorly for heat flow measurements and they may be sampled inadequately to characterize thermal conductivity. Few determinations have been made in holes drilled for petroleum exploration because of the difficulty of obtaining adequate conductivity samples and undisturbed temperature measurements. In prospecting for geothermal energy, large local anomalies, often in surficial sediments, are the targets, and substantial uncertainties can be tolerated. Such holes, commonly drilled to depths of about 50 m, can, however, give valuable heat flows under favorable hydrologic and topographic conditions. Even in holes drilled for regional heat flow in crystalline rock, depths greater than 250 m rarely can be justified, and uncertainties regarding the regional significance of an individual determination can be substantial.

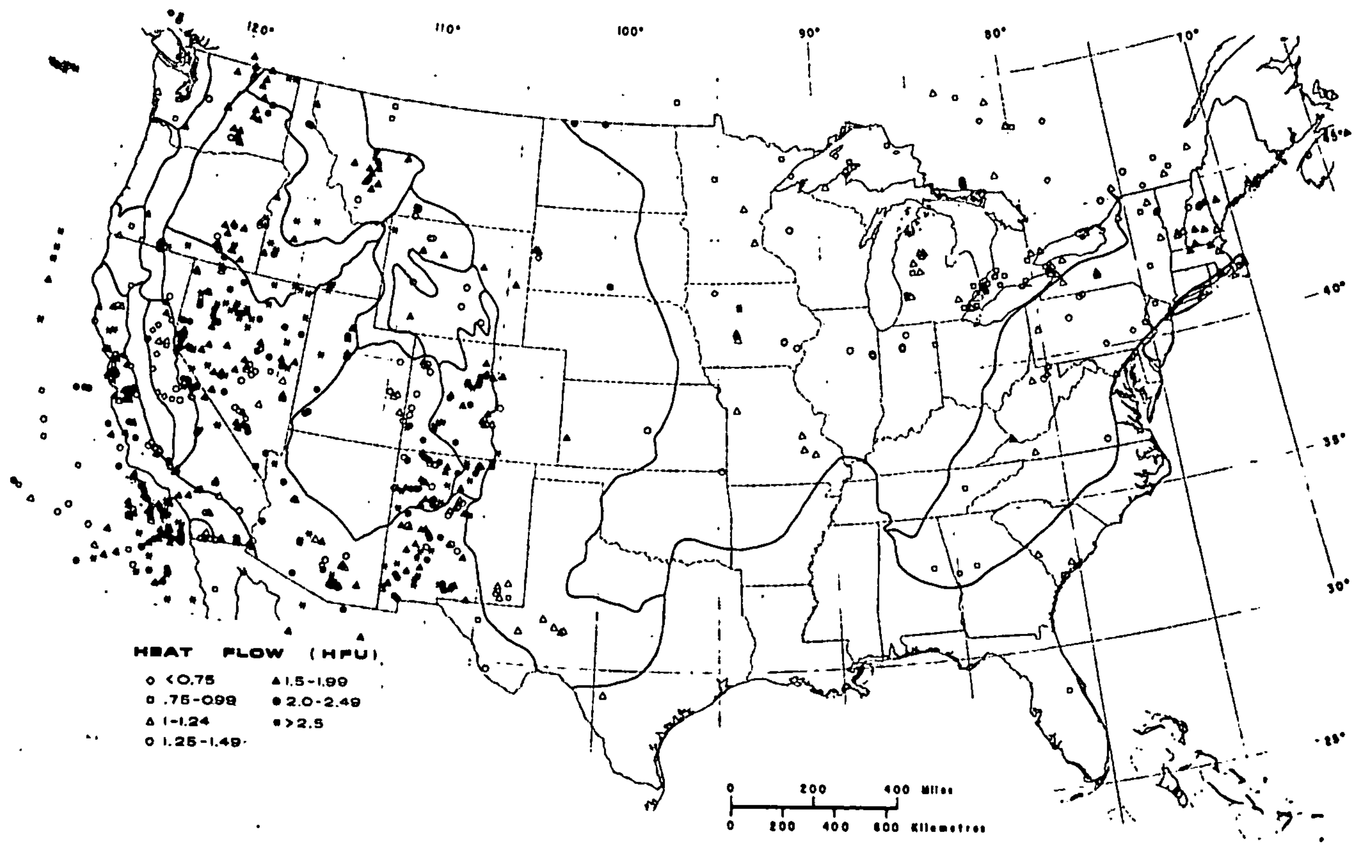

Fig. 1. Observed heat flow in the conterminous United States and some peripheral regions. Physiographic boundaries generalized from Fenneman [1946], (1 HFU = 10^{-6} cal/cm^2 s = 41.8 mW/m^2).

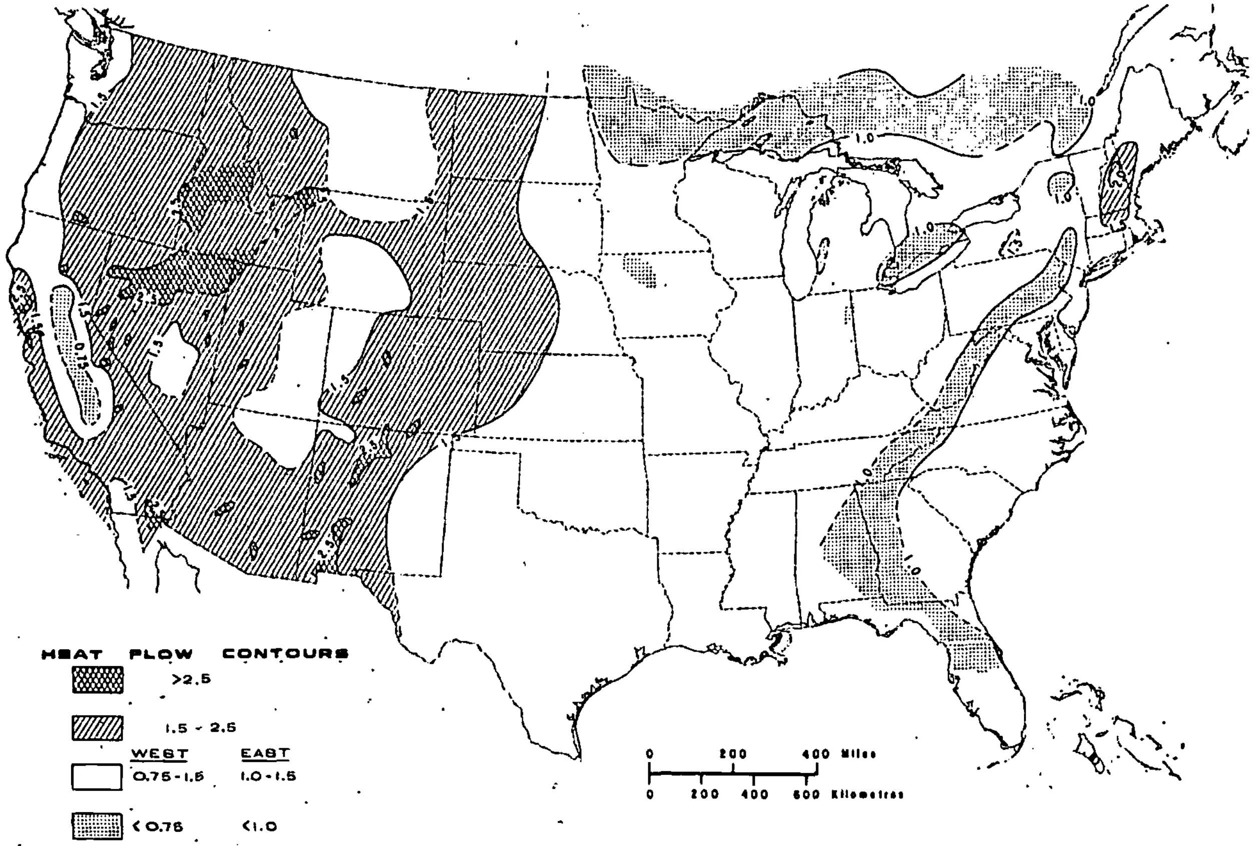

Fig. 2. A generalized heat flow contour map of the conterminous United States.

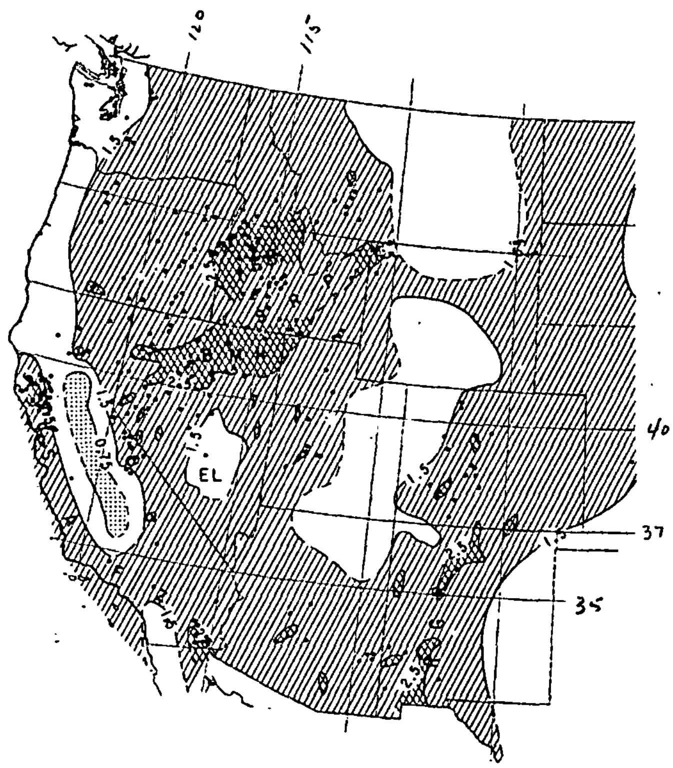

Fig. 3. Regional heat flow and distribution of hydrothermal systems. Dots show locations of hydrothermal systems in the conterminous United States with estimated reservoir temperatures greater than 90°C [Renner et al., 1975]. Abbreviations are BMH for Battle Mountain High, EL for Eureka Low, IB for Idaho batholith, SRP for eastern and central Snake River Plain, Y for Yellowstone thermal area, RGR for Rio Grande Rift, and SAFZ for San Andreas Fault zone.

In studies of regional heat flow it has been customary in the past to avoid regions of hot springs because of their local complexity. However, current interest in volcanic processes and the origin of geothermal energy resources requires that these hot spring areas be understood in relation to their regional thermal and tectonic settings. Figure 3 shows locations of the hotter known hydrothermal systems in the United States. Extending regional heat flow studies into these areas poses problems; the conductive flux at the surface can vary from zero to several hundred heat flow units over distances of a few kilometers, and substantial amounts of heat may be discharged convectively by lateral underflow in shallow aquifers into streams and lakes or at the surface by springs and fumaroles. Under these conditions there is some question about what we should define and map as 'heat flow.' In many regions we cannot feel confident, without hydrologic information, that heat transport in the upper few kilometers is exclusively conductive. However, hydrologic details are generally unknown; the heat flows selected for presentation in Figure 1 represent the upward conductive flux determined

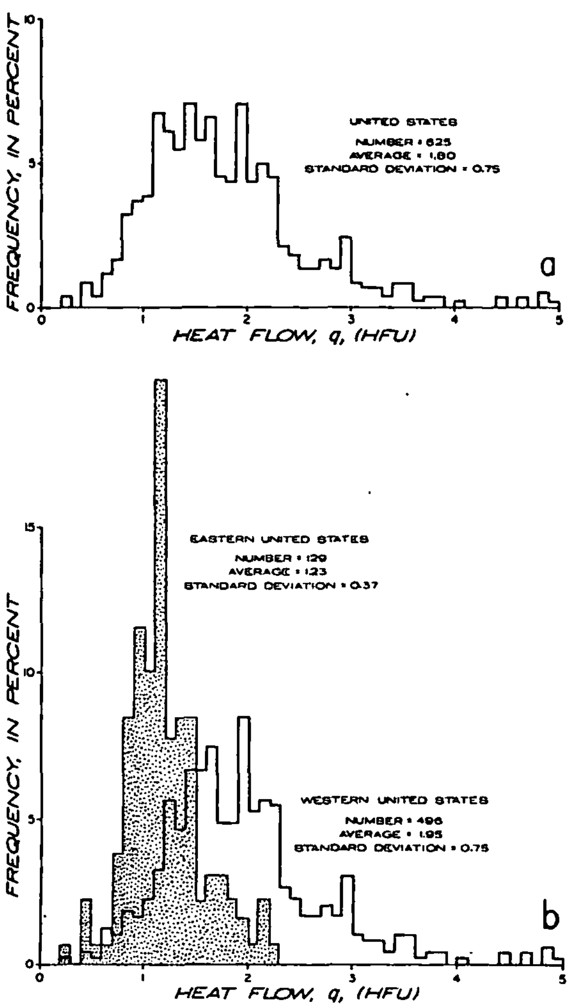

Fig. 4. Histograms of heat flow (a) for the conterminous United States as a single population and (b) for the portion east of the Great Plains (stippled) and the remainder of the conterminous United States (unstippled), treated separately. (For location of the Great Plains, see Figures 1 and 14.)

in holes (usually to depths of at least 100 m) at all sites not obviously disturbed by local water movements. Figure 2 indicates the generalized distribution of heat flow we should expect for observations under these conditions. The data are summarized in histograms in Figure 4.

The gross features shown in earlier regional heat flow maps [Roy et al., 1972; Diment et al., 1972; Blackwell, 1971; Sass et al., 1971; Diment et al., 1975] persist in Figure 2. These are a generally low-to-normal heat flow in the eastern United States (1.5 HFU is approximately the world average) and a generally high heat flow in the west, with zones of lower heat flow in the Colorado Plateau and near the Pacific Coast and very low values in the Sierra Nevada (for identification of the provinces, see Figure 14). The contours in the east are essentially unchanged from the map of Diment et al. [1972]. However, in the west, more information is now available from the work of Combs and Simmons [1973] in the Great Plains, Reiter et al. [1975] and Decker and Smithson [1975] in the Rio Grande Trough and Rocky Mountains, and by D. D. Blackwell, R. G. Bowen, and their associates [Blackwell, 1974; Bowen, 1973; Bowen et al., 1976; Brott et al., 1976] in the Pacific Northwest. Many new data from the USGS, largely in Nevada and the Pacific states, are also available [Lachenbruch and Sass, 1973; Diment et al., 1975].

In the map by Sass et al. [1971] a subprovince of exceptionally high heat flow, the 'Battle Mountain High,' was identified in the northern Great Basin, and one of normal and low heat flow, the 'Eureka Low,' was found in the southern Great Basin. The subsequent measurements tend to confirm the existence of both of these features. It now appears that the Battle Mountain High may be considerably larger than originally indicated, extending across northeastern Nevada at least to the Idaho and Utah borders. It is separated by the Snake River Plain from other regions of exceptionally high heat flow and hydrothermal activity in the Yellowstone, Wyoming, area to the northeast and the Idaho batholith to the north (Figure 3) [Blackwell, 1971; Urban and Diment, 1975; Morgan et al., 1977]. Recent volcanism and hot springs suggest that much of the Snake River Plain (particularly in the east) might have exceptionally large heat loss, although the surface heat flow is complicated by hydrologic conditions [Brott et al., 1976]. Hence a region of exceptionally high heat loss might extend northeastward almost continuously for 1000 km from the vicinity of Steamboat Springs near Reno, Nevada, to Yellowstone Park in Wyoming (see Figure 3). Another feature of the new map is the accumulating evidence for high heat flow in western California throughout a broad band that encloses the San Andreas Fault system [Lachenbruch and Sass, 1973].

The control is still poor in the western Colorado Plateau and eastern Great Basin (Figures 1 and 2); the boundaries drawn there are influenced by the distribution of hot springs and other geophysical data. Although heat flow data are accumulating in some volcanic regions such as parts of the Pacific Northwest [Bowen et al., 1976; Sass et al., 1976b; Brott et al., 1976], it is difficult to evaluate the regional significance of some of them because the rocks are often very permeable with temperatures influenced by hydrologic convection. In the Great Plains and much of the central and eastern United States the control is so poor that contours are rather arbitrarily drawn and a few new measurements could change them over large areas. Work is continuing at heat flow laboratories across the country, and better representations of the geographic distribution of heat flow are expected in the near future; good discussions of the major regional features have already been presented [Roy et al., 1972; Blackwell, 1971; Sass et al., 1971]. Therefore in this paper we shall focus on the general interpretation of heat flow within provinces that seem to have distinct regimes, rather than on the significance of the geographic distribution of the provinces themselves. In particular, we shall discuss the Sierra Nevada, the stable eastern and central United States, and the Basin and Range with its emerging subprovinces. The first represents the coldest crust in the United

States, and the Basin and Range subprovinces are probably among the hottest. Much of the discussion is general and applies to regions outside of these provinces where the heat flow is not as well known. In the San Andreas Fault zone of western California the crustal thermal regime may be unique; it has been discussed elsewhere [Lachenbruch and Sass, 1973; Brune et al., 1969; Henyey and Wasserburg, 1971].

In the next section we present some general background material as context for the discussions to follow. We hope it will make the paper more useful to readers not specialized in the study of terrestrial heat flow.

The symbols most frequently used in the text are as follows:

- Θ temperature, °C;
- t time, s;
- K thermal conductivity, cal/°C s cm;
- ρ, ρ' density of static and moving material, respectively, g/cm^3;
- c, c' heat capacity of static and moving material, respectively, cal/g °C;
- $\alpha = K/\rho c$, thermal diffusivity, cm^2/s;
- q vertical conductive heat flux, HFU (10^{-6} cal/cm^2 s);
- q^* intercept value from heat flow-heat production curve, HFU;
- q_c vertical combined heat flux (convective plus conductive), HFU;
- q_r reduced heat flow, HFU;
- A heat generation, HGU (10^{-13} cal/cm^3 s);
- A_o radioactive heat production in surface rock, HGU;
- v vertical (seepage) velocity or volume flux of water or magma, cm^3/cm^2 s;
- $s = k/\rho' c' v$, characteristic length for groundwater convection, cm;
- k permeability, cm^2;
- $\tau(z)$ conductive time constant for distance z;
- $\ell(t)$ conduction length for time t;
- D characteristic depth for radioactivity or slope of heat flow-heat production curve, km;
- Γ thermal gradient for pure conduction, °C/km;
- z depth;
- h depth of circulation in hydrothermal system;
- H depth to top of magma
- Θ_m magma temperature, °C.

Some General Considerations and Rules of Thumb

General

In discussing the geothermal regime it is useful to refer to the following general equation which relates the temperature and the processes that generate, transport, and store heat in the crust.

$$-\nabla \cdot \hat{q} \equiv \nabla \cdot (K\nabla\Theta) \tag{1a}$$

$$-\nabla \cdot \hat{q} = -A + \rho' c' \hat{v} \cdot \nabla\Theta + \rho c \frac{\partial\Theta}{\partial t} \tag{1b}$$

Here $\hat{q}$ is the conductive flux vector, Θ is the temperature, and K is the thermal conductivity. The rate of heat generation per unit volume is denoted by A; it could represent the effects of radioactive decay, frictional heating, phase change, or chemical reaction. The values ρ and c are the density and heat capacity of material at any point, and ρ' and c' are the corresponding properties for material (usually water or magma) moving with velocity $\hat{v}$. If the movement is through pores or fractures in a fixed framework, $\hat{v}$ represents the volume flux ('seepage velocity') and not particle velocity. In general, all of the parameters in (1), including $\hat{v}$, are functions of x, y, and z, and some can have significant dependence on temperature or pressure.

Although three-dimensional effects must be kept in mind, useful simple interpretations generally involve quasi-one-dimensional models in which all of the quantities in (1) vary only with depth beneath the surface z. It is customary in geophysics to define the 'heat flow' q as the upward component of conductive flux and to reverse the sign convention; i.e.,

$$q \equiv K \frac{\partial \Theta}{\partial z} \qquad (2)$$

Unless otherwise specified, q will represent the conductive heat flow near the earth's surface z = 0. It is convenient also, in the one-dimensional models, to take the upward velocity v to be positive, although it is in the direction of negative z. With these conventions, (1) for the one-dimensional case reduces to

$$\frac{\partial q}{\partial z} = -A - \rho' c' v \frac{\partial \Theta}{\partial z} + \rho c \frac{\partial \Theta}{\partial t} \qquad (3)$$

where q is the upward conductive heat flux, v is the upward volume flux of material with volumetric heat capacity $\rho'c'$, and ρc is the corresponding quantity in any stationary element.

Interpretation of regional heat flow in terms of crustal regime

Heat flow is determined from measurements of K and $\partial\Theta/\partial z$ (equation (2)) in holes typically drilled to depths of 100-300 m. Whether the value is typical of conditions in the underlying crust must be judged on the basis of internal consistency of observations within each hole and among neighboring ones. Regionally significant heat flows are expected to vary only smoothly over lateral distances much less than a crustal thickness, and as a minimum condition there should be a substantial interval in each hole throughout which the measured heat flow is redundant, i.e., over which the right side of (3) vanishes (after correction, if necessary, for laterally variable temperature and topography at the earth's surface; see, e.g., Blackwell [1973], Birch [1950] and Lachenbruch et al. [1962]). As the earth's surface is a source of temperature change ($\partial\Theta/\partial t \neq 0$) and hydrologic disturbance ($v \neq 0$) we generally have greater confidence in results from deeper holes. The internal consistency of measurements within and among holes in uniform granitic rocks at stations 30 km apart in the Sierra Nevada (Figure 5) provides some confidence that a regional condition is being measured there. By contrast, determination of the heat discharge and its regional significance in hydrothermal areas such as Long Valley, California (Figure 6) poses special problems.

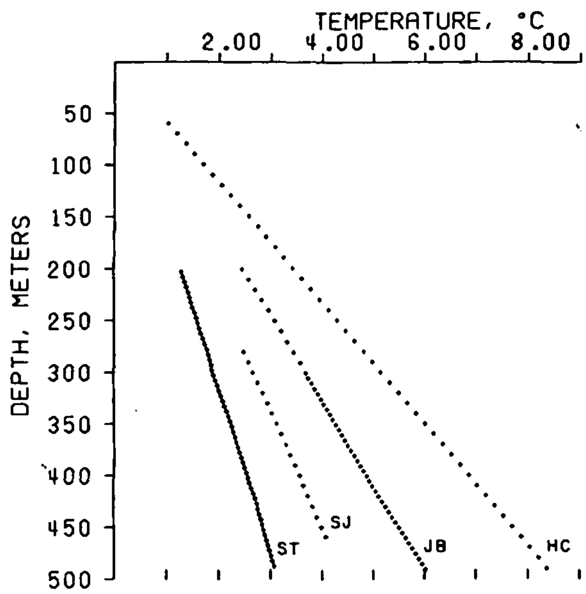

Fig. 5. Temperature measurements in granitic rocks of the Sierra Nevada province adjusted to a common temperature origin at the surface. Stations are about 30 km apart on a line from the western margin (ST) to the range crest (HC) [Lachenbruch, 1968].

The heat flow, normally measured in the upper 1% of the crust, provides only a boundary condition from which we should like to determine the thermal regime of the crust, i.e., to determine q(z) throughout the entire crust. This requires a knowledge of how the terms on the right side of (3) vary throughout the crust. To provide meaningful constraints on these terms we must obtain insight into the physical processes that they represent. Interpretations of the crustal regime generally represent attempts to integrate (3) with simplifications believed to be appropriate for specific regions.

In our discussion, A will represent heat generated by radioactive decay of U, Th, and ^{40}K, elements present in minute amounts in crustal rocks. The process goes on steadily, irrespective of what else might be happening in the earth. The second term on the right in (3) represents effects of relative vertical movement of crustal (and upper mantle) masses; they may be solid blocks moving along faults or magmatic and aqueous fluids generally moving through fractures created by faulting or through pore spaces. As these movements are generally intermittent or short-lived, they generate transient disturbances represented by the last term in (3). Surface indicators of these mass movements are earthquakes, young volcanic rocks, and hot springs, which are shown with the heat flow distribution in Figures 3, 7, and 8. These manifestations are generally concentrated in the western regions of anomalously high heat flow, suggesting that the anomalies there are due primarily to convection and associated transients (i.e., to effects of the last two terms in (3)). The manifestations are rare in regions of low heat flow in the Sierra Nevada and the eastern half of the United States, and the crustal

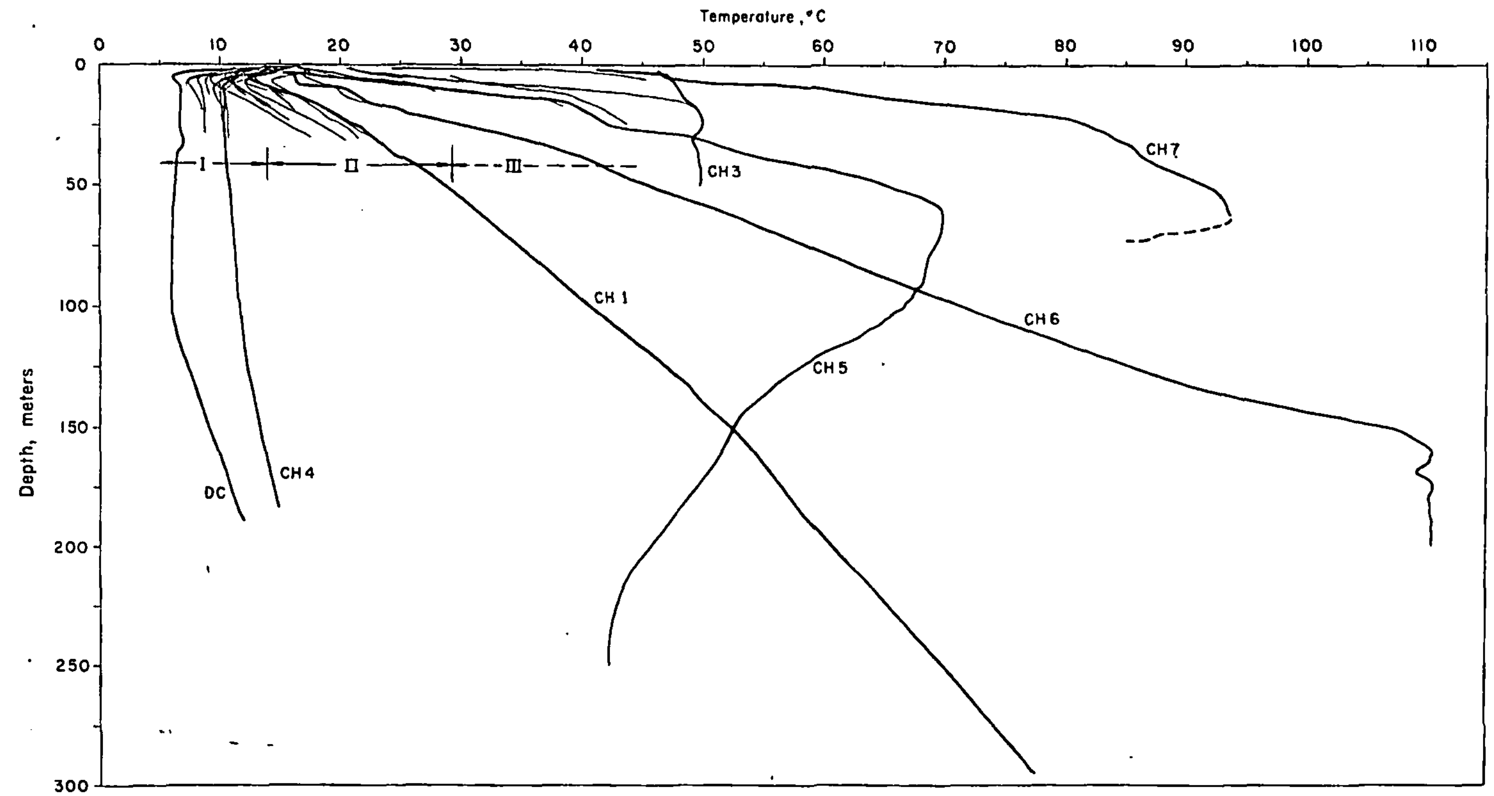

Fig. 6. Temperature measurements in the Long Valley caldera in California, a region with dimensions of about 20 km x 30 km [Lachenbruch et al., 1976b].

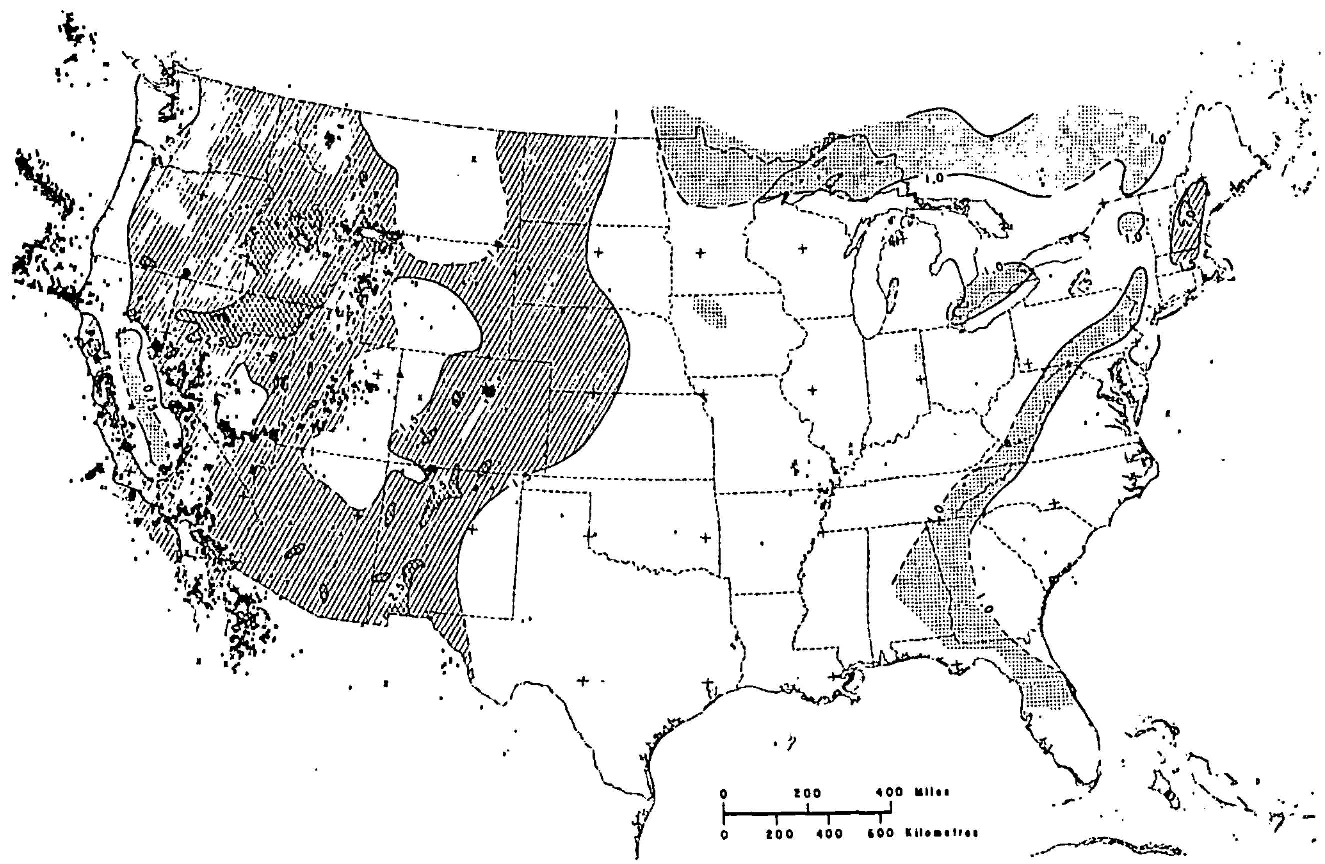

Fig. 7. Regional heat flow and distribution of seismic epicenters for the period 1961-1970. Dots represent earthquakes of magnitude about 3 to 5, crosses greater than 5. National Oceanographic and Atmospheric Administration epicenters have been replotted by J. C. Lahr and P. R. Stevenson of the USGS (personal communication, 1976).

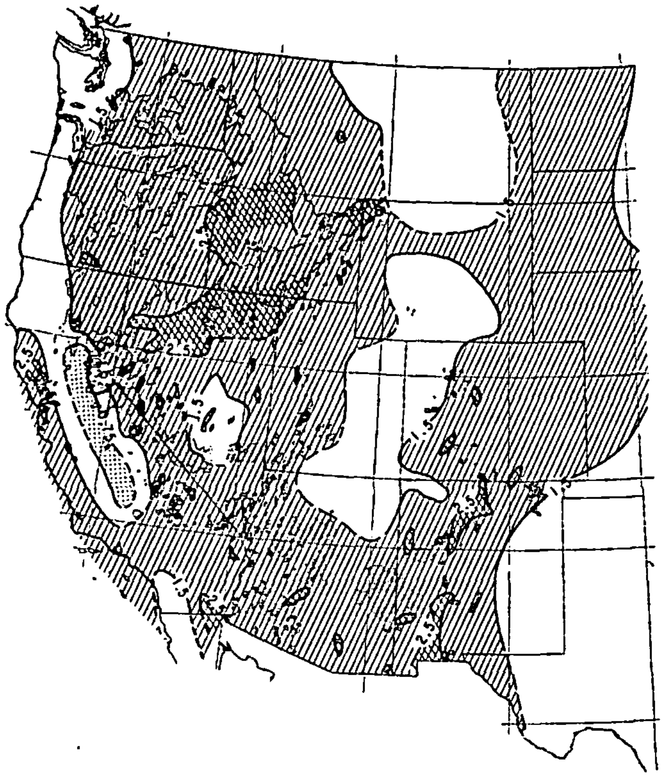

Fig. 8. Regional heat flow and the distribution of volcanic rocks erupted in the last 17 m.y. in the conterminous United States. Distribution of volcanic rocks adapted from Plate II of Stewart and Carlson [1977].

regime in these regions seems to be dominated by radioactivity (first term on the right in (3)).

Heat production and conductive transients

To estimate the relative importance of the terms in (3) we consider the contribution Δq to the surface heat flow that each term might make in a layer of thickness $\Delta z = z_2 - z_1$:

$$\Delta q = \int_{z_2}^{z_1} \frac{\partial q}{\partial z}\, dz \tag{4a}$$

$$\Delta q = A\Delta z + \rho' c' v \Delta\theta - \rho c \frac{\partial \theta}{\partial t} \Delta z \tag{4b}$$

where the parameters in (4b) are taken as appropriate average values and $\Delta\theta$ is the temperature difference across the layer.

If Δz represents a 30-km crust, then the contribution of the first term on the right can be written in dimensional form as follows:

$$\Delta q \text{ (HFU)} = 0.3A \text{ (HGU)} \tag{5}$$

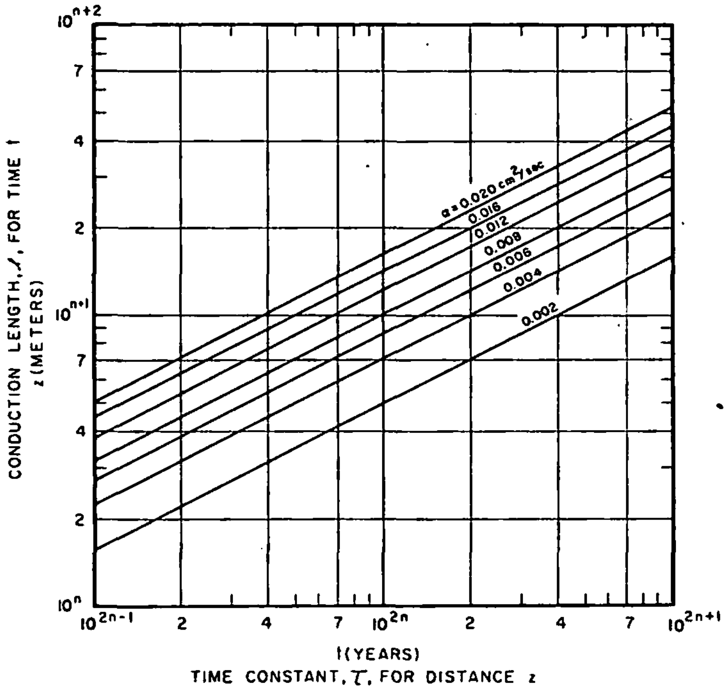

Fig. 9 Relation between conduction length ℓ and time t, or between time constant τ and distance z, for the range of thermal diffusivities (α) of natural earth materials. The scale parameter n may be assigned any convenient value. (For example, if α = 0.008 cm^2/s and t = 1 m.y., set n = 3 to obtain ℓ = 10 km. Conversely, given z = 10 km, then τ = 1 m.y.).

Radioactive decay results in generation of heat at the rate of 1-10 HGU in most crustal rocks exposed at the surface. According to (5), if such rocks were distributed throughout the crust, they could account for much or all of the observed surface heat flow. Hence the distribution A(z) is important to an understanding of the crustal regime, and it has been the subject of considerable study.

Skipping to the last term in (4b), we set ρc = 0.6 cal/cm^3 °C and Δz = 30 km to represent the crust. The contribution of temperature change can be written

$$\Delta q \text{ (HFU)} \sim -0.6 \times 10^5 \times \frac{\partial \Theta}{\partial t} \text{ (°C/yr)} \qquad (6)$$

Thus cooling of the entire crust at rates $\sim 10^{-5}$ °C/yr could contribute significantly to measured heat flow; a total of 20°C or 30°C of crustal cooling could account for heat flow at the observed rates for a million years with no other contributions. However, the rate at which the crust can cool is controlled by the mode of heat transfer within it. Hypothetical circulatory convection systems can be contrived to remove heat from the crust at almost any desired rate, but if the heat transfer is by conduction, the rate at which heat may be discharged or stored is severely constrained by the low conductivity and substantial volumetric heat capacity of crustal materials. These constraints can be discussed in terms of simple limiting heat conduction models that can be reduced to convenient rules of thumb for the purpose of general discussion.

The solutions to many simple conduction problems can be expressed in terms of the single dimensionless ratio $z/\sqrt{4\alpha t}$. Normally, t is the time since some sort of disturbance occurred, z is a distance, usually from the source of disturbance, and α represents thermal diffusivity ($k/\rho c$). We define a characteristic 'conduction length' ℓ and a characteristic 'conduction time constant' τ as follows:

$$\ell(t) \equiv \sqrt{4\alpha t} \qquad (7a)$$

$$\tau(z) \equiv z^2/4\alpha \qquad (7b)$$

Hence

$$\frac{z^2}{4\alpha t} \equiv \left(\frac{z}{\ell(t)}\right)^2 = \frac{\tau(z)}{t} \qquad (7c)$$

and the approach to steady conditions can be expressed in terms of how large t is in relation to τ or how large ℓ is in relation to z, depending on which variables are known. For convenient reference the conduction length ℓ can be found for any t, and the time constant τ can be found for any z for the range of diffusivities for natural earth materials in Figure 9. A reasonable average diffusivity for the entire crust may be around 0.01 cm^2/s.

Some convenient rules of thumb relevant to the measurement of heat flow or the interpretations to be presented are as follows:

1. A periodic temperature change with amplitude B and period P will have a negligible effect (a few percent of B) at depth $\ell(P)$. Thus diurnal fluctuations ($P \sim 3 \times 10^{-3}$ years) are negligible in sediments ($\alpha \sim 0.002$-0.008 cm^2/s) at depths of 30-50 cm (Figure 9, n = -1). The annual wave (Figure 9, P = 1 year, n = 0) penetrates about 5-10 m in poorly conducting sediments and 15 m in crystalline rock ($\alpha = 0.014$ cm^2/s). The temperature pulsations due to repeated intrusion of a deep crustal layer with a period of 10^5 years would be negligible a few kilometers above (and below) the layer (Figure 9, n = 3). The process would therefore have the same effect at the surface as a continuous intrusion with a uniform (time averaged) temperature.

2. A rapid change in surface temperature at time t = 0 in the amount B perturbs the gradient at the surface by about $B/\ell(t)$, and its effect on temperature may be appreciable ($\sim$15% of B) to depth ℓ but is completely negligible (<1% of B) beneath 2ℓ. Thus a 5°C post-Pleistocene warming 10,000 years ago (Figure 9, n = 2) could disturb the surface gradient of the order of 5°C/km in crystalline rocks; temperature effects would be appreciable in holes to several hundred meters. The gradient disturbance would be greater in sediments, but because of the role of thermal conductivity the effect on heat flow would be less. Temperatures below an intruded layer maintained at constant temperature can be treated by these rules.

3. A rapid change in temperature at depth z will not be detectable in surface heat flow until times approaching $1/2\ \tau(z)$, and the surface heat flow will be almost completely adjusted to the change for times exceeding $\tau(z)$. Thus a rapid (step) temperature change due to intrusion

at the base of a 30-km crust ($\alpha \sim 0.01$ cm^2/s) will not affect surface heat flow for about 3 or 4 m.y., but the entire crust will have equilibrated to the change in 8 m.y. or so (Figure 9, $n = 3$).

4. Heating (or cooling) by a constant heat source (or sink) at a depth z from time $t = 0$ will not affect heat flow at the surface until times approaching $\tau(z)$. The surface heat flow will not approach its steady value until $t \gtrsim 100\tau(z)$, but for $t > 3\tau(z)$ temperatures in the layer above depth z can be estimated (within about 10%) by assuming that conditions observed at the surface are steady, i.e., by assuming that heat flow is independent of depth in the layer. The constant source approximates long-term slow intrusion of a sill in which the melt does not survive between intrusive pulses or the thermal recovery of a layer of thickness z after extinction of a hydrothermal system within it. The constant sink approximates effects of a cooling sill after solidification [see Lachenbruch et al., 1976a].

Convection--general considerations

An understanding of regional heat flow in tectonically active areas requires at least a gross understanding of convective processes in the crust. We distinguish between two main types: convection by magma and convection by groundwater. The large-scale effect of magmatic convection on surface heat flow is caused by the upward transport of fluid at temperatures greater than ambient; it always results in a positive contribution to heat flow. The lateral extent of the positive anomaly will be comparable to that of the region intruded. In the steady state the intensity of the anomaly can be determined in terms of the rate (volume flux) of intrusion v from the second term on the right in (3), making allowance in the factor c' for the heat of crystallization. For present purposes, transient effects of convection by magma can be discussed adequately in terms of the rules of thumb presented in the last paragraph.

Groundwater convection is a more difficult problem; it generally involves some flows that are hotter than ambient and others that are colder, and it is mainly confined to the upper crust, close to the surface where heat flow is measured. With the search for geothermal energy it is becoming more important to understand groundwater convection in a regional context. As this process has generally been treated lightly in discussions of regional heat flow, we shall consider it here in somewhat more detail than the processes just discussed.

The magnitude of hydrothermal effects can be estimated by retaining only the second term on the right in (4b). The volumetric specific heat $\rho'c'$ for hot and cold water (and for melted rock as well) is generally from 0.7 to 1 cal/cm^3 °C. Taking the latter value leads to the following dimensional relation for vertical one-dimensional steady convection

$$\Delta q \text{ (HFU)} = 10^6 v \text{ (cm/s)} \, \Delta\Theta \text{ (°C)} \tag{8a}$$

$$\Delta q \text{ (HFU)} \sim v \text{ (ft/yr)} \, \Delta\Theta \text{ (°C)} \tag{8b}$$

Equation (8b) is a useful rule of thumb. Seepage velocities of 1 ft/yr (0.3 m/yr) would result from Darcian flow under unit hydraulic gradient in a medium with a permeability of only 1 mdarcy (10^{-11} cm^2); they are not uncommon in hydrothermal areas. Such a flow rising across a layer with 10°C temperature difference would contribute 10 HFU to the surface flux.

A second useful relation for steady vertical flow is obtained by neglecting the first and third terms on the right in (3) and writing it in the form

$$\frac{\partial q}{\partial z} = -\frac{\rho' c'}{K} vq \qquad (9)$$

Integration yields

$$q(z_1)/q(z_2) = e^{\Delta z/s} \qquad (10)$$

where s is a characteristic distance with the sign of v.

$$s = K/\rho' c' v \qquad (11a)$$

It is most easily expressed as a rule of thumb in terms of feet.

$$s \text{ (feet)} \sim \frac{100}{v \text{ (ft/yr)}} \text{ for 'sediment' } (K = 3 \text{ mcal/cm s °C}) \qquad (11b)$$

$$s \text{ (feet)} \sim \frac{200}{v \text{ (ft/yr)}} \text{ for 'rock' } (K = 6 \text{ mcal/cm s °C}) \qquad (11c)$$

According to (10) and (11b), steady vertical flow at 1 ft/yr through a 500-foot layer (Δz) would increase the gradient and conductive heat flow in the direction of water flow by the factor $e^5 \sim 150$. This can lead to very large (and short-lived) local fluxes and large temperature differences (equation (8)) unless the gradient on the inflow side is very small. Hence the flow will generally cause most of the layer to be nearly isothermal if $\Delta z >> |s|$. Thus for downward flows (s negative) of 1 ft/yr the gradient near the surface and the measured heat flow will generally vanish if the layer is only a few hundred feet thick. Similarly, the surface heat flow will be 'washed out' by downward percolation of only 1 in./yr (a small fraction of annual precipitation) through a few thousand feet of porous rocks. This effect obviates the determination of regional heat flow by conventional means over large areas. Some such areas, mantled by permeable volcanic rocks, are of considerable interest as potential sources of geothermal energy.

Temperature in the layer of thickness Δz (equation (10)) is determined by specifying at least one of the boundary temperatures and the other boundary temperature or one of the boundary heat flows $q(z_1)$ or $q(z_2)$. To be consistent, any physical model must also conserve mass of the flowing water. A useful consistent solution for coupled heat and water flow is obtained by identifying $\Theta(z_1)$ with the mean ground surface temperature and $q(z_2)$ with the regional heat flow. In this case, water flows horizontally along z_2 with no change in temperature, providing a source (or sink) for the vertical mass flow to (or from) the surface. The model yields a useful rule of thumb; viz., whether the surface heat flow ($q(z_1)$) is significantly different from the regional heat flow ($q(z_2)$) depends upon whether the depth of vertical water flow Δz is small or large in relation to $|s|$ (equation (10)). A second application of (10) [Bredehoeft and Papadopulos, 1965] assigns both boundary temperatures $\Theta(z_1)$ and $\Theta(z_2)$. However, unless the assigned temperature $\Theta(z_2)$ is the value determined by uniform flux from below, $q(z_2)$, the water flowing horizontally along z_2 must be a source of heat as well as mass, its temperature must change horizontally, and the one-dimensional model is only approximate. It is useful to note, however, that from a transient solution for this case [Nathenson, 1977] it can be shown that the stationary condition described by (10) is generally approached after one conductive time constant ($\tau(\Delta z)$) for slow water flow between depths held at constant temperature and sooner if the vertical water flow is vigorous ($|s| << \Delta z$).

Equations (8), (10), and (11) give an indication of the enormous effects that hydrologic conditions can have on measured heat flow (see, e.g., Figure 6). In natural systems these effects can be extremely complex, involving variable upward and downward flows (with temperature and pressure dependent properties) in fractures and pore spaces [see, e.g., Sorey, 1975]. These systems may be in delicate balance, vulnerable to the effects of earthquakes or the drilling of wells. The pattern assumed by these flows depends upon the conditions that drive them. There are two distinct cases: (1) the flow is forced by the configuration of fractures and permeable formations and by regional piezometric conditions controlled by precipitation, evaporation, and topography, or (2) the flow results from the instability of groundwater heated from below in a permeable layer. (In general, elements of both driving mechanisms are present.) The second case tends to produce circulating cells with an aspect ratio close to unity [e.g., Sorey, 1975]; it should result in heat flow anomalies that change in sign over lateral distances of the order of the depth of circulation. No such condition applies to the first case, which in extreme circumstances could produce persistent anomalies in surface heat flow on a regional scale (e.g., possibly, the Eureka Low, to be discussed). The foregoing results can be applied to order of magnitude calculations for the first case. We shall now consider the second case, which we shall refer to as hydrothermal systems.

Hydrothermal systems

These systems are initiated when the Rayleigh number R exceeds a critical value [e.g., Lapwood, 1948]. Other things being equal, R increases linearly with the depth of the permeable zone, the permeability of the zone, and the temperature difference across it; increasing any of these could initiate a hydrothermal convection system. To investigate gross relations between these systems and the regional heat flow or magmatism that supplies their heat, we shall discuss some highly idealized quasi-one-dimensional models.

Consider a region near the earth's surface (Figure 10a, $z = 0$) in which the heat transfer is initially conductive and the temperature profile is linear with gradient Γ (Figure 10b, curve I). The heat flow q is then $K\Gamma$. Suppose that in a region of high heat flow at time $t = 0$, fractures open in a layer extending from the earth's surface to depth h and that this increases the permeability so much that the groundwater becomes unstable and starts to circulate. Above regions where the water is moving downward the surface heat flow will diminish, and above regions where it is moving upward the surface heat flow will increase.

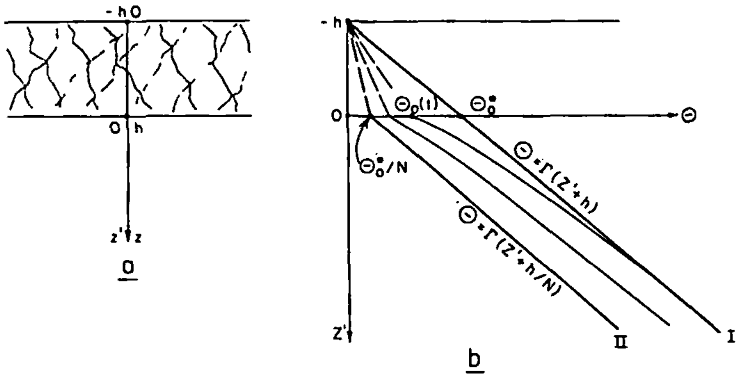

Fig. 10. Idealized one-dimensional model for hydrothermal convection in a surficial layer of thickness h; the heat is supplied by steady regional heat flow (see text).

However, the total heat transport across the layer (integrated over the surface above the fractured region) must increase, as the initial conductive transport is now supplemented by convective transport. For simple one-dimensional order of magnitude calculations we assume that the net effect of convection is to increase the mean heat flux through the layer ($z < h$) by the factor $N > 1$ (e.g., for the layer with uniform vertical flow, upward over half the area and downward over the other half, (10) yields $N = [\exp(h/|s|) + \exp(-h/|s|)]/2$. When the system is in a stationary state and the lower and upper boundaries are held at constant temperatures, N would represent the Nusselt number; in real systems, neither surface would be at uniform temperature. We let $\Theta_o(t)$ be the average temperature at $z = h$ at time t and assume that it is uniform. The surface temperature is assumed to be uniform at the average ambient value taken as zero. This condition would be violated locally by hot springs, the convective discharge of which is included in the factor N. We neglect the change of N that would occur as the system evolves. (A useful discussion of the relation between heat flow and coupled heat and water flow in porous layers has been given by Donaldson [1962] and in isolated fractures by Lowell [1975] and Bodvarsson [1969].)

In this model the mean upward flux *from* $x = h$ will (initially) *exceed* the mean flux into $x = h$ by the factor N. After time t the basal temperature will drop from Θ_o^* to some value $\Theta_o(t)$, and the heat flux through the convecting layer will drop to $NK\Theta_o/h$. The convecting system will continue to mine heat from the earth until the flux through it is equal to the regional conductive flux $K\Gamma$ supplied from below, i.e., equilibrium will be established when

$$NK\Theta_o/h = K\Gamma \equiv K\Theta_o^*/h \qquad (12a)$$

or

$$\Theta_o = (\Theta_o^*/N) \qquad t \to \infty \qquad (12b)$$

To estimate the time required for stabilization, we first neglect the heat capacity of the convecting layer $z < h$ and consider the underlying region $z > h$, which we denote by $z' > 0$ (Figure 10); heat loss from the surface $z' = 0$ is proportional to the temperature $\Theta_o(t)$. The differential equation and conditions are

$$\frac{\partial^2\Theta}{\partial z'^2} = \frac{1}{\alpha}\frac{\partial\Theta}{\partial t} \qquad z' \geq 0 \tag{13a}$$

$$\Theta = \Theta_o^* + \Gamma z' \qquad t = 0 \qquad z' \geq 0 \tag{13b}$$

$$\frac{\partial\Theta}{\partial z'} = \frac{N}{h}\,\Theta_o(t) \qquad z' = 0 \tag{13c}$$

The solution (modified from Carslaw and Jaeger [1959, p. 71]) for temperature Θ_o at the base of the slab is

$$\Theta_o(t) = \Theta_o^* - \Theta_o^*(1 - 1/N)\,[1 - e^{-\beta^2}\,\mathrm{erfc}\,\beta] \tag{14}$$

where $\beta^2 = (N^2\alpha/h^2)t$. Hence $\Theta_o(t)$ approaches its equilibrium value Θ_o^*/N after a time

$$t \sim h^2/N^2\alpha \tag{15}$$

which can be read from Figure 9. For $N = 2$ it is the same as the conductive time constant for the slab of thickness h, and for $N = 6$ it is an order of magnitude less.

The sensible heat lost by the slab as its base cools from Θ_o^* to $(1/N)\Theta_o^*$ (neglected in the above calculation) is roughly $\Theta_o^*(1 - 1/N)h\rho c/2$. This heat could sustain the mean anomalous flux of $NK(\Theta_o^*/h)\ (1 - 1/N)/2$ for a time

$$t \sim h^2/N\alpha \tag{16}$$

The actual time for stabilization of the slab depends upon the complex behavior of coupled temperature and velocity fields; it will generally result in changing N and perhaps in an increase in h, if thermal contraction results in deepening fractures. However, for larger N (say, >2) likely to be of interest we judge from the above that processes internal to the slab (16), not those beneath it (15), will be controlling and that a steady state is likely to be approached in times of the order of $\tau(h)$ (Figure 9) or less. For larger times the surface flux would still have extreme local variations, but perturbations would integrate to zero, and the average combined flux would equal the regional heat flow q. Stabilization times vary from 1,000 years for $h \sim 400$ m to 100,000 years for $h \sim 4$ km (Figure 9). More active systems (large N) probably stabilize more quickly. (For a layer in which circulation is confined to fractures separated by distance λ, the stabilization time will probably be controlled by $\tau(\lambda)$ if $\lambda > h$ [see, e.g., Bodvarsson and Lowell, 1972; Carslaw and Jaeger, 1959, Figure 12].)

Restoration of the steady regional heat flux at the surface after extinction of a hydrothermal system is a very slow process (governed by the conduction rule of thumb, number 4 above). It can be viewed crudely as the conductive return of curve II, now the initial condition, to curve I, the final condition (Figure 10b). The heat flow anomaly Δq at the surface can be shown to be

$$\Delta q = -q(1 - 1/N) \operatorname{erf} \frac{h}{\sqrt{4\alpha t}} \tag{17}$$

where q is the steady regional heat flow. According to (17) the anomaly would be half its initial value when $t \sim h^2/\alpha$ (or $4\tau(h)$) and 10% of its initial value when $\tau \sim 110\tau(h)$.

We illustrate these results with a highly idealized numerical example. A 'one-dimensional' hydrothermal system with depth h = 2 km develops in a region with steady regional flux q of 2.5 HFU. Assume that N = 5 and (perhaps unrealistically) that this value and the depth h persist as the system ages. In early stages the average heat flow from the system will be Nq, i.e., 12 or 13 HFU. After some 25,000 years (τ(2 km)) or less the average flux will fall to the regional value with 80% (i.e., 1 - 1/N) or 2 HFU being supplied by convective transfer. If the circulation suddenly stopped (e.g., from earthquakes or sealing of fractures), the mean flux would fall to 0.5 HFU, producing a mean local anomaly of -2 HFU; negative anomalies of 0.5 and 0.2 HFU would still persist 1/2 and 3 m.y. after circulation stopped, respectively. Although the example is extreme, it serves to illustrate why the heat flow might be extremely variable in tectonically active provinces where hydrothermal convection systems are common; the relation of the anomalies to the systems that produced them may be obscure.

These highly simplified considerations suggest the following generalizations regarding hydrothermal convection systems supported by regional heat flow in permeable surface layers:

1. The heat flow q (and combined flux q_c) will vary over horizontal distances of the order of depth of circulation, h, during all phases.
2. During an initial phase which might last $\sim\tau(h)$ the mean combined flux from the surface will exceed the regional heat flow.
3. If the system survives, it will reach a stationary stable phase in which the mean combined flux will equal the regional heat flow.
4. In a waning or recovery phase, probably longer by a factor of 10^2 than the initial phase, the mean surface flux will be less than regional heat flow.
5. The mean combined flux at the surface integrated over all phases will equal the regional heat flow; if there was convective loss into surface drainage, the integrated conductive flux will be less than the regional value.

If we can view the Basin and Range province (which is $\sim 10^7$ m.y. old) as containing a random sample of such systems (with life cycles of $\lesssim 10^6$ years), the average combined flux will equal the regional heat flow, and the average conductive flux will be less. Similar generalizations apply to systems confined to widely separated fractures as long as they are sustained by regional heat flow (or a source of heat at depth that is uniform for times much larger than the stabilization time for the hydrothermal system).

In the foregoing discussion, hydrothermal instability was initiated by introducing fractures which increased the permeability k or depth of the fractured layer, h. We assumed a steady 'regional' conductive flux from great depth. Even in the Battle Mountain High the regional flux

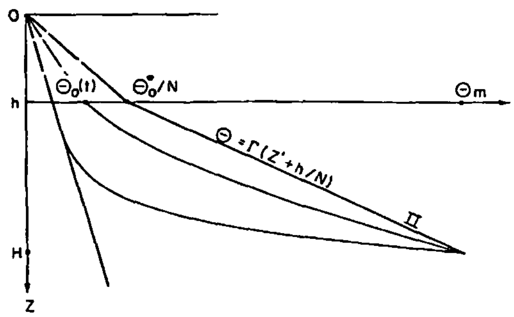

Fig. 11. Idealized one-dimensional model for hydrothermal convection in a surficial layer of thickness h; the heat is supplied by upper crustal magma at depth H (see text).

does not exceed about 3 HFU, and it leads to regional gradients generally in the range of 50°-100°C/km. Intrusions in the upper crust could, of course, produce much higher heat flows locally; if the melts persist long enough, they can generate a steady thermal condition in the overburden, heating the rock all the way to the surface. Under such conditions, hydrothermal instability could be initiated by raising the basal temperature Θ_o of the fractured zone rather than by increasing its permeability. This condition is illustrated in Figure 11 for the simple one-dimensional case of intrusion at depth H with temperature Θ_m. If the magma supply is sufficient to maintain the isothermal condition at $z = H$ during the initial stages, a stationary thermal condition will be approached in the overlying rocks in about $\tau(H)$ (see Figure 9); otherwise, it will take longer [Lachenbruch et al., 1976a]. This stationary condition is represented by curve II in Figure 11, which, of course, is the same (mathematically) as curve II in Figure 10b. In this case, however, the mean surface flux from the developing system may be less than the flux in the steady state, and the steady flux may be much greater than the regional value. In the steady state the mean combined flux q_c from the system can be written

$$q_c = K\Gamma \tag{18a}$$

$$q_c = \overline{K}\Theta_m/H \tag{18b}$$

$$q_c = K\Theta_m/[H - h(N - 1)/N] \tag{18c}$$

where (18c) is obtained by substituting for $\overline{K}$ the harmonic mean conductivity of the overburden (H), using the effective conductivity NK in the fractured zone. The expression in brackets in (18c) could be called the 'effective depth' of magma; it is the depth that would be implied by heat flow observations if convection were absent.

$$H - h\frac{N - 1}{N} = K\frac{\Theta_m}{q_c} \tag{19}$$

At the Long Valley caldera in California the mean combined flux at the surface has been estimated by hydrochemical means to be greater than 10

HFU by Sorey and Lewis [1976] and about 16 HFU by White [1965]. The caldera has been a source of volcanism for 2 m.y., and hydrothermal activity has been in progress at least 300,000 years, more intense in the past [Bailey et al., 1976]. If we assume a stationary state and take $q_c \sim 13$ HFU, $\Theta_m = 800°C$, and K = 5 mcal/cm s °C, we obtain for the effective depth of magma

$$H - h\frac{N-1}{N} \approx 3 \text{ km}$$

This implies that hydrothermal convection must extend downward (to depth h) within 3 km of the magma with very high N or even closer if the circulation is less vigorous. Structural and seismic evidence [Bailey et al., 1976; Hill, 1976; Steeples and Iyer, 1976] suggests that if magma now exists beneath the caldera, it must be at a depth of at least 6 to 8 km. Thus at least 3 to 5 km is made 'transparent' by hydrothermal convection, and water must be circulating to very great depths.

It has been pointed out that hydrothermal systems supported by regional heat flow probably exhaust the sensible heat in time $\sim\tau(h)$, say, 10^3-10^5 years, and if they survive thereafter, they do not result in anomalous heat loss. In volcanic areas such as Long Valley, hydrothermal systems are evidently supported by upper crustal intrusion, and they can persist for millions of years, discharging heat at an anomalous rate. This behavior imposes severe heat demands on the underlying magmatic system [see Lachenbruch et al., 1976a]. When the effective depth of magma exceeds 10 or 15 km (depending on the choice of K and Θ_m in (18c)), the steady surface flux approaches the regional value characteristic of the Battle Mountain High ($\sim$3 HFU) and the time constant for the overburden becomes large in relation to the stabilization time for hydrothermal systems. Under these conditions the heat supply for hydrothermal systems would be considered as either regional heat flow or a local magmatic anomaly, depending upon whether or not the magmatic condition were widespread. Both situations probably occur in the Basin and Range province.

Convection and Regional Heat Flow

In general, convection by groundwater in upper crustal rocks poses the greatest obstacle to determining from surface observations the heat flow associated with crustal conditions at depth. Obvious effects can often be eliminated by judicious selection of study sites or by the criterion of internal consistency applied to measurements in deep holes and in neighboring holes. However, because hydrologic effects can be subtle, lingering uncertainties may persist. For regional interpretation it is important to know whether undetected hydrologic anomalies are likely to be the exception or the rule. It has already been pointed out that in some regions of porous volcanic and sedimentary rocks they may be the rule. Thus it is difficult to determine the regional significance of heat flow measurements throughout portions of the Pacific Northwest, including the Cascade volcanos, parts of the Columbia Plateau, and the important Snake River Plain [Brott et al., 1976], and in other recent volcanic areas such as the San Francisco peaks at the edge of the Colorado Plateau. Very detailed hydrologic studies and deep drilling might be required to detect heat from magmatic reservoirs

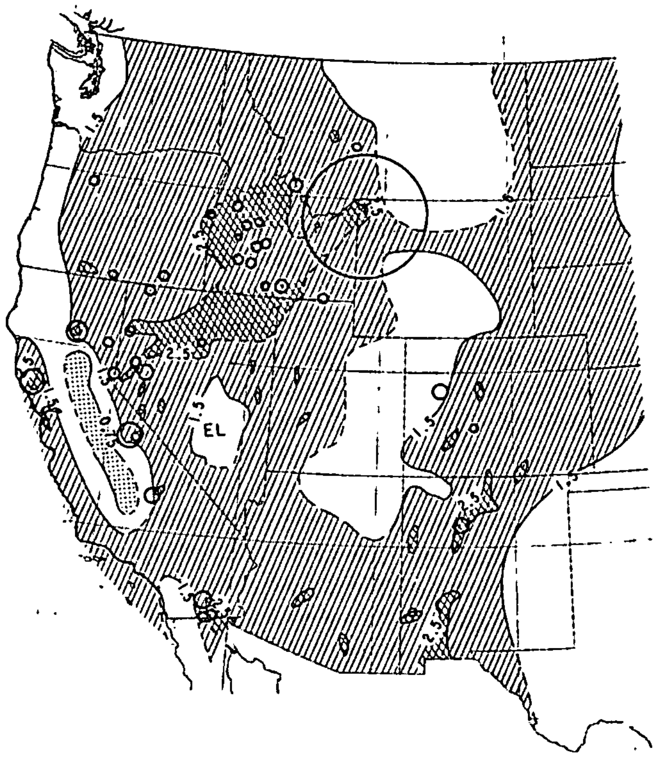

Fig. 12. Regional heat flow and the natural heat discharge of known hydrothermal systems with reservoir temperatures greater than 90°C. Each circle is centered at the location of the system it represents. A heat flow of 1 HFU through the circular area is equivalent to the rate of combined heat discharge estimated for the system. Systems with estimated discharge of less than 3 x 10^6 cal/s are not shown.

[Smith and Shaw, 1975] likely to underlie some of these regions. A similar problem often occurs in sedimentary basins, and for this reason, sites for regional heat flow studies are often chosen in less permeable rock, despite the more costly drilling.

In interpreting heat flow in the Basin and Range province it will be important to estimate the regional effects of hydrothermal convection systems. Figure 3 shows all the hydrothermal systems with estimated reservoir temperatures greater than 90°C that Renner et al. [1975] were able to identify in the conterminous United States in a recent study. From the data presented by them and from supplementary studies, chiefly those of Olmsted et al. [1975], Mariner et al. [1974], Bowen and Peterson [1970], and Fournier et al. [1976], we have attempted to summarize the natural heat discharge from each of these systems. This discharge comes in varying proportions from conductive loss from the reservoir and from conductive and convective losses from fluid discharged from the reservoir into shallow aquifers or surface drainage. Methods of estimating these discharges have been discussed by Olmsted et al. [1975], White [1965, 1968], Sorey and Lewis [1976], Fournier et al. [1976], and

Morgan et al. [1977]; the methods vary depending upon hydrologic conditions, and, of course, the estimates are subject to substantial uncertainty. Of the 255 systems listed by Renner et al. [1975], we judged that about three dozen had total combined natural discharges greater than about 3 x 10^6 cal/s; they are shown as circles in Figure 12. The area enclosed by each circle is the area through which an anomalous flux of 1 HFU would be equivalent to the total rate of combined (conductive and convective) heat discharge for the system. Typically, the anomalous regions have an area that is an order of magnitude smaller than the circles in which they are centered. The purpose of this representation is only to place some of the better known systems in a regional perspective. More detailed studies of these and other systems (some perhaps with high mass discharge at lower temperature) will surely change the picture.

Insofar as the 255 systems located in Figure 3 are concerned, the cumulative anomalous discharge is small in relation to the integrated regional flux; with the exception of the Yellowstone system, their effects on the thermal balance of the crust would be local. For the anomalous discharge to equal the integrated regional flux the circles (Figure 12) would have to overlap once on the average throughout most of the western United States. For those systems that might be stabilized above upper crustal intrusions the circle indicates the rate at which heat must be supplied by magmatic convection. For those systems that have stabilized and are supported by regional heat flow the circle represents the area over which a negative regional anomaly of 1 HFU would be sufficient to complete the heat balance.

These results offer some hope that we might be able to find a characteristic regional flux to identify with the crustal regime over large areas of the Basin and Range and similar regions; the most reasonable choice would be the most frequently occurring (or modal) value of the conductive flux. The mean would be biased toward large values by effects of undetected upper crustal intrusions, although the shallower ones would probably be identified by their hot springs and avoided in regional studies. In large regions of high heat flow, most of the local anomalies of unidentified origin are likely to come from hydrothermal convection supported by regional heat flow and modified by the forcing effects of variable topography, permeability, and precipitation. Although the combined anomalous flux from these systems might integrate to zero, the mean conductive flux would be biased toward lower values if there were appreciable convective discharge into surface drainage. (The mode and mean are not appreciably different for the Basin and Range data, possibly because internal drainage minimizes convective loss from shallow aquifers.) If the local convection systems were common, the dispersion of heat flow would be large, and the mode would be poorly defined, making the regional flux more difficult to identify. This is evidently the case in the Basin and Range (to be discussed further below), where highly fractured rocks are difficult to avoid and high heat flow and locally variable topography and precipitation favor small-scale convection systems [Olmsted et al., 1975].

A hydrologic anomaly on a regional scale seems to provide the most reasonable explanation of the Eureka Low subprovince of the Basin and Range (Figure 12). The average of 13 heat flows in this 30,000 km^2 region of south central Nevada is about 1.1 HFU, roughly 1 HFU less than the heat flow believed characteristic of the surrounding Basin and Range province. The deeper holes generally showed thermal evidence of downward moving water; in the deepest hole this evidence persisted to depths greater than 3 km [Sass et al., 1971]. In a careful hydrologic synthesis, Winograd and Thordarson [1975] have shown that an 11,000 km^2 region, straddling the southern boundary of the Eureka Low, is hydrologically integrated into one groundwater basin, although the region contains 10 topographic basins. The interbasin flow occurs to depths up to 1 1/2 km beneath the surface in permeable fractured carbonate rocks underlying the region; discharge is concentrated along a fault line in the Armogosa Desert on the southwestern margin of the system. Eakin [1966] has described a similar system in a 20,000 km^2 region including much of the eastern portion of the Eureka Low, and Dinwiddie and Schroder [1971] report evidence for interbasin flows to depths greater than 2 km in valleys of the central portion of the Eureka Low. A general discussion of the problem has been given by Mifflin [1968], who summarizes evidence for large-scale interbasin flows in regions underlain by fractured carbonate rocks in southeastern Nevada. The observation of interbasin flow systems in this region makes it likely that the entire Eureka Low is caused by such systems and, in fact, that heat flow might be a useful means of studying them. As the heat flow is still poorly known in the Eureka Low, it is likely that the pattern is much more complex than indicated by the single contour that delineates it in Figure 12. Nevertheless, it is useful to make a very simple steady state order of magnitude calculation. Suppose water percolated downward uniformly in the Eureka Low at the average rate of 1 cm/yr, some 5-10% of the local annual precipitation. Then $s \sim -2$ km for 'rock' (equation (11c)). If the average depth of the interbasin conduit were $\sim$1.4 km, according to (10), the surface heat flow would be roughly half the regional heat flow as required. If the recharge velocity ($-v$) were cut to 5 mm/yr, the regional depth of water flow would be 2.8 km. In the system studied by Winograd and Thordarson the average recharge rate required to supply the estimated annual discharge is about 2 mm/yr; for the system studied by Eakin it is about 5 mm/yr. These values seem consistent with the foregoing calculations, especially since the hydrologic systems studied each overlap the Eureka Low and may have somewhat higher mean heat flows. If the average heat flow anomaly in the Eureka Low is indeed about -1 HFU, the discharge required to complete the thermal balance can be compared to that of the hydrothermal systems by comparing the circles in Figure 12 to the mapped size of the Eureka Low. Next to the Yellowstone system the Eureka Low would have the greatest heat discharge. However, the temperature of the flow would be low, 30°-60°C above surface ambient according to (10) (when $-v =$ 1 cm/yr and 5 mm/yr are used). Much of this heat is probably discharged convectively by warm springs; if it were not, it could cause a substantial positive heat flow anomaly. The possibility of interbasin flows on the scale suggested by the present configuration of the Eureka Low requires further investigation in connection with proposals for underground storage of nuclear wastes in such areas [see also Hunt and Robinson, 1960].

We shall return to the problem of convective transport in a later section; the next section considers the simpler crustal regime characteristic of regions where convection is unimportant.

Sierra Nevada and Eastern United States: Effects of Radioactivity

It has been pointed out (5) that most crustal rocks seen at the surface contain enough radioactive uranium, thorium, and potassium to contribute appreciably to surface heat flow if such rocks were distributed uniformly through the crust. The cumulative contribution of crustal radioactivity must be known in order to determine from the surface heat flow the flux from the top of the mantle. Additionally, a knowledge of how crustal radionuclides are distributed vertically should lead to a better understanding of the thermal regime and geochemical evolution of the crust. Substantial progress has been made on these problems by studying the relation between surface heat flow and radioactive heat production of plutonic and highly metamorphosed crystalline rock exposed at the surface. Such rocks are the ones most likely to be related geochemically to the inaccessible material on which they rest.

Figure 13 is a plot of measured heat flow q versus radioactive heat production A_o of crystalline drill core or outcrop material sampled at the heat flow site. The 150 or so points include all published results from the conterminous United States and adjacent Mexico and many new points of our own (heat productions were determined by our colleague, Carl Bunker, in Denver). Locations from which the data of Figure 13 were obtained are shown in Figure 14, to be discussed further below. Birch et al. [1968] discovered that a graph of heat flow versus heat production (q, A_o) for sites in New England yields a straight line, and Roy et al. [1968a] showed that the same line accommodated additional observations in the stable central region of the United States. Their line is shown in Figure 13 and labeled 'Eastern U.S.'; data from all of the locations east of the Great Plains (shown in Figure 14) lie close to this line (solid circles, Figure 13). Two other heat flow provinces were defined by (q, A_o) lines presented by Roy et al. [1968a], one for the Sierra Nevada and one for the Basin and Range province. Both lines are shown in Figure 13. The line for the Sierra Nevada province was confirmed by independent studies [Lachenbruch, 1968], and further confirmation has come from a value published more recently [Lachenbruch et al., 1976a]. Ten of the eleven points (crossed circles, Figure 13) interior to the Sierra Nevada physiographic province lie close to the Sierra line. The eleventh point for the Sierra Nevada (DP, near the top of Figure 13) lies far above the Sierra line, as was expected; the site is only 3 km from the Long Valley volcanic center. Most of the other points in Figure 13 are not close to any of these province lines, and they will be discussed later. However, it will be useful first to outline a simple interpretation of the linear relation for the Sierra Nevada and eastern United States; it provides general insight into conditions in the crust and mantle [Birch et al., 1968; Roy et al., 1968a; Lachenbruch, 1968, 1970].

The simplicity of the linear relation suggests a simple model. We assume one-dimensional steady state, nonconvective transfer and retain only the term for heat production A(z) on the right side of (3).

$$\frac{dq}{dz} = -A(z) \qquad (20)$$

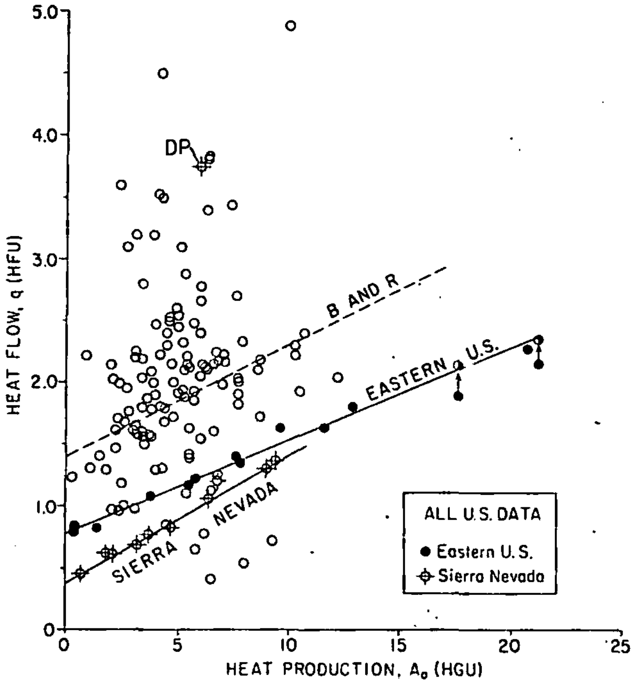

Fig. 13. Observations of heat flow q and radioactive heat production A_o from crystalline rocks in the conterminous United States; linear regression lines are from Roy et al. [1968a] for the Basin and Range (dashed), eastern United States, and Sierra Nevada provinces. Solid circles represent points east of the Great Plains, and crossed circles represent points interior to the Sierra Nevada physiographic province. Vertical arrows represent corrections for finite size of plutons [Roy et al., 1968a]. Three of the open circles on the eastern United States curve at about 1 HFU are from the Klamath Mountains in northern California. The crossed circle slightly above the Sierra Nevada line (q = 1.1) has an uncertain heat production. DP is adjacent to the Long Valley volcanic center.

The linear relation for either province may be written

$$q = q^* + DA_o \tag{21}$$

where q and A_o are heat flow and heat production measured near the surface $z = 0$, and q^* and D are the intercept and slope parameters that define the heat flow province. Rocks at sites satisfying (21) vary greatly in age and have different histories of uplift and erosion; unless the relation (21) is an accident of the present, it should remain valid after erosion by an arbitrary amount z at any location. Thus if at any site a layer of thickness z is eroded away, A_o will take on a new value A(z) depending on how radioactivity is distributed with depth, and q will take on a new value q(z), but (21) should still apply. Hence we let q be a function of z and replace A_o by A(z) in (21). Then substi-

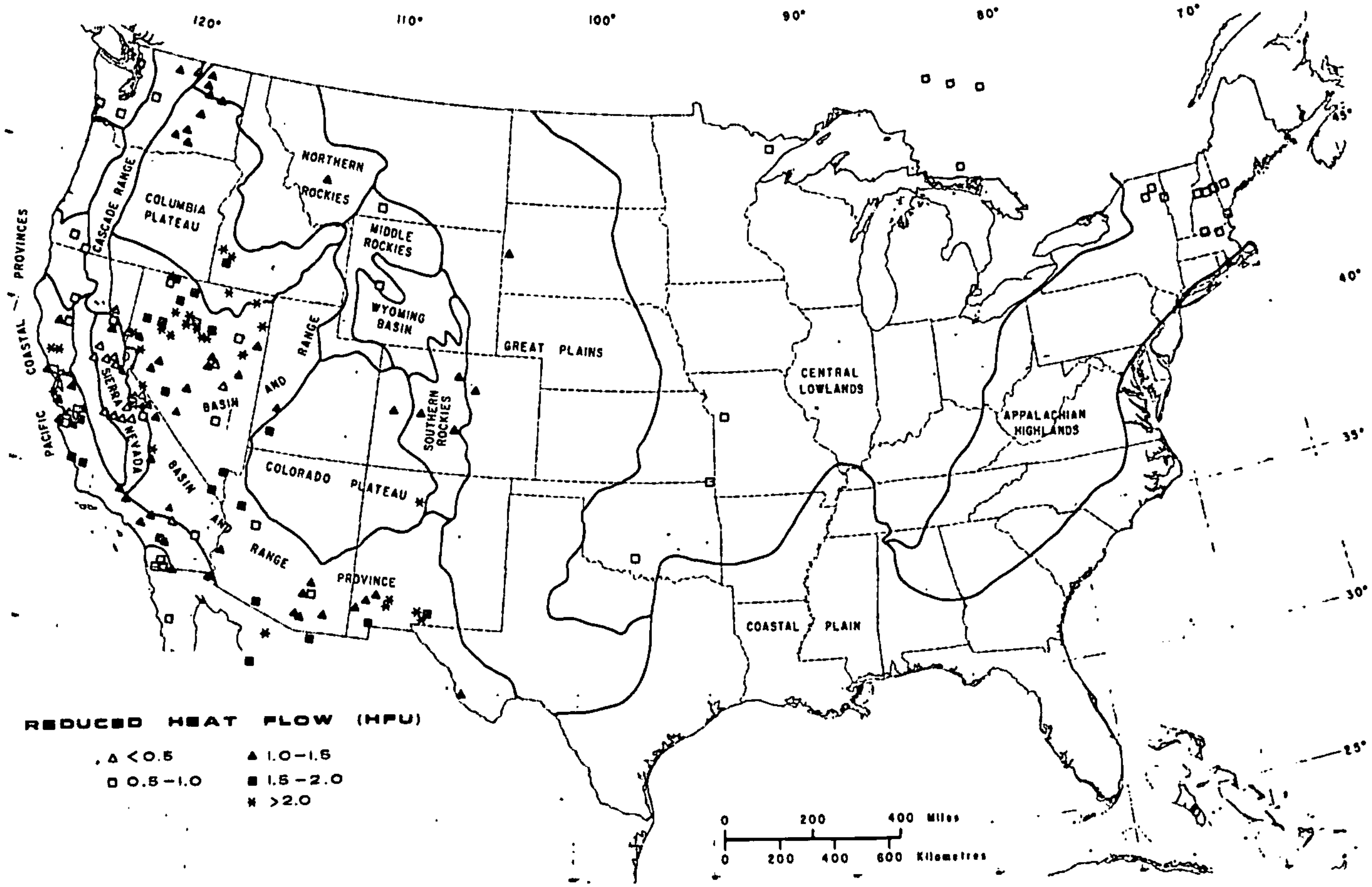

Fig. 14. Reduced heat flows and physiographic provinces (modified from Fenneman [1946].) Abbreviations are KM for Klamath Mountains, SAFZ for San Andreas Fault zone, and GV for Great Valley of California.

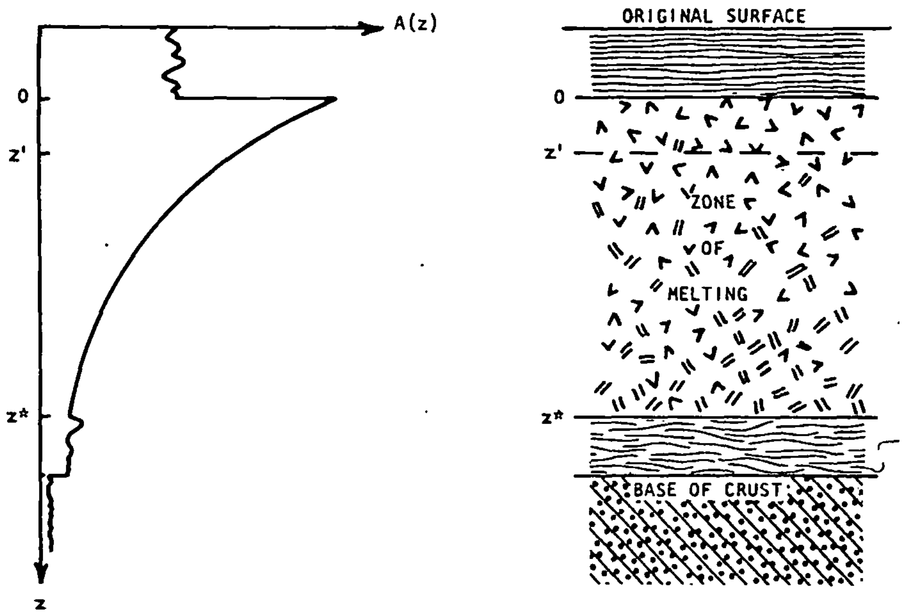

Fig. 15. Conceptual model for the distribution of heat production A(z) in the continental crust (see text).

tuting (21) in (20) yields a unique result for heat production as a function of depth

$$A(z) = A_o e^{-z/D} \tag{22}$$

where A_o is the value on the presently exposed surface, z = 0. Suppose that this distribution extends to some depth z* and that q(z*) is the heat flow at that depth. Then by using (22) the surface heat flow q is

$$q = q(z^*) + \int_{z^*}^{0} A(z)\, dz \tag{23a}$$

$$q = [q(z^*) - DA_o e^{-z^*/D}] + DA_o \tag{23b}$$

The expression in brackets represents the empirically determined intercept q* (equation (21)). The slope parameter D is about 7.5 km for the eastern United States and 10 km for the Sierra. Hence if the exponentially fractionated layer z* extends throughout all or most of the crust (z* >> D), the exponential term in (23b) is small, and q(z*) corresponds approximately to q*, which will probably be approximately the same as the mantle contribution. (For a more complete discussion, see Lachenbruch [1970].)

This simple model is illustrated conceptually in Figure 15. In the plutonic and highly metamorphosed rocks thought to make up most of the crust, U, Th, and K are fractionated upward exponentially, presumably by some process taking place during stages of partial melting or migration of metamorphic fluids [e.g., Lambert and Heier, 1967; Albarede, 1975].

The characteristic depth D is a parameter characterizing the fractionation process. If we assume that after equilibrium is established, heat flow into the lower crust q^* becomes uniform throughout the province, then subsequent measurements in exposed crystalline rocks would generally follow the linear relation observed (equation (21)).

Other assumptions regarding radioactivity of the lower crust are possible, and if the constraint imposed by differential erosion is set aside, source distributions in the upper crust other than (22) are permissible [see, e.g., Roy et al., 1968a; Lachenbruch, 1970; Blackwell, 1971]. Any simple source distribution model is, of course, approximate, as large variations are known to occur on all observable scales. Although direct observational evidence on the form of A(z) is weak, statistical studies of heat production in deep boreholes [Lachenbruch, 1971; Lachenbruch and Bunker, 1971] and geologic studies of differentially eroded plutons [Swanberg, 1972] provide some support for the exponential model. In any case, as first pointed out by Birch et al. [1968], in provinces where the linear relation applies, local variations in heat flow are probably caused by variations in radioactivity strongly concentrated in the upper crust, and heat flow through the lower crust is evidently uniform. Important corollaries are that (1) convective heat transfer is probably insignificant in the crust in these provinces, for otherwise it would have to be uniform throughout each province, and (2) if transient conditions occur, they must be uniform throughout the province. This suggests a deep mantle origin for such transients; e.g., a cool subducted slab deep beneath the Sierra Nevada has been suggested to explain the very low q^* there [Roy et al., 1972; Blackwell, 1971].

For the exponential model described, crustal temperatures are given by [Lachenbruch, 1970]

$$\Theta(z) = [q^*z + D^2A_o(1 - e^{-z/D})]/K \tag{24}$$

where K is thermal conductivity. Crustal temperatures for the appropriate province parameters (q^*, D) and for the ranges of heat production observed in each province are given for an assumed uniform conductivity (K = 6 mcal/cm s °C) in Figure 16. Similar curves, some with different assumptions, can be found elsewhere [Roy et al., 1968a; Lachenbruch, 1968, 1970; Roy et al., 1972; Diment et al., 1975; Lachenbruch et al., 1976a; Blackwell, 1971]. However, in provinces where the linear relation is found to apply, crustal temperatures are severely constrained, and models more specialized than this simple one (equation (24)) do not give significantly different results. (The problem has been discussed by Blackwell [1971].) The chief uncertainty is in the choice of conductivity, which might be adjusted by ±15% with a proportional effect on the temperatures shown. For reference we have shown in Figure 16 the curves for the beginning of melting for granodiorite with pore water present (GSS) and without it (GDS); they are discussed further in the next section.

In the highly radioactive rocks of New England (shaded on map, Figure 2) crustal temperatures probably lie between the central and upper (eastern United States) curves (A_o = 10 and 20 HGU) of Figure 16, whereas for most of the eastern United States, temperatures are expected to lie in the lower half of the range shown (between A_o = 0 and A_o = 10 HGU). For the Sierra Nevada curves, temperatures in the upper range

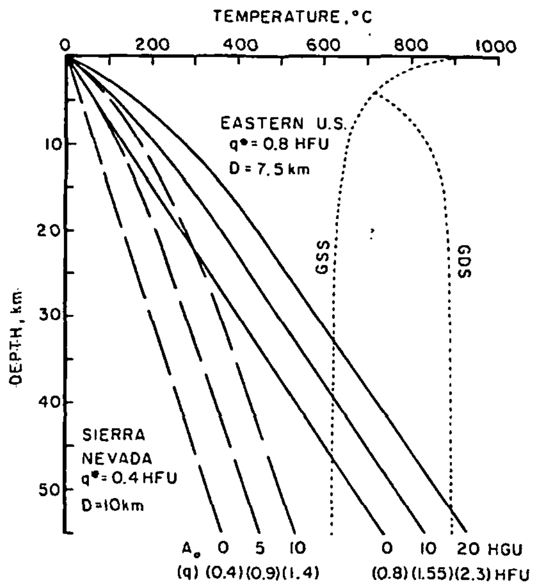

Fig. 16. Steady crustal temperature profiles based on the linear heat flow-heat production relation (equation (24)) for the Sierra Nevada (long-dashed curves) and the central and eastern United States (solid curves) for the range of heat production (A_o) observed in each province. Corresponding values of heat flow (q) are shown in parentheses. Assumed thermal conductivity is 6 mcal/cm s °C. Short-dashed curves GSS (granodiorite saturated solidus) and GDS (granodiorite dry solidus) from Wyllie [1971] show the beginning of melting for rock of intermediate composition.

(A_o = 5 to 10 HGU, Figure 16) are characteristic of the younger (Upper Cretaceous) plutons near the crest of the mountain system, and in the lower range (A_o = 0 to 5 HGU) they generally represent conditions in the western foothills. For the same heat flow, temperatures are lower in the Sierra Nevada, where a smaller fraction of the heat originates at depth (q* ≈ 0.4 HFU in the Sierra and q* ≈ 0.8 HFU in the eastern United States).

The Basin and Range Province: Effects of Radioactivity and Convection

The third heat flow province defined by Roy et al. [1968a] is the Basin and Range province, for which all current (q, A_o) data are shown in Figure 17. The locations from which these data were obtained are indicated by the points within the Basin and Range province boundary in Figure 14 and those points in Mexico south of Arizona [from Smith, 1974]. The regression line (dashed, Figure 17) determined by Roy et al. [1968a] from 12 of 15 available data pairs had a slope D of 9.4 ± 1.3 km and intercept q* of 1.4 ± 0.09 HFU. It is clear from the scatter in Figure 17 that if the Basin and Range province is in some sense represented by this line, it is not in the same sense that the

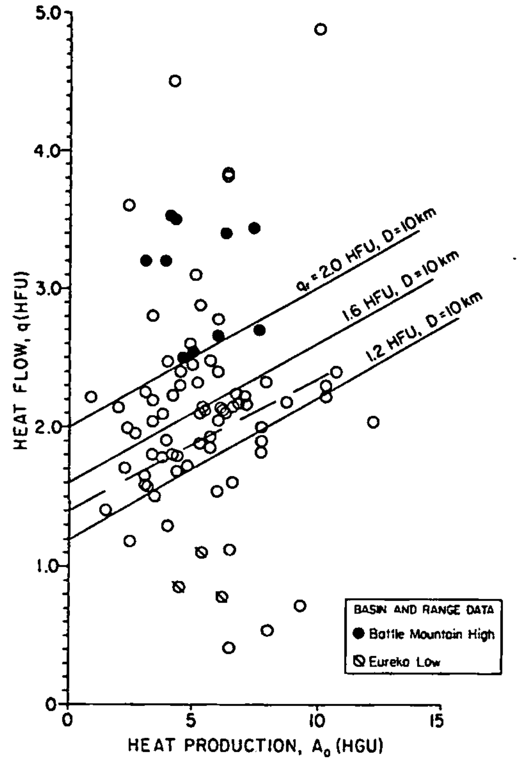

Fig. 17. Observations of heat flow q and radioactive heat production A_o from crystalline rock of the Basin and Range province. Regression line from earlier studies is dashed.

Sierra Nevada and eastern United States provinces are represented by their lines (Figure 13). As the Basin and Range province now has by far the most observations, it could be argued that the linear regression lines will lose their significance in the other provinces, too, as more data are acquired. However, we consider this unlikely, as the density of observation is presently as great in the Sierra Nevada as it is in the Basin and Range, and it was recognized at the outset by Roy et al. [1968a] that the regression analysis was least significant in the Basin and Range province. A more discriminating use of the variable quality data shown in Figure 17 might provide justification for a linear relation in the Basin and Range or parts of it, and this is under study. For the present, however, it appears that the linear regression of q on A_o has little significance in the Basin and Range province, and the question arises whether insights from the foregoing simple model of the linear relation can be applied usefully there.

According to the simple model the steady state contribution from crustal radioactivity is DA_o, where D is a geochemical characteristic of the crust describing its fractionation. This physical interpretation does not depend upon the constancy of lower crustal heat flow (q*) and is reasonable whether or not the linear relation applies. On this basis, we might subtract the term for crustal radioactivity from the

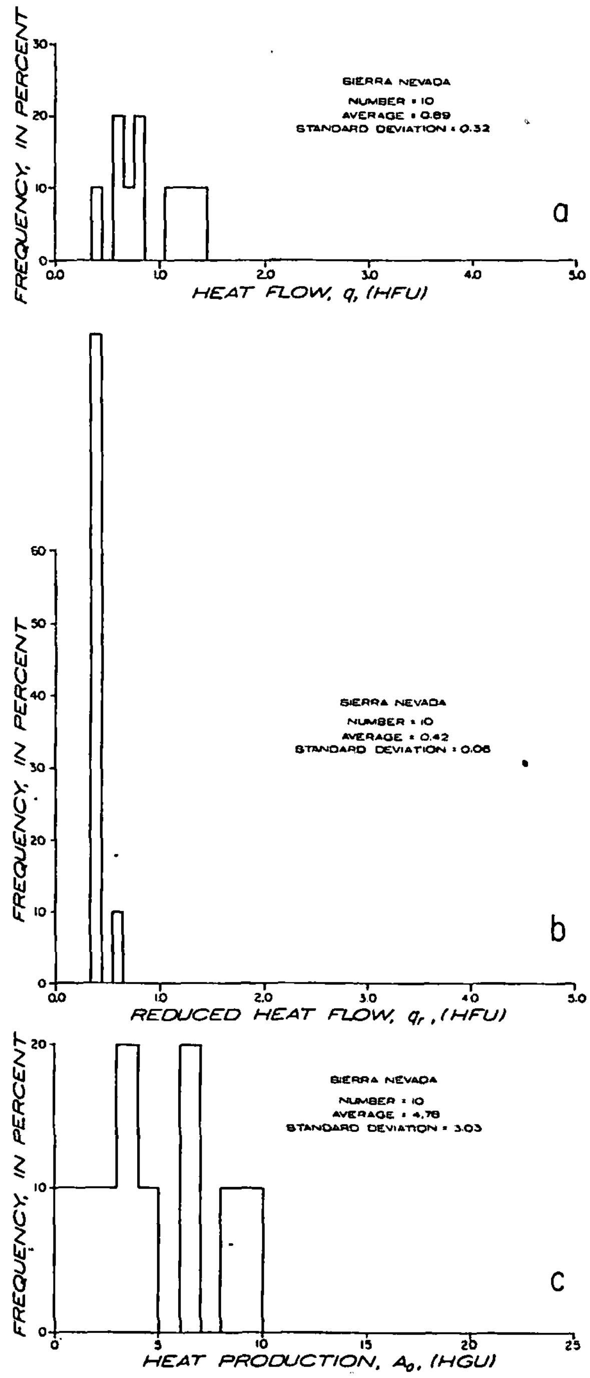

Fig. 18. Histograms of (a) heat flow, (b) reduced heat flow, and (c) radioactive heat production for stations at which both q and A_o were measured in the Sierra Nevada province.

observed heat flow to obtain the 'reduced heat flow' q_r employed by Roy et al. [1972].

$$q_r = q - DA_o \tag{25}$$

Although D is not known directly for the Basin and Range, we might reasonably assume it to have the constant value of 10 km, firmly established in contiguous rocks of the adjacent Sierra Nevada province (granitic rocks in the western Basin and Range province are part of the Sierra Nevada batholith).

Histograms of the three variables in (25), heat flow q, reduced heat flow q_r, and heat production A_o, are shown in parts a, b, and c, respectively, of Figures 18-20 for the three provinces. For a province in which the linear relation applied in a deterministic sense, q_r would be identical to q*, a constant (equation (21)). It is seen from Figures 18 and 19 that this is nearly the case for the Sierra Nevada and eastern United States. In such provinces the simple interpretive model gives q_r a clear-cut physical meaning; it is the uniform flux q* from the mantle or at least the lower crust. No such interpretation is possible for the Basin and Range, where q_r is widely dispersed (Figure 20b). A second distinctive feature of the Basin and Range data (Figure 20b) is the large mean value for q_r, about 1.6 HFU or twice the value for the stable eastern United States usually considered as normal. On the basis of an earlier discussion we believe that the large dispersion results primarily from convection by groundwater, and the large mean, from convection by magma. Before discussing implications of these two inferences we shall consider how widespread the conditions represented by the sample in Figure 20 might be.

In brackets in Figures 20a and 20b, statistics are given for the Basin and Range province excluding determinations in the anomalous subprovinces (10 values from the Battle Mountain High and 3 values from the Eureka Low). For comparison, we show in Figure 21 the corresponding results for the complete population of heat flow measurements in the Basin and Range province; again the brackets enclose statistics determined with the two subprovinces excluded (20 values from the Battle Mountain High and 13 values from the Eureka Low). The fact that the principal mode, the mean, and the standard deviation are essentially the same for data in brackets in Figures 20a and 21 adds a note of generality to the analysis of data in Figure 20. However, without a more careful study of the individual sites than we have yet undertaken, more refined statistical treatment is not warranted. Reduced heat flows reported from the northern and southern Rocky Mountains and the Columbia Plateau (Figure 14) seem commonly to fall in the modal range (1.2-1.6 HFU) characteristic of the Basin and Range data, and those provinces are expected to have similar crustal regimes [see Blackwell, 1969, 1971; Roy et al., 1972]. We have focused on the Basin and Range province because it seems to represent a fairly continuous tectonic unit, and the heat flow coverage there is relatively dense.

The reduction for crustal radioactivity in the Basin and Range province does not significantly reduce the dispersion, and we should be little better off in estimating the heat flow with a knowledge of local radioactivity than without it. This does not mean that the reduction (25) for crustal radioactivity in the Basin and Range is not valid. The

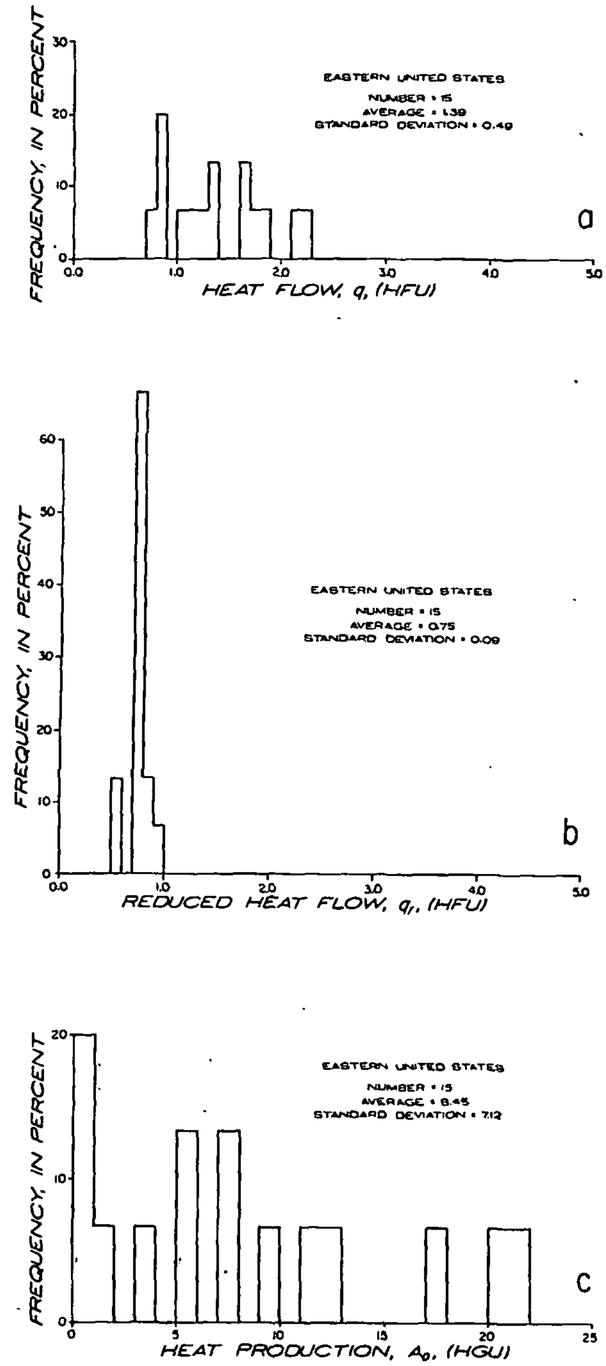

Fig. 19. Histograms of (a) heat flow, (b) reduced heat flow, and (c) radioactive heat production for stations at which both q and A_0 were measured in the eastern United States province (i.e., east of the Great Plains).

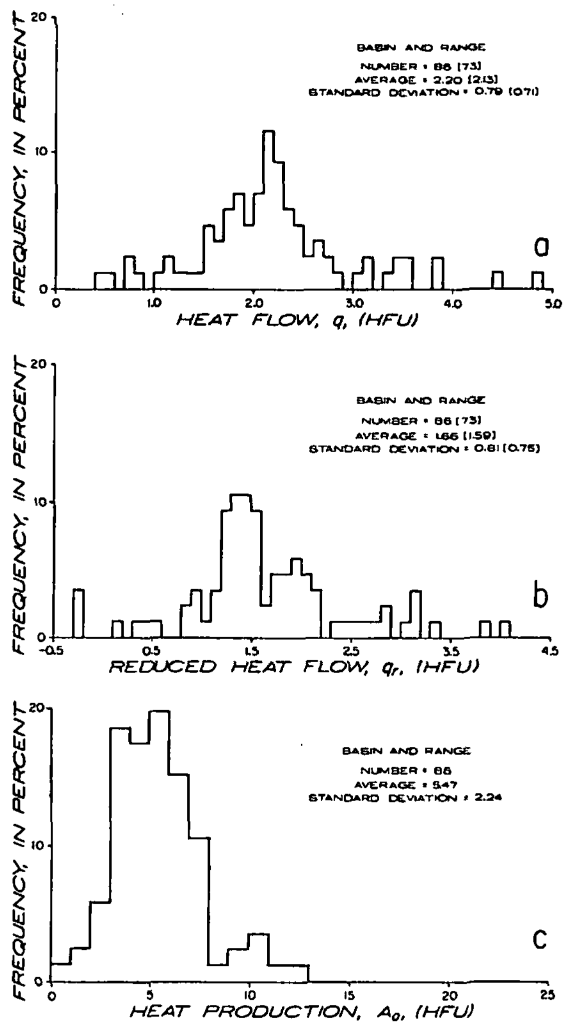

Fig. 20. Histograms of (a) heat flow, (b) reduced heat flow, and (c) radioactive heat production for stations at which both q and A_o were measured in the Basin and Range province. Statistics in brackets in (a) and (b) were determined with data from Battle Mountain High and Eureka Low deleted.

standard deviation of the crustal correction (DA_o with D = 10 km, Figure 20c) is only 0.22 HFU, about one fourth of the standard deviations for both q and q_r. If q and A_o were normally distributed, the reduction from q to q_r (equation (25)) would have an insignificant effect on the standard deviation (∿0.03 HFU). The statistics do suggest that three-dimensional effects, thermal transients, and convection, neglected in the simple theory (equation (20)), are substantially greater (generally by a factor of 3 or 4) than the effects of variable crustal radioactivity. As three-dimensional effects are evidently unimportant in the other provinces, it is likely that the dispersion of

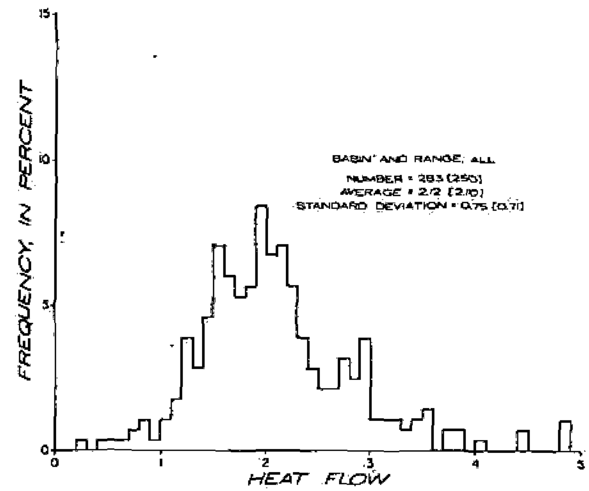

Fig. 21. Histogram of all heat flow data from the Basin and Range province. Statistics in brackets were determined with data from the Battle Mountain High and Eureka Low deleted.

reduced heat flow in the Basin and Range is due primarily to hydrothermal and (to a lesser extent) magmatic convection, including, of course, their time dependent effects, as discussed in an earlier section.

We have mentioned that in the Basin and Range province the mean conductive flux reduced for crustal radioactivity is about twice as large as would be expected in stable regions. We naturally associate this large and variable reduced heat flow with the present pattern of extensional deformation, magmatism, and hot spring activity that has probably characterized the province for the past 17 m.y. [Thompson and Burke, 1974]. It has been shown that convective processes operating solely within the crust over this time (twice the conductive time constant for the crust) would probably reduce the mean conductive flux, not increase it. Hence the excess heat is probably supplied convectively by magma rising across (and possibly beneath) the base of the crust. Regional variations in the intensity of this magmatic upflux are probably responsible for high heat flow subprovinces like the Battle Mountain High and the Rio Grande Trough, and for local silicic volcanic centers like the Long Valley caldera as well. It is likely that these variations are, in turn, caused by local variations in the rate of crustal extension [Lachenbruch et al., 1976a] (A. H. Lachenbruch and J. H. Sass, unpublished models).

It is useful to assume that over large areas the crust is in a quasi-steady state, receiving as much heat by conduction and convection across its base as it gives off by conduction and convection at its surface. As q_r is normally estimated from the conductive heat flow, the actual mantle contribution would be larger than q_r by the amount of convective loss from hot and warm springs and volcanos. However, the heat delivered by post-Oligocene extrusive rocks in the Great Basin is negligible in relation to the conductive heat flow, and judging from Figure 12, the net effect of the hotter known springs might not be important on a regional scale. Nevertheless details of the total hydrologic heat loss are poorly known, and we shall neglect them although they could be significant. In regions where the convective flux is known, it can be accommodated in the computation of q_r (by using combined surface flux q_c instead of q in equation (25)) if the steady state assumption seems to warrant it.

If there is a characteristic flux into the lower crust of the Basin and Range, it is likely that it is represented by the modal value of q_r, with the nonmodal values generally representing superimposed anomalous convective effects. Excluding the two subprovinces, almost half the values of q_r fall in the modal range 1.2-1.6 HFU (Figure 20b). (Interestingly, the value of q^* originally determined from linear regression by Roy et al. [1968a] was 1.4 HFU.) The Battle Mountain High, a positive anomaly with lateral dimensions of many crustal thicknesses, has been defined as a region with $q > 2.5$, but it is essentially unchanged if defined as the region $q_r > 2$. Figure 22 shows crustal profiles (equation (24)) for a steady conductive mantle flux q_r of 1.2 and 1.6, which might bracket the 'characteristic' conditions in the Basin and Range province, and of 2.0 and 2.5, which are intended to represent (lower) limiting and typical conditions in the Battle Mountain High. (The mean for the 20 heat flows in the Battle Mountain High is 3.0 ± 0.4 standard deviation; the mean for the 10 reduced heat flows is 2.5 ± 0.4 standard deviation.) As such large variations in q_r (from 1.2 to 2.5) have a far greater effect on temperature than variations in radioactivity, the curves are shown only for the near-average A_o of 5 HGU (Figure 20c). Likely variations in A_o (of ± 3 HGU, Figure 20c) would change the deep crustal temperatures by only ± 50°C. Variations in thermal conductivity of ± 15% from the assumed value of 6 mcal/cm s °C would change the temperatures in Figure 22 by ± 15%. Shown also in Figure 22 is the curve for the Sierra Nevada ($q^* = 0.4$ HFU) and the curve for $q^* = 0.8$ HFU, which is similar to that for the stable eastern United States except that it is drawn for D = 10 km (instead of 7.5 km) for consistency. The latter is a useful (if somewhat arbitrary) reference for conditions one might expect in the Basin and Range crust if it were underlain by a stable mantle; it differs from the corresponding curve ($q^* = 0.8$ HFU, D = 7.5 km) for the stable eastern United States by less than 45°C.

Although the curves in Figure 22 are drawn as if all of the mantle flux q_r were conducted from the base of the crust, this condition is not required nor is it expected to apply in the hotter regimes. Insofar as our observations at the surface are concerned, the anomalous source may be produced by repeated intrusion at any depth; if the source persists long enough to establish a steady state, the temperatures above it will fall on the appropriate curve of Figure 22. The time $\tau(z)$ required for a sill-like constant temperature source to equilibrate the overburden is shown on the depth axis in Figure 22. (A sill-like source whose strength does not change with time takes about three times as long. During the slow cooling following solidification the average gradient anomaly in the overburden will remain rather close to that measured at the surface, provided that the original source persisted for many τ.) Thus a continuing intrusive process that maintained the 20-km temperature at 900°C for more than 3 m.y. would cause a conductive regime above it as indicated by curve F (Figure 22); thereafter, downward extrapolation from surface observations would correctly identify the 20-km temperature.

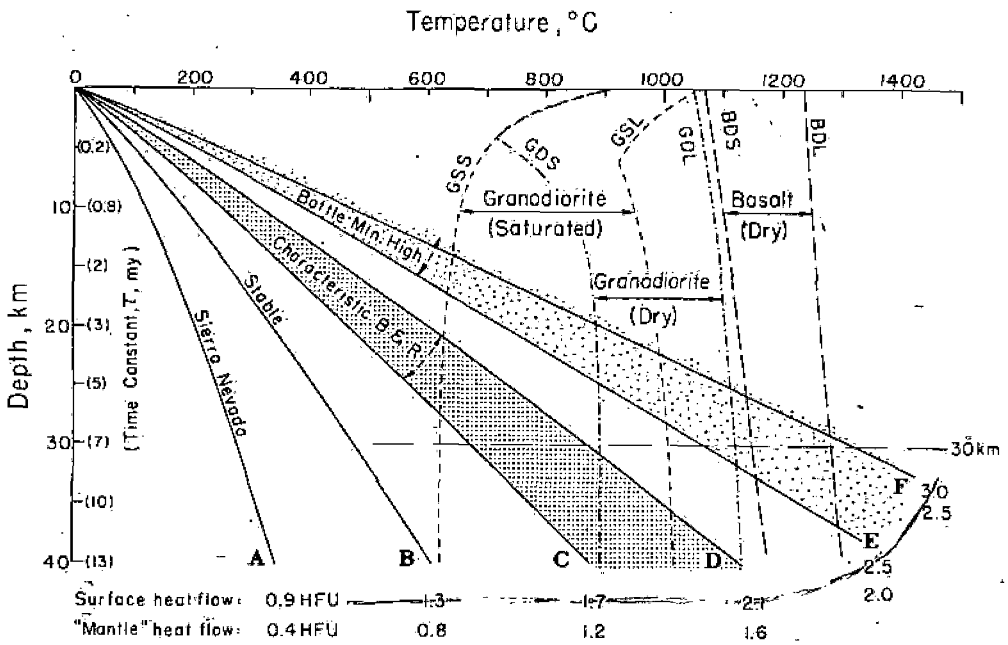

Fig. 22. Generalized conductive temperature profiles for the Sierra Nevada crust (A), a stable reference crust (see text) (B), the characteristic Basin and Range crust (C to D), and lower limiting (E) and typical (F) conditions in the crust of the Battle Mountain High. All curves are drawn for a surface heat production (A_0) of 5 HGU and thermal conductivity (K) of 6 mcal/cm s °C (equation (24)). Corresponding surface heat flow and reduced or 'mantle' heat flow are shown at the bottom of each curve. Melting relations [after Wyllie, 1971] are shown for intermediate crustal rock by the curves GSS (granodiorite saturated solidus), GSL (granodiorite saturated liquidus), GDS (granodiorite dry solidus), and GDL (granodiorite dry liquidus) and for basalt by BDS (basalt dry solidus), and BDL (basalt dry liquidus). In parentheses on the depth axis is shown the time required for the overburden to approach thermal equilibrium after intrusion by a sill maintained at constant temperature.

Above the intrusion we would measure a surface heat flow of 3 HFU and a reduced heat flow of 2.5, and (relative to curve B, Figure 22) the contribution of anomalous convected flux would be 1.7 HFU. The actual anomalous flux into the lithosphere at the time might be greater or less than 1.7 HFU, depending upon whether the lower portion was absorbing or releasing heat, i.e., whether its temperature was approaching the new stationary state from below or above. Convective transfer by magma rising in the lower crust (below 20 km in this example) would cause mean temperatures there to be less than indicated by the conductive curve F (A. H. Lachenbruch and J. H. Sass, unpublished models). Convection in this lower region might involve no more than the upward movement of basalt in narrow conduits en route to the 20-km depth, or it could involve complex networks of basaltic intrusion and secondary diaperic movements of silicic melts and adjustments of solid rock.

In Figure 22 we have shown [from Wyllie, 1971] some limiting melting relations for materials likely to be involved in convective heat transport to and through an anomalously hot crust. The most probable source of anomalous heat is upward migration of basalt (or possibly other mantle-derived magma) beneath or into the base of the crust. For reasonable water contents, most of the crystallization and hence most of the latent heat release will have occurred by the time the basalt cools past its dry solidus (BDS, Figure 22) [Wyllie, 1971; Peck et al., 1966]. Heat introduced by the basalt could raise the temperature and melt fractions of the indigenous crustal material, assumed to have an intermediate (granodiorite) composition. In the presence of excess water ('vapor present condition'), such rocks would begin to melt along the curve GSS (granodiorite saturated solidus) (Figure 22), and melting would be complete at GSL (granodiorite saturated liquidus). If no water occurred in the crustal rock except that bound in hydrous minerals, melting would not begin until temperatures exceeded GDS (granodiorite dry solidus), and it would not be complete until they reached GDL (granodiorite dry liquidus). If a trace of pore water were present, it would dissolve preferentially in a melt (of rhyolite composition) that would begin to form along GSS. With further increase of temperature the increasing melted fraction would become more and more undersaturated, making the residual crystals more difficult to melt; complete melting would not occur until temperatures approached GDL. As the radioactive elements, like the water, move preferentially into the melt, upward migration of the melt might produce the condition illustrated schematically in Figure 15 and at the same time dehydrate the lower crust. Wyllie [1971] has pointed out that unless the lower crust were somehow rehydrated, a second cycle of lower crustal melting would be more difficult, as it would require temperatures in excess of GDS. If repeated cycles did occur, however, we might expect more complete upward fractionation of radioelements. This would appear in surface observations as a decrease in the value of the characteristic depth D (equation (21)).

It is seen from Figure 22 that at the base of a 30-km crust in the Battle Mountain High, basalt melt could be stable, and dry intermediate crustal rock could be completely melted. Hence some heat is probably transferred by magmatic intrusion in the lower crust of the Battle Mountain High, for if it were not, the thermal regime would be conductive, and the base would be nearly or quite all melted. Substantial amounts of melting of most crustal rocks in the presence of pore water could occur near the base of a 30-km crust in the 'characteristic Basin and Range' regimes. Hence 'first cycle' (wet) crustal fractionation could be initiated under the Basin and Range regimes, and 'second cycle' (dry) fractionation could occur under the Battle Mountain High regime. Convection by quasi-steady upward migration of a melted fraction could, of course, convert one regime to the other.

Typically, the upper 20 km of the Basin and Range crust has a seismic velocity ($V_p \approx 6.0$ km/s) characteristic of silicic rocks, including granite, and the lower 10 km or so has a higher velocity ($V_p \approx 6.7$ km/s) characteristic of denser (and presumably more refractory) materials, including basalt [e.g., Hill and Pakiser, 1966]. As temperatures in the Battle Mountain High and similar regions can be in the range 700°-900°C at depths of 15-20 km (curve F, Figure 22), laterally extensive partial silicic melts could occur at midcrustal levels in such regions. Convective transfer attending stretching and intrusion of the extending lithosphere could, however, reduce these temperature estimates by 100°C or so (A. H. Lachenbruch and J. H. Sass, unpublished).

In summary, we have found that the linear relation between heat flow and surface radioactivity does not apply generally in the Basin and Range province. For the linear relation to apply, crustal contributions to heat flow should be exclusively from radioactivity, and the mantle flux should be uniform. We believe that the relation fails in the Basin and Range province because both conditions are violated there. Variations in surface heat flow caused by hydrothermal and magmatic convection overshadow variations caused by crustal radioactivity (they are probably greater by a factor of 3 or 4), and the anomalously large mantle flux is not uniform. Mantle heat flux is probably controlled by magmatic mass flux (into or beneath the base of the crust) which varies in intensity, creating subprovinces like the Battle Mountain High and the Rio Grande Rift, and more local heat flow anomalies and volcanic centers as well (Figure 3). Frequently occurring values of reduced heat flow suggest that the mantle flux throughout much of the province might have characteristic values in the range 1.2-1.6 HFU. These considerations form the basis for construction of generalized crustal temperature profiles which can be discussed in terms of melting relations for crustal rocks. Theoretical temperatures are consistent with the extensive manifestations of magmatic activity observed in the province.

prospecting point!

Discussion and Summary

Our knowledge of regional heat flow in the United States has been acquired only recently. In his review of the status of geothermal investigations in 1954, Birch [1954a] was able to cite only three 'reasonably adequate' determinations (0.93 HFU in northern Michigan [Birch, 1954b], 1.7 HFU in the Colorado Front Range [Birch, 1950], and 1.29 HFU in the Central Valley of California [Benfield, 1947]). Although we now know that each of these values is quite representative of its geologic province, little could be deduced about regional patterns from three determinations. In a review about a decade later, Lee and Uyeda [1965] listed heat flow from about 40 distinct sites in the conterminous United States; the data indicated that heat flow was generally higher in the tectonically active western United States than in the more stable eastern and central portions. A few years later, publication of over 100 new values [Roy et al., 1968b; Blackwell, 1969] revealed correlations between heat flow and higher-order tectonic and geologic features, chiefly, high heat flow in New England and in the Basin and Range province, the northern and southern Rockies, and the Columbia Plateau and a band of lower heat flow near the Pacific Coast, features shown in the maps of Roy et al. [1972] and Blackwell [1971]. A map by Diment et al. [1972] showed the systematic variations of heat flow in the Appalachian Mountain region. Sass et al. [1971] presented 100 or so additional values revealing the strong correlation of heat flow with the major N-S trending tectonic provinces of California, including the San Andreas Fault zone. They also defined subprovinces of high and low heat flow in the Basin and Range province, to which another, the Rio Grande Rift, has more recently been added [Decker and Smithson, 1975; Reiter et al., 1975]. Further detail is shown in the map presented here, and we can, of course, expect the trend to continue.

Our understanding of these heat flow observations was increased substantially in 1968 by the discovery of the linear relation between heat flow and surface radioactivity in New England [Birch et al., 1968], its application to other provinces [Roy et al., 1968a], and its independent confirmation for the Sierra Nevada [Lachenbruch, 1968]. Curiously, 8 years later we still do not know how general this relation might be. It has been shown above that in one of the provinces where the relation was formerly thought to apply approximately (the Basin and Range province), it does not apply. Although the relation is now supported by studies in crystalline rocks of Canada [Cermak and Jessop, 1971], Australia [Jaeger, 1970; Sass et al., 1976c], India [Rao et al., 1976], and Norway [Swanberg et al., 1974], the most convincing results remain those from the provinces in which the relation was first discovered, the eastern United States and the Sierra Nevada. As anticipated by Roy et al. [1968a], data from the Canadian Shield [Cermak and Jessop, 1971] and to a lesser extent those from central Australia are accommodated reasonably well by the line for the stable eastern United States, but the parameters determined from these areas independently are somewhat different; in particular, the values $q^* = 0.64$ HFU and $D = 11.1$ km for nine points in central Australia [Sass et al., 1976c] seem significantly different. Several isolated determinations such as the three from the Klamath Mountains in northern California (Figure 13 and Lachenbruch and Sass [1973]) and two from Precambrian rocks in southern India [Rao et al., 1976] fall on the eastern United States curve. The data from southern Norway [Swanberg et al., 1974] lie rather close to the Sierra Nevada line; the linear regression analysis there yielded $q^* = 0.48$ HFU and $D = 8.4$ km. However, nine points from Precambrian rocks of western Australia [Sass et al., 1976c] yield $q^* = 0.63$ and $D = 4.5$ km, a line quite different from those observed elsewhere, and four points from northern and central India [Rao et al., 1976] yield $q^* = 0.92$ HFU and $D = 14.8$ km. Judging from our experience with the Basin and Range province, many more observations will be needed in all of these areas, and others, to establish the general significance of the relation between heat flow and radioactivity in crystalline rocks. As we have remarked, the importance of this relation is the requirement it places on the vertical distribution of crustal radioactivity and to a lesser extent on the total contribution of crustal radioactivity to surface heat flow. These requirements relate to the processes responsible for evolution of the continental crust. In order for the linear relation to obtain, several other special requirements must be met [Lachenbruch, 1970]; i.e., three-dimensional conductive effects and magmatic and hydrothermal convection must be negligible in the crust, and crustal transients and mantle heat flow must be uniform throughout the province. Thus the linear relation can be expected to apply only in more stable regions, and even there, only under rather special circumstances. Nevertheless, the insight obtained from the relation can provide a basis for estimating the contribution of crustal radioactivity elsewhere on the continents. Thus the 'reduced heat flow,' obtained by subtracting the estimated crustal contribution from observed heat flow [Roy et al., 1972], might be used to interpret continental heat flow where the linear relation does not apply. As the reduction depends upon the value of D, which varies around the world by a factor of 3, according to presently available studies, the reduction must be applied with caution. The justification for using D = 10 km in the Basin and Range province is provided by the linear relation observed in the Sierra Nevada and the observation that granitic rocks in the western Basin and Range at least are part of the Sierra Nevada batholith. Reasonably confident reductions can sometimes be made in regions where crystalline rock is not exposed if enough information on crustal composition is available from other sources. Examples are the California coast ranges, where the thickness of the Franciscan formation (of known radioactivity) is estimated from seismic studies [Lachenbruch and Sass, 1973], and the Pacific Northwest coastal provinces, where the basement rock is believed to be largely mafic [Blackwell, 1971; Sass et al., 1971] and hence to have rather low radioactivity. It is seen from Figure 14 that reduced heat flow estimated for sites along the Pacific Coast is generally in the range characteristic of the eastern United States except in the band through western and south central California enclosing the San Andreas Fault, where it is generally similar to values in the Basin and Range province.

A rather complete description of regional heat flow in the United States and a thorough understanding of its implications for thermal state and processes in the crust will probably be needed for a comprehensive assessment of our geothermal energy resource and the formulation of rational plans for exploring it and exploiting it. As we have seen, even in regions where the heat flow is low and the likelihood of an exploitable resource is slight, the understanding obtained from heat flow studies can be important for unraveling the more complex thermal problems in high heat flow areas. It is seen from Figures 1-3 that only now, with more than 600 determinations, are the areas of extremely high heat flow beginning to emerge as regional features; their boundaries are generally unknown, however, and few areas are sampled adequately for an understanding of hydrothermal systems in a crustal context. Large areas of the heat flow control map (Figure 1) are blank. Ironically, many of these are oil-producing areas where every year more than 10,000 holes are drilled and temperatures are measured. It is likely that a knowledge of regional heat flow in these areas would increase our understanding of the widely discussed 'geopressured' energy resources of the Gulf Coast [see, e.g., Jones, 1969; Jones and Wallace, 1974; Papadopulos et al., 1975] and of the general problem of thermal evolution of sedimentary basins and the maturation of hydrocarbons. A comprehensive compilation of temperature gradient from some 25,000 sites in oil-producing areas of North America has recently been published by the American Association of Petroleum Geologists in cooperation with the USGS [American Association of Petroleum Geologists-U.S. Geological Survey, 1976]; it contains much useful regional information. However, as was emphasized by Birch [1954a], the principal variable affecting temperature gradient in the outer layers of the crust is thermal conductivity (and locally, water movement). Hence a compilation of the temperature gradient alone can be expected to tell us much more about the variations in conductivity (and locally, water movement) than about variations in the more fundamental quantity, heat flow. Regional heat flow studies are proceeding at a modest pace (limited by the availability of drill holes) at a handful of research laboratories across the country. In view of the importance of regional studies to the energy industries and the enormous amount of drilling they undertake, more interaction between these groups should hold substantial advantage for all.

Heat convected by moving groundwater requires careful attention in heat flow studies; it can perturb or completely dominate the regional flux associated with the crustal regime at depth. In tectonically active regions, open fractures, permeable volcanic rocks, and high heat flow may result in circulatory convection systems driven primarily by thermal density differences. Such systems are expected to produce perturbations to surface heat flux which change sign over lateral distances of the order of the depth of circulation, probably up to many kilometers. If the system is sustained by upper crustal magmatic intrusion, the combined flux at the surface might be much greater than the regional value for millions of years. If the system is sustained by regional heat flow, the combined flux will probably fall to the regional value after 10^3-10^5 years (depending on circulation depth), but a lingering conduction anomaly will persist long after the circulation stops. Perturbations caused by these systems create large dispersion in conductive flux from tectonically active regions, making it difficult to identify and interpret the regional heat flow without a dense network of observations [see, e.g., Blackwell and Baag, 1973; Blackwell et al., 1975; Brott et al., 1976; Combs, 1975; Lachenbruch et al., 1976b; Sass and Sammel, 1976; Sass et al., 1976b, d]. Hydrothermal convection systems constitute most of the targets under investigation as potential sources of geothermal energy, and much will no doubt be learned about their inner workings in the next few years. We expect that the increased understanding of the dynamics of these systems will help in the interpretation of regional heat flow and that the better understanding of regional heat flow will, in turn, increase our general understanding of the broader crustal conditions that generate hydrothermal systems. In regions like the Battle Mountain High, where the average heat flow is about 3 HFU, the steady gradient in poorly conducting sediments is typically about 100°C/km, and under favorable conditions a commercial energy resource could exist beneath deep sedimentary basins, even in the absence of hydrothermal convection [see, e.g., Diment et al., 1975].

Large disturbances to regional heat flow can also be caused by groundwater circulation forced by the distribution of precipitation, topography, and permeable formations. In some regions mantled by permeable volcanic rocks, downward percolation can completely 'wash out' the conductive flux, making it impossible to study regional heat flow by conventional means. In other regions like the Eureka Low, effects can be more subtle. Evidence there suggests that a negative heat flow anomaly over an area $\sim 3 \times 10^4$ km^2 might be caused by interbasin flow in deep aquifers fed by downward percolation of a small fraction of the annual precipitation. Heat flow results of this sort can provide useful information on regional hydrologic patterns with important implications for underground disposal of radioactive waste.

Acknowledgments. We are grateful to our colleagues, R. L. Christiansen, W. H. Diment, D. R. Mabey, L. J. P. Muffler, M. Nathenson, F. H. Olmsted, M. L. Sorey, D. E. White, and D. L. Williams, for helpful comments on the manuscript and to B. V. Marshall, S. P. Galanis, Jr., and R. J. Munroe for assistance with computations and illustrations.

References

Albarede, F., The heat flow/heat generation relationship: An interaction model of fluids with cooling intrusions, Earth Planet. Sci. Lett., 27, 73-78, 1975.

American Association of Petroleum Geologists-U.S. Geological Survey, Geothermal gradient map of North America, scale 1:5,000,000, U.S. Geol. Surv., Reston, Virginia, 1976.

Bailey, R. A., G. B. Dalrymple, and M. A. Lanphere, Volcanism, structure, and geochronology of Long Valley caldera, Mono County, California, J. Geophys. Res., 81, 725-744, 1976.

Benfield, A. E., A heat flow value for a well in California, Amer. J. Sci., 245, 1-18, 1947.

Birch, F., Flow of heat in the Front Range, Colorado, Geol. Soc. Amer. Bull., 61, 567-630, 1950.

Birch, F., The present state of geothermal investigations, Geophysics, 19, 645-659, 1954a.

Birch, F., Thermal conductivity, climatic variation, and heat flow near Calumet, Michigan, Amer. J. Sci., 252, 1-25, 1954b.

Birch, F., R. F. Roy, and E. R. Decker, Heat flow and thermal history in New England and New York, in Studies of Appalachian Geology: Northern and Maritime, edited by E. Zen, W. S. White, J. B. Hadley, and J. B. Thompson, Jr., pp. 437-451, Interscience, New York, 1968.

Blackwell, D. D., Heat flow determinations in the northwestern United States, J. Geophys. Res., 74, 992-1007, 1969.

Blackwell, D. D., The thermal structure of the continental crust, in The Structure and Physical Properties of the Earth's Crust, Geophys. Monogr. Ser., vol. 14, edited by J. G. Heacock, pp. 169-184, AGU, Washington, D. C., 1971.

Blackwell, D. D., Surface ground temperature variations in mountainous regions and a new topographic correction technique for heat flow measurements (abstract), Eos Trans. AGU, 54, 1207, 1973.

Blackwell, D. D., Terrestrial heat flow and its implications on the location of geothermal reservoirs in Washington, Wash. Div. Mines Geol. Inform. Circ., 50, 21-33, 1974.

Blackwell, D. D., and C. G. Baag, Heat flow in a 'blind' geothermal area near Marysville, Montana, Geophysics, 38, 941-956, 1973.

Blackwell, D. D., M. J. Holdaway, P. Morgan, D. Petefish, T. Rape, J. L. Steele, D. Thorstenson, and A. F. Waibel, Results and analysis of exploration and deep drilling at Marysville geothermal area, in The Marysville, Montana Geothermal Project, Final Report, pp. E.1-E.116, Battelle Pacific Northwest Laboratories, Richland, Wash., 1975.

Bodvarsson, G., On the temperature of water flowing through fractures, J. Geophys. Res., 74, 1987-1992, 1969.

Bodvarsson, G., and R. P. Lowell, Ocean floor heat flow and the circulation of interstitial waters, J. Geophys. Res., 77, 4472-4475, 1972.

Bowen, R. G., Progress report on geothermal measurements in Oregon, Ore Bin, 35, 6-7, 1973.

Bowen, R. G., and N. V. Peterson, Thermal springs and wells, Oreg. Dep. Geol. Miner. Ind. Misc. Pap., 14, 1970.

Bowen, R. G., D. D. Blackwell, D. A. Hull, and N. V. Peterson, Progress report on heat-flow study of the Brothers fault zone, central Oregon, Ore Bin, 38, 39-46, 1976.

Bredehoeft, J. D., and I. S. Papadopulos, Rates of vertical groundwater movement estimated from the earth's thermal profile, Water Resour. Res., 1, 325-328, 1965.

Brott, C. A., D. D. Blackwell, and J. C. Mitchell, Heat flow study of the Snake River Plain region, Idaho, Geothermal Investigations in Idaho, Water Inform. Bull. 30, part 8, 195 pp., Idaho Department of Water Resources, Boise, 1976.

Brune, J. N., T. L. Henyey, and R. F. Roy, Heat flow, stress, and rate of slip along the San Andreas Fault, California, J. Geophys. Res., 74, 3821-3827, 1969.

Carslaw, H. S., and J. C. Jaeger, Conduction of Heat in Solids, 2nd ed., Oxford University Press, New York, 1959.

Cermak, V., and A. M. Jessop, Heat flow, heat generation and crustal temperature in the Kapuskasing area of the Canadian Shield, Tectonophysics, 11, 287-303, 1971.

Combs, J., Heat flow and microearthquake studies, Coso geothermal area, China Lake, California, Final Report, Order Number 2800, contract N00123-74-C-2099, 65 pp., Advan. Res. Proj. Agency, Washington, D. C., 1975.

Combs, J., and G. Simmons, Terrestrial heat flow determinations in the north central United States, J. Geophys. Res., 78, 441-461, 1973.

Decker, E. R., and S. B. Smithson, Heat flow and gravity interpretation across the Rio Grande Rift in southern New Mexico and west Texas, J. Geophys. Res., 80, 2542-2552, 1975.

Diment, W. H., T. C. Urban, and F. A. Revetta, Some geophysical anomalies in the eastern United States, in The Nature of the Solid Earth, edited by E. C. Robertson, pp. 544-572, McGraw-Hill, New York, 1972.

Diment, W. H., T. C. Urban, J. H. Sass, B. V. Marshall, R. J. Munroe, and A. H. Lachenbruch, Temperatures and heat contents based on conductive transport of heat, U.S. Geol. Surv. Circ., 726, 84-103, 1975.

Dinwiddie, G. A., and L. J. Schroder, Summary of hydraulic testing in and chemical analyses of water samples from deep exploratory holes in Little Fish Lake, Monitor, Hot Creek, and Little Smoky Valleys, Nevada, Central Nevada-40, Tech. Lett. 474-90, 70 pp., U.S. Geol. Surv., Denver, Colorado, 1971.

Donaldson, I. G., Temperature gradients in the upper layers of the earth's crust due to convective water flows, J. Geophys. Res., 67, 3449-3459, 1962.

Eakin, T. E., A regional interbasin groundwater system in the White River area, southeastern Nevada, Water Resour. Res., 2, 251-271, 1966.

Fenneman, N. M., Physical divisions of the United States, U.S. Dep. of the Interior, Washington, D. C., 1946

Fournier, R. O., D. E. White, and A. H. Truesdell, Convective heat flow in Yellowstone National Park, in Proceedings of the Second United Nations Symposium on the Development and Use of Geothermal Resources, pp. 731-739, U.S. Government Printing Office, Washington, D. C., 1976.

Henyey, T. L., and G. J. Wasserburg, Heat flow near major strike-slip faults in California, J. Geophys. Res., 76, 7924-7946, 1971.

Hill, D. P., Structure of Long Valley caldera, California, from a seismic refraction experiment, J. Geophys. Res., 81, 745-753, 1976.

Hill, D. P., and L. C. Pakiser, Crustal structure between the Nevada Test Site and Boise, Idaho, from seismic refraction measurements, in The Earth Beneath the Continents, Geophys. Monogr. Ser., vol. 10, edited by J. S. Steinhart and T. J. Smith, pp. 391-419, AGU, Washington, D. C., 1966.

Hunt, C. B., and T. W. Robinson, Possible interbasin circulation of ground water in the southern part of the Great Basin, U.S. Geol. Surv. Prof. Pap., 400-B, B273-B274, 1960.

Jaeger, J. C., Heat flow and radioactivity in Australia, Earth Planet. Sci. Lett., 8, 285-292, 1970.

Jones, P. H., Hydrodynamics of geopressure in the northern Gulf of Mexico basin, J. Petrol. Technol., 21, 803-810, 1969.

Jones, P. H., and R. H. Wallace, Jr., Hydrogeologic aspects of structural deformation in the northern Gulf of Mexico basin, J. Res. U.S. Geol. Surv., 2, 511-517, 1974.

Lachenbruch, A. H., Preliminary geothermal model of the Sierra Nevada, J. Geophys. Res., 73, 6977-6989, 1968.

Lachenbruch, A. H., Crustal temperature and heat production: Implications of the linear heat flow relation, J. Geophys. Res., 75, 3291-3300, 1970.

Lachenbruch, A. H., Vertical gradients of heat production in the continental crust, 1, Theoretical detectability from near-surface measurements, J. Geophys. Res., 76, 3842-3851, 1971.

Lachenbruch, A. H., and C. M. Bunker, Vertical gradients of heat production in the continental crust, 2, Some estimates from borehole data, J. Geophys. Res., 76, 3852-3860, 1971.

Lachenbruch, A. H., and J. H. Sass, Thermo-mechanical aspects of the San Andreas, in Proceedings of the Conference on the Tectonic Problems of the San Andreas Fault, pp. 192-205, Stanford University Press, Stanford, Calif., 1973.

Lachenbruch, A. H., M. C. Brewer, G. W. Greene, and B. V. Marshall, Temperatures in permafrost, in Temperature--Its Measurement and Control in Science and Industry, pp. 791-803, Reinhold, New York, 1962.

Lachenbruch, A. H., J. H. Sass, R. J. Munroe, and T. H. Moses, Jr., Geothermal setting and simple heat conduction models for the Long Valley caldera, J. Geophys. Res., 81, 769-784, 1976a.

Lachenbruch, A. H., M. L. Sorey, R. E. Lewis, and J. H. Sass, The near-surface hydrothermal regime of Long Valley caldera, J. Geophys. Res., 81, 763-768, 1976b.

Lambert, I. B., and K. S. Heier, The vertical distribution of uranium, thorium, and potassium in the continental crust, Geochim. Cosmochim. Acta, 31, 377-390, 1967.

Lapwood, E. R., Convection of a fluid in a porous medium, Proc. Cambridge Phil. Soc., 44, 508-521, 1948.

Lee, W. H. K., and S. Uyeda, Review of heat flow data, in Terrestrial Heat Flow, Geophys. Monogr. Ser., vol. 8, edited by W. H. K. Lee, pp. 87-190, AGU, Washington, D. C., 1965.

Lowell, R. P., Circulation in fractures, hot springs, and convective heat transport on mid-ocean ridge crests, Geophys. J. Roy. Astron. Soc., 40, 351-365, 1975.

ıriner, R. H., J. B. Rapp, L. M. Willey, and T. S. Presser, The chemical composition and estimated minimum thermal reservoir temperatures of selected hot springs in Oregon, open file report, 27 pp., U.S. Geol. Surv., Menlo Park, Calif., 1974.

Mifflin, M. D., Delineation of ground-water flow systems in Nevada, Hydrol. Water Resour. Publ. 4, 111 pp., Desert Res. Inst., Reno, Nevada, 1968.

Morgan, P., D. D. Blackwell, R. E. Spafford, and R. B. Smith, Heat flow measurements in Yellowstone Lake and the thermal structure of the Yellowstone caldera, J. Geophys. Res., in press, 1977.

Nathenson, M., The effects of a step change in water flow on an initially linear profile of temperature, in Proceedings of the Geothermal Reservoir Engineering Workshop, vol. 2, Stanford Geothermal Program, Stanford, California, in press, 1977.

Olmsted, F. H., P. A. Glancy, J. R. Harrill, F. E. Rush, and A. S. VanDenburgh, Preliminary hydrogeologic appraisal of selected hydrothermal systems in northern and central Nevada, Open File Rep. 75-56, 267 pp., U.S. Geol. Surv., Menlo Park, Calif., 1975.

Papadopulos, S. S., R. H. Wallace, Jr., J. B. Wesselman, and R. E. Taylor, Assessment of onshore geopressured-geothermal resources in the northern Gulf of Mexico basin, U.S. Geol. Surv. Circ., 726, 125-146, 1975.

Peck, D. L., T. L. Wright, and J. G. Moore, Crystallization of tholeiitic basalt in Alae lava lake, Hawaii, Bull. Volcanol., 29, 629-656, 1966.

Rao, R. U. M., G. V. Rao, and H. Narain, Radioactive heat generation and heat flow in the Indian shield, Earth Planet. Sci. Lett., 30, 57-64, 1976.

Reiter, M., C. L. Edwards, H. Hartman, and C. Weidman, Terrestrial heat flow along the Rio Grande Rift, New Mexico and southern Colorado, Geol. Soc. Amer. Bull., 86, 811-818, 1975.

Renner, J. L., D. E. White, and D. L. Williams, Hydrothermal convection systems, U.S. Geol. Surv. Circ., 726, 5-57, 1975.

Roy, R. F., D. D. Blackwell, and F. Birch, Heat generation of plutonic rocks and continental heat flow provinces, Earth Planet. Sci. Lett., 5, 1-12, 1968a.

Roy, R. F., E. R. Decker, D. D. Blackwell, and F. Birch, Heat flow in the United States, J. Geophys. Res., 73, 5207-5221, 1968b.

Roy, R. F., D. D. Blackwell, and E. R. Decker, Continental heat flow, in The Nature of the Solid Earth, edited by E. C. Robertson, pp. 506-543, McGraw-Hill, New York, 1972.

Sass, J. H., and E. A. Sammel, Heat flow data and their relation to observed geothermal phenomena near Klamath Falls, Oregon, J. Geophys. Res., 81, 4863-4868, 1976.

Sass, J. H., A. H. Lachenbruch, R. J. Munroe, G. W. Greene, and T. H. Moses, Jr., Heat flow in the western United States, J. Geophys. Res., 76, 6376-6413, 1971.

Sass, J. H., W. H. Diment, A. H. Lachenbruch, B. V. Marshall, R. J. Munroe, T. H. Moses, Jr., and T. C. Urban, A new heat-flow contour map of the conterminous United States, Open File Rep. 76-756, 24 pp., U.S. Geol. Surv., Menlo Park, Calif., 1976a.

Sass, J. H., S. P. Galanis, Jr., R. J. Munroe, and T. C. Urban, Heat-flow data from southeastern Oregon, Open File Rep. 76-217, 52 pp., U.S. Geol. Surv., Menlo Park, Calif., 1976b.

Sass, J. H., J. C. Jaeger, and R. J. Munroe, Heat flow and near-surface radioactivity in the Australian continental crust, Open File Rep. 76-250, 91 pp., U.S. Geol. Surv., Menlo Park, Calif., 1976c.

Sass, J. H., F. H. Olmsted, M. L. Sorey, H. A. Wollenberg, A. H. Lachenbruch, R. J. Munroe, and S. P. Galanis, Jr., Geothermal data from test wells drilled in Grass Valley and Buffalo Valley, Nevada, Open File Rep. 76-85, 43 pp., U.S. Geol. Surv., Menlo Park, Calif., 1976d.

Sclater, J. G., and J. Francheteau, The implications of terrestrial heat flow observations on current tectonic and geochemical models of the crust and upper mantle of the earth, Geophys. J. Roy. Astron. Soc., 20, 509-542, 1970.

Smith, D. L., Heat flow, radioactive heat generation, and theoretical tectonics for northwestern Mexico, Earth Planet. Sci. Lett., 23, 43-52, 1974.

Smith, R. L., and H. R. Shaw, Igneous-related geothermal systems, U.S. Geol. Surv. Circ., 726, 58-83, 1975.

Sorey, M. L., Numerical modeling of liquid geothermal systems, Open File Rep. 75-613, 66 pp., U.S. Geol. Surv., Menlo Park, Calif., 1975.

Sorey, M. L., and R. E. Lewis, Convective heat flow from hot springs in the Long Valley caldera, Mono County, California, J. Geophys. Res., 81, 785-791, 1976.

Steeples, D. W., and H. M. Iyer, Low-velocity zone under Long Valley as determined from teleseismic events, J. Geophys. Res., 81, 849-860, 1976.

Stewart, J. H., and J. E. Carlson, Generalized maps showing distribution, lithology, and age of Cenozoic igneous rocks in the western United States, scale 1:5,000,000, in Cenozoic Tectonics and Regional Geophysics of the Western Cordillera, Spec. Pap., edited by R. B. Smith and G. P. Eaton, Geological Society of America, Boulder, Colorado, in press, 1977.

Swanberg, C. A., Vertical distribution of heat generation in the Idaho batholith, J. Geophys. Res., 77, 2508-2513, 1972.

Swanberg, C. A., M. D. Chessman, G. Simmons, S. B. Smithson, G. Gronlie, and K. S. Heier, Heat-flow-heat-generation studies in Norway, Tectonophysics, 23, 31-48, 1974.

Thompson, G. A., and D. B. Burke, Regional geophysics of the Basin and Range province, Annu. Rev. Earth Planet. Sci., 2, 213-238, 1974.

Urban, T. C., and W. H. Diment, Heat flow on the south flank of the Snake River Rift (abstract), Geol. Soc. Amer. Abstr. Programs, 7, 648, 1975.

White, D. E., Geothermal energy, U.S. Geol. Surv. Circ., 519, 17 pp., 1965.

White, D. E., Hydrology, activity, and heat flow of the Steamboat Springs thermal system, Washoe County Nevada, U.S. Geol. Surv. Prof. Pap., 458-C, 109 pp., 1968.

Winograd, I. J., and W. Thordarson, Hydrogeologic and hydrochemical framework, South-Central Great Basin, Nevada-California, with special reference to the Nevada Test Site, U.S. Geol. Surv. Prof. Pap., 712-C, 126 pp., 1975.

Wyllie, P. J., Experimental limits for melting in the earth's crust and upper mantle, in The Structure and Physical Properties of the Earth's Crust, Geophys. Monogr. Ser., vol. 14, edited by J. G. Heacock, pp. 279-301, AGU, Washington, D. C., 1971.

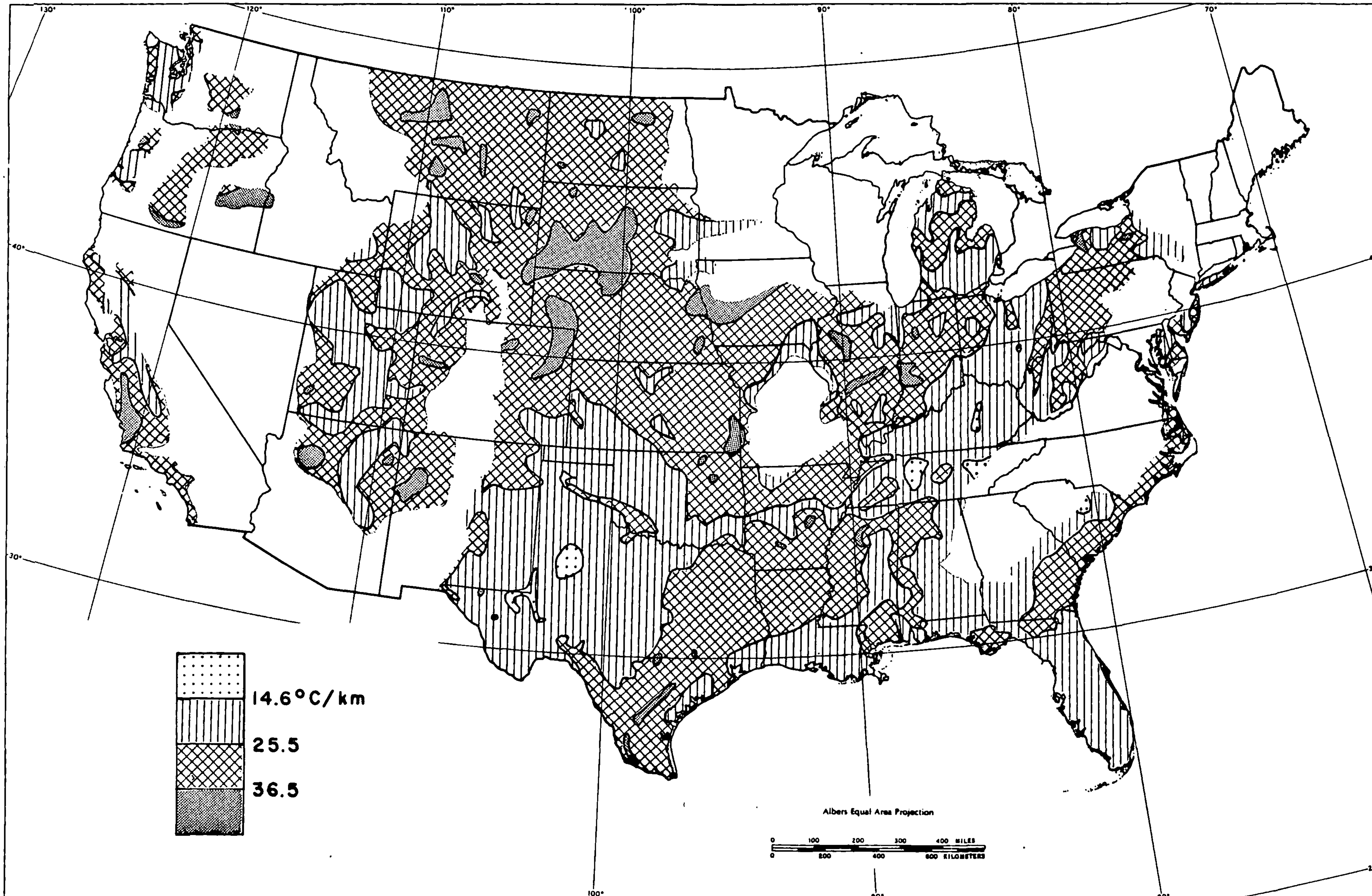

Generalized AAPG-USGS (1976) temperature-gradient map (from Guffanti and Nathenson, 1980).

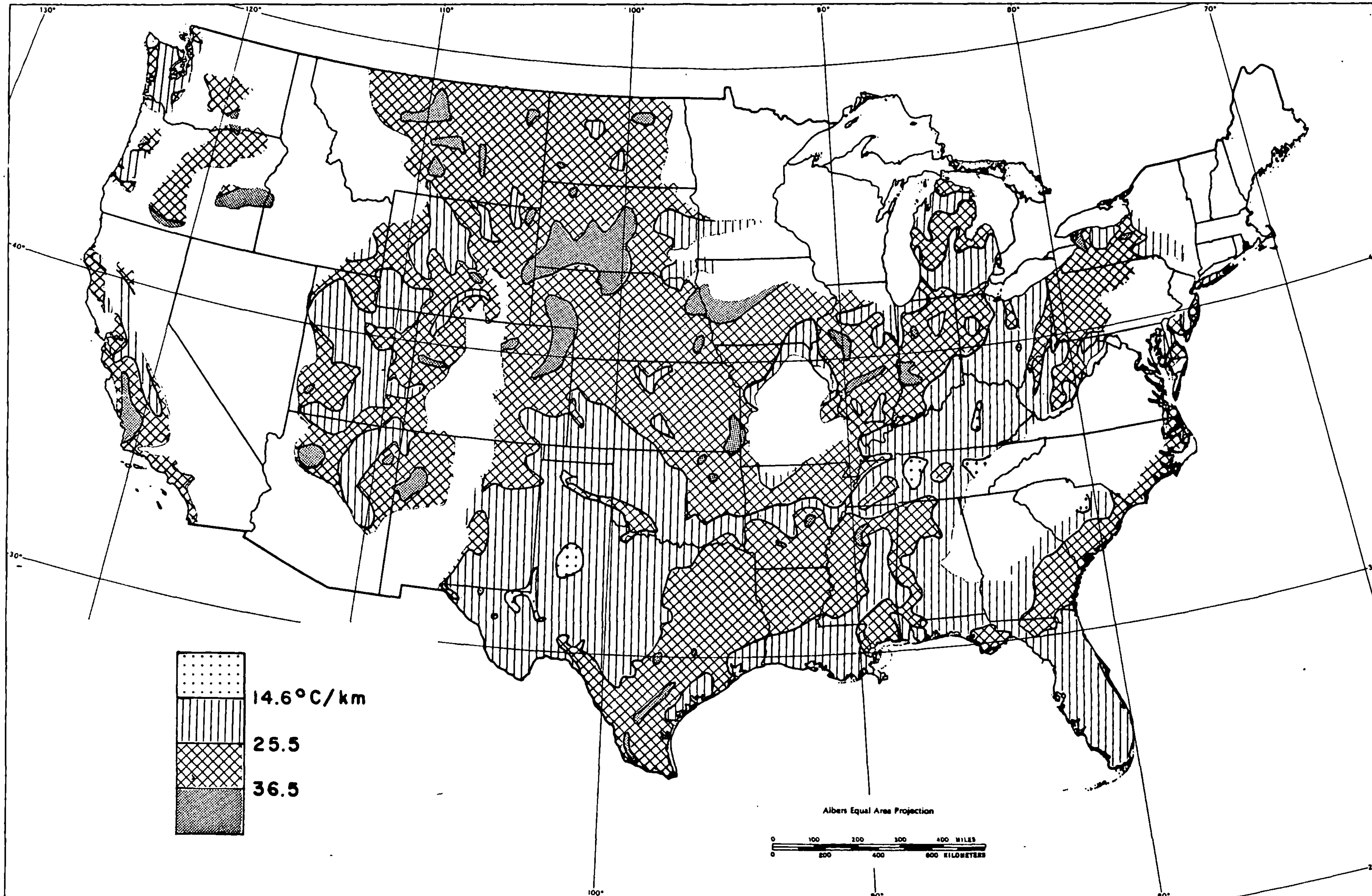

Generalized AAPG-USGS (1976) temperature-gradient map (from Guffanti and Nathenson, 1980).

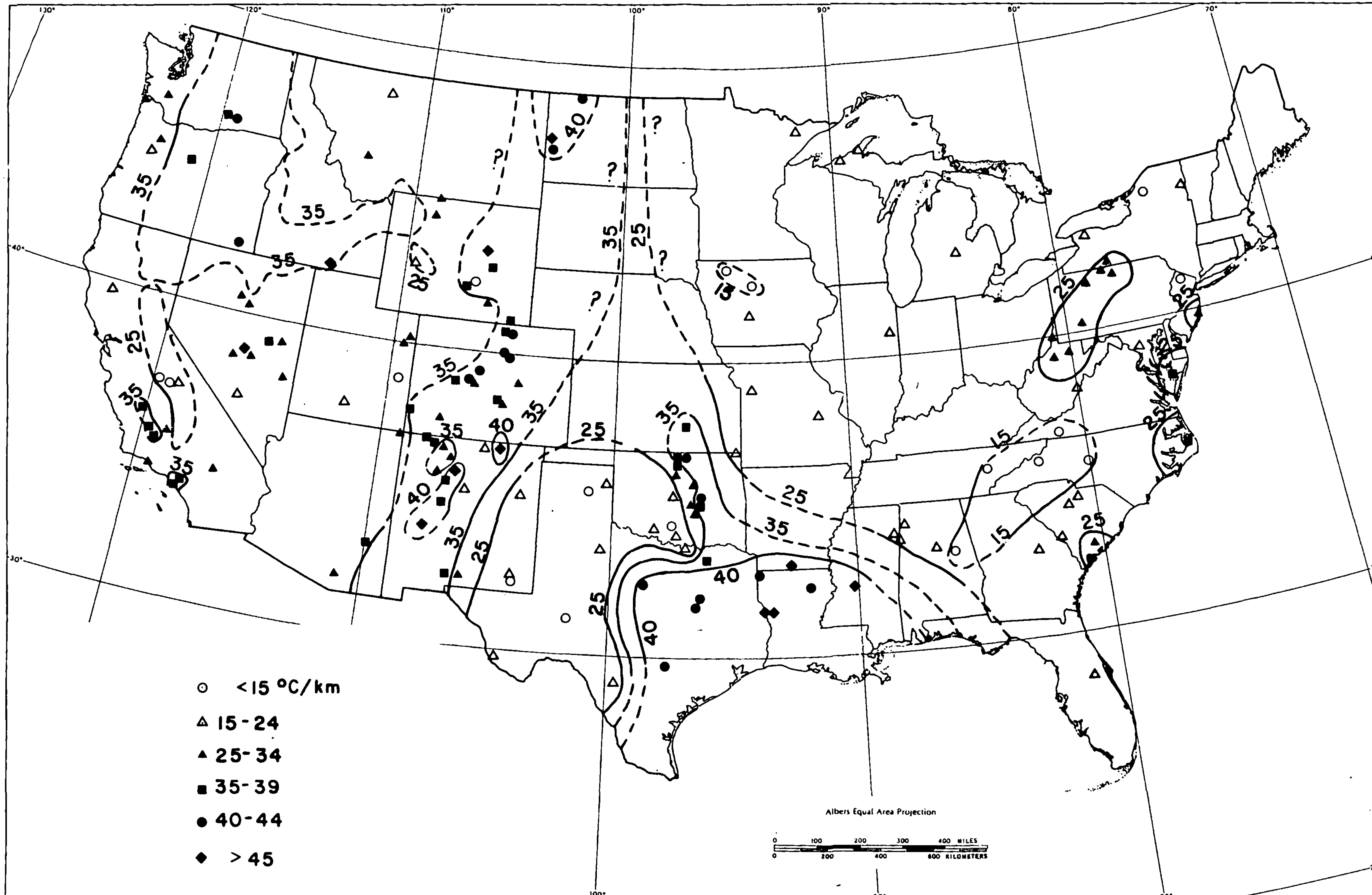

Preliminary temperature-gradient map of the conterminous United States (Guffanti and Nathenson, 1980).

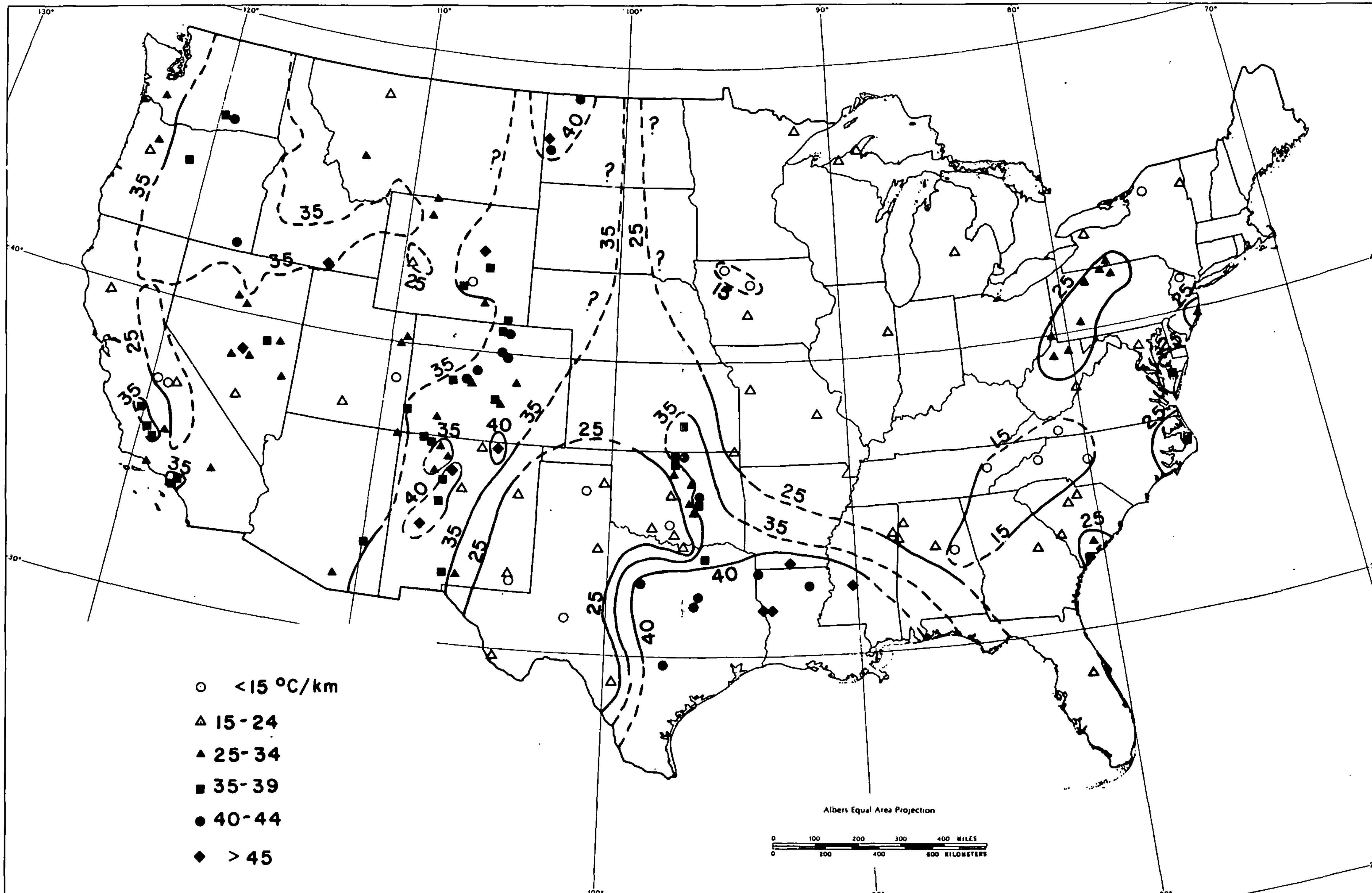

Preliminary temperature-gradient map of the conterminous United States (Guffanti and Nathenson, 1980).

VOL. 76, NO. 26 JOURNAL OF GEOPHYSICAL RESEARCH SEPTEMBER 10, 1971

Heat Flow in the Western United States

J. H. SASS, ARTHUR H. LACHENBRUCH, ROBERT J. MUNROE,
GORDON W. GREENE, AND THOMAS H. MOSES, JR.

U.S. Geological Survey, Menlo Park, California 94025

Between 1962 and late 1970, subsurface temperature measurements were attempted at more than a thousand drilling sites in the western United States. Temperatures from over 150 boreholes at about 100 distinct sites were suitable for estimates of the vertical geothermal flux. These results more than double the data from the western United States and confirm that heat flow is variable but generally high in this region. Within the over-all pattern of high heat flow, there are several distinct geographical regions, each occupying several hundred square kilometers, characterized by low-to-normal heat flow. Normal values were measured in the Pacific northwestern coastal region and the northwestern Columbia Plateaus. Additional results confirm the previously reported trend of very low heat flow in the western Sierra Nevada, increasing to normal near the crest of the range. The present work also confirms that heat flow is high in the northern and southern Rocky Mountains and somewhat lower in the central Rockies. The north-central part of the Colorado Plateau is a region of normal heat flow with higher values near its eastern border with the southern Rockies. The Basin and Range province as a whole is characterized by high heat flow that extends to within 10 to 20 km of the eastern scarp of the Sierra Nevada. The abrupt thermal transition between the Sierra Nevada and the Basin and Range province may occur partly in the Sierra Nevada physiographic province. Between Las Vegas and Eureka, Nevada, there is a large previously undetected zone of low-to-normal heat flow that is most probably the result of a systematic, regional water circulation to depths of a few kilometers. North of this zone, there is an area of several hundred square kilometers characterized by heat flows of 2.5 HFU (μcal/cm^2 sec) or greater. In central California and adjoining western Nevada, a preliminary contour map suggests a heat-flow pattern with alignment parallel to the strike of the major geologic structures.

Since radioactivity was first discovered, the heat flowing from the earth's deep interior has been considered an important constraint on geophysical and geochemical models of the earth. Until fairly recently, however, the measurement of heat flow on land was accorded a low priority compared with other geophysical measurements, so much so that *Birch* [1954] could report only three reliable measurements for the whole of the United States, and only a dozen or so independent regional determinations (attributable largely to E. C. Bullard and his colleagues) for all the continents. During the late 1950's and 1960's, the early efforts of Francis Birch in the United States, J. C. Jaeger in Australia, and A. D. Misener in Canada, among others, were followed up by these workers, their colleagues, and their students, with the result that the number of reports of reliable heat-flow data from continents is approaching one thousand.

Roy et al. [1968b] recently summarized the work of almost a decade by Birch and his students in the conterminous United States. Their paper included data from almost all major physiographic units, and they were able to make a number of generalizations that heretofore were impossible owing to the scarcity of data. Their results confirmed the earlier observation by L. E. Howard [see *Jaeger and Thyer*, 1960; also, *Howard and Sass*, 1964; *Kraskovski*, 1961] that the heat flow in old shield areas was lower, on the average, than that from younger areas. They also were able to confirm that high heat flow was characteristic of the Basin and Range physiographic province and that low-to-normal heat flow was characteristic of the Sierra Nevada, a result indicated also by independent observations [*Clark*, 1957; *Lachenbruch et al.*, 1966].

The data presented by *Roy et al.* [1968b] have been elaborated and interpreted in papers by *Birch et al.* [1968], *Roy et al.* [1968a], *Decker* [1969], *Blackwell* [1969], and *Lachenbruch* [1970]. The discovery that heat flow is a linear function of surface radioactivity for plutonic rocks of the Appalachian region by *Birch et al.* [1968], its independent confirmation for the Sierra Nevada [*Lachenbruch*, 1968*a*], and its extension to other heat-flow provinces in the United States [*Roy et al.*, 1968*a*] has led to new insights profoundly influencing the interpretation of pre-existing data and the direction of studies initiated since 1968. The results remove much of the ambiguity from estimates of crustal temperatures, mantle heat flow, and vertical distribution of crustal radioactivity. In fact, with a few plausible geologic assumptions, crustal radioactivity beneath plutons is uniquely determined (as exponential), and the other quantities are severely constrained [*Lachenbruch*, 1970]. As a result of these findings, much recent work has focused on plutons and on attempts to establish the limits of validity of the heat flow–heat production relation, but many of the results have not yet reached the published literature.

Decker [1969] amplified the results of *Roy et al.* [1968*b*] from the central and southern Rocky Mountain area and interpreted them in the light of the geologic history of the region and of the radioactivity (both measured and inferred) of the area. *Blackwell* [1969] made a similar interpretation of his results from the northwestern States and defined the 'Cordilleran Thermal Anomaly Zone' (CTAZ), comprising the northern Basin and Range, the northern Rocky Mountains, and (by interpolation) the Snake River plain. *Warren et al.* [1969], *Spicer* [1964], and *Costain and Wright* [1968] added several data in the Basin and Range and Colorado Plateaus. *Henyey* [1968] presented several values near strike-slip faults in central and southern California. *Combs* [1970] and *Herrin and Clark* [1956] measured heat flow in the western Great Plains.

The work described here grew out of geothermal studies of permafrost terrane begun around 1950. The portion of that study pertaining to heat flow in the Arctic and the related work in other countries has recently been reviewed [*Lachenbruch and Marshall*, 1969]. Heat-flow studies in Alaska are continuing, and they will be reported separately. In this paper we summarize results of measurements begun in the conterminous United States in about 1962. A progress report on these studies involving some 50 determinations at 23 sites in the western United States was given by *Sass et al.* [1968*b*], and detailed accounts have already been presented for heat-flow results from Menlo Park, California [*Sass et al.*, 1968*c*] and the Sierra Nevada [*Lachenbruch*, 1968*a*].

Of necessity, *Roy et al.* [1968*b*] broke with the geothermal tradition of detailed documentation of individual heat-flow data. They presented their data essentially as a summary table in which, for each borehole (or mine or tunnel), the principal elements of the heat-flow calculation and, of course, the heat-flow value itself, were presented in a single line.

The present paper is similar in scope and format to the work of *Roy et al.* [1968*b*]. It should be noted, however, that a detailed compilation of basic data (temperatures, thermal conductivities, terrain information, etc.) for these and other recent heat-flow determinations from the United States is in preparation, and when published it will allow critical evaluation of recent results from all United States heat-flow groups.

The following symbols and units are used in this paper:

- T, temperature, °C.
- Γ, vertical temperature gradient ($\partial T/\partial z$), °C/km.
- N, number of thermal conductivity samples.
- K, thermal conductivity, mcal/cm sec °C.
- R, electrical resistance, ohms.
- q, heat flow; 1 heat-flow unit (HFU) = 1 μcal/cm² sec.
- $\pm$, refers to the standard error in all cases.

TEMPERATURE MEASUREMENTS

Temperature gradients generally were determined from temperature measurements made at discrete depths in boreholes. The measuring system consisted of a multiconductor cable and hoist, a thermistor thermometer, and a resistance measuring system. In general, measurements were obtained by one of the following three modes of operation:

1. *The well-logging mode.* A truck- or trailer-mounted, hydraulically powered winch with up to 5 km of standard 4-conductor well-logging cable is driven to the site. The truck

contains an instrument rack with the appropriate measuring equipment.

2. *The portable mode.* Some sites are inaccessible by truck or are a long drive from home. In these cases, a portable winch containing up to 1.5 km of light 3-conductor cable armored in stainless steel, which could be backpacked or carried in a light aircraft, is combined with a lightweight (~4·kg) resistance bridge.

3. *The suitcase mode.* This is a compromise between modes 1 and 2, ideally suited to very deep holes at distant locations where commercial well-logging units or other suitable hoist-cable units are available. In this mode, the lightweight resistance bridge, temperature transducers, and suitable adaptors are packed into a suitcase and sent as part of the operator's baggage on common carriers. This mode has been used by one of us (THM) to obtain useful temperature measurements at sites as far apart as Amchitka Island, Mindanao, and Tehran, Iran [*Sass and Munroe*, 1970; *Sass et al.*, 1971]. Th choice among the three modes was usually di tated by logistical requirements, and there essentially no difference among them in the bas equipment, principles of measurement, or th accuracy of the data obtained. The minor di ferences that do exist are discussed below.

Figure 1 illustrates the basic principles of th transducers and surface equipment.

Resistance measurement. The resistanc bridges (Figure 1*a*) are all identical in princip to the Siemens variant of the wheatstone bridg illustrated in Figure 1*a* of *Roy et al.* [1968*b*] The bridge compensates almost completely fo the series resistance of the cable conducto (there is a small relative error, less than 0.01°C approximately equivalent to the variation i $|R_1-R_3|$). There is no provision to compensat for the shunt resistance of the cable [see, e.g *Beck*, 1965] because (1) when the cables wer functioning properly, the shunt resistance be

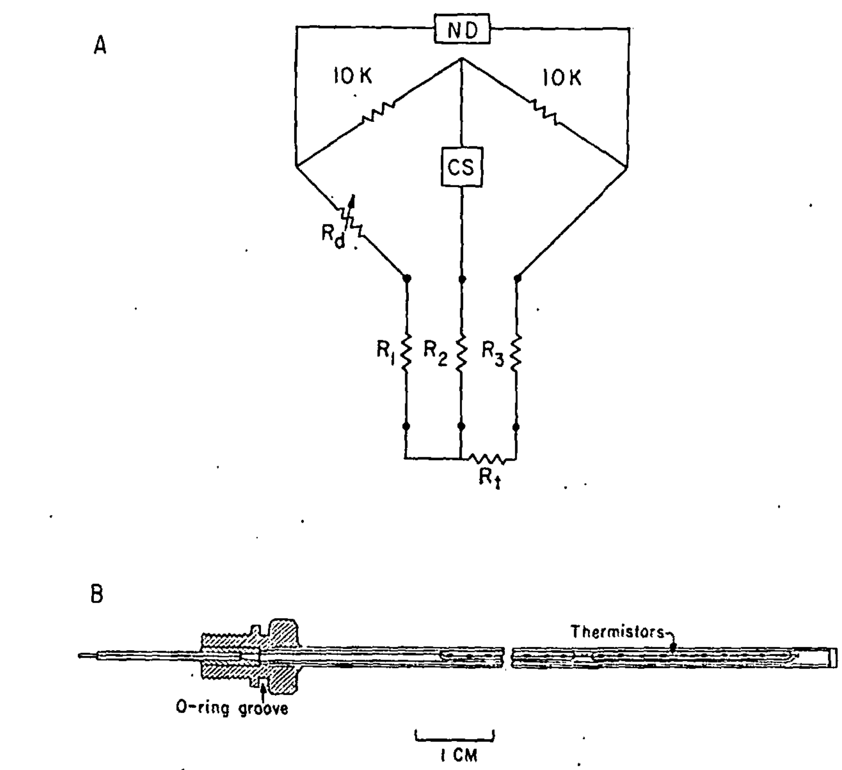

Fig. 1. (*a*) R_t, thermistor; R_1, R_2, and R_3, lead resistances; R_d, 6-decade variable resistor; *CS*, current source (1.35-volt mercury cell with voltage divider); ND, battery-operated null detector. (Redrawn from *Roy et al.* [1968*b*].) (*b*) Sketch of thermistor probe.

tween individual conductors always exceeded 10 megohms, a value high enough to preclude absolute errors of more than a few hundredths of a degree for the usual range of thermistor resistances (1 to 20 kilohms) and (2) when the shunt resistance fell below a few megohms (usually because of failure of the cable-head), there was a noticeable increase in the noise level of the null detector and difficulty in obtaining a null balance. When this occurred, repairs were effected or another cable unit was substituted for the defective one.

The resistive components of the bridges were chosen for their simplicity of operation, stability, and temperature insensitivity. The various bridges have been compared with one another and with precise secondary standard resistors traceable to the National Bureau of Standards. In no case has the discrepancy in resistance exceeded a few tenths of an ohm. Furthermore, the portable bridges have been operated in conditions ranging from the jungles of Panama and Liberia to the arctic environments of Greenland and the north slope of Alaska without serious operational problems.

Temperature transducers. Figure 1*b* illustrates the essential features of the thermistor probe assembly that formed the basis of most temperature sondes. It is basically a stainless steel tube 0.4 cm in outer diameter and 15 cm long containing, in its lower 9 cm, a series-parallel network of 20 thermistor beads having a nominal resistance of 8 to 10 kΩ at 20°C and a temperature coefficient of resistance of about $-4\%/°C$. The thermistor section is filled with a silicone lubricant of low viscosity, which facilitates thermal contact with the probe wall. An air space is left above the thermistor section to accommodate the compressive stresses encountered in deep holes without transmitting them to the thermistors. The probe has a time constant of about 2 sec in still water and will dissipate 100 μw in still water with a temperature rise of less than 10^{-3}°C. Recent advances in solid-state technology have resulted in rugged, portable, and inexpensive electronic null detectors capable of a sensitivity of 10^{-4}°C with a current of only a few μa, so that the high-power dissipation characteristic is no longer important, and single beads can be used.

For modes 1 and 3, the sondes were constructed by machining a 9-cm length of cylindrical stock (SAE #4130 steel or Lexan, a high-impact–strength plastic), 2.54 cm in diameter to accommodate one- or three-probe assemblies at one end and a cablehead of 2.54-cm diameter at the other. In the three-element variety the sonde could be operated with only one element in the circuit or with all three elements in series (this to preserve sensitivity at high temperatures). The mode 2 sondes were simply aluminum cableheads that were 8 cm long and 1.27 cm in diameter, fitted to a single thermistor assembly with O-ring seals.

For all modes, slotted metal 'sinker bars' were attached to the cable above the sonde to provide line tension and/or to aid in penetration of viscous well fluids. With metal cableheads, a short (20- to 30-cm) length of 'Lexan' was usually inserted between the sonde and the sinker-bar column to thermally decouple the sonde from the sinker bars. In modes 1 and 3, the winches were fitted with high-quality slip rings that allowed continuous monitoring of the transducers. In mode 2, considerations of weight versus contact resistance resulted in the sacrifice of this convenience, and a signal lead was plugged in to the winch when the cable was stationary. Temperatures were measured at regular discrete intervals ranging from less than 1 meter (for short-cored intervals) to 15 meters in deep holes (>1 km) in crystalline rocks.

Thermistor calibration. Most thermistor probes were calibrated at the factory at 10° intervals between −10° and +150°C. The precision of each calibration point was about ±0.1°C, but by fitting a series of segments of the form

$$T = (A/\text{Log } R + B) - C \qquad (1)$$

to overlapping 30° temperature ranges and adjusting erroneous values to produce smooth fits, it was possible to obtain values of A, B, and C for which differential temperatures for the same thermistor could be calculated to a precision of better than 0.01°C. This precision is adequate for most heat-flow purposes. There are, however, some instances where very high precision is required. These include precise temperature-gradient determinations at ~1-meter intervals, measurements near the freezing point in permafrost terranes, and measurements at different levels in mines using different sondes. To be prepared for these cases, most thermistors were recalibrated over the range $-10°$ to $80°$ or $100°C$ in our laboratory. The recalibrations were made at $10°$ intervals, but to a precision of ±1 or 2×10^{-3}°C relative to a standardized platinum resistance thermometer. This thermometer was checked, in turn, in a triple-point cell every three to four months. For the past three years, the platinum standard has been drifting upward fairly steadily at the rate of about 0.01°C/year, and the appropriate corrections have been applied to thermistors. Recent batches of thermistor probes have proved extremely stable, with drift rates of 0.01°C/year or less when operated in the temperature range of $-10°$ to $+150°C$.

The recalibrated thermistors give values of A, B, and C (equation 1) for which the precision of differential temperatures approaches the sensitivity of the system (10^{-4}°C). The error in absolute temperature is more difficult to assess because of the many possible sources of error; however, on the basis of repeated measurements in the same hole with different probes and cables, and of comparisons with independent measurements by systems claiming a similar relative accuracy (R. F. Roy, personal communication), the error in absolute temperature is probably only a few hundredths of a degree, and certainly is no greater than one or two tenths of a degree centigrade in the worst case.

Some of the early temperature measurements were made with strings of thermistors originally designed to be frozen in place in Arctic locations [see *Lachenbruch et al.*, 1962]. With these, the temperatures at successive depths were measured with different thermistors, and errors of up to 0.1°C could occur in the temperature difference between adjacent thermistors, although they were usually much smaller. The high relative error does not seriously affect temperature-gradient estimates when these are determined by least-squares straight-line fits, as was done in most of this work.

THERMAL CONDUCTIVITY

By far the majority of thermal-conductivity measurements were made with the modified Birch-type [*Birch*, 1950] divided-bar apparatus described below.

With soft and poorly consolidated rocks, the needle-probe technique [*Von Herzen and Maxwell*, 1959] was used to determine conducti
The probe system is used routinely for con
tivity determinations on ocean-bottom cores
was described by *Lachenbruch and Mar*
[1966]. Whenever possible, the samples
sealed in plastic tubes (which, in turn,
dipped in paraffin wax) immediately after b
removed from the ground to preserve t
moisture content.

The quality of the needle-probe data va
considerably. Fine-grained, clayey sedim
gave satisfactory results, but for pebbly s
ments, there were contact problems and p
lems associated with the size of particles r
tive to the volume sampled by the probe.
some instances, the sample had been allowe
dry, and water was introduced prior to m
urement. In the most favorable cases, nee
probe determinations were very precise (±1
A more common uncertainty is probably ab
$\pm10\%$, with errors of $\pm20\%$ possible in so
'problem' cases.

For many holes, the only samples availa
were drill cuttings. For others, the rock
so badly weathered or so poorly cemented t
suitable disks could not be prepared for
divided bar, but the grains were too hard
permit drilling of the long small-diameter ho
required for a needle-probe determination.
these instances, conductivities were measured
fragments using the chip technique descri
by *Sass et al.* [1971]. For a given determinati
this technique has an over-all accuracy
$\pm10\%$, which is adequate in view of the f
that the standard deviation of a single (p
cise) conductivity determination due to co
positional heterogeneity on the scale of a f
centimeters is of the same order.

The divided-bar apparatus. The apparat
consists of four units of the type depict
schematically in Figure 2, connected in paral
to a pair of constant-temperature baths. T
cylindrical elements usually are either 3.81 cm
2.86 cm in diameter. The basic principles
operation of this apparatus are well kno
[see, e.g., *Birch*, 1950]. Briefly, cylindrical ro
specimens of unknown conductivity are plac
in series with copper disks containing wells f
temperature transducers and with standa
disks of known conductivity (0.3-cm-thick fus
silica disks in this case). The extreme ends
this 'stack' are held at different, constant tem

peratures, the entire apparatus is allowed to achieve a thermal steady state, and the temperature drops across standard disks are compared with those across samples of unknown conductivity. The latter conductivity is determined from the ratios of the temperature drops and thicknesses between sample and standard. In the configuration illustrated in Figure 2, the conductivities of two unknowns are determined simultaneously.

The apparatus was calibrated using *Ratcliffe*'s [1959] values for quartz and fused silica as standard values. It was usually operated at a mean temperature of about 25°C, with a total temperature drop of 7° to 10°C between the warm and the cold baths. Over a period of 20 minutes or so (the average duration of a determination), each bath can be maintained at a mean temperature constant to within a few thousandths of a degree. Short-period (~1 to 10 sec) variations of up to a few hundredths of a degree are damped out by 0.2-cm-thick disks of Micarta (laminated plastic and linen) at each end of the stack.

The divided bar is very simple in principle, but there are two practical problems that must be carefully managed to avoid large errors. These are radial heat losses and contact resistance. The first is minimized by careful lagging with styrofoam. Three procedures are followed to reduce contact resistances to negligible levels.

1. The faces of all disks are made as flat and as parallel as possible. For standards and copper disks the tolerances are ±0.0005 cm. For samples they are relaxed to ±0.002 cm for flatness and ±0.005 cm for parallelism. (The rubber pad beneath the cold bath, shown in Fig. 2, easily accommodates wedges of this magnitude.)

2. The faces of all disks are coated with a very thin film of a paste or liquid of relatively high conductivity (1 or 2 mcal/cm sec °C). A commercial mixture of silicone grease and metal oxide or a liquid household detergent were used as contact films.

3. Axial pressure of 80 to 100 bars is applied to the stack to extrude the excess contact material and to minimize the variation in contact resistance within a series of determinations.

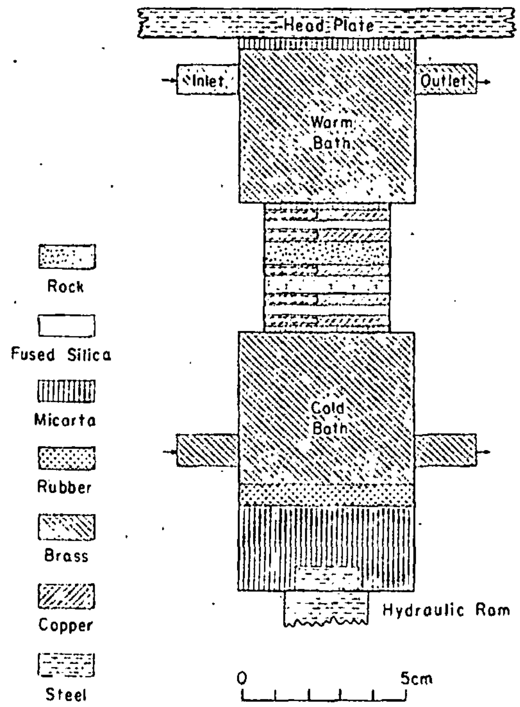

Fig. 2. Schematic representation of the divided-bar apparatus: The dashed lines in the copper sections are projections of cylindrical thermistor wells.

Walsh and Decker [1966] have demonstrated that even for rocks of low porosity, significant errors in conductivity can result if the rocks are not saturated (their normal condition in situ). All rocks were saturated with water under vacuum prior to measurement.

For many rocks, thermal conductivity is sufficiently sensitive to temperature that corrections must be made if the in situ temperature is more than 5° or 10°C different from that at which the conductivity determination is made. The temperature coefficients of thermal resistivity for a number of common rocks were determined by *Birch and Clark* [1940]. Checks between 20° and 50°C on a few of the samples from the present work gave values consistent with those of Birch and Clark, and the appropriate coefficients were used in correcting the measured conductivity to in situ temperatures.

CALCULATION OF HEAT FLOW

In general the heat flow q is obtained by combining in some way the measured thermal conductivities and temperature gradients according to

$$q = K\Gamma \tag{2}$$

The most appropriate way of doing this depends on the actual distribution of conductivity and temperature with depth and on how well these distributions are known at any site. The common methods of data reduction are reviewed by *Hyndman and Sass* [1966]. The three methods that were used in this study are described in detail in the next section.

The quantity determined from (2) is usually referred to as the uncorrected heat flow. It is based on the assumption that all the heat transfer is by one-dimensional steady-state conduction. Departures from this condition can lead to local heat-flow determinations quite unrepresentative of the regional vertical conductive flux. An effort was made to identify such departures at each site and either to account for them or to allow for them in evaluating the reliability of the determinations. Effects considered include vertical water flow [see e.g., *Birch,* 1947; *Bredehoeft and Papadopulos,* 1965], drilling disturbance [*Bullard,* 1947; *Lachenbruch and Brewer,* 1959; *Jaeger,* 1961], climatic change [*Birch,* 1948], uplift, erosion, and sedimentation [*Birch,* 1950; *Jaeger,* 1965], effects of lakes, rivers, and other regions of anomalous surface temperature [*Lachenbruch,* 1957*a*, *b*], and the steady-state effects of topographic relief and thermal refraction in dissimilar rocks. Only the last two warrant discussion here. It is important, however, that many conditions leading to nonconductive, transient, or two- and three-dimensional heat flow can go undetected, and this must certainly contribute to the scatter of internally consistent heat-flow determinations.

Topographic corrections. Topographic relief can distort the temperature field sufficiently to cause errors in heat-flow determinations. The map reading involved in detailed topographic corrections is very tedious, and it is often impossible to judge, simply by looking at a topographic map, whether the effects are significant. In view of this, we considered the problem of terrain correction in two stages. If topographic relief in the area exceeded a few tens of meters, we made a preliminary estimate of its steady-state effect based on an exaggerated two-dimensional approximation to the true topography. The approximations were Lees-type hills, valleys, or monoclines [see *Jaeger and Sass,* 1963] or plane slopes [*Lachenbruch,* 1968*b*]. In the rare instances where the two-dimensional representation seemed a reasonable approximation to the true topography (some ridges and fault scarps, or fairly distant relief) this correction was used. In the majority of cases, however, the two-dimensional correction was not used. If it did not exceed 5% (about 70% of the cases), no topographic correction was made. If it did exceed 5%, a three-dimensional Birch-type correction [*Birch,* 1950] was performed in which the effect of all topography outward from the borehole collar to at least 90% of the solid angle subtended by the lowest temperature measurement point was calculated. These corrections were invariably substantially smaller than the two-dimensional approximations, so that we felt justified in ignoring topography where the latter correction was 5% or less. It should be noted that the first-order correction of *Birch* [1950] can result in large errors if steep slopes occur at or near the station [see e.g. *Lachenbruch,* 1968*b*].

For all topographic corrections, we assumed that the ground-surface temperature decreased 5°C/km with increasing elevation, a generalized value obtained from weather bureau records and from shallow holes. Although this simple one-dimensional model can introduce significant errors in rare cases [see, e.g., *Blackwell,* 1969], the available information on local variations is usually too scant to define the exact local conditions, and the simple assumption is the best that can be made.

Refraction. When heat flow is determined from measurements near steeply inclined contacts between rocks of contrasting conductivity, the one-dimensional interpretation can result in substantial errors. Heat flow will be underestimated if the measurements are in the lower conductivity rocks and overestimated for measurements in the higher conductivity rocks. *Howard and Sass* [1964] discussed an example of a probable underestimate of nearly 100% near Rum Jungle in northern Australia.

Corrections for refraction are sensitive to geometric details that are usually unknown; however, rough estimates of its effect can often be obtained from simple models [see e.g., *Roy*, 1963; *Hyndman and Sass*, 1966; *Sass et al.*, 1968*a*; *Von Herzen and Uyeda*, 1963; *Lachenbruch and Marshall*, 1966]. In a region like the Basin and Range province, where alluvial valleys conceal down-faulted bedrock pediments that can have conductivities three or four times as high as the valley sediments, refraction anomalies can be very large [see *Lachenbruch*, 1968*b*, p. 399]. A series of measurements near Tucson, Arizona (discussed below), provides an example of the probable effects of unknown conductivity structure.

THE HEAT-FLOW VALUES

The heat-flow values are presented in Tables 1 through 8, one table for each major physiographic-tectonic province in the western United States. The boundaries of these provinces, based on those of *Fenneman* [1928] are shown in Figure 3, together with the locations of previously published heat flows and the present values. (See also Figure 4.)

In most papers on heat flow, the standard error or some other statistical measure of scatter is calculated for each of the principal elements of the heat-flow calculation (conductivity and temperature gradient). These are combined in some way to arrive at a formal statistical estimate of the reliability of the heat-flow value. It is then pointed out that the formal standard error does not adequately take account of the possible sources of error, but that (hopefully) the values are accurate to within some reasonable limits. This is the general procedure followed here, but we have defined three broad categories to take some account of the large range of quality among the data. In assigning a heat flow to one category or another we were guided by the objective general criteria listed below, but, in some borderline cases, rather subjective judgments based on experience in other areas decided the issue.

Each of the eight tables presents data in at least one of the following three categories:

Category 1. These are determinations of the highest quality. Temperature profiles are smooth, with no sign of hydrologic disturbances below depths of a few tens of meters. Sufficient samples of rock are available to characterize the effective conductivity of the measured section, and no variations that cannot be explained and corrected are apparent. If conductivity stratification is present, component heat flows for the various individual strata are in good agreement. Typical uncertainties for category 1 are less than $\pm 10\%$.

Category 2. For this category, the uncertainty in heat flow is greater than for category 1, but it probably is no greater than $\pm 20\%$. Included here are temperature profiles in which there are suggestions of local hydrologic disturbances. Also included are cases where the conductivity sample is unsatisfactory, owing to either too few samples or an unusually large scatter in conductivity values. In the stratified cases, if component heat flows do not agree satisfactorily and there is not enough structural information to resolve the disagreement with refraction calculations, the average of the components is taken and the value is relegated to this category.

Category 3. Values in this category are little more than rough estimates, and, taken individually, they do not yield much information. When combined with higher-quality data on a regional basis, however, these heat flows can be quite useful. In the tables, the values in category 3 are given to the nearest 0.5 HFU. The implication here is that the uncertainty is of this order. For some of the higher values, the uncertainty can exceed 1 HFU. Category 3 values are shown within parentheses in the relevant figures to emphasize the point that they are merely estimates.

For each site, the principal elements of the heat-flow calculation are given in Tables 1 through 8. Each table consists of twelve columns. The first four columns identify the location of the site by name, hole, or well number (where appropriate), latitude and longitude to the nearest minute, and surface elevation. Column 5 gives the depth range applicable for each line of the table. The columns headed N and K refer to the number of conductivity specimens and the arithmetic mean conductivity ($\pm$ standard error), respectively. If most conductivities in a given set were obtained by measurements on solid disks with the divided-bar apparatus, the average conductivity is not flagged in any way. The superscripts f and n in the K column denote that the majority of

TABLE 1. Heat Flow from the California Coastal Province

Locality	North Latitude	West Longitude	Elevation, meters	Depth Range, meters	N	K, mcal/cm sec °C	Γ, °C/km	q(unc), HFU	q(corr), HFU Category 1	Category 2	Category 3
Fort Bragg	39° 26′	123° 44′	120	444–1207	0	~4*	48.3 ±6.5	2			2
Willitts (EC-1)	39° 34′	123° 07′	1100	153–344	6	8.41 ±0.28	21.40 ±0.06	1.80 ±0.06	1.8		
Cold Creek (EG-8)	39° 42′	122° 53′	1186	175–327	10	10.3 ±0.5	20.43 ±0.05	2.11 ±0.10	1.6		
Cottonwood Glade (EG-7)	39° 42′	122° 48′	1585	220–1245	39	6.95 ±0.31	16.2 ±0.02	1.13 ±0.05	1.17		
Berkeley (BER)	37° 52′	122° 15′	122	33–159	6	5.0 ±1.0	36.74 ±0.07	1.84 ±0.4			2
Tracy (TRA)	37° 48′	121° 35′	19	33–246	34	3.27[a] ±0.14	(29.3)[b]	0.96 ±0.02	0.96		
Menlo Park	37° 27′	122° 10′	16	68–218	165	3.99[a] ±0.03	(54.1)[c]	2.16	2.16		
				218–240	53	5.1 ±0.5	42.5 ±0.2	2.2 ±0.2	2.2		
				Best value					2.2		
Dumbarton SF Bay #1	37° 29′	122° 08′	1	114–117	10	3.72[a] ±0.15	63.85 ±0.78	2.37 ±0.10	2.4		
				155–157	5	4.13[a] ±0.13	51.5 ±2.1	2.13 ±0.11	2.1		
				Mean					2.25		
Sunnyvale (SV)	37° 27′	122° 02′	12	160–258	42	3.44[a] ±0.06	58.6 ±0.6	2.02 ±0.04	2.02		
Permanente	37° 19′	122° 07′									
586			509	183–204	7	6.40[f] ±0.49	21.87 ±0.65	1.40 ±0.11		1.9	
659			483	92–155	21	10.05[f] ±0.25	12.03 ±0.22	1.21 ±0.04		2.2	
				155–181	11	7.04[f] ±0.38	27.6 ±0.8	1.94 ±0.12		2.4	
				Mean (2 holes)						2.2	
La Panza (TS)	35° 26′	120° 30′	427	76–166	14	6.90 ±0.16	32.90 ±0.66	2.25 ±0.07	2.06		

Locality	North Latitude	West Longitude	Elevation, meters	Depth Range, meters	N	K, mcal/cm sec °C	Γ, °C/km	q(unc), HFU	Category 1	Category 2	Category 3
				Mean (2 holes)						2.2	
La Panza (TS)	35° 26′	120° 30′	427	76–166	14	6.90 ±0.16	32.90 ±0.66	2.25 ±0.07	2.06		

TABLE 1. *(continued)*

Locality	North Latitude	West Longitude	Elevation, meters	Depth Range, meters	N	K, mcal/cm sec °C	Γ, °C/km	q(unc), HFU	q(corr), HFU Category 1	Category 2	Category 3
Elk Hills											
366-24Z	35° 18′	119° 34′	365	1782–1864	22	5.08^n ±0.16	19.2 ±0.8	0.98 ±0.05	1.0		
385-24Z	35° 18′	119° 33′	361	1496–1756	20	3.76^n ±0.28	$(31.1)^i$	1.17 ±0.05	1.2		
326-28R	35° 17′	119° 31′	441	685–838	7	3.58^f ±0.25	36.9 ±1.0	1.32 ±0.10			
				1420–1850	23	3.47^n ±0.08	35.81 ±0.20	1.24 ±0.03			
				Mean					1.26		
372-35R	35° 17′	119° 28′	405	2098–2113	6	4.90^n ±0.15	$(27.3)^i$	1.34 ±0.14		1.3	
343-4G	35° 16′	119° 24′	317	1391–2142	26	3.82^n ±0.16	$(29.3)^i$	1.12 ±0.03	1.12		
382-3G	35° 16′	119° 23′	277	2115–2141	5	4.23^n ±0.35	$(32.2)^i$	1.36 ±0.20			
				2207–2331	19	4.58^n ±0.16	27.10 ±0.30	1.24 ±0.04			
				Mean					1.26		
344-35S	35° 17′	119° 22′	222	2091–2152	7	4.05^n ±0.28	$(28.4)^i$	1.15 ±0.25		1.2	
Los Angeles Basin (LB-1)	33° 53′	118° 02′	21	2073–3223	40	5.04 ±0.16	34.5 ±0.1	1.75 ±0.05	1.74		
Santa Ana AC-1	33° 58′	117° 38′	300	30–183	17	3.6^n ±0.1	46.0 ±2.2	1.66 ±0.09			
				183–305	13	2.35^n ±0.04	64.2 ±2.9	1.51 ±0.07			
				Mean						1.6	

Definitions (applicable to Tables 1–8): q(corr), corrected heat flow; q(unc), uncorrected heat flow; superscript b, Bullard method; superscript f, measured on fragments; superscript i, interval method; superscript n, needle-probe method.

* Estimated conductivity.

TABLE 2*a*. Heat Flow from the Sierra Nevada

Locality	North Latitude	West Longitude	Elevation, meters	Depth Range, meters	N	K, mcal/cm sec °C	Γ, °C/km	q(unc), HFU	q(corr), HFU Category 1	Category 2	Category 3
Moonlight Valley											
ML-9	40° 13′	120° 48′	1710	238–334	15	7.99 ±0.25	19.64 ±0.19	1.57 ±0.05		1.60*	
ML-43	40° 14′	120° 48′	1670	46–148	14	8.11 ±0.36	24.97 ±0.13	2.03 ±0.09	1.92		
				Best value					1.9		
San Juan Ridge SJR-1	39° 24′	120° 52′	1378	246–256	6	7.84 ±0.14	8.79 ±0.11	0.69 ±0.02	0.65		
SJR-2	39° 24′	120° 53′	1406	274–276	9	13.0 ±1.0	5.74 ±0.05	0.75 ±0.06		0.72	
				Mean					0.69		
Auburn Dam AD-34	38° 52′	121° 03′	295	30–183	20	9.00 ±0.10	15.05 ±0.27	1.35 ±0.03		0.72†	
AD-117	38° 53′	121° 03′	150	44–152	12	8.65 ±0.30	(17.7)§	1.53 ±0.11		0.72‡	
AD-212	38° 53′	121° 03′	157	60–130	19	7.17 ±0.17	(19.8)§	1.42 ±0.06		0.67‡	
				Mean						0.70	
Sherman Thomas Ranch (ST)	37° 10′	120° 04′	110	203–488	90	7.13 ±0.04	6.35 ±0.02	0.45 ±0.01	0.45		
San Joaquin Experimental Range (SJ)	37° 06′	119° 44′	335	280–459	201	6.97 ±0.06	8.90 ±0.04	0.62 ±0.01	0.61		
Jose Basin (JB)	37° 06′	119° 23′	1000	201–491	191	6.05 ±0.03	12.2 ±0.03	0.74 ±0.01	0.77		
Helms Creek (HC)	37° 08′	118° 59′	2510	60–490	203	7.09 ±0.03	17.2 ±0.01	1.22 ±0.01	1.30		

* There is evidence for downward water movement above 238 meters.
† Correction made for 1°C temperature drop about 80 years ago. The drop could have been caused by a landslide or by hydraulic mining operations.
‡ On the edge of a river; corrections made assuming a temperature difference of 4°C between land and water.

TABLE 2*b*. Heat Flow from the Tehachapi Mountains

Locality	North Latitude	West Longitude	Elevation, meters	Depth Range, meters	N	K, mcal/cm sec °C	Γ, °C/km	q(unc), HFU	q(corr), HFU Category 1	Category 2	Category 3
Helms Creek (HC)	37° 08′	118° 59′	2510	60–490	203	7.09 ±0.03	17.2 ±0.01	1.22 ±0.01	1.30		

* There is evidence for downward water movement above 238 meters.
† Correction made for 1°C temperature drop about 80 years ago. The drop could have been caused by a landslide or by hydraulic mining operations.
‡ On the edge of a river; corrections made assuming a temperature difference of 4°C between land and water.

TABLE 2b. Heat Flow from the Tehachapi Mountains

Locality	North Latitude	West Longitude	Elevation, meters	Depth Range, meters	N	K, mcal/cm sec °C	Γ, °C/km	q(unc), HFU	q(corr), HFU Category 1	Category 2	Category 3
Tejon Ranch, California											
DH-61	34° 57′	118° 49′	506	107–153	9	7.23 ±0.24	18.4 ±2.1	1.33 ±0.16		1.31	
DH-62	34° 56′	118° 49′	476	76–130	10	6.35 ±0.44	23.93 ±0.39	1.52 ±0.11	1.33		
DH-65	34° 56′	118° 49′	791	244–433	31	6.95 ±0.25	18.51 ±0.08	1.29 ±0.05	1.38		
				Mean (3 holes)					1.36		
DH-43	34° 53′	118° 46′	1119	122–183	6	8.13 ±0.26	21.75 ±0.09	1.77 ±0.06	1.83		

TABLE 3. Heat Flow from the Pacific Northwest Coastal Province

Locality	North Latitude	West Longitude	Elevation, meters	Depth Range, meters	N	K, mcal/cm sec °C	Γ, °C/km	q(unc), HFU	q(corr), HFU Category 1	Category 2	Category 3
Chehalis, Washington	46° 32′	122° 50′									
SU-4			165	100–380	59*	2.58ª ±0.1	32.8 ±0.2	0.85 ±0.03			
				710–760	5	4.23 ±0.03	19.4 ±0.6	0.82 ±0.02			
SU-11			157	100–340	59	2.56ª ±0.1	34.6 ±0.2	0.89 ±0.04			
SU-14			156	100–400	59	2.56ª ±0.1	33.8 ±0.1	0.86 ±0.03			
				Best value	77	2.74ª ±0.10	(30.3)		0.83		

* Core was obtained from SU-4 and from four other wells, all of which were within a few hundred meters of the holes in which temperatures were measured.

TABLE 4. Heat Flow from the Columbia Plateaus

Locality	North Latitude	West Longitude	Elevation, meters	Depth Range, meters	N	K, mcal/cm sec °C	Γ, °C/km	q(unc), HFU	q(corr), HFU		
									Category 1	Category 2	Category 3
Nevada											
White Elephant Butte, EB-1	41° 53′	115° 05′	2010	100–366	7	8.68 ±0.28	43.4 ±0.2	3.76 ±0.12		3.3*	
Washington											
Rattlesnake Hills RS-1	46° 26′	119° 47′	875	900–2500	6	3.75 ±0.3	(34.8)*	1.31 ±0.1		1.39	
RS-2				58–119	14	4.12 ±0.10	28.0 ±0.2	1.15 ±0.03	1.36		
				Best value (2 holes)					1.4		
Richland DH-3	46° 21′	119° 17′	120	305–608	16	3.95 ±0.17	38.95 ±0.15	1.54 ±0.07	1.54		
				608–1079	15	3.64 ±0.08	34.58 ±0.28	1.26 ±0.03		1.3	
				Best value					1.5		
Willa, DH-1	46° 35′	119° 31′	168	53–183	19	4.08 ±0.08	37.2 ±0.3	1.52 ±0.03	1.52		

* Water flowing steadily from the collar at about 2 to 3 liters/minute [cf. *Birch*, 1947].

TABLE 5. Heat Flow from the Colorado Plateau Province

TABLE 5. Heat Flow from the Colorado Plateau Province

Locality	North Latitude	West Longitude	Elevation, meters	Depth Range, meters	N	K, mcal/cm sec °C	Γ, C/km°	q(unc), HFU	q(corr), HFU Category 1	Category 2	Category 3
Colorado											
Yellow Creek											
CH-1	40° 03′	108° 20′	1830	46–671	25	3.40	43.3	1.47			
						±0.26	±0.2	±0.11			
				671–881	14	2.25	63.4	1.43			
						±0.25	±0.9	±0.16			
				Mean					1.5		
CH-2	39° 58′	108° 28′	2011	76–404	10	3.42	30.1	1.03			
						±0.28	±0.2	±0.08			
				404–488	6	2.58	57.0	1.47			
						±0.27	±0.3	±0.15			
				663–716	5	2.52	50.9	1.28			
						±0.39	±1.9	±0.20			
				Best value						1.4	
CH-3	40° 03′	108° 21′	1937	617–983	14	2.64	56.4	1.49	1.5		
						±0.21	±0.7	±0.12			
Barcus Creek	40° 03′	108° 31′	1920	411–544	17	2.87	67.4	1.93			2*
BC-1						±0.36	±0.7	±0.24			
Rio Blanco	39° 46′	108° 09′	2070	46–107	8	3.79	57.9	2.19			
TG2-3						±0.16	±0.4	±0.09			
				201–322	16	2.69	49.4	1.33			
						±0.20	±1.4	±0.11			
				Mean							1.5
New Mexico											
Gobernador	36° 41′	107° 12′	2194	1052–1288	9	6.6	(30.6)	2.02	2.01		
GB-1						±0.8		±0.08			
Utah											
Ouray	39° 59′	109° 36′	1520	61–533	11	5.63	25.13	1.42			
W-Ex-1						±0.17	±0.06	±0.04			
				541–907	51	4.90	32.19	1.60			
						±0.18	±0.28	±0.06			
				Mean					1.50		

* Strong vertical water movement above 400 meters.

TABLE 6. Heat Flow from the Rocky Mountain Province

Locality	North Latitude	West Longitude	Elevation, meters	Depth Range, meters	N	K, mcal/cm sec °C	Γ, °C/km	q(unc), HFU	q(corr), HFU Category 1	Category 2	Category 3
Colorado											
Rocky Mountain Arsenal, Denver	39° 51′	104° 51′	1501	368–2535	42	5.83[f] ±0.65	(38.6)[i]	2.25 ±0.11		2.14	
				3017–3597	19	8.96 ±0.60	24.7 ±1.0	2.21 ±0.16		1.88	
				Mean						2.0	
Idaho											
Galena mine, Wallace (GAL)	47° 29′	115° 58′	928	957–1201	30	11.9* ±1.8	21.42 ±0.01	2.55 ±0.38		2.3	
Montana											
Verdigris Creek											
Hole M-22	45° 23′	109° 54′	2151	83–209	24	8.80 ±0.17	17.8 ±0.1	1.57 ±0.03	1.63		
Hole M-19A	45° 23′	109° 55′	2140	111–171	11	8.4 ±0.4	16.9 ±0.2	1.42 ±0.07	1.35		
				171–269	21	7.15 ±0.21	21.2 ±0.2	1.52 ±0.05	1.47		
				Mean (2 holes)					1.52		
Nye Basin Hole NB-2	45° 22′	109° 49′	2470	163–253	6	7.8 ±0.4	18.7 ±0.4	1.46 ±0.08	1.39		
Wyoming											
Pinedale (DHPW)	42° 46′	109° 34′	2218	305–1356	27	7.21 ±0.26	19.21 ±0.04	1.38 ±0.05	1.38		
				2088–2906	29	6.79 ±0.12	16.41 ±0.03	1.14 ±0.02	1.25		
				Mean					1.3		
Green River (GR1-1)	41° 32′	109° 25′	1890	53–152	7	3.64 ±0.34	44.1 ±0.8	1.61 ±0.15	1.6		

* Temperatures were measured near a vertical contact between rocks of contrasting conductivities. The standard error in conductivity includes the uncertainty in the structural effect.

(GR1-1)		±0.34	±0.8	±0.15

[a] Temperatures were measured near a vertical contact between rocks of contrasting conductivities. The standard error in conductivity includes the uncertainty in the structural effect.

TABLE 7. Heat Flow from the Great Plains Province

Locality	North Latitude	West Longitude	Elevation, meters	Depth Range, meters	N	K, mcal/cm sec °C	Γ, °C/km	q(unc), HFU	q(corr), HFU Category 1	Category 2	Category 3
Kansas											
Lyons					91[a]	7.93[a] ±0.42					
Hole 1	38° 23′	98° 10′	525	99–229		3.82 ±0.38	36.42 ±0.56	1.39 ±0.14			
				252–328		12.5 ±1.0	13.35 ±0.20	1.67 ±0.14			
Hole 2	38° 22′	98° 10′	512	128–212		3.70 ±0.37	40.84 ±0.30	1.51 ±0.15			
				235–311		11.9 ±1.0	12.63 ±0.21	1.50 ±0.13			
				Mean (2 holes)					1.50		
South Dakota											
Windy Flats Hole NBH-1	44° 18′	103° 40′	1652	383–516	7	5.12 ±0.29	9.10 ± 0.07	0.47 ±0.03		0.5	
Moonshine Gulch Hole NBH-2	44° 08′	103° 43′	1695	126–250	13	6.70 ±0.46	7.77 ±0.04	0.52 ±0.04		0.5	
Dacy Hole RTM-1	44° 22′	103° 53′	1790	204–334	7	7.3 ±1.0	25.6 ± 0.05	1.87 ±0.26		1.9	

[a] The holes penetrated interbedded, flat-lying, sedimentary layers of contrasting conductivities. An arithmetic mean conductivity was calculated for each distinct rock type. These averages were used, together with relative abundances from detailed core logs, to calculate a harmonic mean conductivity for each gradient interval.

TABLE 8. Heat Flow from the Basin and Range Province

Locality	North Latitude	West Longitude	Elevation, meters	Depth Range, meters	N	K, mcal/cm sec °C	Γ, °C/km	q(unc), HFU	q(corr), HFU Category 1	Category 2	Category 3
Arizona											
Yuma	32° 44′	114° 37′	50	220–338	15	5.6	34.3	1.92		1.92	
LCRP-26						±0.5	±1.1	±0.18			
LCRP-13	32° 41′	114° 37′	60	30–137	7	5.0	44.9	2.24			
						±0.5	±0.5	±0.22			
				137–223	3	5.3	35.6	1.88			
						±0.5	±1.2	±0.19			
				Mean				2.06		2.1	
Phoenix	33° 32′	112° 20′	331	107–229	9	3.7^f	85.9	3.18			
						±0.5	±0.5	±0.43			
ST-1				238–268	6	8.1^f	50.9	4.12			
						±0.4	±1.1	±0.22			
				268–1365	0*	13.0	14.8	1.92			
						±1.0	±1.0	±0.20			
				Mean							>3
Tempe	33° 25′	112° 01′	340	107–175	4	3.7^n	29.6	1.09		1.1	
A-1-3						±0.5	±0.2	±0.15			
Higley	33° 19′	111° 43′	395	100–280	22	3.79^f	45.7	1.73		1.7	
D-1-6						±0.11	±0.6	±0.06			
Red Rock	32° 36′	111° 36′	500	100–260	2	2.8^n	30.19	0.85			
						±0.2	±0.25	±0.06			
D-9-7				260–353	6	3.77	22.6	0.85			
						±0.30	±0.4	±0.07			
				Mean					0.85		
Eloy	32° 47′	111° 29′	480	200–230	6	3.70^n	34.2	1.27	1.3		
D-7-8						±0.33	±0.2	±0.11			
Christmas	33° 02′	110° 41′	762	168–320	12	7.61	18.84	1.43	1.4		
SM-1						±0.58	±0.15	±0.11			
San Manuel	32° 40′	110° 42′	1053	914–1372	42	8.72	17.61	1.54	1.54		
DH-34						±0.34	±0.14	±0.06			
Tucson	32° 11′	111° 07′	795	152–442	70	8.61	29.69	2.56	2.56		
KCL-7						±0.29	±0.08	±0.09			
Helmet Peak	31° 58′	111° 04′	1033	91–335	8	8.09	26.40	2.14	2.14		
A-545						±0.23	±0.07	±0.06			
Twin Buttes	31° 54′	111° 03′	1017	198–472	46	9.31	22.6	2.10	2.10		
A-644						±0.29	±0.3	±0.07			
A-911	31° 54′	111° 02′	1025	137–366	43	8.37	23.7	1.98	1.98		

[illegible]	[illegible]	[illegible]	[illegible]	[illegible]	8	8.09	[illegible]	2.14	2.14		
A-545						±0.23	±0.07	±0.06			
Twin Buttes	31° 54′	111° 03′	1017	198–472	46	9.31	22.6	2.10	2.10		
A-644						±0.29	±0.3	±0.07			
A-911	31° 54′	111° 02′	1025	137–366	43	8.37	23.7	1.98	1.98		
						±0.21	±0.1	±0.05			

TABLE 8. *(continued)*

Locality	North Latitude	West Longitude	Elevation, meters	Depth Range, meters	N	K, mcal/cm sec °C	Γ, °C/km	q(unc), HFU	q(corr), HFU Category 1	Category 2	Category 3
Arizona (continued)											
A-616	31° 53′	111° 02′	1010	183–396	23	8.82	21.3	1.88	1.88		
						±0.42	±0.3	±0.09			
A-940	31° 53′	111° 02′	993	183–335	31	7.48	20.9	1.56	1.56		
						±0.22	±0.2	±0.05			
California											
Black Rock	37° 41′	118° 32′	2110	183–206	0	6*	33.5	2.0			2
BR							±1.6				
Deep Springs	37° 24′	118° 00′	1630	250–305	55	6.6	28.76	1.89		1.8	
DS-1A						±0.7	±0.27	±0.20			
Eagle Mountain	33° 52′	115° 26′	285	350–426	10	6.48	19.9	1.29	1.29		
CK-3						±0.22	±0.5	±0.05			
Nevada											
Adelaide	40° 50′	117° 32′	1780	38–107	8	8.1	42.8	3.47	3.32		
GV-1						±0.8	±0.9	±0.34			
				107–305	10	6.80	51.1	3.47	3.41		
						±0.62	±0.2	±0.32			
				Mean					3.4		
Panther Canyon	40° 33′	117° 34′									
BM-3			1608	61–160	11	6.81	64.3	4.38		3.5	
						±0.38	±0.7	±0.25			
BM-37			1635	122–241	13	8.32	57.6	4.79		4.0	
						±0.58	±1.2	±0.25			
				Mean (2 holes)					3.8		
Elder Creek	40° 41′	117° 04′	1510	26–252	7	9.5	35.06	3.33	3.2		
EC-4						±1.1	±0.06	±0.39			
Buckingham	40° 37′	117° 04′									
B-6			1780	61–247	8	8.8	33.2	2.92	2.8		
						±1.3	±0.3	±0.43			
B-11			1830	152–311	5	8.7	29.66	2.58	2.5		
						±0.6	±0.15	±0.18			
				Mean (2 holes)					2.7		
Iron Canyon	40° 33′	117° 06′	1675	259–1410	46	11.2	31.24	3.50	3.50		
Hole IC-1						±0.5	±0.08	±0.16			

TABLE 8. *(continued)*

Locality	North Latitude	West Longitude	Elevation, meters	Depth Range, meters	N	K, mcal/cm sec °C	Γ, °C/km	q(unc), HFU	q(corr), HFU Category 1	Category 2	Category 3
Nevada (continued)											
Lander Hole TN-1	40° 20′	116° 43′	1670	61–411	10	11.3 ±1.2	30.6 ±0.3	3.46 ±0.35	3.16		
				442–747	12	14.16 ±1.1	24.35 ±0.06	3.45 ±0.28	3.31		
				747–1218	18	7.82 ±0.28	34.1 ±0.1	2.67 ±0.10	2.63		
				Mean					3.0		
Tenabo Hole TN-2	40° 18′	116° 40′	1525	76–343	9	11.72 ±0.48	30.7 ±0.2	3.59 ±0.15	3.53		
Gold Acres GAP-1	40° 16′	116° 45′	1676	122–177	8	9.16 ±0.55	27.2 ±0.2	2.49 ±0.15	2.5		
Swales Mountain Hole SM-2	40° 57′	116° 01′	1829	122–152	9	6.68 ±0.03	22.2 ±0.04	1.48 ±0.01		1.7	
Washington Hill VC-4	39° 28′	119° 38′	1634	61–134	6	4.91 ±0.23	45.8 ±0.6	2.25 ±0.11	2.1		
Lousetown VC-2	39° 23′	119° 38′	1770	30–108	6	4.00 ±0.12	54.7 ±3.3	2.19 ±0.15		2.0	
VC-3	39° 23′	119° 38′	1800	46–111	8	6.24 ±0.54	62.5 ±1.6	3.90 ±0.35		3.5	
Virginia City C-63	39° 18′	119° 39′	1920	107–151	4	8.1 ±0.6	87.7 ±3.4	7.1 ±0.6		.7	
Silver City CV-1	39° 15′	119° 40′	1585	137–320	26	6.62 ±0.16	27.60 ±0.04	1.83 ±0.04	1.81		
				320–389	8	11.54 ±0.87	17.66 ±0.21	2.04 ±0.16	1.95		
				389–476	9	9.8 ±1.1	22.50 ±0.36	2.20 ±0.25		2.14	
				Mean					1.93		
Pine Nut Canyon PN-10	38° 53′	119° 35′	1850	58–88	7	7.24 ±0.72	40.34 ±0.25	2.92 ±0.29		2.6	
				88–104	4	8.72 ±1.3	34.4 ±0.3	3.00 ±0.45		2.6	
PN-19	38° 52′	119° 35′	1890	99–183	12	7.05 ±0.63	36.3 ±0.2	2.56 ±0.23	2.26		
				183–383	16	7.95 ±0.19	32.49 ±0.05	2.58 ±0.06	2.38		
				Best value					2.3		

TABLE 8. (continued)

Locality North Latitude West Longitude Elevation, meters Depth Range, meters N K, mcal/cm sec °C Γ, °C/km q(unc), HFU q(corr), HFU Category 1 Category 2 Category 3

[illegible]						±0.72	±0.25	±0.29			
				88–104	4	8.72 ±1.3	34.4 ±0.3	3.00 ±0.45		2.6	
PN-19	38° 52′	119° 35′	1890	99–183	12	7.05 ±0.63	36.3 ±0.2	2.56 ±0.23	2.26		
				183–383	16	7.95 ±0.19	32.49 ±0.05	2.58 ±0.06	2.38		
				Best value					**2.3**		

TABLE 8. *(continued)*

Locality	North Latitude	West Longitude	Elevation, meters	Depth Range, meters	*N*	*K*, mcal/cm sec °C	Γ, °C/km	*q*(unc), HFU	*q*(corr), HFU Category 1	Category 2	Category 3
Nevada (continued)											
Yerington L-2	38° 55′	119° 04′	1463	137–260	9	8.76† ±0.41	20.52 ±0.31	1.80 ±0.09			
L-7	38° 56′	119° 04′	1460	107–350	24	8.29 ±0.16	22.56 ±0.10	1.87 ±0.04			
L-48	38° 56′	119° 04′	1450	107–411	34	8.06 ±0.27	22.80 ±0.14	1.84 ±0.06			
				Mean (3 holes)				1.84	1.84		
Sand Springs	39° 12′	118° 22′									
PM-1			1633	180–320	8	7.04 ±0.03	22.5 ±0.1	1.58 ±0.01	1.58		
PM-2			1621	180–265	0	6.86	18.8 ±0.2	1.29		1.26	
PM-3			1561	70–250	11	6.87 ±0.15	30.8 ±0.1	2.12 ±0.05	1.69		
USBM-1			1585	90–316	0	6.86	24.7 ±0.1	1.69		1.58	
				Mean (4 holes)‡	143	6.86 ±0.04	(22.9)		1.57		
Eureka											
703	39° 30′	116° 00′	1989	165–189	8	6.02 ±0.22	15.6 ±0.3	0.94 ±0.04	0.88		
608	39° 30′	115° 59′	2115	159–245	14	8.18 ±0.10	7.18 ±0.19	0.59 ±0.02	0.58		
720	39° 29′	115° 59′	2318	61–366	5	9.4 ±1.8	10.7 ±0.7	1.01 ±0.20		1.08	
706	39° 29′	115° 59′	2232	31–183	5	9.6 ±1.1	11.2 ±0.4	1.07 ±0.13		1.13	
713	39° 30′	115° 59′	2139	183–450	8	8.38 ±0.12	6.92 ±0.10	0.58 ±0.01	0.60		
				Mean (5 holes)					0.88		
Monitor Valley UCe-3	38° 58′	116° 38′	2165	401–597	9	3.94 ±0.26	51.7 ±0.4	2.04 ±0.13	2.0		
Little Fish Lake Valley UCe-12A	38° 55′	116° 20′	2111	228–455	9	2.52 ±0.07	49.9 ±0.6	1.26 ±0.04			

TABLE 8. *(continued)*

Locality	North Latitude	West Longitude	Elevation, meters	Depth Range, meters	N	K, mcal/cm sec °C	Γ, °C/km	q(unc), HFU	q(corr), HFU Category 1	Category 2	Category 3
Nevada (continued)											
				455–582	4	3.62 ±0.36	42.9 ±2.7	1.55 ±0.18			
				582–697	4	5.09 ±0.21	32.3 ±0.4	1.64 ±0.07			
				Mean					1.4		
UCe-9	38° 49′	116° 27′	2088	154–866	0	3.0§	39.4 ±0.2	1.2		1.2	
UCe-10	38° 41′	116° 28′	1980	150–780	7	2.34 ±0.07	49.0 ±0.5	1.15 ±0.04	1.2		
Little Smoky Valley UCe-14	38° 43′	116° 02′	1902	282–393	3	3.0 ±0.3	38.0 ±0.2	1.14 ±0.11			
				424–449	4	5.5 ±0.2	31.5 ±0.9	1.73 ±0.08			
				Best value							1.5
Patterson Pass	38° 36′	114° 44′									
PP-2			2250	76–151	6‖	7.72′ ±0.20	16.21 ±0.45	1.25 ±0.05		1.25	
PP-3			2260	76–305	21	8.92′ ±0.34	13.5 ±0.8	1.20 ±0.08		1.20	
				Mean (2 holes)						1.2	
Luning M-4	38° 29′	118° 12′	1585	30–249	18	8.11 ±0.18	88.2 ±1.5	7.15 ±0.20		7.2	
Pilot Mountains	38° 19′	117° 52′									
DH-1			1978	76–191	10	6.73′ ±0.67	28.07 ±0.16	1.89 ±0.19	1.98		
DH-2			1933	99–332	11	6.91′ ±0.20	28.17 ±0.06	1.95 ±0.06	1.92		
DH-3			1940	99–267	10	6.94′ ±0.36	28.69 ±0.06	1.99 ±0.10	1.98		
				Mean (3 holes)					1.95		
Ralston Valley UCe-1	38° 34′	116° 56′	2150	198–609	153	7.15 ±0.03	25.58 ±0.08	1.83 ±0.01	1.79		
Hot Creek Valley UCe-18	38° 35′	116° 12′	1757	192–1292	11	3.56	36.8	1.31	1.29		

Locality | North Latitude | West Longitude | Elevation, meters | Depth Range, meters | N | K, mcal/cm sec °C | Γ, °C/km | q(unc), HFU | q(corr), HFU Category 1 | Category 2 | Category 3
Nevada (continued) ±0.11 ±0.1 ±0.03

Ralston Valley UCe-1	38° 34′	116° 56′	2150	198–609	153	7.15 ±0.03	25.58 ±0.08	1.83 ±0.01	1.79		
Hot Creek Valley UCe-18	38° 35′	116° 12′	1757	192–1292	11	3.56 ±0.22	36.8 ±0.2	1.31 ±0.08	1.29		
				1292–1664	14	4.94	25.4	1.25	1.24		

TABLE 8. *(continued)*

Locality	North Latitude	West Longitude	Elevation, meters	Depth Range, meters	N	K, mcal/cm sec °C	Γ, °C/km	q(unc), HFU	q(corr), HFU Category 1	Category 2	Category 3
Nevada (continued)											
						±0.11	±0.4	±0.03			
				Mean					1.28		
Stone Cabin Valley UCe-2	38° 18′	116° 35′	1890	40–162	6	3.84 ±0.28	45.6 ±0.6	1.75¶ ±0.13			
				202–405	9	4.37 ±0.11	25.20 ±0.07	1.10 ±0.03			
				Mean						1.3	
Bristol Range ESP-3	38° 06′	114° 36′	2061	602–762	28	7.13 ±0.24	23.32 ±0.14	1.66 ±0.06	1.74		
ESP-1	38° 04′	114° 36′	2274	30–457	18	10.44 ±0.74	13.54 ±0.48	1.41 ±0.11	1.72		
				549–579	6	7.18 ±0.15	20.98 ±0.23	1.51 ±0.04	1.65		
				Mean (2 holes)					1.72		
Manhattan Gap MAN-2	37° 58′	114° 36′	2103	152–191	8	7.97 ±1.12	22.16 ±0.74	1.76 ±0.26	1.71		
				198–305	12	9.54 ±1.03	19.44 ±0.20	1.85 ±0.20	1.87		
				Mean					1.83		
MAN-3	37° 57′	114° 36′	2164	30–274	9	8.66 ±0.51	18.05 ±0.22	1.56 ±0.09	1.67		
				305–404	5	16.80 ±0.42	11.38 ±0.09	1.91 ±0.05	2.00		
				404–456	8	8.7 ±1.2	17.93 ±0.17	1.56 ±0.22	1.62		
				Mean					1.75		
MAN-4	37° 58′	114° 36′	2210	296–414	19	9.31 ±0.52	18.1 ±0.2	1.69 ±0.10	1.80		
MAN-7	37° 58′	114° 35′	2200	152–305**	25	9.29 ±0.33	17.08 ±0.16	1.59 ±0.06	1.69		
				305–389††	13	9.28 ±0.48	17.02 ±0.22	1.58 ±0.08	1.67		
				Mean					1.68		
MAN-9	37° 58′	114° 36′	2260	389–509	15	6.91	21.84	1.51	1.59		

TABLE 8. (continued)

Locality	North Latitude	West Longitude	Elevation, meters	Depth Range, meters	N	K, mcal/cm sec °C	Γ, °C/km	q(u[illegible]), H[illegible]			
Nevada (continued)											
						±0.29	±0.29	±0.[illegible]			
				Mean (5 holes)							
Silverpeak	37° 43′	117° 47′									
LC-1			2118	107–228	18	5.44 ±0.18	38.68 ±0.17	2.10 ±0.07			
LC-4			2136	172–201	8	5.32 ±0.15	41.47 ±0.48	2.21 ±0.07			
				Mean (2 holes)							
Goldfield Hole 1	37° 43′	117° 12′	1771	330–465	14	8.76 ±0.22	30.73 ±0.19	2.69 ±0.07			
Hole 2	37° 45′	117° 11′	1731	146–316	11	5.52 ±0.11	35.71 ±0.20	1.97 ±0:04			
				Mean (2 holes)					2.3‡‡		
Tempiute											
SDH-17A	37° 38′	115° 33′	2128	215–288	6	7.76 ±0.23	12.74 ±0.19	0.99 ±0.03	1.05		
SDH-7	37° 38′	115° 33′	2076	447–507	9	8.10 ±0.95	13.03 ±0.10	1.06 ±0.12	1.13		
SDH-18	37° 39′	115° 33′	1975	182–211	12	8.28 ±0.31	13.19 ±0.30	1.09 ±0.05	1.09		
				Mean					1.1		
Pahute Mesa											
PM-2	37° 21′	116° 34′	1703	457–610	4	2.32 ±0.08	56.8 ±0.6	1.32 ±0.05			
				610–732	3	3.15 ±0.15	48.7 ±0.8	1.53 ±0.08			
				732–792	3	4.40 ±0.18	38.2 ±1.9	1.68 ±0.11			
				Mean						1.5	
PM-1	37° 17′	116° 24′	1999	610–914	4	3.06 ±0.25	28.8 ±0.1	0.88 ±0.07			

TABLE 8. (continued)

Locality	North Latitude	West Longitude	Elevation, meters	Depth Range, meters	N	K, mcal/cm sec °C	Γ, °C/km	q(unc), HFU	q(corr), HFU		
									Category 1	Category 2	Category 3

				Mean						1.5	
PM-1	37° 17′	116° 24′	1999	610–914	4	3.06 ±0.25	28.8 ±0.1	0.88 ±0.07			

TABLE 8. *(continued)*

Locality	North Latitude	West Longitude	Elevation, meters	Depth Range, meters	*N*	*K*, mcal/cm sec °C	Γ, °C/km	*q*(unc), HFU	*q*(corr), HFU Category 1	Category 2	Category 3
Nevada (continued)											
				914–1219	4	4.83 ±0.44	24.4 ±0.1	1.18 ±0.11			
				Mean						1.0	
Dolomite Hill DOL	37° 11′	116° 12′	1950	152–320	7	11.7 ±0.3	16.40 ±0.11	1.92 ±0.05	1.9		
Yucca Flat TW-E	37° 03′	116° 00′	1272	213–457	9	1.34 ±0.11	48.2 ±0.7	0.65 ±0.05			
				518–701	11	2.27 ±0.07	33.8 ±0.5	0.77 ±0.03			
				Mean					0.7		
Yucca Mountain TW-6	36° 48′	116° 24′	1011	61–290	4	4.4 ±0.2	35.4 ±0.8	1.56 ±0.08		1.6	
Hampel Hill TW-F	36° 46′	116° 07′	1263	564–808	11	4.42 ±0.18	41.77 ±0.07	1.85 ±0.08	1.81		
Frenchman Flat TW-3	36° 46′	115° 52′	1062	137–350	6	6.5 ±0.5	39.9 ±0.7	2.6 ±0.2	2.2		
Rock Valley TW-5	36° 38′	116° 18′	931	61–244	8	6.3 ±0.4	31.1 ±0.6	1.96 ±0.13	2.0		
Indian Spring Valley TW-4	36° 36′	115° 47′	1060	396–457	3	14.2 ±0.4	15.7 ±0.5	2.23 ±0.09		2.17	
Utah											
Cedar City DE-175	37° 42′	113° 17′	1703	76–206	20	7.88 ±0.26	27.09 ±0.32	2.13 ±0.07	2.13		
DE-163	37° 42′	113° 17′	1703	76–335	42	6.98 ±0.21	28.46 ±0.18	1.99 ±0.06	1.99		
DE-104	37° 42′	113° 19′	1725	76–274	28	7.08 ±0.22	29.07 ±0.22	2.06 ±0.07	2.06		
DE-114	37° 41′	113° 19′	1736	53–320	24	6.72 ±0.29	30.39 ±0.21	2.04 ±0.09	2.04		

TABLE 8. (*continued*)

Locality	North Latitude	West Longitude	Elevation, meters	Depth Range, meters	N	K, mcal/cm sec °C	Γ, °C/km	q(unc), HFU	q(corr), HFU Category 1	Category 2	Category 3
DE-161	37° 41′	113° 19′	1743	76–366	25	8.93 ±0.48	26.47 ±0.40	2.36 ±0.13	2.36		
DE-105	37° 41′	113° 19′	1744	46–290	34	8.48 ±0.40	25.22 ±0.15	2.14 ±0.10	2.14		
N-6	37° 38′	113° 26′	1810	46–107	10	8.97 ±0.27	24.45 ±0.44	2.19 ±0.08	2.19		
				Best value	29	6.70 ±0.09	(28.06)¶	1.88 ±0.04	1.88		

* Estimated conductivity.
† K from *Roy* [1963].
‡ All but 19 of the conductivity samples came from nearby holes (<1 km away) in the same material.
§ K is a regional average for 35 samples of the same material.
|| Samples from PP-3.
¶ Tuffs, above static-water level. If the regional average K (3) is used, q(unc) is 1.4.
** Temperatures measured in air.
†† Temperatures measured in water.
‡‡ A combination of conductivity structure and sampling bias resulted in an overestimate of q(unc) in hole 1, and an underestimate in hole 2.

conductivities in that particular data set were measured on fragments or by the needle probe, respectively (see section on conductivity, above).

The gradient Γ (column 8) is represented in three different ways, depending on which of the following methods of heat-flow reduction was used:

1. If there was conductivity stratification on a scale of 50 meters or larger, one line of the table is devoted to each stratum. Γ is the least-square temperature gradient (± standard error) over the depth range indicated (column 5), and the uncorrected heat flow q(unc), column 9, is the product of this gradient and the mean conductivity (column 7).

2. If conductivity stratification was on a smaller scale, then the heat flow for each of the layers is determined as in 1, and their weighted mean for the depth range indicated (column 5) is entered in column 9. For consistency, the arithmetic mean conductivity (and its standard error) for the entire depth range is entered in column 7, and the gradient consistent with that conductivity and the heat flow (column 9) is entered in column 8. This derived gradient is shown in parentheses with a superscript i (for interval method).

3. In inhomogeneous materials in which the conductivity stratification is not clearly defined, the resistance integral technique of *Bullard* [1939] was used to determine q(unc). As in method 2, a derived gradient consistent with K (column 7) and q(unc) (column 9) is entered in parentheses in column 8. The gradient entry has the superscript b (for Bullard method).

The final three columns headed q(corr) represent the best estimate of heat flow with corrections where appropriate and category assignments according to criteria outlined above. In the majority of cases if a correction was applied, it was for steady-state topography, but estimates of other sources of disturbance were sometimes made in evaluating a heat flow and assigning it to a category. As stated in the introduction, detailed documentation for each of the heat-flow determinations in Tables 1 through 8 is in preparation.

In areas where there were two or more holes within a small area (~10 km²), a single value is given below all the others, representing the best estimate of the heat flow in the area. This is generally the mean (weighted by the length of the applicable depth interval) of all holes, but this can be altered by local factors. For example, the average q from eight holes near Cedar City, Utah (see Table 8), is about 2.1. There is, however, a strong suggestion of sampling bias toward silicic rocks in some of the heterogeneous sedimentary formations. Sampling was not a problem in the Homestake limestone, a dense, marine limestone formation. Here, 24 component heat flows calculated by the interval method were tightly grouped about a mean of 1.88 ± 0.04, and this value was adopted for the area.

DISCUSSION

The foregoing tables contain about 150 new heat-flow determinations representing roughly 100 distinct sites separated from one another by at least a few kilometers. As this more than doubles the published heat-flow data from the western United States, it is worth looking briefly at the present status of the observations. Interpretive studies of these data and additional results being obtained in such key areas as the Klamath Mountains are under way, and they will be reported separately.

Figure 3 distinguishes between the locations of heat flows reported herein (squares) and those previously published (triangles). Figure 4 distinguishes between all heat flows with values in the 'low-to-normal' range (defined by $q \leq 1.5$ HFU) and those 'higher than normal' (defined by $q \geq 1.6$ HFU, with all values rounded to the nearest 0.1 HFU). It is seen from Figure 3 that the western United States as a whole is still very poorly sampled. From Figure 4 and the histogram, Figure 5, it is seen that the heat flow as we now know it is extremely variable and is dominated by higher-than-normal values. That part of the western United States to the west of the Great Plains corresponds to the 'Mesozoic-Cenozoic orogenic areas' of *Lee and Uyeda* [1965]. The most recent compilation of 159 values from such areas throughout the world [*Lee*, 1970] yielded a mean of 1.76 and standard deviation of 0.58. These values are almost identical to those shown for the western United States in Figure 5. This tends to confirm Lee's results even

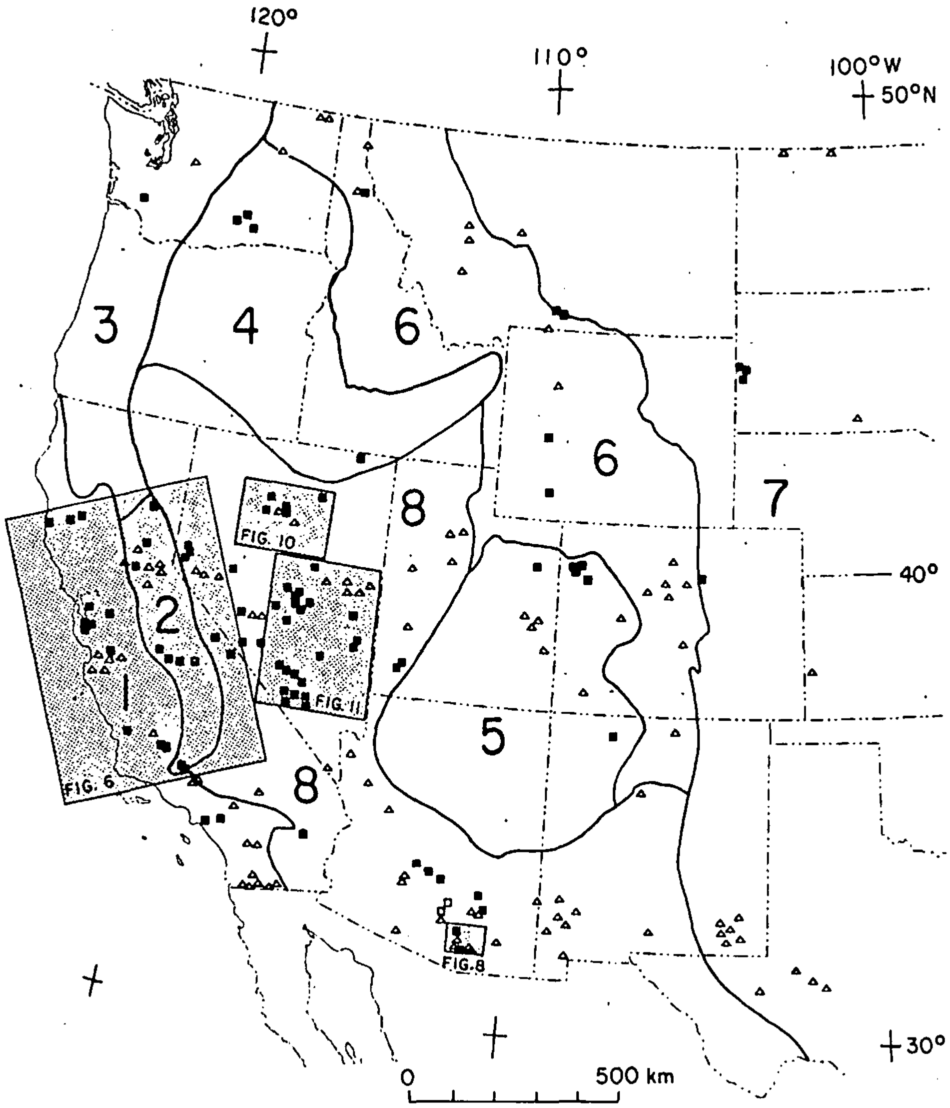

Fig. 3. Sketch map of the western United States showing the locations of heat-flow measurements: Triangles, previously published data (see text for references); squares, U.S. Geological Survey data. The stippled rectangles are shown in greater detail in Figures 6, 8, 10, and 11. The numbers refer to the same physiographic provinces in the corresponding tables.

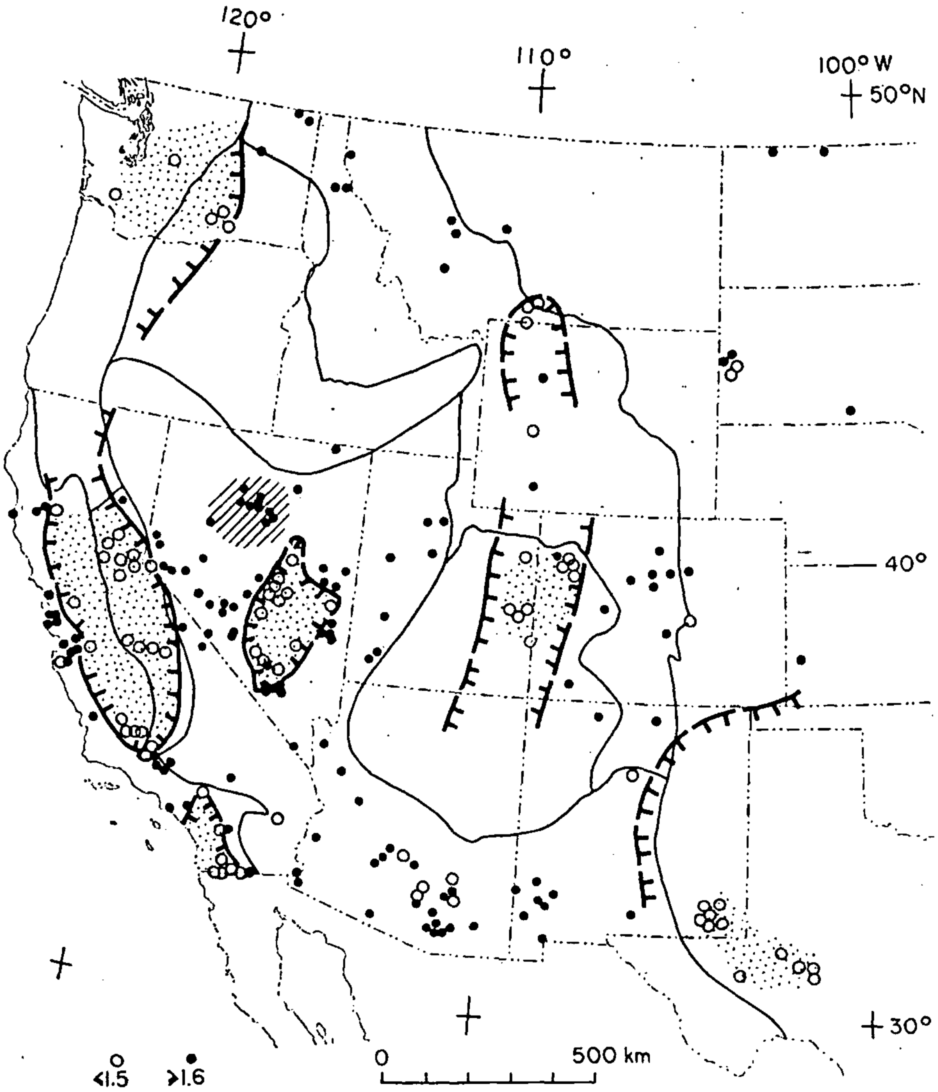

Fig. 4. Generalized representation of heat-flow data from the western United States. Stippled areas are characterized by heat flows of 1.5 and less; the heavy lines are 1.5 HFU contours. The cross-hatched area is characterized by heat flow of 2.5 and greater.

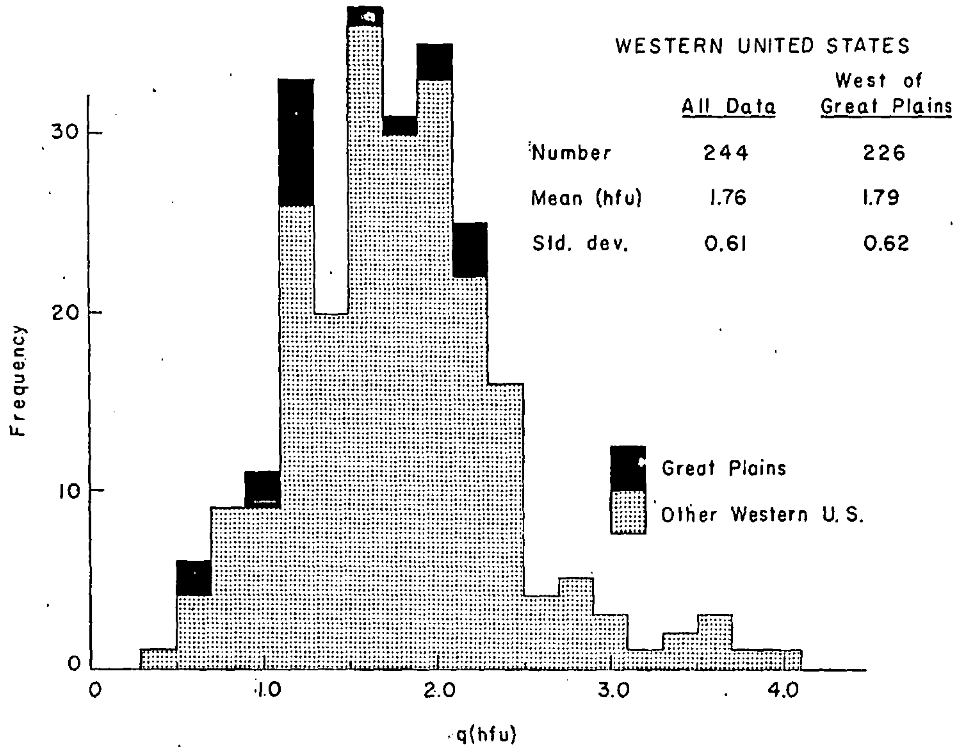

Fig. 5. Histogram of all heat-flow determinations in the western United States. Values greater than 4 HFU were omitted from the analysis.

though almost 100 values are common to both analyses.

From the simple binary division of heat-flow values in Figure 4, it is clear that heat flow from the western United States need not be treated as a homogeneous population. This fact has, of course, been recognized for some time, and many of the features in Figure 4 have been identified by *Roy et al.* [1971] from previously published data. Although the predominant heat flow in the western United States seems to be higher than normal, several regions of lower heat flow with lateral dimensions an order of magnitude greater than crustal thickness can be identified (stippled areas, Figure 4). The heavy dashed lines enclosing these regions (Figure 4) represent a preliminary interpretation of the 1.5 HFU contour. (It is of some interest to note the general coincidence of this contour and the lines enclosing the region of intermediate crustal seismic velocity in Figure 2, *Pakiser and Zietz* [1965].) More refined contouring is probably warranted only in the Sierra Nevada–Great Valley–Coast Range area of California shown in Figure 6.

The semicontinuous band of lower heat flows paralleling the west coast and its gross relation to the San Andreas transform fault system in California suggest explanations in terms of lithospheric subduction and related tectonic processes [see e.g., *Blackwell and Roy*, 1971; *Roy et al.*, 1971]. These models are sensitive to assumptions regarding the magnitudes and distribution in time and space of the opposing effects of cooling by descending plates and heating by friction, compression, radioactivity, and ascending melts. Our present ignorance of the mechanics of these processes permits a broad range of assumptions and a wide variety of explanations of the heat-flow pattern. It is hoped that work in progress at several institutions will increase the heat-flow coverage of this region sufficiently to obtain more useful constraints for models of the continental margin.

One region of conspicuously high heat flow

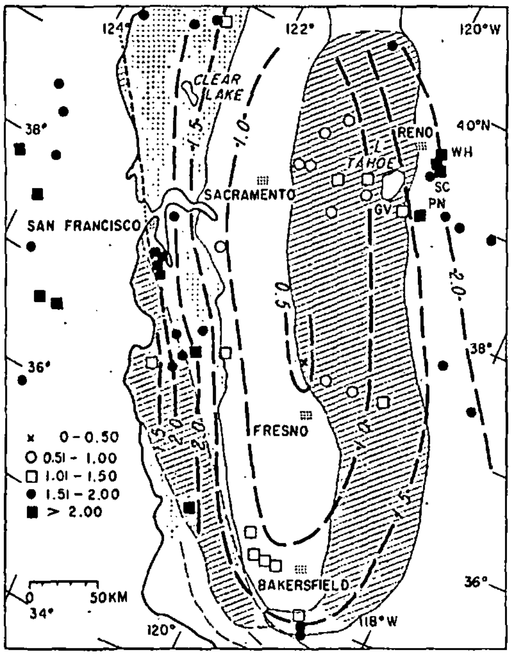

Fig. 6. Heat-flow values in central California and western-central Nevada. (See Figure 3 for location.) Contour interval, 0.5 HFU. The offshore measurements are from *Foster* [1962] and *Burns and Grim* [1967]. The strippled area is the Franciscan block; shaded areas, the Sierra Nevada and Salinian blocks.

occurs in north-central Nevada (cross hatching, Figure 4). The boundaries of this region, and possibly others as yet undetected, could be delineated by more systematic heat-flow coverage. This could provide useful guidance in the search for economically exploitable geothermal fields.

Some comments on the status of observations in the individual provinces follow.

California coastal province (Table 1). This province includes such diverse physiographic regions as the great Central Valley, the Coast Ranges, the peninsular ranges, and the Los Angeles basin. The range of heat flow reflects the heterogeneity of the province.

Heat flow is high in the Franciscan terrane in the vicinity of San Francisco Bay, where all values are around 2.0, irrespective of distance from the major strike-slip faults. This is consistent with measurements farther south by *Brune et al.* [1969], and *Henyey* [1968], which showed no significant heat-flow anomalies associated with strike-slip faults in California. The numerous hot springs in the Coast Ranges north of the San Francisco Bay area up to Clear Lake at about latitude 39°N [*Waring*, 1965] indicate that the band of high heat flow extends northwestward at least that far. North of Clear Lake, heat flow seems high near the coast but decreases inland to a normal value near the eastern limit of Franciscan rocks (Figure 6). The measurements along the western margin of the Central Valley are low to normal, consistent with the earlier result of *Benfield* [1947] near Bakersfield. Measurements in the Los Angeles basin and near Santa Ana indicate a region of high heat flow there (Figure 4).

Sierra Nevada (Table 2). With seven measurements less than 0.75 HFU, the western margin of the Sierra Nevada is now one of the best documented areas of low heat flow on the continents. This finding came as a surprise to many because of the observed masses of granite that were thought to contain sufficient heat sources to account for much higher heat flows. It is consistent, however, with low values reported from the ocean side of circum-Pacific granitic rocks in Chile [*Diment et al.*, 1965], Amchitka Island [*Sass and Munroe*, 1970], and northeastern Honshu Island [*Uyeda and Horai*, 1964] in what might be related tectonic settings. Theoretical considerations indicate that the paradox results primarily from anomalously low heat flow from the mantle underlying the Sierra Nevada province and secondarily from the low heat production of granitic rocks in the western part of the Sierra [*Roy et al.*, 1968*b*; *Lachenbruch*, 1968*a*, 1970]. It now appears that the mantle (or deep crustal) heat flow in the Sierra (0.4 HFU) is only about half that characteristic of stable regions and less than one-third that of the Basin and Range province to the east. The increase in heat flow eastward to the Sierra crest (Figure 6) seems generally to correspond to an increase in crustal heat production. The transition at the Basin and Range boundary is discussed in a later paragraph.

Physiographically, the Tehachapi Mountains are the southern 'toe' of the Sierra Nevada. They are, however, different from the Sierra with respect to structure, origin, and geological history [*Buwalda*, 1954].

Many holes were drilled by the California Division of Water Resources along the proposed route for the California aqueduct system. Suitable temperatures were measured in four of the holes, and heat flows are listed in Table 2*b*. For DH 43 and DH 65, the heat flows are in reasonable agreement with later measurements in the same holes by *Henyey* [1968]. The Tehachapi range appears to provide a thermal as well as a physiographic boundary between the San Joaquin Valley (low-to-normal heat flow) and the Mojave block of the Basin and Range province, which is probably characterized by higher-than-normal heat flow (Figures 4 and 6).

Pacific Northwest coastal province. Table 3 presents one of the first reliable estimates of heat flow from this province. This low value near Chehalis, Washington, raises the possibility that the crustal heat production in the area is low or, alternatively, that this province is similar to the Sierra Nevada, having a very low heat flow from the mantle. Intrusive rocks were not encountered at Chehalis, and they are rare in the area. Where Tertiary intrusive rocks are seen, they are mafic sills of gabbro or basalt porphyry [see e.g., *Snavely et al.*, 1958; *Henriksen*, 1956]. H. C. Wagner and P. D. Snavely, Jr., reported in 1966 that the pre-Tertiary crystalline basement of western Washington (not exposed in the Chehalis area) is principally gneissic amphibolite and quartz diorite (in unpublished report of U.S. Congressional Committee on Interior and Insular Affairs, 89th Congress, 2nd Session, pp. 37–46). Thus the small amount of information available on deep crustal composition indicates a rather mafic crust containing few radiogenic heat sources, an observation consistent with the low observed heat flow and a moderate heat flow from the mantle.

Columbia Plateaus. Largely on the basis of observed volcanism, hot spring activity, and seismicity, *Blackwell* [1969] included the Columbia Plateau in his postulated 'Cordilleran Thermal Anomaly Zone' (CTAZ) of high heat flow. From the present results (Table 4) it appears that at least the western part of the plateaus may be part of a province of low-to-normal heat flow (see also Figure 4). A single high value from northeastern Nevada supports the assumption that the Snake River Plain is part of the CTAZ (Figure 4).

The Colorado Plateau (Table 5). A heat flow of 2.01 was obtained near the eastern boundary of the plateau. This high value is consistent with the findings of *Decker* [1969, and personal communication] in this part of the plateau and the neighboring southern Rocky Mountains, and with the suggestion [*Edwards*, 1966] that this part of the plateau is underlain by granitic rocks. In the northern part of the plateau, five new sites give normal values with only one (category 3) value as high as 2 (Figures 3 and 4). This part of the plateau evidently is underlain by a Precambrian sedimentary terrane [*Edwards*, 1966]. Low heat flow in the northern Colorado Plateau is also consistent with *Porath*'s [1971] interpretation of the depth to an electrically conductive layer in this region on the basis of observed magnetic variation anomalies.

Rocky Mountain province (Table 6). A value of 2.3 was measured in the Galena mine near Wallace, Idaho, confirming the high values measured by *Blackwell* [1969] slightly to the east. The five estimates of heat flow from the central Rocky Mountains are all in the range 1.3 to 1.6 HFU. The high value measured at Denver is included in the Rocky Mountains even though Denver is physiographically part of the Great Plains. This is higher than the nearest neighboring point, *Decker*'s [1969] value of 1.52 at Golden, but it is consistent with the general pattern of high heat flow in the southern Rocky Mountains.

Great Plains province (Table 7). The only heat-flow estimates made in the Great Plains during this work were at three sites in the Black Hills of South Dakota and one near Lyons, Kansas (not shown in Figures 3 and 4). The Black Hills values show a very large variation over a relatively small area, and none is in category 1. The hole at Dacy (which agrees with *Blackwell*'s [1969] estimate at Lead) had been completed only 10 days before the temperature measurements were made, and there was evidence of residual drilling disturbances in the temperature profile. Water was flowing slowly but steadily from the collars of both holes from which heat flow is low. Examination of the temperature profiles (Figure 7), however, indicated no vertical water movement below the zone of influx of the Artesian flow, and the vertical temperature profiles below these points were linear and mutually consistent. The low heat flows may well be the result of some fairly deep seated regional hydrologic effect of long duration that has, in effect, thermally decoupled the rocks penetrated by these holes from the earth below. On the other hand, the possibility that the high heat flows at Lead and Dacy are the result of some local anomalous situation cannot be ignored. We do not have enough information to define a regional heat flow for the Black Hills.

Basin and Range province (Table 8). The majority of the data presented in this paper are from the Basin and Range physiographic province, and they generally confirm that this province is one of high heat flow (Figure 4). In addition, however, the new data define some distinct subprovinces, and they place further constraints on the nature of the transition between the Sierra Nevada and the Basin and Range provinces.

Tucson area. A detailed examination of the 15 heat-flow determinations in a 100 km² area near Tucson serves to illustrate some of the problems of measuring heat flow in the Basin and Range province and to emphasize that even a 'first-rate' single determination in a region of unknown, complicated structure can be a poor indicator of the actual regional heat flux.

Our six values in this region are all in category 1, and, from the information given in their table, it appears that all the values of *Roy et al.* [1968b] are also in this category. There is, however, a spread of nearly a factor of 2 between the extreme values (Figures 8 and 9 and Table 9). Despite the variation within each set of determinations, the mean heat flow determined from one set is not significantly different from that calculated from the other (see Table 9).

The structural complexity and the range of heat-flow values encountered in this region are similar to those encountered at Mt. Isa, Queensland, by *Hyndman and Sass* [1966]. In the present instance, even though the general structure of the region is well known from drilling and mining operations, there is insufficient knowledge of detailed structure to make the necessary corrections. The combination of steeply dipping beds of contrasting conductivity and ubiquitous faults on every scale probably results in a 'worst case' situation in this region, and several holes are needed to arrive at a reliable estimate of regional heat flux. The coefficient of correlation between q and K is about 0.23 (Figure 9), a value typical of many found by *Horai and Nur* [1970] on a larger scale. This poor correlation implies a complicated situation that cannot be resolved by simple geometrical refraction models even on a scale as small as that illustrated in Figure 8.

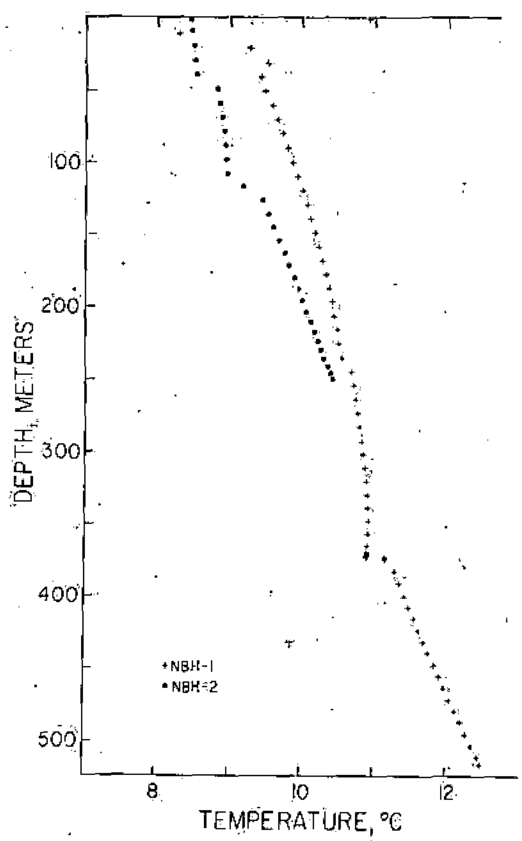

Fig. 7. Temperature profiles from Windy flats (NBH-1) and Moonshine gulch (NBH-2), South Dakota. See Table 7.

Subprovinces in the Basin and Range. Most heat-flow values in this province are in the range 1.5 to 2.5 HFU. There are some isolated very high and low-to-normal values that are most probably related to local hydrologic conditions. In addition, however, there are clusters of consistently high or low values of regional extent for which we must seek more deep-seated causes. From the present work, we define the 'Battle Mountain high' (Figure 10) and the 'Eureka low' (Figure 11). There is also a single category-1 datum of 1.3 HFU near Eagle

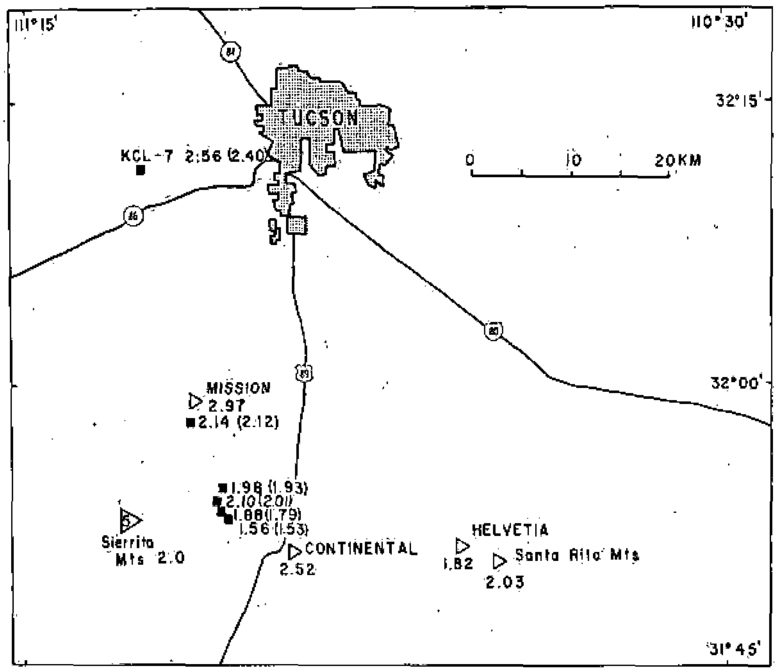

Fig. 8. Heat flows near Tucson, Arizona (see Figure 3 for location). Triangles, values from *Roy et al.* [1968*b*]; squares, U.S. Geological Survey values. The values in parentheses were calculated in the same way as those of Roy et al.

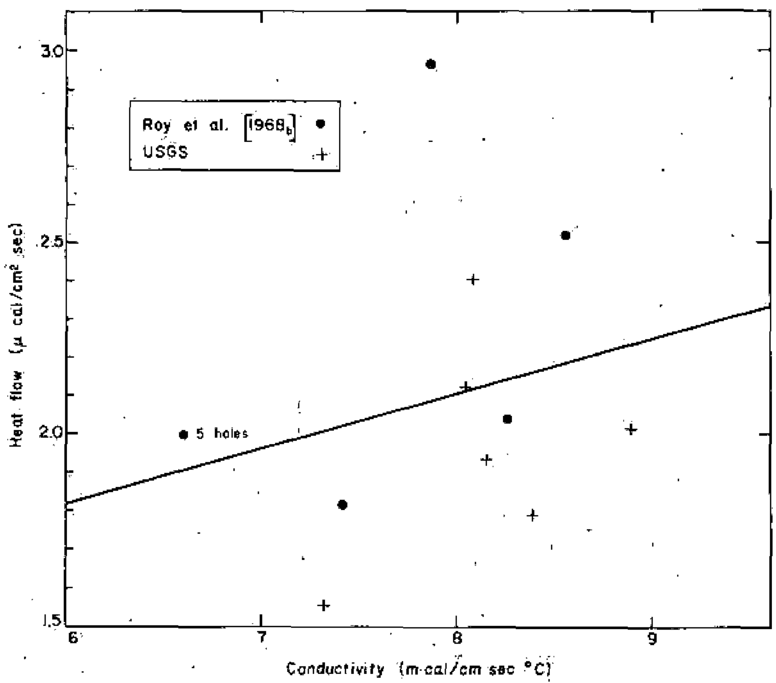

Fig. 9. Heat flow versus mean conductivity for the locations shown in Figure 8.

TABLE 9. Mean Heat Flows in HFU for the Region South and West of Tucson, Arizona (Range of individual values, 1.56 to 2.97)

Source of Data	Number of Holes	Total Length,* meters	Average Heat Flow	Standard Error
Present work	6	1400	2.04	0.13
Roy et al. [1968*b*]	9	1430	2.15	0.12
Present work and *Roy et al.* [1968*b*]	15	2830	2.10†	0.09
Present work and *Roy et al.* [1968*b*]	15	2830	2.12‡	0.06

* This includes only those parts of the holes for which temperatures were used to calculate heat flow.
† Simple average of all values.
‡ Mean weighted according to the length of individual holes.

Mountain, California (in the Mojave Block), which may form part of a region of normal heat flow.

It is interesting that there are no thermal springs near Eagle Mountain and that within the Eureka low the thermal springs are less common and are cooler than in the surrounding areas [see *Waring*, 1965]. By contrast, the Battle Mountain high contains a fairly dense, regular distribution of warm-to-hot-water springs including the well-known Beowawe geysers (Figure 10).

The high mean heat flow from the Basin and Range province has been interpreted in terms of near-melting conditions in the lower crust and upper mantle [see e.g. *Roy and Blackwell*, 1966; *Roy et al.*, 1968*b*, 1971; *Lachenbruch*, 1970], and it seems reasonable to interpret the Battle Mountain high as a transient effect of fairly recent crustal intrusion. This view is supported by evidence of Quaternary volcanism within the region [see e.g., *Roberts*, 1964].

Figure 11 shows a large area north of Las Vegas, which we have called the 'Eureka low,' characterized by heat flows in the range of 0.7 to 1.5 HFU. (The relatively high value of 1.9

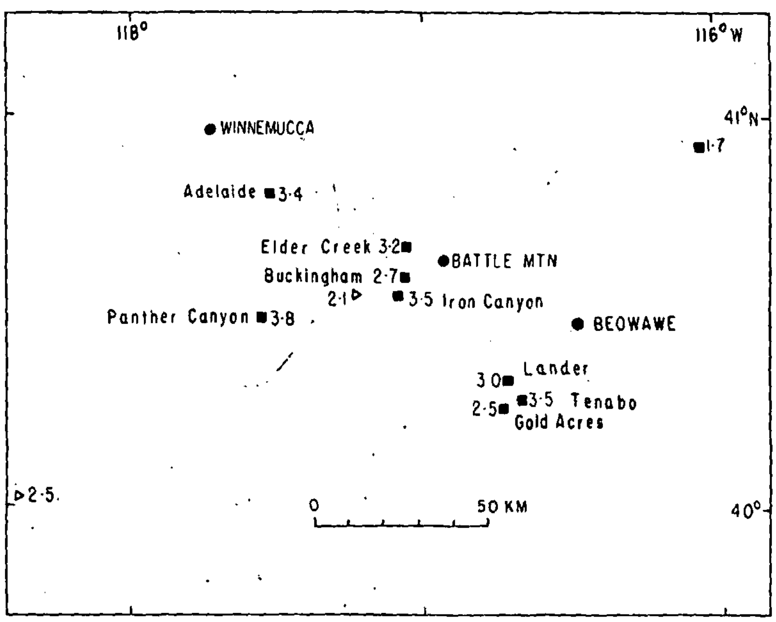

Fig. 10. Heat flows within the 'Battle Mountain high' (see Figure 3 for location). The symbols are as in Figure 8.

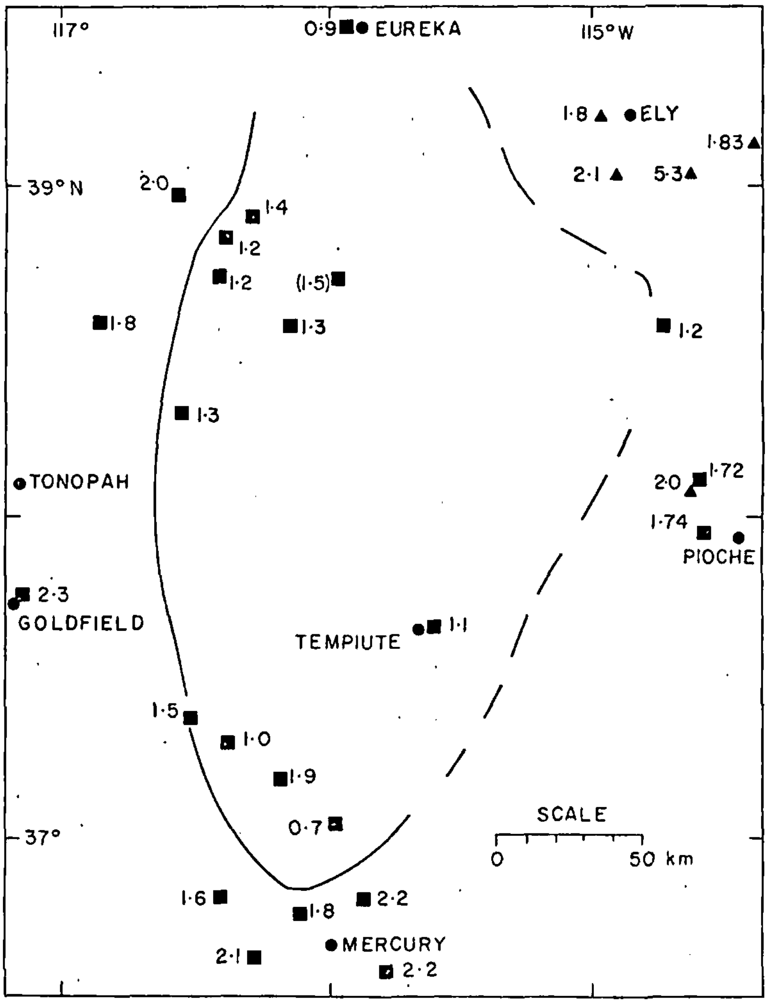

Fig. 11. Heat flows between Mercury and Eureka, Nevada (see Figure 3 for location); the heavy line is a 1.5-HFU contour defining the 'Eureka low.' Symbols are as in Figure 8.

near the southern end of the Eureka low was measured in dolomite near a contact with volcanic rocks and may be caused, in part, by refraction.) This large apparent anomaly in the normally 'hot' Basin and Range may be interpreted in at least two ways. It could represent a systematic hydrologic effect of regional extent or it might be a region where temperatures in the lower crust and upper mantle have been below the solidus for some time. However, the abrupt transitions on the margin of the feature (Figure 11) favor a fairly shallow origin for the anomaly. Our fragmentary temperature data from very deep holes in southern Nevada suggest an explanation in terms of systematic though complex interbasin ground water flow with appreciable vertical velocity components to depths of about 3 km (~1 km below sea level). The identification of such flow patterns is, of course, fundamental to an understanding of the hydrology of this large arid area [see e.g. *Winograd and Thordarson*, 1968]. It is also fundamental to the evaluation of regional heat-flow analyses, since the conductive flux determined in the upper kilometer is usually identified tacitly with heat loss from the earth's interior. It is seen (Table 8) that several heat flows in the Eureka low have been assigned to the 'highest quality' category (1) on the basis of usually applied criteria of internal consistency. Only under exceptional circumstances will supplementary information be available to reveal the possible occurrence of deep-seated 'hydrologic decoupling' on a regional scale.

The Sierra Nevada–Basin and Range transition. *Roy and Blackwell* [1966] and *Roy et al.* [1968*b*, 1971] have concluded that the transition between these two provinces takes place over a short distance (on the order of 100 km) within the Basin and Range province. Data now available suggest a more abrupt transition that might extend into the eastern Sierra Nevada.

Figure 6 shows all the previously published data along the transition together with the present results. The most striking increase in heat flow is that between Gardnerville (GV) and the Pine Nut Canyon (PN). If equal weight is given to the two values, then we must conclude that the transition occurs within 20 km. North of these points the new data firmly establish high heat flow between Carson City and Reno, only 15 to 20 km from the physiographic boundary of the Sierra province. Although independent evidence [*Becker*, 1882] indicates that the very high heat flows near the Comstock lode are from local hydrologic effects, no such effects are evident at Washington Hill (WH), Silver City (SC), or Pine Nut Canyon (PN) (Figure 6). Measurements at Black Rock and Deep Spring 150 km to the south, (10 and 35 km from the physiographic boundary), also indicate high heat flow extending very close to the edge of the Basin and Range province.

As previously mentioned, interpretive studies suggest that the thermal transition from the Basin and Range province to the Sierra Nevada might involve a change in heat flow from the deep crust or mantle by a factor of 3. Such a transition would be extremely difficult to explain by almost any model if it occurred over a lateral distance of only 10 or 20 km (a situation that must exist if we assume that the transition zone is in the Basin and Range province). It therefore seems probable that, like the Basin and Range faulting, the heat-flow transition extends into the eastern Sierra. This view is supported by recent heat-flow results from Lake Tahoe presented by *Lee and Henyey* [1970].

Acknowledgments. We are greatly indebted to many individuals connected with the mining and petroleum industries, without whose willing help the majority of the determinations presented here would not have been possible. We are grateful to other governmental agencies, in particular the Atomic Energy Commission, the Bureau of Mines, the Bureau of Reclamation, and the California Division of Water Resources, for allowing access to their boreholes. Many colleagues in the U.S. Geological Survey were very helpful in supplying information on regional and local geology and in arranging access to exploratory borings in their areas. We thank R. F. Roy for kindly giving us a preprint of *Roy et al.* [1971] and for allowing us to cite the manuscript. John Tanida and Ming Ko rendered valuable assistance in the processing of the vast number of primary data. G. Brent Dalrymple, William H. Diment, William B. Joyner, and Donald E. White read the manuscript and offered valuable comments.

Publication has been authorized by the Director, U.S. Geological Survey.

REFERENCES

Beck, A. E., Techniques of measuring heat flow on land, in *Terrestrial Heat Flow, Geophys. Monogr. Ser.*, vol. 8, edited by W. H. K. Lee, pp. 24–57, AGU, Washington, D. C., 1965.

Becker, G. F., *Geology of the Comstock Lode and the Washoe District, U.S. Geol. Surv. Monogr. 3*, 422 pp., 1882.

Benfield, A. E., A heat flow value for a well in California, *Amer. J. Sci., 245*, 1–18, 1947.

Birch, Francis, Temperature and heat flow in a well near Colorado Springs, *Amer. J. Sci., 245*, 733–753, 1947.

Birch, Francis, The effects of Pleistocene climatic variations upon geothermal gradients, *Amer. J. Sci., 246*, 729–760, 1948.

Birch, Francis, Flow of heat in the Front Range, Colorado, *Geol. Soc. Amer. Bull., 61*, 567–630, 1950.

Birch, Francis, The present state of geothermal investigations, *Geophysics, 19*, 645–659, 1954.

Birch, Francis, and Harry Clark, The thermal conductivity of rocks and its dependence on temperature and composition, *Amer. J. Sci., 238*, 529–558 and 613–635, 1940.

Birch, Francis, R. F. Roy, and E. R. Decker, Heat flow and thermal history in New England and New York, in *Studies of Appalachian Geology: Northern and Maritime*, edited by E-an Zen, W. S. White, J. B. Hadley, and J. B. Thompson, Jr., pp. 437–451, Interscience, New York, 1968.

Blackwell, D. D., Heat-flow determinations in the northwestern United States, *J. Geophys. Res., 74*, 992–1007, 1969.

Blackwell, D. D., and R. F. Roy, Geotectonics and Cenozoic history of the western United States (abstract), *Geol. Soc. America, Cordil-*

leran Sect., 67th Annu. Meet., Riverside, Calif., 1971, Abstr. Programs, 3, 84–85, 1971.

Bredehoeft J. D., and I. S. Papadopulos, Rates of vertical groundwater movement estimated from the earth's thermal profile, *Water Resour. Res., 1,* 325–328, 1965.

Brune, J. N., T. L. Henyey, and R. F. Roy, Heat flow, stress, and rate of slip along the San Andreas fault, California, *J. Geophys. Res., 74,* 3821–3827, 1969.

Bullard, E. C., Heat flow in South Africa, *Proc. Roy. Soc. London, Ser. A, 173,* 474–502, 1939.

Bullard, E. C., The time necessary for a borehole to attain temperature equilibrium, *Mon. Not. Roy. Astron. Soc., Geophys. Suppl., 5,* 127–130, 1947.

Burns, R. E., and P. J. Grim, Heat flow in the Pacific Ocean off central California, *J. Geophys. Res., 72,* 6239–6247, 1967.

Buwalda, J. P., Geology of the Tehachapi Mountains, California, in *Geology of Southern California,* edited by R. H. Jahns. *Calif. Dep. Natur. Resour. Div. Mines Bull., 170*(6), 131–142, 1934.

Clark, S. P., Jr., Heat flow at Grass Valley, California, *Eos Trans. AGU, 38,* 239–244, 1957.

Combs, J. B., Terrestrial heat flow in north central United States, Ph.D. thesis, Massachusetts Institute of Technology, Cambridge, 1970.

Costain, J. K., and P. M. Wright, Heat flow and geothermal measurements in Utah (abstract), *Eos Trans. AGU, 49,* 325, 1968.

Decker, E. R., Heat flow in Colorado and New Mexico, *J. Geophys. Res., 74,* 550–559, 1969.

Diment, W. H., Francisco Ortiz O., Louis Silva R., and Carlos Ruiz F., Terrestrial heat flow at two localities near Vallenar, Chile (abstract), *Eos Trans. AGU, 46,* 175, 1965.

Edwards, Jonathan, Jr., The petrology and structure of the buried Precambrian basement of Colorado, *Quart. Colo. School Mines, 61*(4), 436 pp., 1966.

Fenneman, N. M., Physiographic divisions of the United States, *Ann. Ass. Amer. Geogr., 18,* 261–353, 1928.

Foster, T. D., Heat-flow measurements in the northeast Pacific and in the Bering Sea, *J. Geophys. Res., 67,* 2991–2993, 1962.

Henriksen, D. A., Eocene stratigraphy of the lower Cowlitz River-eastern Willapa Hills area, southwestern Washington, *Wash. Dep. Conserv. Div. Mines Geol. Bull., 43,* 122 pp., 1956.

Henyey, T. L., Heat flow near major strike-slip faults in central and southern California, Ph.D. thesis, California Institute of Technology, Pasadena, 1968.

Herrin, Eugene, and S. P. Clark, Jr., Heat flow in west Texas and eastern New Mexico, *Geophysics, 21,* 1087–1099, 1956.

Horai, Ki-iti, and Amos Nur, Relationship among terrestrial heat flow, thermal conductivity, and geothermal gradient, *J. Geophys. Res., 75,* 1985–1991, 1970.

Howard, L. E., and J. H. Sass, Terrestrial heat flow in Australia, *J. Geophys. Res., 69,* 299–308, 1964.

Hyndman, R. D., and J. H. Sass, measurements at Mount Isa, Que *Geophys. Res., 71,* 587–601, 1966.

Jaeger, J. C., The effect of the drilling temperatures measured in boreholes, *phys. Res., 66,* 563–569, 1961.

Jaeger, J. C., Application of the theory conduction to geothermal measureme *Terrestrial Heat Flow, Geophys. Monog.* vol. 8, edited by W. H. K. Lee, pp. 7–23, Washington, D. C., 1965.

Jaeger, J. C., and J. H. Sass, Lee's topogra correction in heat flow and the geothermal in Tasmania, *Geofis. Pura Appl., 54,* 53–63, 19

Jaeger, J. C., and R. F. Thyer, Report on progr in geophysics: Geophysics in Australia, *Ge phys. J., 3,* 450–461, 1960.

Kraskovski, S. A., On the thermal field in shields, *Izv. Akad. Nauk. SSSR, Ser. Geofiz.,* 247–250, 1961.

Lachenbruch, A. H., Three-dimensional heat flow in permafrost beneath heated buildings, *U.S. Geol. Surv. Bull. 1052-B,* 51–69, 1957*a*.

Lachenbruch, A. H., Thermal effects of the ocean on permafrost, *Geol. Soc. Amer. Bull., 68,* 1515–1529, 1957*b*.

Lachenbruch, A. H., Preliminary geothermal model of the Sierra Nevada, *J. Geophys. Res., 73,* 6977–6989, 1968*a*.

Lachenbruch, A. H., Rapid estimation of the topographic disturbance to superficial thermal gradients, *Rev. Geophys. Space Phys., 6,* 365–400, 1968*b*.

Lachenbruch, A. H., Crustal temperature and heat production: Implications of the linear heat-flow relation, *J. Geophys. Res., 75,* 3291–3300, 1970.

Lachenbruch, A. H., and M. C. Brewer, Dissipation of the temperature effect of drilling a well in arctic Alaska, *U.S. Geol. Surv. Bull. 1083-C,* 73–109, 1959.

Lachenbruch, A. H., and B. V. Marshall, Heat flow through the Arctic Ocean floor: The Canada basin-Alpha rise boundary, *J. Geophys. Res., 71,* 1223–1248, 1966.

Lachenbruch, A. H., and B. V. Marshall, Heat flow in the Arctic, *Arctic, 22,* 300–311, 1969.

Lachenbruch, A. H., M. C. Brewer, G. W. Greene, and B. V. Marshall, Temperatures in permafrost, in *Temperature—Its Measurement and Control in Science and Industry,* edited by C. M. Herzfeld, vol. 3, pp. 791–803, Reinhold, New York, 1962.

Lachenbruch, A. H., H. A. Wollenberg, G. W. Greene, and A. R. Smith, Heat flow and heat production in the central Sierra Nevada, preliminary results (abstract), *Eos Trans. AGU, 47,* 179, 1966.

Lee, T. C., and T. L. Henyey, Heat flow in Lake Tahoe, California-Nevada (abstract), *Eos Trans. AGU, 51,* 824, 1970.

Lee, W. H. K., On the global variation of terrestrial heat flow, *Phys. Earth Planet. Interiors, 2,* 332–341, 1970.

Lee, W. H. K., and Seiya Uyeda, Review of heat flow data, in *Terrestrial Heat Flow, Geophys. Monogr. Ser., vol. 8,* edited by W. H. K. Lee, pp. 87–190, AGU, Washington, D. C., 1965.

Pakiser, L. C., and Isidore Zietz, Transcontinental crustal and uppermantle structure, *Rev. Geophys. Space Phys., 3,* 505, 1965.

Porath, H., Magnetic variation anomalies and seismic low-velocity zone in the western United States, *J. Geophys. Res., 76,* 2643, 1971.

Ratcliffe, E. H., Thermal conductivities of fused and crystalline quartz, *Brit. J. Appl. Phys., 10,* 22–28, 1959.

Roberts, R. J., Stratigraphy and structure of the Antler Peak quadrangle, Humboldt and Lander counties, Nevada, *U.S. Geol. Surv. Prof. Pap. 459-A,* A1–A93, 1964.

Roy, R. F., Heat flow measurements in the United States, Ph.D. thesis, Harvard University, Cambridge, Mass., 1963.

Roy, R. F., and D. D. Blackwell, Heat flow in the Sierra Nevada and western Great Basin (abstract), *Eos Trans. AGU, 47,* 179–180, 1966.

Roy, R. F., D. D. Blackwell, and Francis Birch, Heat generation of plutonic rocks and continental heat flow provinces, *Earth Planet. Sci. Lett., 5,* 1–12, 1968*a*.

Roy, R. F., E. R. Decker, D. D. Blackwell, and Francis Birch, Heat flow in the United States, *J. Geophys. Res., 73,* 5207–5221, 1968*b*.

Roy, R. F., D. D. Blackwell, and E. R. Decker, Continental heat flow, in *The Nature of the Solid Earth,* edited by E. C. Robertson, McGraw-Hill, New York, in press, 1971.

Sass, J. H., and R. J. Munroe, Heat flow from deep boreholes on two island arcs, *J. Geophys. Res., 75,* 4387–4395, 1970.

Sass, J. H., P. G. Killeen, and E. D. Mustonen, Heat flow and surface radioactivity in the Quirke Lake syncline near Elliot Lake, Ontario, Canada, *Can. J. Earth Sci., 5,* 1417–1428, 1968*a*.

Sass, J. H., A. H. Lachenbruch, G. W. Greene, T. H. Moses, Jr., and R. J. Munroe, Progress report on heat-flow measurements in the western United States (abstract), *Eos Trans. AGU, 49,* 325–326, 1968*b*.

Sass, J. H., R. J. Munroe, and A. H. Lachenbruch, Measurement of geothermal flux through poorly consolidated sediments, *Earth Planet. Sci. Lett., 4,* 293–298, 1968*c*.

Sass, J. H., A. H. Lachenbruch, and R. J. Munroe, Thermal conductivity of rocks from measurements on fragments and its application to heat-flow determinations, *J. Geophys. Res., 76,* 3391–3401, 1971.

Snavely, P. D., Jr., R. D. Brown, Jr., A. E. Roberts, and W. W. Rau, Geology and coal resources of the Centralia Chehalis district, Washington, *U.S. Geol. Surv. Bull., 1053,* 159 pp., 1958.

Spicer, H. C., Geothermal gradients and heat flow in the Salt Valley anticline, Utah, *Boll. Geof. Teor. Appl., 6,* 263–282, 1964.

Uyeda, Seiya, and Ki-iti Horai, Terrestrial heat flow in Japan, *J. Geophys. Res., 69,* 2121, 1964.

Von Herzen, R. P., and A. E. Maxwell, The measurement of thermal conductivity of deep-sea sediments by a needle probe method, *J. Geophys. Res., 64,* 1557–1563, 1959.

Von Herzen, R. P., and Seiya Uyeda, Heat flow through the eastern Pacific floor, *J. Geophys. Res., 68,* 4219–4250, 1963.

Walsh, J. B., and E. R. Decker, Effect of pressure and saturating fluid on the thermal conductivity of compact rock, *J. Geophys. Res., 71,* 3053–3061, 1966.

Waring, G. A., Thermal springs of the United States and other countries of the world, a summary, *U.S. Geol. Serv. Prof. Pap., 492,* 1965.

Warren, R. E., J. G. Sclater, Victor Vacquier, and R. F. Roy, A comparison of terrestrial heat flow and transient geomagnetic fluctuations in the southwestern United States, *Geophysics, 34,* 463–478, 1969.

Winograd, I. J., and William Thordarson, Structural control of groundwater movement in miogeosynclinal rocks of south-central Nevada, in *Nevada Test Site, Mem. 110,* edited by E. B. Eckel, pp. 35–48, Geological Society of America, Boulder, Colo., 1968.

(Received March 22, 1971.)

Heat-Flow Determinations in the Northwestern United States

DAVID D. BLACKWELL[1]

Hoffman Laboratory, Harvard University, Cambridge, Massachusetts 02138

Eleven new heat-flow determinations in the northwestern United States, based on data from twenty-one drill holes and two mine shafts, together with previously available data, suggest a heat-flow pattern similar to that observed in the southwestern United States. In particular the high heat flow found in the Basin and Range province, about 2.0 μcal/cm² sec, is characteristic of the Northern Rocky Mountains province and possibly the Columbia Plateaus as well. This region of high heat flow is referred to in this paper as the Cordilleran thermal anomaly zone. Most of central Wyoming, central Montana, and western Washington may have normal heat flow. A heat-flow determination in the Black Hills is high. The Northern Rocky Mountains and Basin and Range provinces have similar regional heat flow, crustal structure, upper mantle P_n velocity, and Cenozoic geologic history. Thus, tectonic schemes that emphasize the Basin and Range province as a unique area on the North American continent must be reevaluated.

INTRODUCTION

The geophysical characteristics of the crust and upper mantle in the western United States have been the subject of active investigation in the past few years [*Lee and Uyeda*, 1965; *Roy et al.*, 1968b; *Sass et al.*, 1968; *Henyey*, 1968]. The heat flow is normal in the Great Plains province and high (>1.6 μcal/cm² sec) in the Southern Rocky Mountains. The heat flow seems to be normal in at least part of the Colorado Plateaus province but is uniformly high (the average is approximately 2 μcal/cm² sec) in the Basin and Range province. The heat flow in the Sierra Nevada Mountains and the Southern California batholith is normal to low. The Franciscan belt east of the San Andreas fault appears to have a high heat flow while the crystalline belt west of the San Andreas has a normal heat flow. The object of this study is to investigate the heat-flow pattern in the northwestern United States.

The locations of the new heat-flow determinations are shown in Figure 1. Precambrian metamorphic and igneous rocks form the basement in the Dakotas, Wyoming and eastern and central Montana. One heat-flow value was obtained near the edge of the Beartooth Plateau, part of the large outlier of very old Precambrian basement (K-Ar ages >2.5 b.y.) in Wyoming [*Gast et al.*, 1958; *Goldich et al.*, 1966]. The site is only about 70 km from the thermal areas in Yellowstone National Park. Two determinations, one on either side of the outlier of old basement, were made in younger Precambrian metamorphic rocks, in the Black Hills of South Dakota, and in the Little Belt Mountains in Montana. The rocks of the Black Hills and Little Belt Mountains were last metamorphosed about 1700 and 1900 m.y. ago, respectively [*Goldich et al.*, 1966; *Catanzaro and Kulp*, 1964]. A determination is also reported for a site in the Absaroka Mountains of northwestern Wyoming. The Absaroka Mountains are composed of early Cenozoic volcanic and volcanic detrital units and are atypical of the Middle Rocky Mountains. The bedrock in most of northwestern Montana and northern Idaho is late Precambrian sedimentary rocks of the Belt Series; four heat-flow determinations are reported from this terrain. A value in northeastern Washington is in Paleozoic sediments that are a part of a highly deformed belt of sedimentary rocks called the Kootenay Arc [*Yates et al.*, 1966]. The basement in central Idaho and northern Washington is composed of Mesozoic intrusives and metamorphic rocks. The only determination in these rocks is in the Colville batholith in northern Washington. The age of the Colville batholith is about 100 m.y. [*Becraft and Weiss*, 1963, p. 32].

[1] Now at Dallas Geophysical Laboratory, Southern Methodist University, Dallas, Texas 75222.

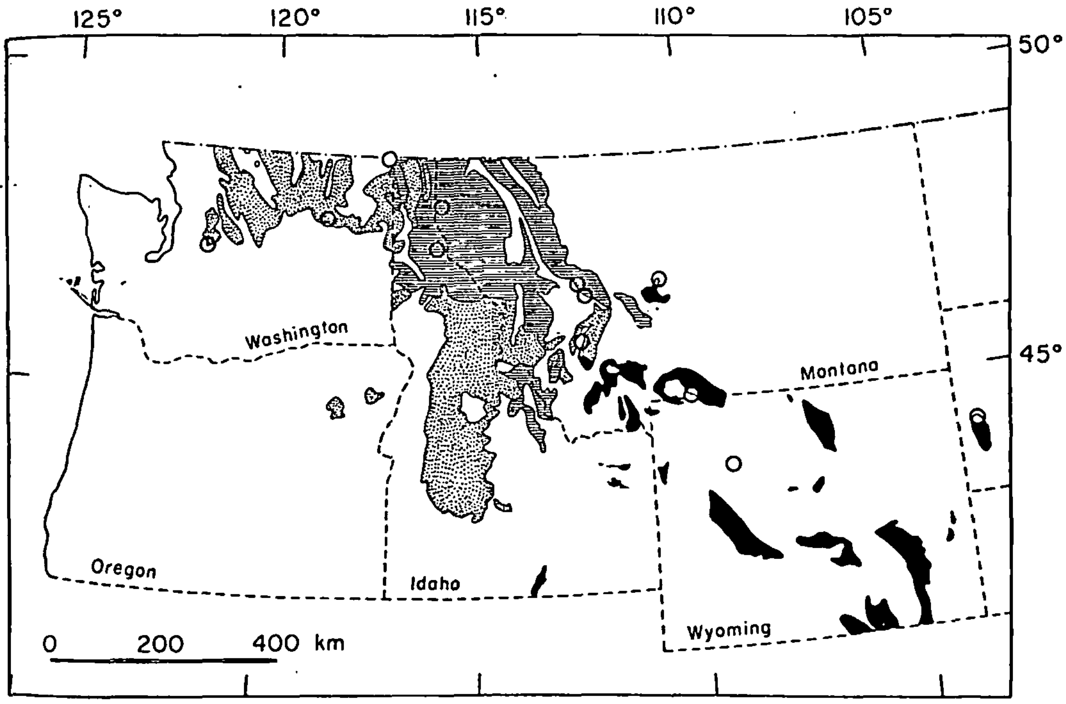

Fig. 1. Large outcrops of basement rocks in the northwestern United States. Solid pattern, Precambrian metamorphic rocks; line pattern, Precambrian sedimentary rocks; dotted pattern, Mesozoic and Cenozoic intrusive rocks.

In addition, a determination in the Late Cretaceous Boulder batholith of western Montana (Blackwell and Robertson, in preparation) will be mentioned. A single determination was made in the northern Cascades in the Snoqualmie batholith. According to K-Ar dating, the batholith was intruded only 17 m.y. ago [*Lipson et al.*, 1961], a date which is in agreement with stratigraphic evidence. Several estimated heat flow values in the Wyoming basin, the Columbia Plateaus in Oregon, and along the Washington coast furnish evidence on the heat flow in areas for which no precise data are available.

Data

Eleven heat-flow determinations based on measurements from 21 drill holes and 2 mine shafts are reported. Because of the large amount of data, only the briefest summary of the details pertinent to each heat-flow determination is possible. The data and a more comprehensive discussion of each determination may be found in the author's thesis [*Blackwell*, 1967].

The mechanical details of the data acquisition and reduction are summarized by *Roy et al.* [1968*b*]. All the heat-flow determinations discussed were made by using holes drilled for the purpose of mineral exploration. The heat-flow determinations are listed in Table 1 and in *Roy et al.* [1968*b*]. All of the heat-flow values, except as noted, were calculated by the resistance integral method. The gradients are least-squares straight lines fitted to the temperature-depth data in the given interval. The conductivity values listed are mean harmonic averages. The errors shown beneath the heat-flow values are statistical and relate only to the internal consistency of the data. The error limits shown for the best value for each area are discussed more fully in the section pertaining to that particular heat-flow determination. Temperature-depth curves for most of the drill holes are shown in Figures 2–5. For clarity only points at 20-meter intervals are plotted although the heat flow values were calculated using measurements made at 10-meter intervals.

Several of the heat flow determinations presented have rather large topographic corrections.

The procedure suggested by *Jeffreys* [1938] and modified by *Birch* [1950] gives satisfactory results if corrections are no greater than 10–15%. The method is much more accurate for drill holes in valleys than on hills, but in both situations the tendency is to overcorrect. Additional error for large corrections may arise owing to departures from the assumed uniform rate of variation of surface temperature with elevation or lateral variations in thermal conductivity. The details are reserved for a later publication, but in two areas the correction calculated in the normal manner was modified to allow for the inaccuracies of the plane approximation. The resulting error of the heat-flow determinations from this source should be no more than 10–15%.

Because the northwestern United States is an area of rugged topography, the effect of topographic evolution was considered for all of the drill holes. For all but two areas the maximum reasonable corrections are not significant (<5%) and so are neglected.

Heat-Flow Determinations

Lead, South Dakota. Temperature data from the Yates and No. 4 and No. 5 Shafts were supplied by the Homestake Mining Company (see Figure 2). The technique of temperature measurement is described by *Noble* [1948]. The formations shown in Figure 2 are described by *Noble and Harder* [1948]. The variation in gradient in the Yates Shaft correlates with conductivity variations between formations, so the change in gradient noted by *Noble* [1948] is due to a change in thermal conductivity and there is no evidence for an increase in heat flow with depth.

Meeteetse, Wyoming. A temperature-depth curve for DDH-17 is shown in Figure 3 (curve 4). The drill hole is in a tuff pipe intruded into the Wiggins Formation of late Eocene and

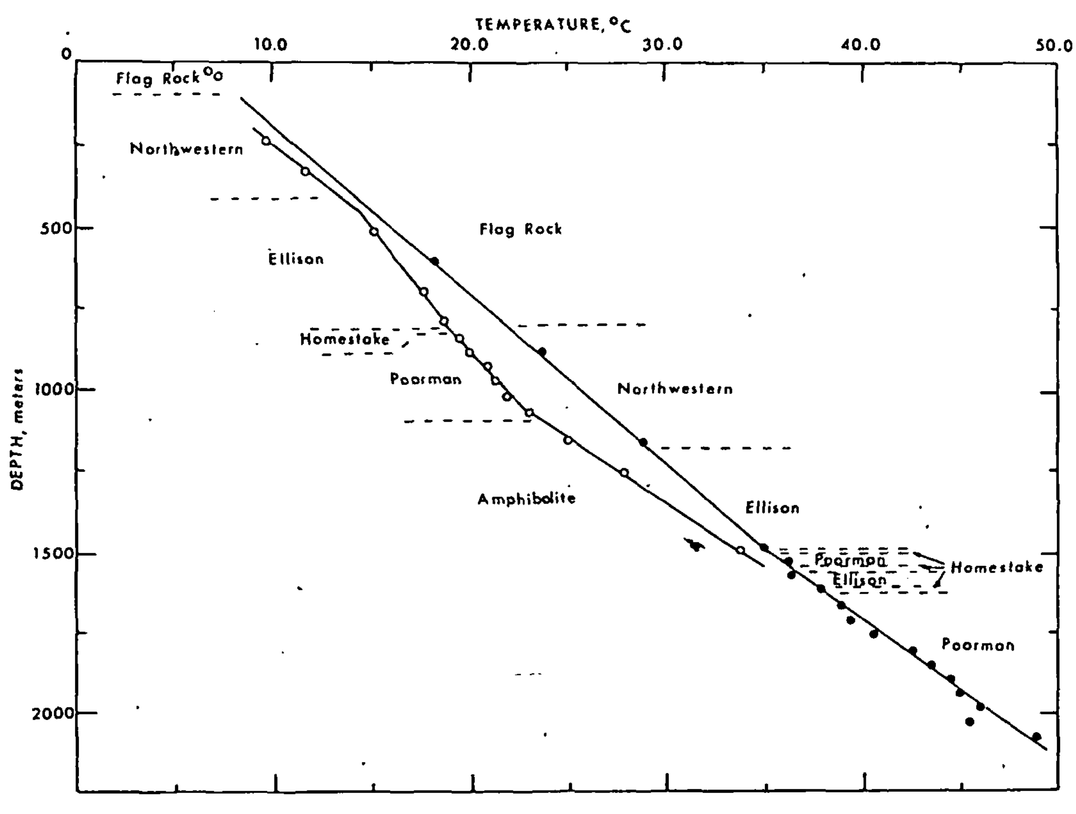

Fig. 2. Temperature-depth curves and rock units in Yates (open circles) and No. 4 and No. 5 (solid circles) Shafts, Homestake Mine, Lead, South Dakota.

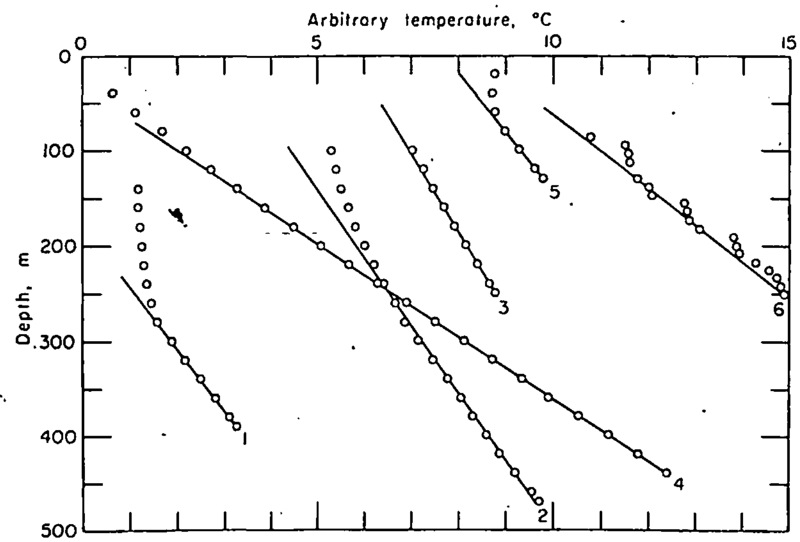

Fig. 3. Temperature-depth curves: 1: Libby, Montana; 2, 3: Wilbur, Washington; 4: Meeteetse, Wyoming; 5, 6: North Bend, Washington.

Oligocene age [*Wilson*, 1964]. The thermal conductivity contrast between the tuff and the surrounding volcanics appears to be small so refraction is not important, although the tuff body may be rather small. A time-dependent terrain correction was applied to the determination. The value listed in Table 1 was calculated assuming uplift of 1.8 km and erosion of 0.6 km in the last 2–9 m.y. [see *Love*, 1939, p. 114].

Cooke City, Montana. The determination is based on data from two drill holes in the Cooke City mining district [*Lovering*, 1929]. The holes penetrate Cambrian sedimentary rocks and the underlying Precambrian granitic rocks. Only DDH-1 is represented by a temperature-depth curve (Figure 4, curve 1). The change in gradient in DDH-1 is matched by a change in thermal conductivity. The heat flow in both drill holes is undisturbed at a depth of only 50 meters.

Neihart, Montana. The heat flow is based on data from two drill holes in the Precambrian metamorphic core of the Little Belt Mountains, but only DDH-37 is illustrated (Figure 4, curve 2). Several porphyry dikes of about the same conductivity as the metamorphic rocks are cut by the drill holes. Above 170 meters in DDH-37 the temperatures are disturbed by flowing water and are not used in the calculation of the heat flow.

Marysville, Montana. Results from three drill holes in contact metamorphosed Belt sediments and Tertiary dikes in the Marysville mining district [*Barrell*, 1907] give abnormally high heat-flow values. The gradients are abnormal (see Figure 5), not the conductivity, so the high values cannot be attributed to refraction. Because there are no hot springs in the area, the best explanation for the high values seems to be a shallow recent intrusion or an untapped reservior of hot water at depth.

Lincoln, Montana. The two drill holes (DDH-1 and DDH-29, curves 3 and 4, Figure 4) cut flat-lying Belt argillite and quartzite and altered quartz monzonite intrusives. The conductivity for DDH-1 was estimated from samples from above 66 meters and from samples in DDH-29. The uncorrected values differ by 25% but the terrain-corrected values differ by only 5%.

Libby, Montana. Temperatures measured in a drill hole in Belt sediments in extreme northwestern Montana are isothermal above 280 meters due to water circulation. Below that depth the gradient is quite linear (curve 1, Figure 3). The sediments in the vicinity of the drill hole are almost flat-lying, although in general the deformation is moderate to intense [*Gibson*, 1948]. The terrain correction is large, but because of the depth of the drill hole the probable error is small. The large estimated

TABLE 1. Measurements of Harmonic Conductivity, Gradient and Heat Flow*

Locality	N. Lat.	W. Long.	Elev., meters	Depth Range, meters	K, mcal/cm sec °C	No.	$\frac{\Delta T}{\Delta z}$, °C/km	Heat Flow, μcal/cm² sec Unc.	Heat Flow, μcal/cm² sec Corr.
Idaho									
Crescent Mine	47°30′	116°05′	1341	1538–1604	12.6	21	17.6	2.20	2.22
					0.2		0.2	0.03	
Silver Summit Mine	47°30′	116°02′	1189	1382–1435	11.7	9	18.8	2.23	2.25
					0.3		0.2	0.03	
Mean									2.2 ± 0.1
Montana									
Cooke City 1	45°30′	109°57′	2793	50–300	7.2	30	18.4	1.29	1.25
					0.2		0.2	0.01	
Cooke City 2†			2870	50–150	8.1	13	18.0	1.45	1.37
					0.4		0.4	0.05	
Mean									1.3 ± 0.1
Libby	48°14′	115°55′	1682	280–390	8.9	26	15.5	1.38	1.75 ± 0.3
					0.4		1.0	0.04	
Lincoln 1†	47°02′	112°23′	1597	100–250	8.8		27.5	2.4	2.1
							0.2		
Lincoln 29			1919	170–270	11.2	10	17.0	1.92	2.22
					0.4		0.2	0.03	
Mean									2.2 ± 0.1
Marysville 2	46°43′	112°21′	2043	100–210	11.7	13	70.4	8.0	
					0.8		2.1	0.2	
Marysville 4			2001	50–270	8.4	13	72.5	6.38	
					0.4		0.5	0.07	
Marysville 6			2043	100–280	9.0	13	72.5	6.68	
					0.6		1.6	0.15	
Best value								6.5 ± 0.2	
Neihart 36	46°58′	110°43′	2006	70–150	6.6	10	24.3	1.56	1.60
					0.6		0.6	0.02	
Neihart 37			1939	170–280	6.5	12	29.1	1.82	1.72
					0.2		0.2	0.03	
Mean									1.7 ± 0.1
South Dakota									
Lead No. 4 Shaft	44°21′	103°45′		1455–2048	7.9	13	23.4	1.82	1.84
					0.3		0.8	0.07	
Yates Shaft			1618	584–1508	10.7	15	19.0	1.98	1.96
					0.8		1.2	0.05	
Mean									1.9 ± 0.1
Washington									
Leadpoint 1	48°55′	117°36′	711	100–240	14.3	16	23.9	3.43	3.00
					0.1		0.1	0.01	
Leadpoint 3			820	290–340	14.4	16	22.0	3.16	2.93
					0.1		0.1	0.02	
Best value‡									2.0 ± 0.3
North Bend 1	47°30′	121°22′	838	80–130	9.4	9	16.2	1.52	1.18
					0.5		0.3	0.03	
North Bend 2			585	80–251	7.2	24	25.2	1.84	1.34
					0.2		1.0	0.08	
Best value§									1.2 ± 0.2
Wilbur A†	48°04′	118°42′	892	90–170	9.1	2	14.5	1.33	1.77
							0.1		
Wilbur B			1036	130–250	9.9	11	12.0	1.17	1.75
					0.5		0.1	0.03	
Wilbur C			963	200–470	9.1	28	13.5	1.23	1.51
					0.4		0.5	0.03	
Weighted mean									1.6 ± 0.2
Wyoming									
Meeteetse	43°52′	109°17′	3010	140–440	6.97	36	30.35	2.14	1.95
					0.05		0.03	0.01	
Best value§									1.8 ± 0.1

* Standard error shown immediately below mean values.
† Heat flow calculated from product of mean harmonic conductivity and least-squares gradient.
‡ Heat flow corrected for refraction.
§ Heat flow corrected for effects of topographic evolution.

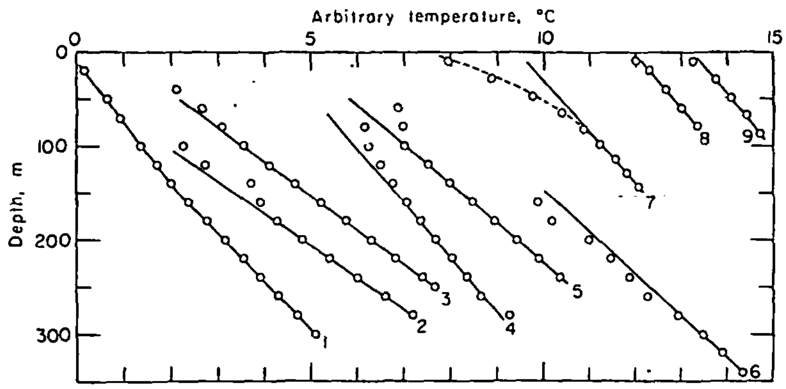

Fig. 4. Temperature-depth curves: 1: Cooke City, Montana; 2: Neihart, Montana; 3, 4: Lincoln, Montana; 5, 6: Leadpoint, Washington; 7, 8, 9: Coeur d'Alene mining district, Idaho.

error for the determination, however, is due to the combined effects of complex geology, possible water circulation, and a large terrain correction.

Coeur d'Alene mining district, Idaho Temperatures were measured in three steeply-inclined underground drill holes, two in the Crescent Mine belonging to the Bunker Hill Mining Company and one in the Silver Summit Mine belonging to the Hecla Mining Company. The geology in the district is complex, and in the vicinity of the mines, on the north limb of an anticline south of the Osburn fault [*Hobbs et al.*, 1965, section B, plates 2 and 3], the average dip is about 70°. The two drill holes in the Crescent Mine (DDH-841, curve 8; DDH-854, curve 9, Figure 4) are only a few meters apart in a recently opened crosscut and are treated as a single value. They penetrate rocks of the Revett quartzite. The drill hole in the Silver Summit Mine (DDH-3417, Figure 4, curve 7) in the St. Regis argillite is in an old crosscut, and the ventilation effects penetrate to 80–90 meters (the calculated effect shown as a dotted curve agrees well with the observed effect). The rocks are anisotropic, and because the drill holes were inclined the vertical conductivity of the samples was obtained from measurements perpendicular to bedding ($K_\perp$) and parallel to bedding ($K_\parallel$). The ratios of $K_\parallel$ to $K_\perp$ range from 1.1 to 1.5 for the quartzites and from 1.7 to 2.5 for the argillites. The average value of $K_\perp$ is 7.9 (ranging from 4.4 to 10.8) for the rocks of the St. Regis formation cored by DDH-3417 and is 10.0 (ranging from 7.8 to 13.6) for rocks of the Revett quartzite cored by DDH-841 and DDH-854. The equivalent average values of $K_\parallel$ are 12.6 and 13.0, so that the more steeply inclined the rocks, the more uniform the vertical thermal conductivity. The agreement of the two heat-flow values is excellent, but the possibility of large-scale refraction cannot be ruled out.

Leadpoint, Washington. Temperature-depth curves from two drill holes in the Cambrian Metaline dolomite are shown in Figure 4 (DDH-1, curve 5; DDH-3, curve 6). The temperatures are disturbed by water movement above 100 meters in DDH-1 and above 290 meters in DDH-3. However, the heat-flow value for the interval 200–340 meters in DDH-3 (3.1 ± 0.1) does not differ from that in the

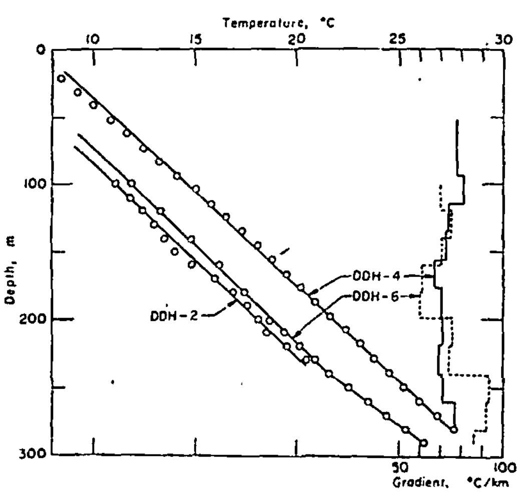

Fig. 5. Temperature-depth curves and gradients, Marysville, Montana.

most stable interval (290–340 meters). The heat flow in both drill holes is abnormally high. Geologic mapping suggests that the dolomite body is pod-shaped [*Yates*, 1964, section *BB'*]. According to the formula given by *Jaeger* [1965] for a horizontal semi-elliptical cylinder of the appropriate size, the heat flow in the country rock at a large distance from the dolomite would be between 1.7 and 2.3 if the average thermal conductivity of the country rock lies between 6.0 and 11.0. The best value of regional heat flow is taken to be 2.0 ± 0.3.

Wilbur, Washington. Temperatures were measured in three holes in an area of high relief and complex alteration. There is a partial conductivity-gradient correlation in DDH-C (Figure 3, curve 2). Data from DDH-B are also shown (Figure 3, curve 3). The terrain corrections were calculated by using surface temperature data from the drill holes rather than an assumed uniform lapse rate. The data will be described in more detail in a later publication. For the purposes of this paper, the best value is taken to be the average (weighting DDH-C twice) of the values.

North Bend, Washington. Data are available in two shallow drill holes in the northern Cascades. Below 70 meters in DDH-1 (Figure 3, curve 5) there is a good gradient-conductivity correlation. The temperature-depth curve in DDH-2 shows abundant evidence of water movement. Least-square lines fitted to all of the data or to the points possibly least disturbed give the same result (the line fitted to the latter data points is shown in Figure 3, curve 6). The heat-flow values calculated for the two drill holes agree in spite of the uncertainties. The terrain-corrected values were increased by 5% to allow for inaccuracies in the correction. A correction for 2 km of uplift and 1.0–1.5 km of erosion in about 6 m.y. was also applied to the data. Geological data indicates that the Snoqualmie batholith was intruded very close to the surface. If so, a correction for the initial heat of the batholith is negligible.

Published and Estimated Heat-Flow Determinations

Although no other heat-flow study has dealt with the northwestern United States, some published information on the heat flow is available (Table 2*A*). *Garland and Lennox* [1962] report heat-flow values of about 1.5 in two oil wells in the Alberta plains at 54°N. In addition, some data on gradients in holes drilled for hydrocarbon exploration in the northwestern United States and Canada are available. Although the gradients alone cannot be used for precise heat-flow determinations, they will in some cases indicate whether the heat flow is high or normal. *Anglin and Beck* [1965] report gradients from two localities in southwestern Alberta, but they do not identify the section involved. *Van Ostrand* [1951] published gradients from many wells in the northwestern United States. Recently *Spicer* [1964] published a tabulation of all of the temperature measurements made during the early 1900's by Van Ostrand and others of the U. S.

TABLE 2*A*. Published Heat-Flow Determinations in the Northwestern United States

Locality	N. Lat.	W. Long.	Rock Type	Heat Flow, $\mu cal/cm^2$ sec	Reference
Idaho					
Wallace			Precambrian sediments	>2.0	*Sass et al.* [1968]
Montana					
Butte	46°03′	112°33′	Boulder batholith	2.2	Blackwell and Robertson, in prep.
Washington					
Metaline	48°55′	117°20′	Cambrian dolomite	2.3	*Roy et al.* [1968*b*]
Central Wash.			Tertiary basalt	'normal'	*Sass et al.* [1968]
Western Wash. (3 values)			Tertiary sediments	'normal'	*Sass et al.* [1968]
Wyoming					
Wind River Mts.			Precambrian granite	1.3	*Sass et al.* [1968]

TABLE 2B. Estimated Heat-Flow Determinations in the Northwestern United States

Locality	N. Lat.	W. Long.	Average Depth, m (no.)*	Rock Type	Average Gradient, °C/km†	Estimated K, millical / cm sec °C	Heat Flow, μcal/cm² sec
Montana							
Conrad	48°20′	111°55′	690(2)	Shale	20.5	4.0 ± 0.5	0.8 ± 0.1
			(1)	Dolomite	10.0	10.0 ± 0.5	1.0 ± 0.1
Kevin-Sunburst	48°45′	111°50′	400(6)	Shale	23.4	4.0 ± 0.5	0.9 ± 0.1
			(2)	Limestone	15.3	6.5 ± 1.0	1.0 ± 0.2
North Dakota							
Lone Tree	48°18′	101°40′	1143(1)	Shale and Limestone	39.8	>3.5	>1.4
Oregon							
Astoria	46°09′	123°53′	1152(1)	Sandstone and shale	30.9	...	...
Burns	43°27′	118°6′	1140(1)	Basalt	40.0–45.0	4.5 ± 0.5	2.0 ± 0.3
Klamath County	42°12′	121°50′	400(4)	Lava and tuffs	48.0–98.0	...	>1.6
Vale	43°46′	117°22′	395(1)	?	77.7	...	>1.6
Washington							
Benton City	46°25′	119°34′	650(1)	Basalt	38.3	4.5 ± 0.5	1.7 ± 0.2
Moclips	47°12′	124°6′	1030(1)	Shale	27.1	4.0 ± 0.5	1.1 ± 0.1
Seattle	47°36′	122°20′	762(1)	?	17.4	...	...
Wyoming							
Big Muddy field	42°51′	106°58′	895(4)	Shale	35.5	4.0 ± 0.5	1.4 ± 0.2
Ferris field	42°10′	107°8′	871(2)	Shale	34.8	4.0 ± 0.5	1.4 ± 0.2
Gebo field	43°48′	108°14′	429(1)	Shale	39.5	4.0 ± 0.5	1.6 ± 0.2
Lance Creek field	43°4′	104°38′	964(3)	Limestone and shale	50.5	4.0 ± 0.5	2.0 ± 0.2
Little Sand Draw field	44°22′	109°0′	914(1)	Shale	31.9	4.0 ± 0.5	1.3 ± 0.2
Lost Soldier field	42°14′	107°34′	730(3)	Shale, sand, and lime	39.3–86.3‡	...	...
Oregon Basin field	44°22′	108°56′	1295(1)	Shale	30.5	4.0 ± 0.5	1.3 ± 0.2
Rock River field	41°40′	106°7′	884(3)	Shale	28.9	4.0 ± 0.5	1.2 ± 0.2
Salt Creek field	43°35′	106°15′	640(25)	Shale	45§	4.0 ± 0.5	1.8 ± 0.2

* Number of wells at each location.
† Temperature data from *Spicer* [1964].
‡ Circulating hot water along faults [*Irwin*, 1929] probably causes the high gradients.
§ Gradient at flank of dome [see *Van Ostrand*, 1934].

Geological Survey; these temperatures were used to calculate least-squares gradients for all suitable wells in the Northwest. The localities, gradients, and, where possible, estimated conductivities and heat-flow values are shown in Table 2B.

Most of the drill holes in Wyoming and Montana penetrate sections composed predominantly of relatively unconsolidated shale with only a small proportion of sand. For such a lithology a reasonable conductivity is 4.0 ± 0.5 mcal/cm sec °C [*Benfield*, 1947; *Garland and Lennox*, 1962]. The wells in the Columbia Plateaus province usually show evidence of water disturbances [see *Van Ostrand*, 1938], and the gradients in several of the wells were estimated from temperature points near the top and bottom of the drill hole. The conductivity of basalt was assumed to be 4.5 ± 0.5 mcal/cm sec °C, the average of several samples of the Columbia River basalt from near Yakima, Washington. The only value to which numerical significance is attached is the heat flow estimated in the Kevin-Sunburst and Conrad fields in north-central Montana. The gradients and estimated conductivities in three distinct lithologies give consistent results of 1.0 ± 0.2. The assumed dolomite conductivity was based on measurements of six samples of the same formation from about 60 km north of the well site.

Discussion

Summary of heat-flow determinations. The heat-flow data available in the northwestern United States are shown in Figure 6. All values in the Northern Rocky Mountain province

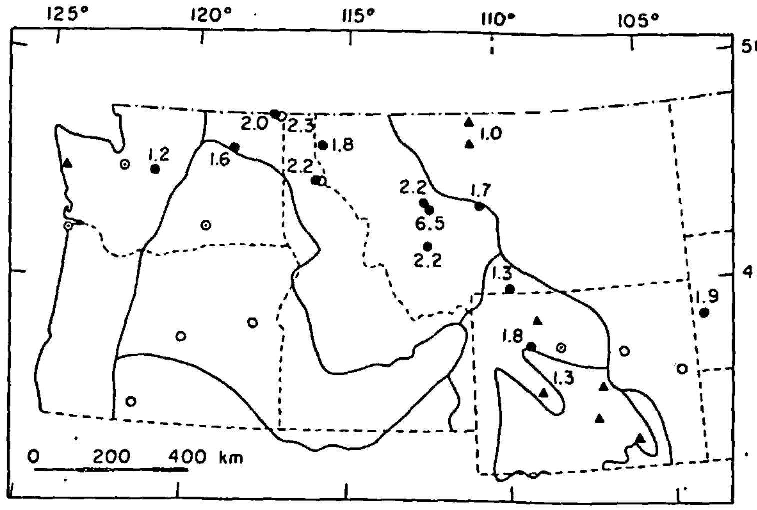

Fig. 6. Heat-flow determinations in the northwestern United States. Solid circles, determinations discussed in this paper; open circles, published or estimated values >1.6; triangles, published or estimated values <1.6; dotted circles, estimated values which could be either above or below 1.6.

are high and, excluding the heat flow of 6.5 at Marysville, Montana, average 2.0 ± 0.1. Scanty data in the Columbia Plateaus province suggest that the regional heat flow may be comparable to that in the Basin and Range and Northern Rocky Mountain provinces. The heat flow in central Montana, central Wyoming, and western Washington is generally normal, while the Black Hills and part of eastern Wyoming appear to have high heat flow.

Presently available heat-flow data in the western United States are summarized in Figure 7. The estimated values from Table 2 are not included, however. All determinations in the Basin and Range, Northern Rocky Mountains, and Southern Rocky Mountains physiographic provinces are above 1.5, while all values in the Colorado Plateaus, Middle Rocky Mountains (except the Absaroka Mountains), Wyoming basin, and Great Plains (except the Black Hills) physiographic provinces are below 1.5. Also all determinations in the Northern Cascades, Washington coast, Sierra Nevada Mountains, and Lower California provinces are below 1.5. Thus the regional zonation of heat flow in the northwestern and southwestern United States is similar.

Birch et al. [1968] and *Roy et al.* [1968*a*] show that surface heat production is an important parameter in the interpretation of heat-flow data. Only three of the heat-flow determinations discussed here are from what might classify as large plutonic bodies. The data on radioactivity from suitable sites are listed in Table 3. The data from the Boulder batholith fall on the line relating heat flow and heat production appropriate for the Basin and Range province while the points from Cooke City and North Bend would plot midway between that line and the line for the eastern United States.

Lateral variation in the electrical conductivity structure in the upper mantle also should supply information on regional heat-flow variation. *Schmucker* [1964] and *Swift and Madden* [1967] infer an upwarping of isothermal surfaces in the southern part of the Basin and Range province based on geomagnetic field variation and magnetotelluric investigations. The boundaries of this temperature anomaly are in excellent agreement with the boundaries of the zone of high surface heat flow [*Warren et al.*, 1968]. *Caner et al.* [1967] present data from geomagnetic field variations in southwestern Canada and the southwestern United States, but the correlation of their results with the distribution of regional heat flow shown in Figure 7 is not close. The reason for the lack of agreement is not known.

The best documented feature of the heat-flow pattern in the Northwest, as in the South-

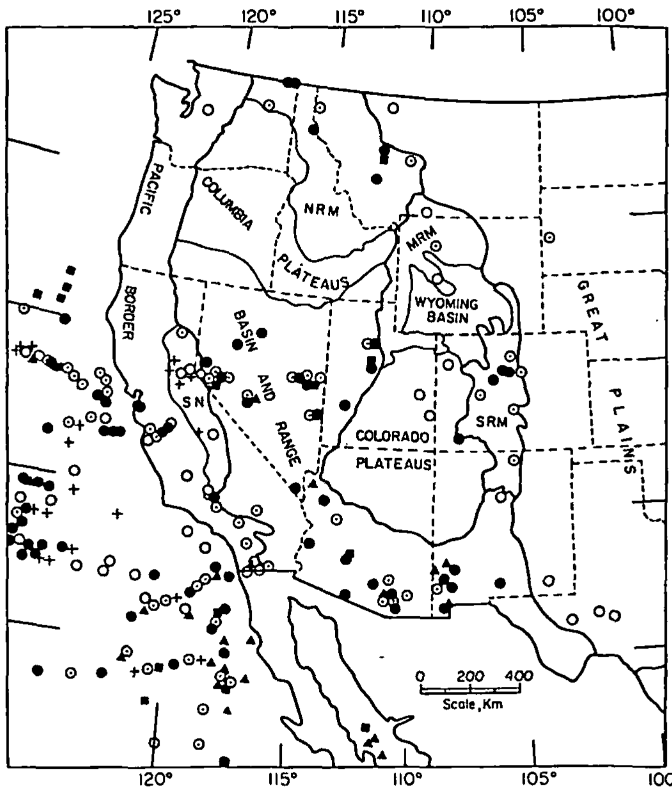

Fig. 7. Heat flow and physiographic provinces in the western United States (from Roy and Blackwell, in preparation). The abbreviations SRM, MRM, NRM, and SN stand for Southern, Middle, and Northern Rocky Mountains and Sierra Nevada Mountains, respectively. Published heat-flow data from *Roy et al.* [1968*b*]; *Lachenbruch et al.* [1966]; *Sass et al.* [1968]; *Warren et al.* [1968]; *Henyey* [1968]; *Costain and Wright* [1968]; *Burns and Grim* [1967]; *Vacquier et al.* [1967]; and *Lee and Uyeda* [1965]. Pluses, heat flow 0–0.99 μ cal/cm^{2}sec; open circles, 1.0–1.49; dotted circles, 1.5–1.99; solid circles, 2.0–2.49; solid triangles, 2.5–2.99; solid rectangles, >3.0.

west, is the broad central zone of above average heat flow in the Basin and Range, Northern Rocky Mountain, and Columbia Plateau provinces. As the zone follows the axis of the Cordilleran mountain chain [see *King*, 1966], from the Mexican to the Canadian borders, for convenience of reference it will be referred to as the Cordilleran thermal anomaly zone (CTAZ) in the remainder of this paper.

Cenozoic normal faulting and volcanism. The identifying physical features of the Basin and Range province are alternating ranges and valleys commonly aligned north-south. Cenozoic volcanic rocks, principally silicic flows or ignimbrites, are abundant in both the ranges and valleys. The controlling factor of the topography seems to be a set of large-scale Cenozoic dip-slip faults; the valleys are either grabens or downtilted blocks and the ranges are either horsts or uptilted blocks.

The Northern Rocky Mountains, southern Idaho, southeastern Oregon, southwestern Montana, and parts of extreme western Wyoming are commonly considered to exhibit Basin and Range structure [see *Gilluly*, 1965]. *Pardee* [1950] points out that the whole western third of Montana is characterized by Basin and Range structure and that the faulting occurred chiefly in the Pliocene. *Yates et al.* [1966] summarize the geology of northwestern Montana, northern Idaho, and northeastern Washington and emphasize the role of normal faulting and volcanism in the Cenozoic history of that region.

A region near the eastern boundary of both the Northern Rocky Mountain and Basin and Range provinces is called the 'zone of great

TABLE 3. Radioactive Heat Production.

Locality	No. of Samples	eU,* ppm	K,† %	A 10^{-13}cal‡ / cm³ sec
Butte, Montana§				8.6
Cooke City, Montana	12	4.6	2.1	3.5
North Bend, Washington	10	4.4	1.6	3.3

* Determined by the method of α-counting.
† Determined by the X-ray fluorescence method.
‡ Heat production determined by using conversion factors given by *Roy et al.* [1968*a*].
§ Data from Boulder [illegible]tholith (Blackwell and Robertson, in preparation).

trenches' by *Eardley* [[illegible], p. 506] because of the presence of a numb[illegible] of large displacement, late Cenozoic normal fa[illegible]. However, the zone is merely the eastern b[illegible]ary of the region of normal faulting (Figur[illegible]). A band of seismic activity, the Rocky M[illegible]ain earthquake zone [*Ryall et al.*, 1966], co[illegible]des with this boundary. As shown in Fig[illegible], normal heat-flow values are confined i[illegible] area east of the normal faulting and th[illegible] [illegible]thquake zone. Thus the position of the Roc[illegible] [illegible]ountain earthquake zone supports the eq[illegible] of the Northern Rocky Mountains an[illegible] Basin and Range province and suggests [illegible] the earthquakes are somehow related to th[illegible]sition in heat flow along which they appe[illegible] occur.

Crustal and upper [illegible]tle structure. The crustal structure of t[illegible] [illegible]uthwestern United States has been extens[illegible] investigated by the technique of seismic [illegible]ion profiling. The resulting picture of crus[illegible]ructure is shown in Figure 9 as a cross sec[illegible] about 39°N. The section is similar to [illegible]blished by *Pakiser* [1963] with modificati[illegible]de to include the results of more recent [illegible] *Eaton et al.*, 1965; *Roller*, 1965; *Jackson* [illegible] [illegible]*kiser*, 1965]. The crust is 10–20 km thi[illegible] beneath the Basin and Range province [illegible] beneath the Sierra Nevada, Colorado Pla[illegible] [illegible]r Southern Rocky Mountains, although th[illegible]ge elevation differences are small. Also [illegible] velocity beneath the Basin and Range [illegible] is low (7.8–7.9 km/sec.). The transitio[illegible] the crustal structure of the Basin and Range to tha[illegible] Sierra Nevada and Colorado Plateau[illegible] to be sharp with dips of 15° or more [illegible] discontinuity [*Eaton*, 1966; *Julian et al*[illegible] In the one place where the heat-flow tra[illegible] from high values in the Great Basin to [illegible] values in the Sierra Nevada, is investiga[illegible] detail the seismic and heat-flow boundar[illegible] coincident and about 50 km east of the [illegible] tural and physiographic boundary [*Ro*[illegible] *Blackwell*, 1966].

Also shown in Figure 9 is a crustal cros[illegible] tion at about 50°N [*White and Savage*, 19[illegible] The similarity between the two crustal sectio[illegible] is obvious. *White and Savage* [1965] found [illegible] decrease in crustal thickness east of the Co[illegible] Range and a low P_n velocity beneath the th[illegible] crust. An increase in crustal thickness was in[illegible] ferred to occur somewhere slightly to the we[illegible] of the eastern edge of the Rocky Mountains[illegible] Both transition zones would be near the region[illegible]

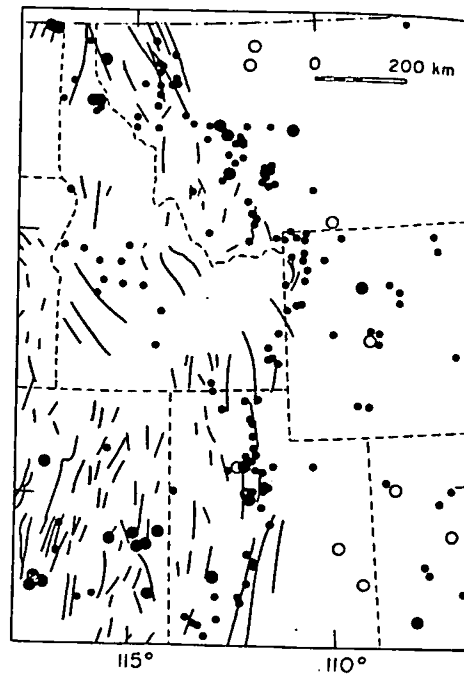

Fig. 8. Heat flow, normal faults, and earthquakes (1869–1954) in the vicinity of the Rocky Mountain earthquake zone. The small dots are earthquake epicenters [*Ross and Nelson*, 1954]. The solid lines are normal faults of large displacement [*Gilluly*, 1953, Figure 18; *Yates et al.*, 1966]. Heat-flow determinations >1.6 are shown as large solid dots and those <1.6 are shown as open circles.

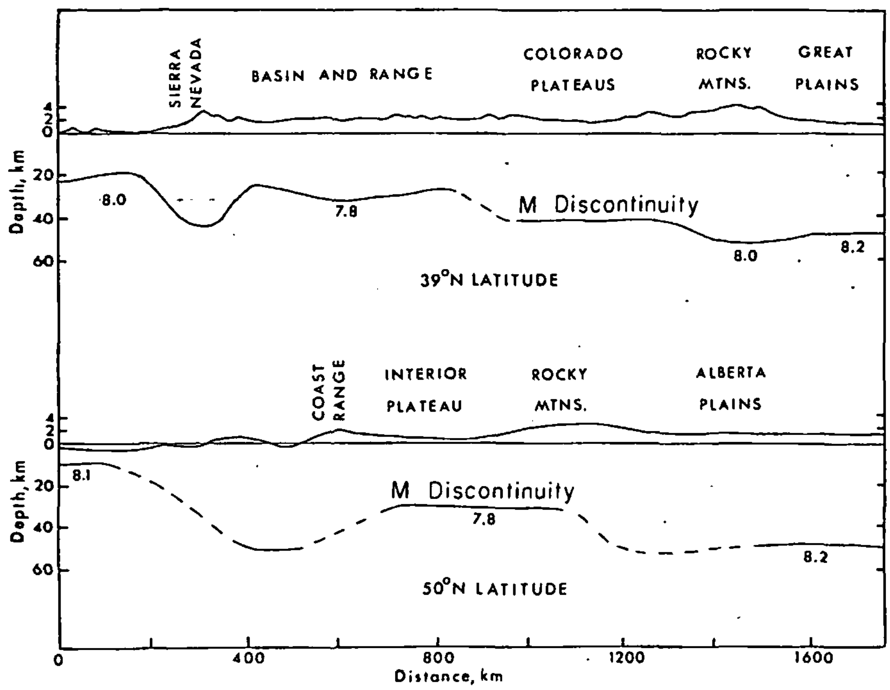

Fig. 9. Crustal cross sections, western North America. See text for references.

where a heat-flow transition is suggested by data from this study.

Data on crustal thickness in the northwestern United States are scanty, but several refraction profiles in Montana exhibit some interesting features. Interpretation of two reversed and several unreversed profiles [*Steinhart and Meyer*, 1961; *McCamy and Meyer*, 1964] shows that the crust in eastern Montana is thick (45–55 km), the average crustal velocity is high, and the upper mantle velocity is normal to high (8.0–8.4 km/sec.). In western Montana a north-south reversed profile indicates that the crust is thinner than in the plains (by 5–20 km) and that the P_n velocity is lower (7.9 km/sec). Two recently published east-west profiles in northwestern Montana [*Asada and Aldrich*, 1966], though not interpreted in such a fashion, are consistent with an abrupt decrease in crustal thickness (M-discontinuity dipping at 10°–15°) of 10–15 km from east to west between 112°W and 113°W and a concomitant decrease in P_n velocity from above 8.0 to 7.9 km/sec.

Thus on the basis of present knowledge, the crust beneath the CTAZ is abnormally thin and the upper mantle seismic velocities are low. The boundaries of the region of anomalous crustal structure (characterized by a 5 to 20-km change in crustal thickness in 25–50 km) appear to coincide with the heat-flow transitions. The data, then, strongly imply a genetic relationship between thin crust, low P_n velocities, and high heat flow.

Origin and extent of the high heat flow. The data discussed in the previous sections establish the similarity of the Cenozoic geological history, crustal structure, and regional heat flow of the Northern Rocky Mountains and the Basin and Range province. No other areas for which data are presently available in the western United States have all the same characteristics. Although the Southern Rocky Mountains have a high regional heat flow, the crust is thick and the P_n velocity is normal. So the relation of that zone of high heat flow to the CTAZ is unknown. It is clear that the CTAZ is a dominant feature of the western Cordillera at the present time and the understanding of its development is one of the key geological and geophysical problems in the western United States.

The main questions raised by the occurrence of the broad zone of high heat flow in the western Cordillera, its origin and the ultimate source of the excess heat flow, remain unanswered. The data from the northwestern United States indicate that the average heat flow there is about the same as in the Southwest. The distance between the heat-flow determination at Cooke City, Montana, and the thermal areas in Yellowstone National Park, which presumably are in the zone of high heat flow, suggests a sharp border to the zone. Because little else is known about the shape of the anomaly in the Northwest, no detailed interpretations of the data are attempted. The model most favored to explain the regional anomaly in the Great Basin involves recurrent, province-wide solid or liquid intrusions in the upper mantle [*Roy and Blackwell*, 1966]. The model is a convective one, but does not involve a current system. Penetrative convection in the crust could explain the heat-flow values above about 3.0, such as the 6.5 at Marysville, Montana. Large continent-wide convection models which have ascending movement beneath the CTAZ and descending movement beyond the borders of the zone will *not* fit the heat-flow data in the western United States, but a model with a small convection cell completely confined to the CTAZ might fit the data.

The extension of the CTAZ beyond the United States is a possible topic of speculation. Seismic refraction data indicate that the zone extends to at least 51°N. A structural feature near the eastern boundary of the zone, the Rocky Mountain trench extends to about 60°N. Directly along the strike of the Rocky Mountain trench, the Tintina trench extends from the Yukon into eastern Alaska in a broad arc. A high heat-flow value was found in the Canadian arctic [*Garland and Lennox*, 1962] not far east of these fault systems. At the western boundary of the CTAZ the Frazer fault system extends to about 51°N and a flood basalt field to 54°N [*White*, 1959]. Between about 60°N and its northern end in extreme northwestern Alaska, the Denali fault parallels the Tintina trench and another fault along the strike of the Tintina trench. The separation of the two parallel fault zones is about 350 km [see *King*, 1966]. Several large exposures of Cenozoic volcanics occur between the eastern and western fault zones in northwestern Canada. Although many of the faults mentioned are not normal faults, it may be significant that the western boundary of the CTAZ in southern California appears to be the San Andreas system of faults [*Henyey*, 1968]. In Mexico typical Basin and Range structure, volcanism, and topography extend for several hundred kilometers south of the border.

East Pacific rise and the western United States. There are many hypotheses about the relation of the East Pacific rise to the geological features of the western United States. It is not the purpose of this section to give a synthesis of all the evidence pertaining to the problem or to give references to the voluminous literature. It will merely be pointed out that the identical nature of the present geophysical characteristics and Cenozoic history of the Basin and Range and Northern Rocky Mountain provinces casts doubt on tectonic schemes which give a unique position to the Basin and Range province [*Wise*, 1963; *Talwani et al.*, 1965; many others]. Also hypotheses which single out part of the CTAZ, such as the 'zone of great trenches' as the extension of the rise [*Heezen*, 1960; *Cook*, 1962] do not appear to be justified by the data; the rise must be a regional feature if the CTAZ and the East Pacific rise are considered equivalent. The possibility that the Colorado Plateaus mark the axis of the extension of the rise [*Menard*, 1960] appears to be discounted by the heat-flow data. Furthermore it is now clear that there are several separate regions of high heat flow in the western United States and northeastern Pacific (Figure 7). Thus, whatever the relation of the East Pacific rise and the western United States, it is obviously not as simple as was previously supposed.

The possibility must be considered that the CTAZ is due to other causes than the continental extension of an oceanic rise system. The zone follows the axis of the Cordilleran mountain chain in the western United States so it might be related to the development of the mountain belt rather than superimposed on it. Furthermore, similar zones of high heat flow around the Pacific basin in Australia and Japan do not appear to be the extension of rise systems.

Acknowledgments. The cooperation of the following mining companies and others made this study possible: American Metal Climax, Inc.; American Zinc, Lead and Smelting Company; The Anaconda Company; Bunker Hill Mining

Company; Hecla Mining Company; Homestake Mining Company. The author is particularly indebted to A. L. Slaughter, Chief Geologist, and G. C. Mathisrud of the Homestake Mining Company for permission to use temperature measurements made by the company. The support of Professor Francis Birch as thesis advisor is gratefully acknowledged. Professor Birch also provided data on thermal conductivity measurements made on samples from the Yates Shaft of the Homestake Mine. Kathy Knight and Charles Bickel measured many of the conductivity samples and Robert G. Davis and James R. Otis assisted in the field.

For 4 years the National Science Foundation provided support to the author in the form of a graduate fellowship. The Committee on Experimental Geology and Geophysics, Harvard University, and Harvard National Science Foundation projects GP-701 and GA-416 provided for field and equipment expenses. The manuscript was completed during the tenure of a post-doctoral appointment at California Institute of Technology.

References

Anglin, F. M., and A. E. Beck, Regional heat-flow pattern in western Canada, *Can. J. Earth Sci., 2*, 176–182, 1965.

Asada, T., and L. T. Aldrich, Seismic observations of explosions in Montana, in *The Earth beneath the Continents, Geophys. Monograph 10*, edited by J. S. Steinhart and T. J. Smith, pp. 382–390, American Geophysical Union, Washington, D. C., 1966.

Barrell, J., Geology of the Marysville mining district, Montana, 178 pp., *U. S. Geol. Surv. Profess. Paper 57*, 1907.

Becraft, G. E., and D. L. Weiss, Geology and mineral deposits of the Turtle Lake Quadrangle, Washington, 73 pp., *U. S. Geol. Surv. Bull. 1131*, 1963.

Benfield, A. E., A heat-flow value for a well in California, *Am. J. Sci., 245*, 1–18, 1947.

Birch, F., Flow of heat in the Front Range, Colorado, *Bull. Geol. Soc. Am., 61*, 567–630, 1950.

Birch, F., R. F. Roy, and E. R. Decker, Heat flow and thermal history in New York and New England, in *Studies of Appalachian Geology: Northern and Maritime*, edited by W. White and E-an Zen, ch. 33, Interscience, New York, in press, 1968.

Blackwell, D. D., Terrestrial heat-flow determinations in the northwestern United States, Ph.D. thesis, Harvard University, 1967.

Burns, R. E., and D. J. Grim, Heat flow in the Pacific Ocean off central California, *J. Geophys. Res., 72*, 6239–6247, 1967.

Caner, B., W. H. Cannon, and C. E. Livingstone, Geomagnetic depth sounding and upper mantle structure in the Cordillera region of western North America, *J. Geophys. Res., 72*, 6335–6351, 1967.

Catanzaro, E. J., and J. L. Kulp, Discordant zircons from the Little Belt (Montana), Beartooth (Montana) and Santa Catalina (Arizona) Mountains, *Geochim. Cosmochim. Acta, 28*, 87–127, 1964.

Cook, K. L., The problem of the mantle-crust mix: Lateral inhomogeneity in the uppermost part of the earth's mantle, *Advan. Geophys., 9*, 295–360, 1962.

Costain, J. K., and P. M. Wright, Heat-flow and geothermal gradient measurements in Utah (abstract), *Trans. Am. Geophys. Union, 49*, 325, 1968.

Eardley, A. J., *Structural Geology of North America*, 2nd ed., 743 pp., Harper and Row, New York, 1962.

Eaton, J. P., Crustal structure in northern and central California from seismic evidence, *Calif. Div. Mines Geol. Bull. 190*, 419–426, 1966.

Eaton, J. P., J. H. Healy, W. H. Jackson, and L. C. Pakiser, Upper mantle velocity and crustal structure in the eastern Basin and Range Province determined from Shoal and chemical explosions near Delta, Utah (abstract), *Geol. Soc. Am. Spec. Paper 82*, 250–251, 1965.

Garland, G. D., and D. H. Lennox, Heat flow in western Canada, *Geophys. J., 6*, 245–262, 1962.

Gast, P. W., J. L. Kulp, and L. E. Long, Absolute age of early Precambrian rocks in the Bighorn Basin of Wyoming and Montana, and southeastern Manitoba, *Trans. Am. Geophys. Union, 39*, 322–334, 1958.

Gibson, R., Geology and ore deposits of the Libby quadrangle, Montana, 128 pp., *U. S. Geol. Surv. Bull. 956*, 1948.

Gilluly, J., The tectonic evolution of the western United States, *Quart. J. Geol. Soc. London, 119*, 133–174, 1963.

Gilluly, J., Volcanism, tectonism, and plutonism in the western United States, 69 pp., *Geol. Soc. Am. Spec. Paper 80*, 1965.

Goldich, S. S., E. G. Lidiak, C. E. Hedge, and F. G. Walthall, Geochronology of the midcontinent region, United States, 2, Northern area, *J. Geophys. Res., 71*, 5389–5408, 1966.

Heezen, B. C., The rift in the ocean floor, *Sci. Am., 203*, 98–110, 1960.

Henyey, T. L., Heat flow near major strike-slip faults in California, Ph.D. thesis, California Institute of Technology, Pasadena, 1968.

Hobbs, S. W., A. B. Griggs, R. E. Wallace, and A. B. Campbell, Geology of the Coeur d'Alene district, Shoshone County, Idaho, 139 pp., *U. S. Geol. Surv. Profess. Paper 478*, 1965.

Irwin, J. S., Oil and gas fields of Lost Soldier District, Wyoming, in *Structure of Typical American Oil Fields*, vol. 2, edited by S. Powers, pp. 636–666, American Association of Petroleum Geologists, Tulsa, Oklahoma, 1929.

Jackson, W. H., and L. C. Pakiser, Seismic study of crustal structure in the southern Rocky Mountains, *U. S. Geol. Surv. Profess. Paper 525-D*, 85–92, 1965.

Jaeger, J. C., Applications of the theory of heat conduction to geothermal measurements, in *Terrestrial Heat Flow, Geophys. Monograph 8*, edited by W. H. K. Lee, pp. 7-23, American Geophysical Union, Washington, D. C., 1965.

Jeffreys, H., The disturbance of the temperature gradient in the earth's crust by inequalities of height, *Monthly Notices Roy. Astron. Soc., Geophys. Supp., 4*, 309-312, 1938.

Julian, B. R., R. F. Roy, and D. D. Blackwell, Travel times from the nuclear explosion Gasbuggy in the Colorado Plateau and Basin and Range provinces (abstract), *Trans. Am. Geophys. Union, 49*, 290, 1968.

King, P. B., The North American Cordillera, in *Tectonic History and Mineral Deposits of the Western Cordillera, Special Volume 8*, pp. 1-25, Canadian Institute of Mining and Metallurgy, Montreal, 1966.

Lachenbruch, A. H., H. A. Wollenberg, G. W. Greene, and A. R. Smith, Heat flow and heat production in the central Sierra Nevada, preliminary results (abstract), *Trans. Am. Geophys. Union. 47*, 179, 1966.

Lee, W. H. K., and S. Uyeda, Review of heat-flow data, in *Terrestrial Heat Flow, Geophys. Monograph 8*, edited by W. H. K. Lee, pp. 87-190. American Geophysical Union, Washington, D. C., 1965.

Lipson, J., R. E. Follinsbee, and H. Baadsgaard, Periods of orogeny in the western Cordillera, *Ann. N. Y. Acad. Sci., 91*, 459-462, 1961.

Love, J. D., Geology along the southern margin of the Absaroka Range, Wyoming, *Geol. Soc. Am. Spec. Paper 20*, 134 pp.. 1939.

Lovering, T. S., The New World or Cooke City mining district, Park County, Montana, 87 pp., *U. S. Geol. Surv. Bull. 811-A*, 1929.

McCamy, K., and R. P. Meyer, A correlation method of apparent velocity measurement, *J. Geophys. Res., 69*, 691-699, 1964.

Menard. H. W., The East Pacific rise, *Science, 132*, 1737-1746, 1960.

Noble, J. A., Evidence for a steepening of geothermal gradients in some deep mines and drill holes, *Am. J. Sci., 246*, 426-440, 1948.

Noble, J. A., and J. O. Harder, Stratigraphy and metamorphism in a part of the northern Black Hills and the Homestake Mine, Lead. South Dakota, *Bull. Geol. Soc. Am., 59*, 941-976, 1948.

Pakiser, L. C., Structure of the crust and upper mantle in the western United States, *J. Geophys. Res., 68*, 5747-5756, 1963.

Pardee, J. T., Late Cenozoic block faulting in western Montana, *Bull. Geol. Soc. Am., 61*, 359-406, 1950.

Roller, J. C., Crustal structure in the eastern Colorado Plateaus province from seismic refraction measurements, *Bull. Seismol. Soc. Am., 55*, 107-119, 1965.

Ross, C. P., and W. H. Nelson, Regional seismicity and a brief history of Montana earthquakes, *U. S. Geol. Surv. Profess. Paper 435*, 25-30, 1964.

Roy, R. F., and D. D. Blackwell, Heat flow in the Sierra Nevada and western Great Basin (abstract), *Trans. Am. Geophys. Union, 47*, 179-180, 1966.

Roy, R. F., D. D. Blackwell, and F. Birch, Heat generation of plutonic rocks and continental heat-flow provinces, *Earth Planetary Sci. Letters, 5*(1), 1-12, 1968*a*.

Roy, R. F., E. R. Decker, D. D. Blackwell, and F. Birch, Heat flow in the United States, *J. Geophys. Res., 73*, 5207-5221, 1968*b*.

Ryall, A., D. B. Slemmons, and L. D. Gedney, Seismicity, tectonism, and surface faulting in the western United States during historic time, *Bull. Seismol. Soc. Am., 56*, 1105-1135, 1966.

Sass, J. H., A. H. Lachenbruch, G. W. Greene, T. H. Moses, Jr., and R. J. Munroe, Progress report on heat-flow measurements in the western United States (abstract), *Trans. Am. Geophys. Union*, 49, 325-326, 1968.

Schmucker, U., Anomalies of geomagnetic variations in the southwestern United States, *J. Geomagnet. Geoelec., Koyoto, 15*, 192-221, 1964.

Spicer, H. C., A compilation of deep-earth temperature data, U.S.A. 1910-1945, *U. S. Geol. Surv. Open File Rept. 147*, 74 pp., 1964.

Steinhart, J. S., and R. P. Meyer, Explosion studies of continental structure, *Carnegie Inst. Wash. Publ. 622*, 409 pp., 1961.

Swift, C. M., Jr., and T. Madden, A magnetotelluric investigation of the electrical conductivity anomaly in the upper mantle of the western United States (abstract), *Trans. Am. Geophys. Union, 48*, 210, 1967.

Talwani, M., X. Le Pichon, J. R. Heirtzler, East Pacific rise: The magnetic pattern and the fracture zones, *Science, 150*, 1109-1120, 1965.

Vacquier, V., J. G. Sclater, and C. E. Cory, Studies of the thermal state of the earth, *Bull. Earthquake Res. Inst., 45*, 375-393, 1967.

Van Ostrand, C. E., Some possible application of geothermics to geology, *Bull. Am. Assoc. Petrol. Geol., 18*, 13-38, 1934.

Van Ostrand, C. E., Temperatures in the lava beds of east-central and south-central Oregon, *Am. J. Sci., 235*, 22-46, 1938.

Van Ostrand, C. E., Observed temperatures in the earth's crust, in *Internal Constitution of the Earth*, edited by B. Gutenberg, pp. 107-149, Dover Publications, New York, 1951.

Warren, R. E., J. G. Sclater, V. Vacquier, and R. F. Roy, A comparison of terrestrial heat flow and transient geomagnetic fluctuations in the southwestern United States, *Geophysics*, 1968.

White, W. H., Cordilleran tectonics in British Columbia, *Bull. Am. Assoc. Petrol. Geologists, 43*, 60-100, 1959.

White, W. R. H., and J. C. Savage, A seismic refraction and gravity study of the earth's crust in British Columbia, *Bull. Seismol. Soc. Am., 55*, 463-486, 1965.

Wilson, W. H., The Kirwin mineralized area, Park County, Wyoming. *Geol. Surv. Wyo. Prelim. Rept. 2*, 12 pp., 1964.

Wise, D. U., An outrageous hypothesis for the tectonic pattern of the North American Cordillera, *Bull. Geol. Soc. Am., 74*, 357-362, 1963.

Yates, R. G., Geologic map and sections of the Deep Creek area, Stevens and Pend Oreille Counties, Washington. *U. S. Geol. Surv. Misc. Geol. Invest., Map I-412*, 1964.

Yates, R. G., G. E. Becraft, A. B. Campbell, and R. C. Pearson, Tectonic framework of northeastern Washington, northern Idaho, and northwestern Montana, in *Tectonic History and Mineral Deposits of the Western Cordillera, Special Volume 8*, pp. 47-59, Canadian Institute of Mining and Metallurgy, Montreal, 1966.

(Received July 29, 1968;
revised October 24, 1968.)

VOL. 78, NO. 2 JOURNAL OF GEOPHYSICAL RESEARCH JANUARY 10, 1973

Terrestrial Heat Flow Determinations in the North Central United States

JIM COMBS[1] AND GENE SIMMONS

Department of Earth and Planetary Sciences, Massachusetts Institute of Technology
Cambridge, Massachusetts 02139

Twenty-six new heat flow determinations in the north central United States range from 0.90 to 2.2 HFU (μcal/cm²sec). Two distinct provinces are characterized on the basis of both heat flow and physiography, although all the stations are located in the stable continental interior. The Interior Lowlands are characterized by a regional mean value of 1.4 HFU, whereas the regional value for the northern Great Plains is about 2.0 HFU. Local variations of heat flow in the Interior Lowlands are attributed to differences in basement rock type and the attendant contrasts in radiogenic heat production and thermal conductivity. Because basement lithologies and crustal thicknesses are quite similar in the Interior Lowlands and the northern Great Plains, most regional deviations in heat flow must be attributed to temperature differences in the upper mantle. The lower heat flow values ($\leq$1.5 HFU) are associated with negative seismic travel time anomalies, whereas the high values ($\geq$1.8 HFU) are related to positive station residuals. Lower P_n velocities are also associated with high heat flux in the northern Great Plains. These correlations support the conclusion that difference in regional heat flux can be attributed to differences in the temperature structure in the upper mantle.

The area investigated in this study is situated between the Appalachian and the Rocky mountains and is part of the physiographic province that *King* [1959] terms the central stable region of North America. The northern part of the area is divided into two distinct regions, the Interior Lowlands and the northern Great Plains (see Figure 1). Both regions consist of a thick sedimentary sequence overlying the Precambrian basement [*King*, 1959], and both have been subjected to only mild tectonic disturbances since Precambrian time. The basement configuration reflects the basin and arch provinces recognized in the Paleozoic rocks of this region. Basement is defined here as the uppermost igneous or metamorphic rocks underlying the predominately sedimentary section.

Lithologic studies of a considerable number of well samples indicate that the basement in the midcontinent is predominately granitic [*Muehlberger et al.*, 1964]. Gravity and magnetic anomalies in Iowa, Indiana, and Michigan appear to be caused by Keweenawan-type basalts and sediments superimposed on the granite [*Thiel*, 1956; *Henderson and Zietz*, 1958; *Zietz and Griscom*, 1964; *Rudman and Blakely*, 1965; *Rudman et al.*, 1965; *Zietz et al.*, 1966; *Cohen and Meyer*, 1966]. The differences in basement rock types provide an extremely useful input for the interpretation of the heat flow field.

Determination of terrestrial heat flow requires measuring the geothermal gradient and the thermal conductivity of the rocks in which the temperature gradient has been measured [*Ingersoll et al.*, 1954; *Carslaw and Jaeger*, 1959]. In the present investigation geothermal gradients were obtained from both continuous and discrete temperature measurements in vertical boreholes. Thermal conductivities have been obtained from measurements on rock cores from either the same boreholes or, in a few cases, from adjacent ones. An important point demonstrated later is that, with the excellent control on gradients afforded by continuous temperature logs, one can obtain precise values of the geothermal gradient over short intervals (10 meters), measure the thermal conductivity on a few representative samples for these selected intervals, and obtain precise estimates of the value of the

[1] Now at Department of Geological Sciences and Institute of Geophysics and Planetary Physics, University of California, Riverside, California 92502.

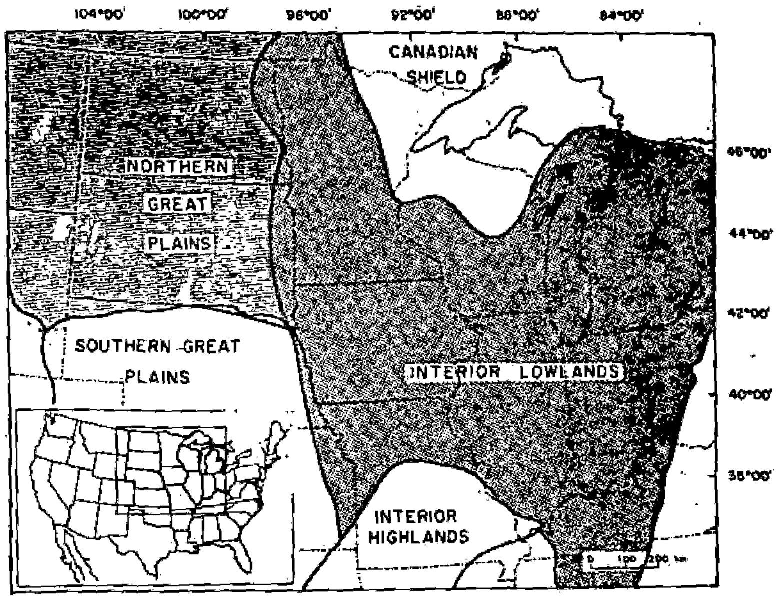

Fig. 1. Location map showing physiographic provinces in north central United States.

heat flow. Two or more such intervals in a borehole yield heat flow values that agree very closely (Table 1). This technique has been used by *Sass et al.* [1968, 1971*a*], *Combs and Simmons* [1969], and *Combs* [1970].

The average value of 26 new heat flow determinations in this area, 1.36 ± 0.35 HFU (μcal/cm^2 sec), is slightly lower than the average value of 1.49 ± 0.51 HFU for the Interior Lowlands of North America of *Horai and Simmons* [1969]. Although approximately 400 measurements of heat flow on land are published or are in various stages of completion, a comprehensive picture of both the local and the regional variation of heat flow has been presented for only a few continental areas (for example, the study of Lake Superior by *Hart et al.* [1968] and the areas studied in detail by *Sass et al.* [1971*b*]). The closely spaced data presented by *Combs* [1970] are summarized in this paper in an attempt to relate heat flow to local and regional geological, geochemical, and geophysical data.

The following symbols and units are used in this paper.

- T temperature (°C).
- Γ vertical temperature gradient $\partial T/\partial z$ (°C/km).
- N number of thermal conductivity samples.
- K thermal conductivity (mcal/cm sec °C).
- Q heat flow (1 HFU = 1×10^{-6} cal/cm^2 sec).
- A heat production (1 HGU = 1×10^{-13} cal/cm^3 sec).
- ± refers to standard error.

TABLE 1. Comparison of Heat Flow Values for Intervals Measured in Taden 1, Crescent City Field, Illinois

Depth Interval, meters	Average Geothermal Gradient, °C/km	Mean Thermal Conductivity, mcal/cm sec °C	Heat Flow, HFU
205	19.7	7.25 (1)	1.43
250 to 254	19.5	7.27 (2)	1.42
262 to 269	18.4	7.89 (2)	1.45
308 to 328	17.4	8.10 (3)	1.41
337 to 344	19.6	7.34 (2)	1.44
413 to 416	10.8	13.38 (2)	1.45
778 to 789	11.2	13.00 (3)	1.46

Numbers in parentheses indicate number of samples measured for interval.

TEMPERATURE MEASUREMENTS AND GEOTHERMAL GRADIENTS

Most of the published values of heat flow in continental areas have been derived from temperatures measured at discrete points in boreholes. All temperature measurements discussed in this paper were obtained as a continuous function of depth, except those from the Linkville and Monroeville fields in Indiana. The continuous temperature logging equipment used during this work has been described by *Simmons* [1965].

It is well known that high precision, but not high accuracy, in the temperature measurements is required for heat flow determinations. The repeatability of the measured temperatures (that is, the precision of our system) was about 0.01°C, whereas the absolute accuracy of the system was probably no better than 0.1°C.

Bullard [1947], *Jaeger* [1961], and *Lachenbruch and Brewer* [1959] have discussed the effect of drilling on the temperature distribution along a borehole. Because all the boreholes except S-44 and S-55 in Royal Center and Hoffman 1 in Vincent had been quiescent for at least several months, there were no disturbances in the geothermal gradients that might have been caused by circulation of the drilling fluid. Although disturbances caused by circulation of the drilling fluid are evident on the temperature logs for the three holes mentioned above, we could obtain reliable estimates of the heat flow values. Circulation of ground water was not observed in any of the boreholes measured; neither was there any indication on the temperature logs of such circulation.

Temperatures in some boreholes at depths of less than about 100 meters below ground level were somewhat irregular. These temperatures were presumably influenced by surface effects; therefore only temperatures from depths of >100 meters were used in this study. Because most boreholes were deeper than 300 meters, many checks were available to examine the effect of using the upper parts of boreholes to obtain heat flow data.

A problem incurred in obtaining geothermal gradients arises if there is no fluid in the borehole. When there is a column of air in the borehole, temperature-depth curves are somewhat erratic. These erratic temperatures are caused by convective heat transfer and lack of equilibrium between thermistor and air column produced by the longer time constant of the temperature probe in air and the self-heating of the probe. When there was a column of water in the borehole, however, no erratic behavior was detected, and the geothermal gradients are easily determined. The temperature log for the N-203 Northville borehole (Figure 2) is an example. The upper section was logged with air in the column, whereas below 750 meters the borehole was filled with water. When there is air in the vertical column of the borehole, the temperatures are erratic, but this behavior is eliminated if the borehole is filled with water. Nevertheless, reliable gradients can be obtained from the measurements made in a gas-filled borehole if the gradients are averaged over considerable depth range.

Geothermal gradients were obtained by simply 'eyeballing' a least-squares fit to the temperature-depth curves at the depth or over the particular intervals where the thermal conductivity was determined. The original temperature-depth curves were recorded on a scale of 1°C/30.5 mm. Because all the boreholes penetrated sedimentary sequences, there was a considerable range of thermal gradients. Gradients in some sandstone sections were as low as 6.0°C/km, whereas those in some shale sections were as high as 70.0°C/km.

Depth measurements in this study are accurate to at least 0.1%, and the temperatures were measured to within 0.01°C [*Simmons*, 1965]. If errors in the depth and temperature measurements are random, they cause a maximum error of 1% in a geothermal gradient of 20°C/km obtained over a 100-meter interval.

Because the maximum topographic relief within a 1-km radius of any of the boreholes is only a few tens of meters, the effects of hills and valleys on the geothermal gradient tend to cancel. Therefore in this investigation no topographic corrections were deemed necessary. Finally, no corrections to the geothermal gradients for climatic changes, glaciation, isostatic uplift, or erosion have been made.

THERMAL CONDUCTIVITY

Both transient (needle probe) and steady state (divided-bar apparatus) methods have been used in this investigation to determine thermal conductivities. Using the needle probe technique of *Von Herzen and Maxwell* [1959], we obtained values that were within 5% of the steady state determinations. A divided-bar apparatus with four stacks, similar to the one described by *Birch* [1950], was used for the steady state measurements. Copper and Lexan disks

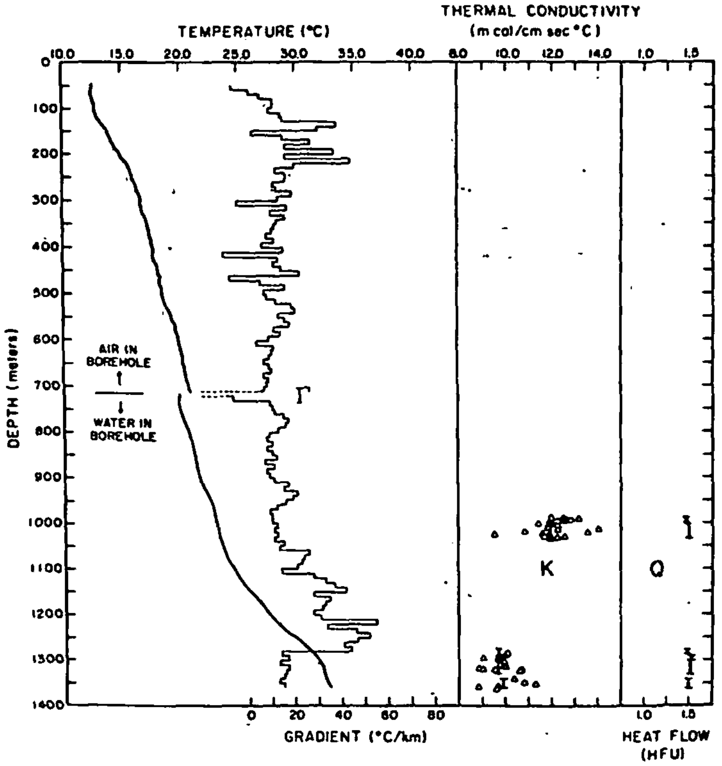

Fig. 2. Temperature T, gradient Γ, thermal conductivity K, and heat flow Q versus depth in borehole N-203, Northville, Michigan. Individual vertical lines represent averages over individual intervals. Note that all temperatures are plotted at 5-meter intervals for convenience of presentation.

served as the fixed parts of the thermal bar, and insulation was used to eliminate most side heat losses. A single measurement consisted of observing the potentials across four thermocouples. The thermocouples were measured with a potentiometer and a nanovoltmeter. Readings were made to 0.5 μv, and the ratios of temperatures on the flat and parallel ground rock specimens were reproducible to $\pm 2\%$ or better. Most of the specimens were ground to a ± 0.050-mm tolerance.

All samples were saturated by using the technique described by *Brace et al.* [1965]. The effect of saturation was studied on a number of samples of varying porosity, and it was found that the thermal conductivity of a shelf-dried rock with a porosity of 5–10% could be as low as 60% of that of a saturated rock.

Most of the samples were measured with an axial stress of ≥ 50 bars. Several disks were run at stresses of 25 and 75 bars to determine the average correction for pressure. The pressure effects were small, $<1\%/500$ bars, and consequently are neglected.

The temperature coefficients of the thermal conductivity for the rock disks ranged from $-1\%/10°C$ and were important in most cases. Each sample was measured at two to six different temperatures and graphed to estimate the conductivity of the rocks at the in situ temperature.

Our apparatus used samples with diameters between 8.9 and 10.2 cm, whereas most other heat flow workers use diamond drill cores not ordinarily exceeding a diameter of 5 cm. Because of the large size of our cores, a disk of crystalline quartz could not be obtained. Therefore all the thermal conductivities reported in this investigation are relative to the thermal conductivity of fused silica (General Electric Company type G/P 125). The value of the thermal conductivity of fused silica obtained by

Ratcliffe [1959] was used. The combined systematic and random errors in the measurement of a single rock disk are <5%, much less than the variation from specimen to specimen in most rocks.

DATA AND ANALYSIS

Illinois. The boreholes in Illinois are located on the low Kankakee arch, which structurally separates the Michigan basin from the Illinois basin. The local stratigraphic section consists of essentially flat-lying Paleozoic sediments overlying a crystalline basement [*King*, 1959]. Using samples from deep boreholes, *Aldrich et al.* [1960], *Muehlberger et al.* [1964], and *Bradbury and Atherton* [1965] have shown that the Illinois basement is chiefly granitic or is of closely related composition. No Precambrian mafic igneous rocks or metasediments have been observed in the 15 wells penetrating to the basement in Illinois. Recovery of only granitic basement rocks, combined with available gravity and magnetic data [*McGinnis and Heigold*, 1961; *Beck*, 1965; *McGinnis*, 1966, 1970], suggests that the local basement can be considered as a large essentially homogeneous body of granitic-type rock. Because the radiogenic elements (chiefly U, Th, and K) that could be sources of local heating are rare in the Paleozoic sedimentary section in northern Illinois and since there would be no local large-scale thermal conductivity contrasts in a homogeneous basement, the measured heat flow values are not altered by near-surface effects; therefore they probably represent a good estimate for regional heat flux in northeastern Illinois. Lithologic logs for the four wells studied indicate that the sedimentary sequence is essentially the same in these two fields. This observation is substantiated by comparing the temperature-depth plots for the four wells (Figure 3). Cores were intermittently recovered between depths of 200 and 1100 meters, a number of different rock types were sampled, and the range of thermal conductivity for 47 samples was from 6.79 to 14.58 mcal/cm sec °C.

Indiana. The Linkville field, located in Marshall county, is approximately 5 × 6 km. The large number of boreholes in this limited area allowed us to examine the spatial variation of heat flow. Eight different holes scattered uni-

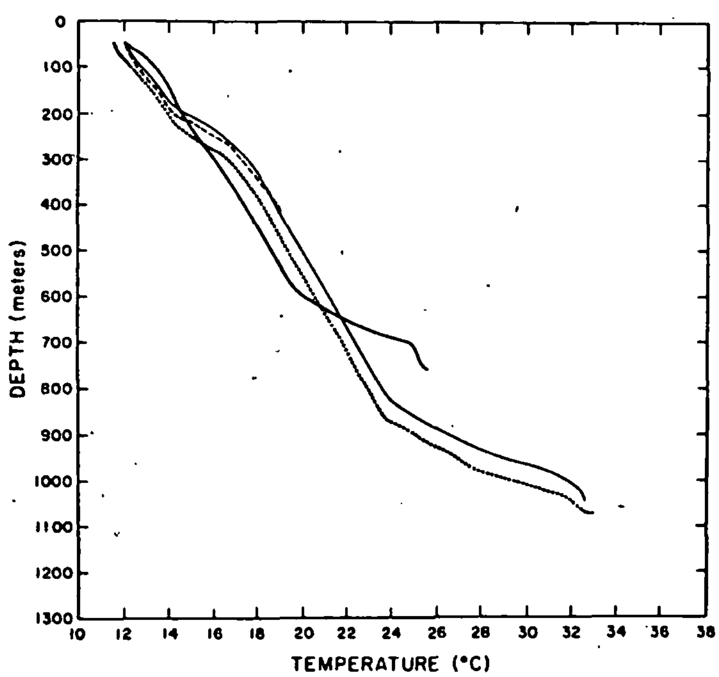

Fig. 3. Temperature-depth curves for the four boreholes investigated in Illinois. Dotted line represents Condit 1; dashed line, Wessel 1; thin line, Musser 1; thick line, Taden 1.

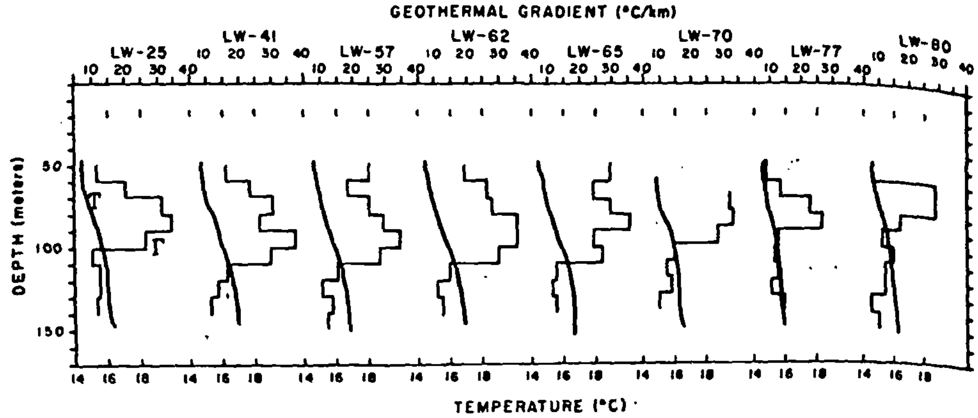

Fig. 4. Temperature T and geothermal gradient Γ versus depth in eight boreholes logged in the Linkville field, Indiana.

formly throughout the field were logged (see Figure 4). Three wells were logged at two different times to verify that steady state temperatures were being measured. Only one set of rock cores was available. Because the lithology differs between the upper and lower sections of the cores, the average conductivity was determined over two intervals (100–120 meters and 120–150 meters). Table 2 contains the average thermal gradients over the two intervals and the corresponding heat flow values for all the wells.

The Royal Center field, located in Cass and Fulton counties, is approximately 6.5 × 8.0 km. Continuous temperature-depth curves were obtained in five wells in this field. Only four of the five wells had core samples available for thermal conductivity determinations. In addition, both S-44 and S-55 had been drilled only a short time before the temperature logs were run and therefore showed a somewhat erratic behavior. However, as is shown in Table 3, even though individual temperatures were erratic, the geothermal gradients over the two depth intervals tabulated are similar. From the similarity of gradients in these closely spaced boreholes, one can deduce that reliable heat flow determinations can be obtained by measuring the thermal conductivity in one well and the geothermal gradient in an adjacent well, if the rock types remain essentially the same throughout the different boreholes. In other words, similar gradients through a particular lithologic unit in two different boreholes would strongly imply that the thermal properties of the units are the same. It would be most fortuitous if the heat flow and the thermal conductivity changed sympathetically and in just the right amount to yield a uniform gradient. Finally, it should be noted that slight transient disturbances in the temperature profile do not necessarily indicate

TABLE 2. Geothermal Gradients and Heat Flow Values in Linkville Field, Indiana

Well	Depth Interval from 100 to 120 Meters: Geothermal Gradient, °C/km	Depth Interval from 100 to 120 Meters: Heat Flow, HFU	Depth Interval from 120 to 150 Meters: Geothermal Gradient, °C/km	Depth Interval from 120 to 150 Meters: Heat Flow, HFU
LW-25	12.0	0.88	12.5	1.32
Lw-41	23.5	1.72	13.0	1.37
LW-57	22.5	1.64	12.7	1.34
LW-62	22.5	1.64	12.5	1.32
LW-65	20.0	1.46	12.5	1.32
LW-70	13.0	0.95	11.0	1.16
LW-77	12.5	0.91	13.0	1.37
LW-80	13.3	0.97	10.0	1.06

TABLE 3. Comparison of Geothermal Gradients in Royal Center Field, Indiana

	Geothermal Gradient, °C/km	
Well	200 to 300 meters	300 to 350 meters
S-36	46.5	13.9
S-38	48.8	13.6
S-44	47.1	14.0
S-46	46.6	13.6
S-55	47.3	14.0

that the geothermal gradient will be useless for a heat flow determination.

Indiana is part of the central stable region of North America that has undergone only mild deformation since the beginning of Paleozoic time [*King*, 1951]. Upper Cambrian sedimentary rocks rest directly on the Precambrian basement complex throughout the state. Although the lithology of the sedimentary sequence is essentially the same throughout the state, there is a general thickening toward the west and the southwest into the region of the Illinois basin. Basement sample studies and geophysical data of previous workers [*Henderson and Zietz*, 1958; *Muehlberger et al.*, 1964; *Rudman and Blakely*, 1965; *Rudman et al.*, 1965] indicate that the basement underlying the Linkville and Royal Center fields is granitic, whereas the Monroeville field is underlain by basalt closely resembling the Keweenawan flows of the midcontinent region. Furthermore, the Monroeville field is located on a pronounced magnetic high that has been interpreted by *Henderson and Zietz* [1958] as a large basaltic plug intruded into the granitic basement.

The contrast between the contents of radiogenic elements (U, Th, and K) of granitic and basaltic rocks [*Birch*, 1951] can yield a relationship between the heat flow values and the associated basement complex. In particular, the low value at Monroeville (0.97 HFU) is associated with a basaltic basement, whereas the other values in Indiana (1.28–1.41 HFU) are associated with a granitic basement. In addition, the work of *Horai and Nur* [1970] suggests that the geometry of the basalt basement and the thermal conductivity contrast between granitic and basaltic rocks can account for this difference in heat flow. Because both effects would produce the low heat flow value and since the detailed structure, the thermal conductivity, and the heat production are not known, one cannot separate the effects. If, however, one combines estimates of the corrections for the thermal conductivity contrast and the heat source differences, the low heat flow value at Monroeville can be made to coincide with the regional heat flow value of approximately 1.4 HFU.

Iowa. Iowa lies on the flank of the Wisconsin arch, and the sedimentary strata dip gently southwestward in a broad homocline toward the Forest City basin and southward toward the Illinois basin [*King*, 1959]. From wells that have penetrated the basement, it is known that most of Iowa is a part of the widespread midcontinental granitic province [*Aldrich et al.*, 1960; *Bell et al.*, 1964; *Muehlberger et al.*, 1964; W. J. Yoho, unpublished data, 1962]. The midcontinent gravity and magnetic high extends across the central part of the state in a generally NE-SW direction. Combined geophysical and borehole basement sample data indicate that the gravity and magnetic high can be traced northward to an exposed basement, where these striking magnetic and gravity anomalies can be correlated with basalt flows and sedimentary rocks of Keweenawan age [*Thiel*, 1956; *Muehlberger et al.*, 1964; *Zietz and Griscom*, 1964; *Zietz et al.*, 1966; *Cohen*, 1966]. The positive gravity anomaly originates from dense basalt flows of Keweenawan age, whereas the adjacent parallel negative gravity anomalies probably result from mass deficiencies associated with low-density Keweenawan sediments. Four boreholes were logged in the Vincent field, and, as is seen in Figure 5, the temperature-depth curves are quite similar. One particular change in gradient in all boreholes is noticeable: a high geothermal gradient between 350 and 400 meters. From the lithologic logs for this field, this high gradient is seen to correspond to a thin shale sequence located between two thick predominately dolomitic sections. From the correlation between lithologic logs and temperature logs for this field, as well as from similar evidence from other fields in the midcontinent, it is thus shown that continuous temperature-depth curves can provide a useful tool for determining the distribution of subsurface rock types. Because drilling in Hoffman 1 had been completed only a few days before the temperatures were measured, the

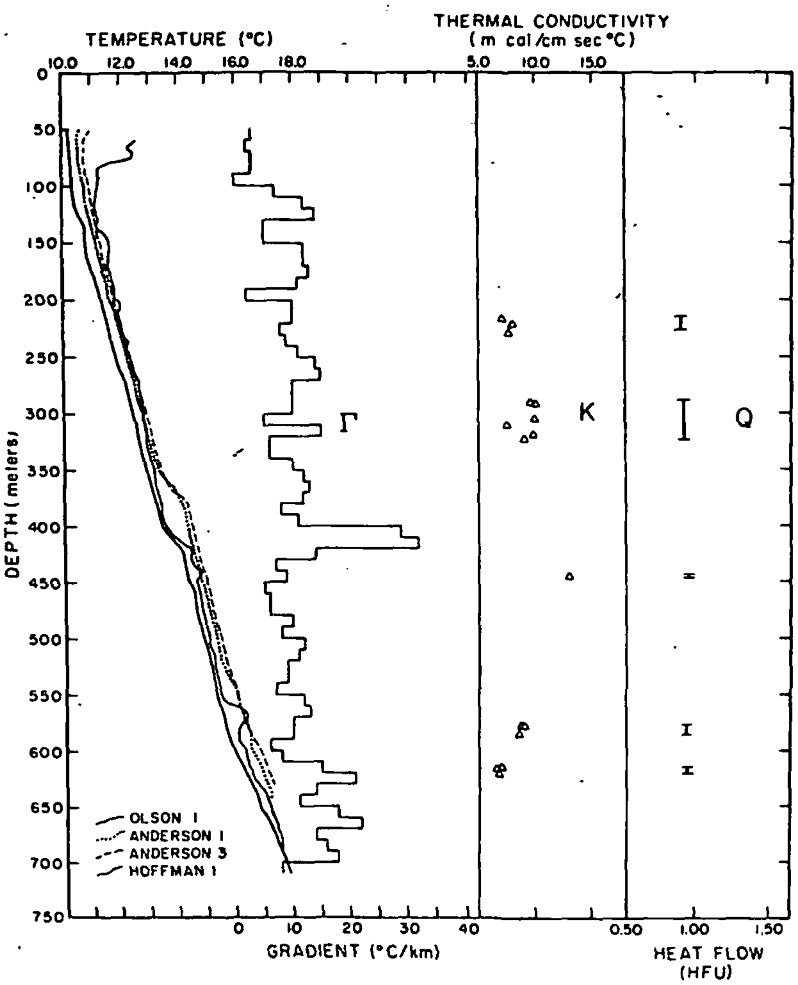

Fig. 5. Comparison of the temperature-depth curves for the four boreholes investigated in the Vincent field, Iowa, with the gradient Γ, thermal conductivity K, and heat flow Q versus depth for Hoffman 1 borehole. Individual vertical lines represent averages over individual intervals.

values are somewhat erratic. However, comparison of the heat flow values from Hoffman 1 with those measured in the other three holes indicates that it is possible to obtain a valid estimate of the heat flow (to perhaps 15 or 20%) from a borehole shortly after drilling.

Hart et al. [1968] reported on 83 heat flow stations in Lake Superior. The values range from 0.50 to 1.24 HFU and can be used to characterize two distinct regions: a belt along the western shore characterized by low values (0.5–0.9 HFU) and a central region of higher but uniform values (1.0–1.2 HFU). Some of our heat flow determinations in Iowa, as well as those of Hart and his co-workers, are on the midcontinent gravity and magnetic anomaly. The spatial relationships and the heat flow values are comparable for both regions. There appears to be no direct correlation between the heat flow values and the available gravity and magnetic data. However, a correspondence between the basement lithology and the heat flow data is seen in three wells in the Vincent field that penetrated the basement of diabase (or basalt) and in the Redfield field, where six boreholes have encountered an altered diabase. The usual low content of radioactive elements in basic rocks, in addition to a thermal conductivity lower than that of the otherwise granitic basement, can account for these low heat flow values. Although there are no deep boreholes in the Keota or Cairo fields, it is predicted from the magnetic data and from the lithologic data in surrounding wells that the basement is granitic.

Michigan. The heat flow determined for borehole 972 in Marion is one of the least precise of the present values. Only one 15-meter interval had been cored, and no other wells were available in the Winterfield field to substantiate the heat flow value. Because only this interval was available, the variation in the thermal conductivity (i.e., 10%) was used as an estimate of the error in the final heat flow.

Because of the availability of core samples, borehole N-203 in the Northville field provided an opportunity to examine the hypothesis that for an essentially homogeneous geologic section a few thermal conductivities, in addition to a precise geothermal gradient, yield as precise a value for the heat flow as can be obtained from measuring many thermal conductivity samples combined with a less precise gradient. Table 4 contains the data obtained from an original set of 16 thermal conductivity samples, as well as those from the 23 additional samples measured. The resulting differences in the average thermal conductivity and, therefore, the calculated value of heat flow can be seen in Table 5. The advantage of measuring thermal conductivity on 16 disks rather than on 39 or more is obvious.

If the structure and the lithology of the basement rocks are disregarded, negative gravity and magnetic anomalies should be associated with the Michigan basin, owing to the generally less dense nonmagnetic sediments filling the basin in comparison with the adjacent basement rocks, but this is not the case. In fact, the principal anomaly on both gravity and magnetic maps is positive and extends through the center of the basin [*Hinze*, 1963]. The magnitude of the anomalies as well as the excellent correlation between gravity and magnetic highs suggests a basic basement complex as the origin of the anomalies. Some investigators [e.g., *Rudman et al.*, 1965; *Muehlberger et al.*, 1964] have postulated that the linear anomalies in Michigan, like those in Iowa, Wisconsin, and Minnesota, are caused by basalt flows of Keweenawan age. Although no basement samples are available from the area, the low heat flow values for 972 in Marion (1.10 HFU) and S-503-E in Burnips (1.07 HFU) are compatible with the hypothesis that the basement consists mostly of basic rocks. Further interpretation, perhaps similar to that presented for the Iowa data, must be delayed until the nature of the basement has been established. However, at least six basement samples have been recovered from the southeast corner of the southern peninsula of Michigan [*Muehlberger et al.*, 1964]. All were granite or granitic gneiss. The borehole in the

TABLE 4. Depth, In Situ Temperature, Density, and Thermal Conductivity for Each Core Disk from Borehole N-203, Northville Field, Michigan

Depth, meters	Temperature, °C	Density, g/cm³	Thermal Conductivity, mcal/cm sec °C
989	23.04	2.82	12.04
991*	23.08	2.74	12.58
993	23.10	2.77	13.21
995*	23.12	2.81	12.85
997*	23.14	2.76	12.31
1001*	23.18	2.83	12.17
1003*	23.21	2.84	11.47
1004	23.22	2.87	11.96
1006	23.24	2.83	12.29
1011	23.29	2.81	11.89
1014	23.33	2.89	14.02
1016*	23.35	2.78	12.29
1020	23.40	2.77	10.84
1023	23.43	2.80	13.53
1024*	23.45	2.81	11.64
1027	23.47	2.80	11.98
1028	23.50	2.80	9.55
1030*	23.52	2.81	12.57
1031	23.53	2.76	11.70
1033	23.55	2.81	12.28
1286	31.72	2.82	10.08
1289	31.85	2.82	10.03
1299*	32.16	2.84	9.07
1300*	32.20	2.83	9.70
1302	32.23	2.85	9.88
1305	32.28	2.84	9.55
1315*	32.43	2.84	9.94
1316*	32.44	2.82	10.02
1318	32.48	2.83	8.88
1323	32.56	2.83	10.69
1326*	32.60	2.81	9.06
1328	32.63	2.82	9.53
1329	32.64	2.82	10.69
1344	32.90	2.82	10.39
1350*	33.03	2.83	10.82
1354	33.10	2.82	11.33
1357	33.15	2.84	8.88
1358*	33.18	2.80	9.74
1361*	33.22	2.85	9.68

*Data obtained in original set of thermal conductivity determinations.

TABLE 5. Thermal Conductivities, Geothermal Gradients, and Heat Flows Calculated for Borehole N-203, Northville Field, Michigan

Depth Interval, meters	Average Thermal Conductivity,* mcal/cm sec °C	Average Thermal Conductivity,† mcal/cm sec °C	Geothermal Gradient, °C/km	Heat Flow,* HFU	Heat Flow,† HFU
988 to 998	12.58 (3)	12.58 (5)	10.9	1.37	1.37
1000 to 1035	12.03 (5)	11.98 (15)	11.6	1.40	1.39
1280 to 1290		9.74 (2)	14.2		1.38
1296 to 1298	9.07 (1)	9.07 (1)	15.5	1.41	1.41
1300 to 1330	9.68 (4)	9.70 (10)	14.4	1.39	1.40
1342 to 1364	9.95 (3)	9.91 (6)	14.0	1.39	1.39

Numbers in parentheses indicate number of samples measured for depth interval.

*Data obtained from original set of thermal conductivity determinations.

†Data obtained from total set of thermal conductivity determinations.

Northville field, N-203, has a value of 1.39 HFU. There is an apparent similarity between this area and most of the areas in Illinois, Indiana, and Iowa; that is, a heat flow value of approximately 1.4 HFU is associated with all these midcontinental areas underlain by a granitic basement.

North Dakota and South Dakota. A lithologic log of the stratigraphic section from the surface to 305 meters was constructed from drill cutting from Assman 1. The borehole penetrated Tertiary sediments from the surface to 122 meters and a continuous section of Pierre shale (Cretaceous) from 122 to 305 meters [*Geotechnical Corporation*, 1964]. No samples were available for thermal conductivity measurements. Similarly, no core was available for either well in North Dakota, but detailed knowledge of the lithology (from cuttings) permits one to make reasonable estimates of the average thermal conductivity. Both boreholes in North Dakota penetrate a thick gray marine shale of Upper Cretaceous age [*Carlson and Anderson*, 1965]. The Pierre formation represents the major part of the stratigraphic section. No sandstones or carbonates were penetrated by these wells.

Because the three boreholes in the Dakotas penetrated shale sequences and since no core was available, a best estimate for the thermal conductivity must be made to obtain an estimate of the heat flow. The Pierre shale has been investigated in detail by *Tourtelot* [1962]. From microscope work, X rays, and chemical analyses of borehole samples in the two areas where the present boreholes are located, he determined that the Pierre shale is composed of 70–85% clay minerals, 15% quartz, and 2% feldspar, and two samples contained 5% calcite. If the thermal conductivity of the minerals observed in these analyses is used, the thermal conductivity of the Pierre shale will be <5.0 mcal/(cm sec °C). J. H. Sass (personal communication, 1971) had indicated that the chip measurements on 42 shale samples (mainly Pierre shale) from the Rocky Mountain Arsenal [*Sass et al.*, 1971*b*, Table 6, page 6390] had a mean thermal conductivity of 5.83; however, this value did not take into account either anisotropy or porosity. If a porosity of 20–25% is assumed, the effective conductivity would be in the range 4.0–4.5 (J. H. Sass, personal communication, 1971). In addition, *Benfield* [1947], in a heat flow determination for a well in California, investigated 31 shale samples. These samples were saturated, and the mean wet conductivity was 3.90 with a range from 2.76 to 5.61. In an investigation of heat flow in western Canada

Garland and Lennox [1962] measured 23 samples that they classified as shales. The mean for these saturated samples was 3.97, and the range was from 2.2 to 6.0. The average value for most of the other shale conductivities that have been published is approximately 4.0 [*Clark*, 1966]. Therefore the estimated average value used for the Pierre shale of this investigation is 4.0 mcal/(cm sec °C). Both the present study and the earlier work of *Blackwell* [1969] and *Sass et al.* [1971*b*] indicate that the best heat flow value for the regional flux is 2.0 HFU. This

TABLE 6. Published Heat Flow Determinations in North Central United States

Locality	Location	Elevation, meters	Heat Flow, HFU	Reference†
Colorado				
Canon City	38°30'N, 105°20'W	1937	1.84	*a*
Colorado Springs*	38°30'N, 104°45'W	1890	1.2	*b*
Front Range*	49°27'N, 105°43'W	2530	1.7	*c*
Golden	39°47'N, 105°16'W	1905	1.52	*a*
Iowa				
Spencer	43°10'N, 95°11'W		0.44	*a*
Kansas				
Lyons hole 1	38°23'N, 98°10'W	525	1.53	*d*
Lyons hole 2	38°22'N, 98°10'W	512	1.50	*d*
Michigan				
Calumet			0.93	*e*
Delaware	47°24'N, 88°01'W	390	0.99	*a*
White Pine N-55	46°45'N, 89°34'W	280	1.04	*a*
White Pine N-65	46°44'N, 89°34'W	310	1.06	*a*
White Pine Mean			1.05	*a*
Minnesota				
Ely 3	47°49'N, 91°43'W	463	0.81	*a*
Ely 4	47°49'N, 91°43'W	456	0.87	*a*
Mean			0.82	*a*
Missouri				
Boss USA-7	37°39'N, 91°10'W	380	1.3	*a*
Bourbon B-20	38°09'N, 91°15'W	290	1.24	*a*
Ironton K-13	37°30'N, 90°40'W	365	1.24	*a*
Levasy	37°05'N, 94°10'W	220	1.17	*a*
Oklahoma				
Picher 43-C	36°59'N, 94°52'W	255	1.46	*a*
Picher P-5	36°59'N, 94°52'W	253	1.35	*a*
Mean			1.4	*a*
North Dakota				
Lone Tree	48°18'N, 101°40'W		>1.4	*f*
South Dakota				
Dacy	48°18'N, 103°53'W	1790	1.9	*d*
Lead 4 shaft	44°21'N, 103°45'W		1.84	*a*
Yates shaft	44°21'N, 102°45'W	1618	1.96	*a*
Mean			1.9	*a*
Moonshine Gulch	44°08'N, 103°43'W	1695	0.5	*d*
Windy Flats	44°18'N, 103°40'W	1652	0.5	*d*
Wyoming				
Lance Creek field	43° 4'N, 104°38'W	964	2.0	*f*
Salt Creek field	43°35'N, 106°15'W	640	1.8	*f*

*Latitude and longitude determined by the authors.
†Letters refer to the following: *a*, *Roy et al.* [1968*b*]; *b*, *Birch* [1947]; *c*, *Birch* [1950]; *d*, *Sass et al.* [1971]; *e*, *Birch* [1954]; *f*, *Blackwell* [1969].

TABLE 7. Measurements of Harmonic Thermal Conductivity, Geothermal Gradient, and Terrestrial Heat Flow

Well Name and Field	Location	Elevation, meters	Maximum Depth, meters	Number of Disks*	Mean Harmonic Thermal Conductivity, mcal/cm sec °C	Geothermal Gradient, °C/km	Terrestrial Heat Flow,† HFU
Illinois							
Musser 1, Ancona	41°01.2'N, 88°53.7'W	194	765	8	11.58 ± 2.18	12.2 ± 3.5	1.41 ± 0.02
Condit 1, Crescent City	40°48.6'N, 87°53.6'W	194	1065	14	12.25 ± 1.31	11.6 ± 1.1	1.42 ± 0.02
Taden 1, Crescent City	40°45.3'N, 87°47.3'W	198	1040	15	8.87 ± 2.62	16.1 ± 3.7	1.44 ± 0.02
F. Wessels 1, Crescent City	40°45.7'N, 87°48.4'W	197	415	10	9.87 ± 2.49	14.0 ± 2.9	1.39 ± 0.01
Indiana							
Leuenberger well, Monroeville	40°58.5'N, 84°52.1'W	243	420	12	11.18 ± 0.72	8.7 ± 0.6	0.97 ± 0.02
Linkville field	41°23.0'N, 86°14.0'W	247	150	15	9.16 ± 1.69	14.0 ± 4.4	1.28 ± 0.26
S-36, Royal Center	40°53.4'N, 86°28.3'W	226	420	12	9.85 ± 1.40	14.3 ± 2.4	1.41 ± 0.01
S-38, Royal Center	40°53.4'N, 86°28.0'W	226	405	3	7.24 ± 0.24	19.2 ± 1.9	1.39 ± 0.02
S-46, Royal Center	40°54.5'N, 86°27.8'W	226	410	5	7.81 ± 1.37	17.9 ± 3.5	1.41 ± 0.01
S-55, Royal Center	40°55.1'N, 86°27.1'W	227	1050	14	8.99 ± 2.74	15.4 ± 4.6	1.39 ± 0.01
Iowa							
Anderson 1, Vincent	42°38.3'N, 94°01.5'W	348	630	16	8.46 ± 1.59	10.6 ± 1.6	0.90 ± 0.01
Anderson 3, Vincent	42°38.3'N, 94°01.2'W	350	645	16	8.45 ± 1.59	10.9 ± 1.6	0.92 ± 0.02
Book 1, Redfield	41°33.7'N, 94°06.2'W	312	675	5	8.74 ± 1.76	13.4 ± 2.5	1.17 ± 0.02
Broderick 1, Redfield	41°39.6'N, 94°09.7'W	313	365	3	8.23 ± 0.87	14.3 ± 1.7	1.17 ± 0.03
Hoffman 1, Vincent	42°37.8'N, 94°02.8'W	347	690	12	8.12 ± 1.27	11.7 ± 2.4	0.97 ± 0.07
J. Anderson 1, Keota	41°23.2'N, 91°54.9'W	231	365	11	8.31 ± 2.52	18.0 ± 4.4	1.49 ± 0.02
L. Vogel 1, Keota	41°21.6'N, 91°54.5'W	242	355	11	8.34 ± 2.53	17.7 ± 4.2	1.49 ± 0.02
Olson 1 'G', Vincent	42°37.6'N, 94°03.2'W	349	710	16	8.47 ± 1.59	10.8 ± 1.6	0.93 ± 0.02
P. Hutchinson 2, Cairo	41°12.3'N, 91°19.6'W	201	255	7	7.75 ± 1.09	18.9 ± 2.0	1.47 ± 0.02
Price 1, Redfield	41°41.5'N, 94°10.4'W	309	585	4	5.25 ± 0.34	22.2 ± 0.8	1.16 ± 0.02
Michigan							
972, Marion	44°03.1'N, 85°05.4'W	330	500	8	9.53 ± 0.65	11.5 ± 0.2	1.10 ± 0.11
N-203, Northville	42°25.5'N, 83°33.8'W	296	1360	39	10.89 ± 1.38	12.9 ± 1.6	1.39 ± 0.01
S-503-B, Burnips	42°43.4'N, 85°49.1'W	203	810	10	9.04 ± 1.44	11.9 ± 1.7	1.07 ± 0.03
South Dakota							
Assman 1, Winner	43°15.1'N, 100°11.7'W	792	300	§	4.0 ± 0.5	52.0 ± 5.0	2.1 ± 0.4
North Dakota							
Carrie Hovland 1, Flaxton	48°55.3'N, 102°26.0'W	573	1800	§	4.0 ± 0.5	56.0 ± 6.0	2.2 ± 0.4
E. L. K. 1 Nelson, Roth	48°56.1'N, 100°49.6'W	457	940	§	4.0 ± 0.5	55.0 ± 6.0	2.2 ± 0.4

*Number of disks measured to obtain thermal conductivity.
†Heat flow value is arithmetic mean of all depth intervals measured.
§No core available; therefore conductivity estimated (see text for details).

value is higher than that of 1.4 HFU found in the Interior Lowlands.

Approximately 100 basement samples scattered uniformly throughout North Dakota have been studied, but only one of them was a basic rock type, a diabase from Oliver county [*Muehlberger et al.*, 1964]. Muehlberger and his co-workers encountered only four basic rocks (two basalts, a gabbro, and a diabase) in the 100 wells that they examined in South Dakota. Considering the correlation of heat flow with basement lithology noted for the Interior Lowlands, one would predict that the value of heat flow for the northern Great Plains should be 1.3–1.4 HFU. The observation of a heat flux of 2.0 HFU will be discussed more completely in the next section.

DISCUSSION AND CONCLUSIONS

Twenty-six new heat flow values were determined for the north central United States. Previously published values (see Table 6) as well as these new values (see Table 7) are shown in Figure 6. The values obtained in this investigation range from 0.90 to 2.2 HFU. However, there are two distinct regions on the basis of both physiography and heat flow. The Interior Lowlands (see Figure 1) are characterized by a regional flux of 1.4 HFU, whereas the regional value for the northern Great Plains is about 1.0 HFU. The sedimentary section in both regions is essentially devoid of radiogenic elements; therefore any heat sources must be located in the crust below the sediments or in the mantle. From their data on heat flow and heat production *Roy et al.* [1968a] suggested that heat flow variations in the central stable region, which includes this area, may reflect areal changes of heat generation in the basement. Their conclusion is confirmed in the present study. Local variations from the regional value in the Interior Lowlands can be attributed to the presence of mafic rocks in the basement complex. The attendant contrasts in heat productivity and thermal conductivity within the predominately sialic basement can account for the low heat flow values. Gravity and magnetic data in addition to basement sample studies have indicated these differences in basement rock types. Lithologic data obtained from well samples reveal that the basement throughout the north central United States is predominately granitic [*Muehlberger et al.*, 1964].

Seismic crustal structure studies [*Slichter*, 1951; *Steinhart and Meyer*, 1961; *McCamy and Meyer*, 1964; *McEvilly*, 1964; *Cohen*, 1966;

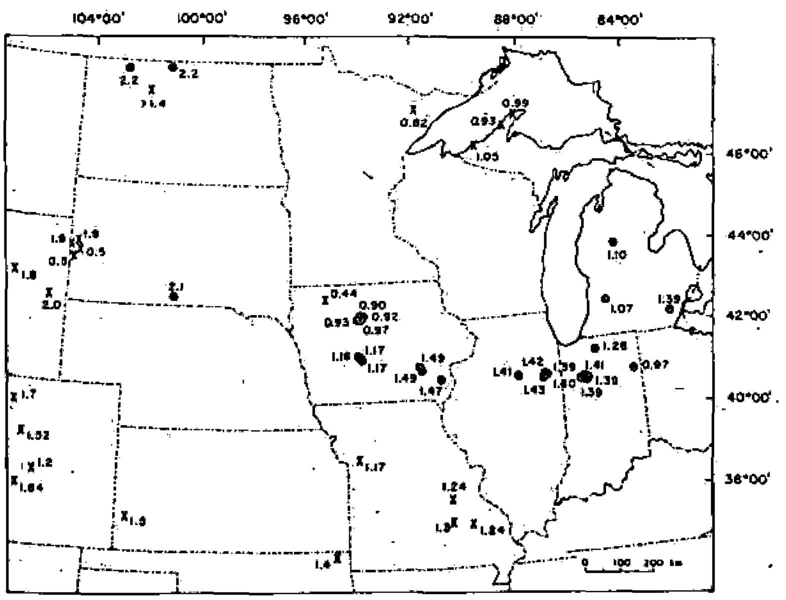

Fig. 6. Terrestrial heat flow values in north central United States. The circles indicate determinations made in this study, and the crosses refer to published values (see Table 6 for references). All heat flow values are in HFU.

*Number of disks measured to obtain thermal conductivity.
†Heat flow value is arithmetic mean of all depth intervals measured.
‡No core available; therefore conductivity estimated (see text for details).

James and Steinhart, 1966; *Green and Hales*, 1968] indicate that there is little difference between the crustal thickness of the Interior Lowlands and that of the northern Great Plains. The crustal thickness varies randomly from 45 to 55 km. The difference in heat flow, therefore, cannot be explained on the basis of a thicker crust in the northern Great Plains. Because the crust appears to be essentially homogeneous, heterogeneity in the upper mantle must explain the difference between the regional heat flux of the Interior Lowlands and that of the northern Great Plains.

Hales and Doyle [1967] pointed out that heat flow values in southeastern Australia are high [*LeMarne and Sass*, 1962; *Sass and LeMarne*, 1963; *Jaeger and Sass*, 1963; *Sass et al.*, 1967; *Howard and Sass*, 1964] where the station anomalies and travel time residuals are positive, whereas in Queensland and southwestern Australia [*Howard and Sass*, 1964; *Sass*, 1964*b*] the station anomalies are negative [*Cleary*, 1967] and the heat flow is normal or subnormal [*Hyndman*, 1967]. This correlation has also been observed in the western United States [*Roy et al.*, 1968*a*; *Decker*, 1969; *Blackwell*, 1969]. Undoubtedly, some travel time deviations arise from differences of composition in the crust, but the study of *Hales and Doyle* [1967] strongly suggests that most deviations arise from differences in temperatures in the upper mantle. Because station travel time residuals originate largely in the upper mantle, it would appear that the high heat flows are associated with higher temperatures and lower seismic velocities in the upper mantle.

The relative travel time anomalies for both compressional waves (Figure 7) and shear waves (Figure 8) [*Cleary and Hales*, 1966; *Hales and Doyle*, 1967; *Doyle and Hales*, 1967; *Herrin*, 1969; *Hales and Roberts*, 1970] for the north central United States indicate a correlation between the station residuals and the heat flow. *Horai and Simmons* [1968] suggested that the major cause of seismic travel time anomalies is differences in mantle temperature associated with anomalous heat flow. Travel time delays were obtained for each heat flow station by interpolating the station residuals of *Cleary and Hales* [1966]. Figure 9 shows a correlation similar to that indicated by *Horai and Simmons* [1968, Figure 9]. Lower heat flow values (≤ 1.5 HFU) are associated with negative station anomalies, whereas the high values (≥ 1.8 HFU) are related to positive station residuals (compare Figures 7 and 8 with Figure 6). Re-

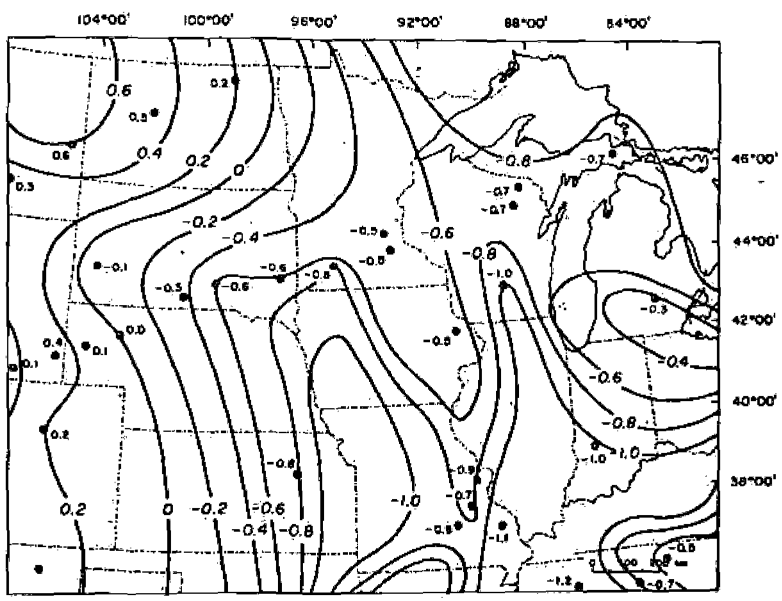

Fig. 7. Relative travel time anomalies for compressional waves contoured on a 0.2-sec interval; data from *Cleary and Hales* [1966] with contours similar to those of *Archambeau et al.* [1969].

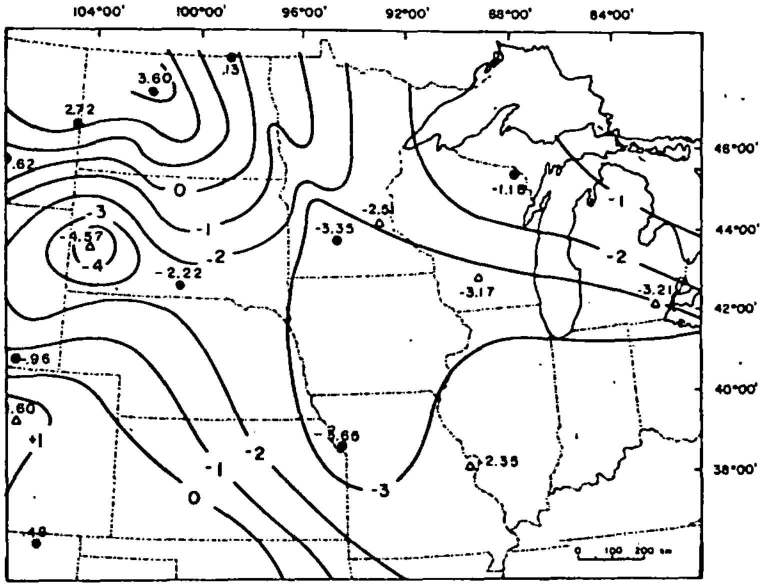

Fig. 8. Relative travel time anomalies for shear waves contoured on a 1.0-sec interval [after *Hales and Roberts*, 1970].

gional differences in heat flow, therefore, may be attributed to differences in the temperature of the upper mantle.

The P_n phase used to estimate P wave velocity in the uppermost mantle is observed to be slower under areas of high heat flow. From a consideration of the difference in apparent P_n velocities for the Interior Lowlands and the northern Great Plains, a simple model consistent with the observed difference in regional heat flux can be constructed. The difference in P_n velocity (see Figure 10) is approximately 0.08–0.12 km/sec [*Herrin and Taggart*, 1962; *Herrin*, 1969], whereas the crustal thickness for both regions is approximately 50 km. If we assume that the upper mantle is composed of a mineral assemblage characterized by olivine, pyroxene, garnet, and spinel, the rate of change of the compressional velocity with respect to temperature is approximately -5×10^{-4} km/sec °C [*Ander-*

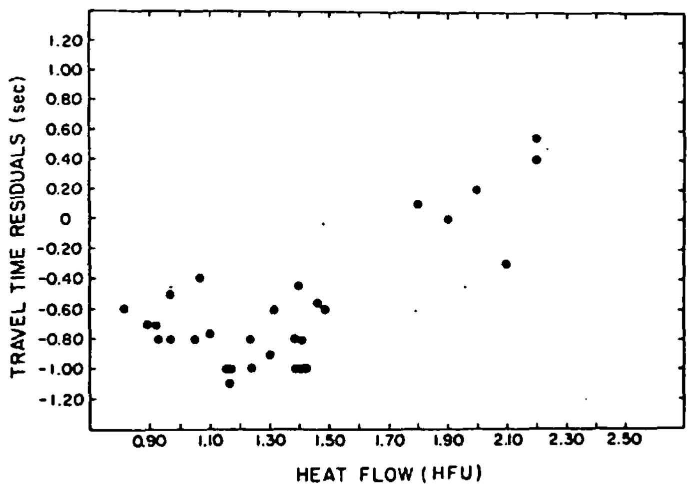

Fig. 9. Correlation of P wave travel time anomalies and terrestrial heat flow.

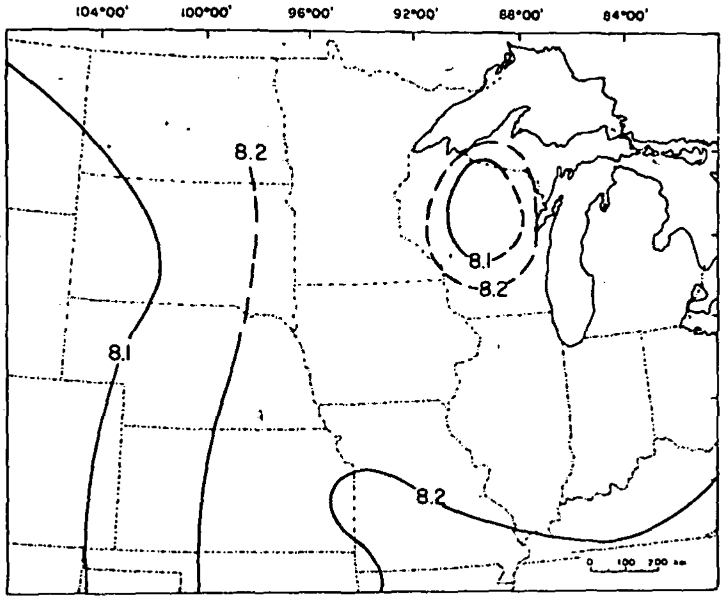

Fig. 10. Estimated P_n velocity in north central United States. Velocities are in kilometers per second [after *Herrin*, 1969].

son et al., 1968; *Kumazawa and Anderson*, 1969]. When these parameters are used, a temperature difference of about 150°–250°C at a depth of 45–55 km is suggested.

On the other hand, the difference in the temperature at the M discontinuity calculated from the thermal models discussed below can be interpreted in terms of the stable mineral assemblages and their corresponding seismic velocities. Comparing the temperatures calculated in the several models with the 'equilibrium' curve for basalt-eclogite [*Ringwood and Green*, 1966, Figure 1] indicates that the stable mineral assemblage at a depth of 50 km for the Interior Lowlands would be eclogite, whereas garnet granulite would be the stable assemblage for the northern Great Plains. Eclogites have seismic *P* velocities between 8.2 and 8.6 km/sec, whereas garnet granulites are characterized by a wide range of velocities between 7 and 8 km/sec. From a consideration of the P_n velocity data, we cannot distinguish, therefore, between temperature differences and compositional differences in the upper mantle.

From a study of the regional differences in seismic travel times at teleseismic distances and the corresponding P_n anomalies, *Hales et al.* [1968] suggested that variation in the anomalies between the western and eastern United States can be explained by a change in the thickness of the upper mantle low-velocity layer. In particular, there is a marked low-velocity layer in the west, which either does not exist or is vestigial in the central and eastern United States [see *Hales et al.*, 1968, Figure 11]. Because of the high temperatures in the northern Great Plains, the pyrolite solidus, a possible mantle material, is probably reached at shallow depths in the mantle. If our modeled temperature-depth curves (Figure 11) for the northern Great Plains are extended downward, they intersect the solidus for dry pyrolite [*Clark and Ringwood*, 1964] at 60–70 km; if a small amount of water were present, partial melting would occur at shallower depths. The presence of a partially molten zone at shallow depths in the upper mantle is consistent with the seismic data in the northern Great Plains [*Hales et al.*, 1968; *Helmberger and Wiggins*, 1971; B. Julian, personal communication, 1970]. Temperature-depth curves for the Interior Lowlands do not intersect the solidus for dry pyrolite at depths of <100 km. Even if there is no partial melting, there is a considerable temperature difference between the two regions, and thus there would be a small temperature-induced difference in the velocity structure.

Birch et al. [1968], *Roy et al.* [1968a], and

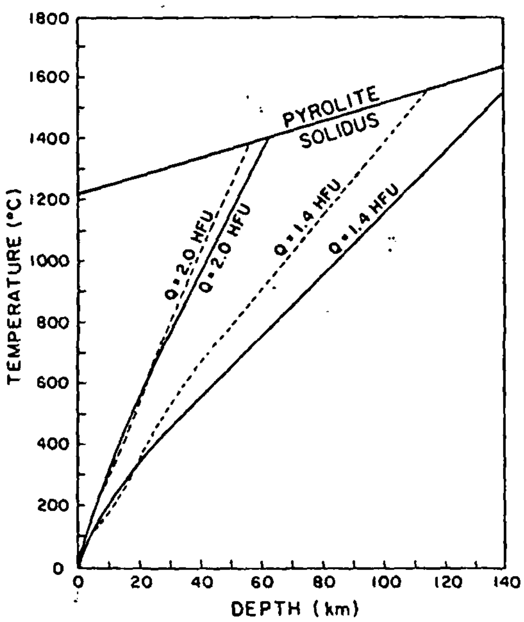

Fig. 11. Temperature-depth curves for heat production models. Solid lines are for constant heat source distribution, and dashed lines are for exponential distribution. Both models are for an upper crustal layer 8 km thick.

Lachenbruch [1968] recently described a linear relationship between heat flow Q and heat production A of the surface rock in plutons from many localities in the United States. The relationship has the form

$$Q = a + bA \qquad (1)$$

where a has the dimensions of heat flow and b has the dimension of depth. *Roy et al.* [1968*a*] defined several heat flow provinces on the basis of this relationship. Of the unlimited class of radioelement distributions that appear to be consistent with the linear relation, three particular problems that have been investigated are constant heat production, linear decrease in heat production with depth, and exponential decrease in heat production with depth in the crust. *Lachenbruch* [1968, 1970, 1971] has investigated each of these problems and has suggested that the heat sources in the crust are distributed exponentially. Data of *Lachenbruch and Bunker* [1971] suggest a general decrease in heat production with depth, consistent with the exponential source model, but alternate models are not precluded. On the basis of the geochemical data of *Lambert and Heier* [1967], *Hyndman et al.* [1968] explained different regional values of heat flow by variations in the thickness of the heat-producing layer, the mantle contribution being considered to be almost constant everywhere. However, *Roy et al.* [1968*a*] suggest that the thickness of the heat-producing surface layer varies little (7–10 km in the areas that they discussed), whereas the different regional values arise from variations in the heat flow from the lower crust and mantle.

To obtain crustal temperatures, we can use the equations relating temperature to surface heat flux and subsurface heat sources derived by *Jaeger* [1965] and *Lachenbruch* [1970]. We will consider four possible models, using both a constant and an exponential heat source distribution for the two regions. We will examine the following cases.

Case 1. Heat sources for both areas are concentrated in the upper 8 km of the crust, as *Roy et al.* [1968*a*] have suggested is the case for the central and eastern United States.

Case 2. Heat sources for both areas are concentrated in the upper 20 km of the crust, which is the depth to the sialic-mafic interface as determined from the seismic data [*Steinhart and Meyer*, 1961; *McCamy and Meyer*, 1964; *Green and Hales*, 1968; *Hales et al.*, 1968].

Case 3. The crustal layering and the heat source distribution are different for both areas, but the mantle contribution to the heat flux is constant.

Case 4. Temperatures at the M discontinuity are the same for both regions.

The crustal thickness of 50 km in all models is based on seismic data. For constant heat source models, we consider that the crust consists of two layers. In the temperature calculations, we have neglected the existence of the sedimentary layer, since the thickness of the sedimentary layer (1–2 km) is negligible in comparison with the depth of the crust (~50 km). Although a change of thermal conductivity in our models affects temperatures at all depths, the expected change is small because of the limited range of values of thermal conductivity for crustal rocks at high temperatures [*Birch and Clark*, 1940*a*, *b*]. One consequence of assuming constant conductivity is that the temperature-depth curves will be more concave towards the depth axis than they would be for temperature-dependent conductivity. The mean conductivity assumed for the lower layer is, if anything, high. Because the thermal conductivity decreases with temperature over the range considered in the models, the temperatures estimated are minimum values. The differences between the two regions would be somewhat larger if the variation of thermal conductivity with temperature was included.

The following are the conclusions for each of the cases.

For case 1, if we assume values of heat production similar to those of *Roy et al.* [1968*a*], $A_1 = 5.5$ HGU and $A_2 = 1.5$ HGU, where A_1 is for the upper layer and A_2 is for the lower layer in our two-layer crustal model, the temperatures at the base of the crust in the northern Great Plains may be higher than those at the base of the crust beneath the Interior Lowlands by 400°C or more, and the mantle contribution beneath the northern Great Plains is at least 0.6 HFU higher than that for the Interior Lowlands. If lower values for heat source distribution are used, the crustal temperatures are increased. *Renick*'s [1969] magnetotelluric investigations indicate that these temperatures are not unreasonable. The exponential distribution gives slightly higher temperatures throughout the crust, but the conclusions are similar to those for the constant heat source distribution.

For case 2, if we use the heat productivities used in case 1 but assume that the heat sources are concentrated in the 20-km-thick layer, all crustal temperatures in our models are lowered by <100°C, but, more importantly, the heat production in the upper layer must be considerably less than normal for a sialic layer or the heat production in the lower layer must be <0.01 HGU, which is less than the measured value for most basic and ultrabasic rocks by an order of magnitude [*Adams et al.*, 1959; *Heier*, 1963; *Clark*, 1966; *Lambert and Heier*, 1967] or there must be some combination of these effects.

For case 3, even if reasonable limits for the differences in heat production and layer thicknesses are used, the temperature difference between the two areas remains >200°C.

For case 4, if we assume that the temperature at the base of the crust is the same for both regions, the crust in the northern Great Plains must have an average heat productivity of 3.5 HGU. Such a value is incompatible with estimates of the composition of the crust based on seismic and geochemical data.

In summary, for the available data a model similar to case 1 or case 3 appears to be the most plausible one. Even if the layer thickness and the values of heat production are different for the two regions, the temperature difference at 50 km between the two areas remains greater than about 200°C. Therefore it is impossible to obtain a self-consistent interpretation of the regional difference in heat flux without requiring lateral temperature differences in the upper mantle.

Acknowledgments. The cooperation of the following companies and others made this study possible: Cardinal Oil Company, Consumers Power Company, Teledyne-Geotech, Illinois Geological Survey, Iowa Geological Survey, Michigan Gas Storage Company, Natural Gas Pipeline Company of America, North Dakota Geological Survey, Northern Illinois Gas Company, Northern Indiana Public Service Company, Northern Natural Gas Company, and the Subsurface Laboratory of the University of Michigan. We extend thanks to David Riach, who prepared the equipment for measuring the thermal conductivity disks. We thank Philip Spencer and Anthony England for temperature-logging nine of the boreholes. We thank D. D. Blackwell, L. H. Cohen, A. J. Erickson, Ki-iti Horai, J. H. Sass, R. P. Von Herzen, and W. H. Diment for their very helpful comments on the manuscript.

The investigation was completed while one of us (J.C.) held a traineeship from the National Aeronautics and Space Administration. Financial support for the logging of the boreholes was provided by Air Force Office of Scientific Research contract AF-AFOSR 49 (638)-1694. Equipment for the thermal conductivity measurements was provided by National Aeronautics and Space Administration contract NAS 9-8102 and NASA grant NGR-22-009-176.

REFERENCES

Adams, J. A. S., J. K. Osmond, and J. J. W. Rogers, The geochemistry of thorium and uranium, *Phys. Chem. Earth, 3*, 298-348, 1959.

Aldrich, L. T., G. W. Wetherill, M. N. Bass, G. R. Tilton, and G. L. Davis, Mineral age measurements and earth history, *Carnegie Inst. Washington Yearb.*, *59*, 209-218, 1960.

Anderson, O. L., E. Schreiber, R. C. Liebermann, and N. Soga, Some elastic constant data on minerals relevant to geophysics, *Rev. Geophys. Space Phys.*, *6*, 491-524, 1968.

Archambeau, C. B., E. A. Flinn, and D. G. Lambert, Fine structure of the upper mantle, *J. Geophys. Res.*, *74*, 5825–5865, 1969.

Beck, M. E., Jr., Aeromagnetic map of northeastern Illinois and its geologic interpretation, *Geophys. Invest. Map GP-523*, U.S. Geol. Surv., Washington, D. C., 1965.

Bell, A. F., E. Atherton, T. C. Buschbach, and D. H. Swann, Deep oil possibilities of the Illinois basin, *Ill. Geol. Surv. Circ.*, *368*, 1–38, 1964.

Benfield, A. E., A heat-flow value for a well in California, *Amer. J. Sci.*, *245*, 1–18, 1947.

Birch, F., Temperature and heat flow in a well near Colorado Springs, *Amer. J. Sci.*, *245*, 733–753, 1947.

Birch, F., Flow of heat in the Front Range, Colorado, *Geol. Soc. Amer. Bull.*, *61*, 567–630, 1950.

Birch, F., Recent work on the radioactivity of potassium and some related geophysical problems, *J. Geophys. Res.*, *56*, 107–126, 1951.

Birch, F., Thermal conductivity, climatic variation, and heat flow near Calumet, Michigan, *Amer. J. Sci.*, *252*, 1–25, 1954.

Birch, F., and H. Clark, The thermal conductivity of rocks and its dependence upon temperature and composition, 1, *Amer. J. Sci.*, *238*, 529–558, 1940*a*.

Birch, F., and H. Clark, The thermal conductivity of rocks and its dependence upon temperature and composition, 2, *Amer. J. Sci.*, *238*, 613–635, 1940*b*.

Birch, F., R. F. Roy, and E. R. Decker, Heat flow and thermal history in New England and New York, in *Studies of Appalachian Geology: Northern and Maritime*, edited by E-an Zen, W. S. White, J. B. Hadley, and J. B. Thompson, Jr., pp. 437–451, Interscience, New York, 1968.

Blackwell, D. D., Heat flow determinations in the northwestern United States, *J. Geophys. Res.*, *74*, 992–1007, 1969.

Brace, W. F., A. S. Orange, and T. R. Madden, The effect of pressure on the electrical resistivity of water-saturated crystalline rocks, *J. Geophys. Res.*, *70*, 5669–5678, 1965.

Bradbury, J. C., and E. Atherton, The Precambrian basement in Illinois, *Ill. Geol. Surv. Circ.*, *382*, 1–13, 1965.

Bullard, E. C., The time necessary for a borehole to attain temperature equilibrium, *Mon. Not. Roy. Astron. Soc., Geophys. Suppl. 5*, 127–130, 1947.

Carlson, C. G., and S. B. Anderson, Sedimentary and tectonic history of North Dakota part of Williston basin, *Bull. Amer. Ass. Petrol. Geol.*, *49*, 1833–1846, 1965.

Carslaw, H. S., and J. C. Jaeger, *Conduction of Heat in Solids*, pp. 1–8, Oxford University Press, New York, 1959.

Clark, S. P., Jr., Thermal conductivity, in *Handbook of Physical Constants, Mem. 97* (revised ed.), edited by S. P. Clark, Jr., pp. 459–482, Geological Society of America, Boulder, Colo., 1966.

Clark, S. P., Jr., and A. E. Ringwood, Density distribution and constitution of the mantle, *Rev. Geophys. Space Phys.*, *2*, 35–88, 1964.

Cleary, J., *P* times to Australian stations from nuclear explosions, *Bull. Seismol. Soc. Amer.*, *57*, 773–781, 1967.

Cleary, J., and A. L. Hales, An analysis of the travel times of *P* waves to North American stations, in the distance range 32° to 100°, *Bull. Seismol. Soc. Amer.*, *56*, 467–489, 1966.

Cohen, T. J., Explosion seismic studies of the mid-continent gravity high, Ph.D. thesis, 329 pp., Univ. of Wis., Madison, 1966.

Cohen, T. J., and R. P. Meyer, The midcontinent gravity high, gross crustal structure, in *The Earth beneath the Continents, Geophys. Monogr. Ser.*, vol. 10, edited by J. S. Steinhart and T. J. Smith, pp. 141–165, AGU, Washington, D. C., 1966.

Combs, J. B., Terrestrial heat flow in north central United States, Ph.D. thesis, 317 pp., Mass. Inst. of Technol., Cambridge, 1970.

Combs, J., and G. Simmons, Heat-flow measurements in Iowa (abstract), *Eos Trans. AGU*, *50*, 316, 1969.

Decker, E. R., Heat flow in Colorado and New Mexico, *J. Geophys. Res.*, *74*, 550–559, 1969.

Doyle, H. A., and A. L. Hales, An analysis of the travel times of *S* waves to North American stations, in the distance range 28° to 82°, *Bull. Seismol. Soc. Amer.*, *57*, 761–771, 1967.

Garland, G. D., and D. H. Lennox, Heat flow in western Canada, *Geophys. J. Roy. Astron. Soc.*, *6*, 245–262, 1962.

Geotechnical Corporation, Deep-hole site report, Assman Nos. 1 and 2, Tripp County, South Dakota, *Tech. Rep. 64-131*, 38 pp., Garland, Texas, 1964.

Green, R. W. E., and A. L. Hales, The travel times of *P* waves to 30° in the central United States and upper mantle structure, *Bull. Seismol. Soc. Amer.*, *58*, 267–289, 1968.

Hales, A. L., and H. A. Doyle, *P* and *S* travel time anomalies and their interpretation, *Geophys. J. Roy. Astron. Soc.*, *13*, 403–415, 1967.

Hales, A. L., and J. L. Roberts, The travel times of *S* and *SKS*, *Bull. Seismol. Soc. Amer.*, *60*, 461–489, 1970.

Hales, A. L., J. R. Cleary, H. A. Doyle, R. Green, and J. Roberts, *P* wave station anomalies and the structure of the upper mantle, *J. Geophys. Res.*, *73*, 3885–3896, 1968.

Hart, S. R., J. S. Steinhart, and T. J. Smith, Heat flow, *Carnegie Inst. Washington Yearb.*, *66*, 52–57, 1968.

Heier, K. S., Uranium, thorium, and potassium in eclogitic rocks, *Geochim. Cosmochim. Acta*, *27*, 849–860, 1963.

Helmberger, D., and R. A. Wiggins, Upper mantle structure of midwestern United States, *J. Geophys. Res.*, *76*, 3229–3245, 1971.

Henderson, F. R., and I. Zietz, Interpretation of an aeromagnetic survey of Indiana, *U.S. Geol. Surv. Prof. Pap., 316-B,* 19–37, 1958.

Herrin, E., Regional variations of *P* wave velocity in the upper mantle beneath North America, in *The Earth's Crust and Upper Mantle, Geophys. Monogr. Ser.*, vol. 13, edited by P. J. Hart, pp. 242–246, AGU, Washington, D. C., 1969.

Herrin, E., and J. Taggart, Regional variations in P_n velocity and their effect on the location of epicenters, *Bull. Seismol. Soc. Amer., 52,* 1037–1046, 1962.

Hinze, W. J., Regional gravity and magnetic anomaly maps of the southern peninsula of Michigan, *Mich. Geol. Surv. Rep. Invest., 1,* 1–26, 1963.

Horai, K., and A. Nur, Relationship among terrestrial heat flow, thermal conductivity, and geothermal gradient, *J. Geophys. Res., 75,* 1985–1991, 1970.

Horai, K., and G. Simmons, Seismic travel time anomaly due to anomalous heat flow and density, *J. Geophys. Res., 73,* 7577–7588, 1968.

Horai, K., and G. Simmons, Spherical harmonic analysis of terrestrial heat flow, *Earth Planet. Sci. Lett., 6,* 386–394, 1969.

Howard, L. E., and J. H. Sass, Terrestrial heat flow in Australia, *J. Geophys. Res., 69,* 1617–1626, 1964.

Hyndman, R. D., Heat flow in Queensland and Northern Territory, Australia, *J. Geophys. Res., 72,* 527–539, 1967.

Hyndman, R. D., I. B. Lambert, K. S. Heier, J. C. Jaeger, and A. E. Ringwood, Heat flow and surface radioactivity measurements in the Precambrian shield of western Australia, *Phys. Earth Planet. Interiors, 1,* 129–135, 1968.

Ingersoll, L. R., O. J. Zobel, and A. C. Ingersoll, *Heat Conduction,* pp. 3–20, University of Wisconsin Press, Madison, 1954.

Jaeger, J. C., The effect of the drilling fluid on temperatures measured in boreholes, *J. Geophys. Res., 66,* 563–569, 1961.

Jaeger, J. C., Applications of the theory of heat conduction to geothermal measurements, in *Terrestrial Heat Flow, Geophys. Monogr. Ser.*, vol. 8, edited by W. H. K. Lee, pp. 7–23, AGU, Washington, D. C., 1965.

Jaeger, J. C., and J. H. Sass, Lees's topographic correction in heat flow and the geothermal flux in Tasmania, *Geofis. Pura Appl., 54,* 53–63, 1963.

James, D. E., and J. S. Steinhart, Structure beneath continents: A critical review of explosion studies 1960–1965, in *The Earth beneath the Continents, Geophys. Monogr. Ser.,* vol. 10, edited by J. S. Steinhart and T. J. Smith, pp. 293–333, AGU, Washington, D. C., 1966.

King, P. B., *The Tectonics of Middle North America,* pp. 27–66, Princeton University Press, Princeton, N.J., 1951.

King, P. B., *The Evolution of North America,* pp. 23–40, Princeton University Press, Princeton, N.J., 1959.

Kumazawa, M., and O. L. Anderson, Elastic moduli, pressure derivatives, and temperature derivatives of single-crystal olivine and single-crystal forsterite, *J. Geophys. Res., 74,* 5961–5972, 1969.

Lachenbruch, A. H., Preliminary geothermal model of the Sierra Nevada, *J. Geophys. Res., 73,* 6977–6989, 1968.

Lachenbruch, A. H., Crustal temperature and heat production: Implications of the linear heat flow relation, *J. Geophys. Res., 75,* 3291–3300, 1970.

Lachenbruch, A. H., Vertical gradients of heat production in the continental crust, 1, Theoretical detectability from near-surface measurements, *J. Geophys. Res., 76,* 3842–3851, 1971.

Lachenbruch, A. H., and M. C. Brewer, Dissipation of the temperature effect of drilling a well in arctic Alaska, *U.S. Geol. Surv. Bull., 1083-C,* 73–109, 1959.

Lachenbruch, A. H., and C. M. Bunker, Vertical gradients of heat production in the continental crust, 2, Some estimates from borehole data, *J. Geophys. Res., 76,* 3852–3860, 1971.

Lambert, I. B., and K. S. Heier, The vertical distribution of uranium, thorium, and potassium in the continental crust, *Geochim. Cosmochim. Acta, 31,* 377–390, 1967.

LeMarne, A. E., and J. H. Sass, Heat flow at Cobar, New South Wales, *J. Geophys. Res., 67,* 3981–3983, 1962.

McCamy, K., and R. P. Meyer, A correlation method of apparent velocity measurement, *J. Geophys. Res., 69,* 691–699, 1964.

McEvilly, T. V., Central U. S. crust–upper mantle structure from Love and Rayleigh wave phase velocity inversion, *Bull. Seismol. Soc. Amer., 54,* 1997–2015, 1964.

McGinnis, L. D., Crustal tectonics and Precambrian basement in northeastern Illinois, *Ill. Geol. Surv. Rep. Invest., 219,* 1–29, 1966.

McGinnis, L. D., Tectonics and the gravity field in the continental interior, *J. Geophys. Res., 75,* 317–331, 1970.

McGinnis, L. D., and P. C. Heigold, Regional maps of vertical magnetic intensity in Illinois, *Ill. Geol. Surv. Circ., 324,* 1–12, 1961.

Muehlberger, W. R., R. E. Denison, and E. G. Lidiak, Buried basement rocks of the United States of America and Canada, final report, 749 pp., contract AF 49(638)-1115, Air Force Office of Sci. Res., Washington, D. C., 1964.

Ratcliffe, E. H., Conductivity of fused and crystalline quartz, *Brit. J. Appl. Phys., 10,* 22–25, 1959.

Renick, H., Jr., Magnetotelluric investigations in the area of the Tobacco Root mountains, southwestern Montana, southeastern Montana, and southern Illinois, Indiana, and Ohio, Ph.D. thesis, Indiana Univ., Bloomington, 1969.

Ringwood, A. E., and D. H. Green, Petrological nature of the stable continental crust, in *The Earth beneath the Continents, Geophys. Monogr. Ser.*, vol. 10, edited by J. S. Steinhart and T. J. Smith, pp. 611–619, AGU, Washington, D. C., 1966.

Roy, R. F., D. D. Blackwell, and F. Birch, Heat generation of plutonic rocks and continental heat flow provinces, *Earth Planet. Sci. Lett.*, *5*, 1–12, 1968*a*.

Roy, R. F., E. R. Decker, D. D. Blackwell, and F. Birch, Heat flow in the United States, *J. Geophys. Res.*, *73*, 5207–5221, 1968*b*.

Rudman, A. J., and R. F. Blakely, A geophysical study of a basement anomaly in Indiana, *Geophysics*, *30*, 740–761, 1965.

Rudman, A. J., C. H. Summerson, and W. J. Hinze, Geology of basement in midwestern United States, *Bull. Amer. Ass. Petrol. Geol.*, *49*, 894–904, 1965.

Sass, J. H., Heat-flow values from eastern Australia, *J. Geophys. Res.*, *69*, 3889–3893, 1964*a*.

Sass, J. H., Heat-flow values from the Precambrian shield of western Australia, *J. Geophys. Res.*, *69*, 299–308, 1964*b*.

Sass, J. H., and A. E. LeMarne, Heat flow at Broken Hill, New South Wales, *Geophys. J. Roy. Astron. Soc.*, *7*, 477–489, 1963.

Sass, J. H., S. P. Clark, Jr., and J. C. Jaeger, Heat flow in the Snowy Mountains of Australia, *J. Geophys. Res.*, *72*, 2635–2647, 1967.

Sass, J. H., R. J. Munroe, and A. H. Lachenbruch, Measurement of geothermal flux through poorly consolidated sediments, *Earth Planet. Sci. Lett.*, *4*, 293–298, 1968.

Sass, J. H., A. H. Lachenbruch, and R. J. Munroe, Thermal conductivity of rocks from measurements on fragments and its application to heat flow determinations, *J. Geophys. Res.*, *76*, 3391–3401, 1971*a*.

Sass, J. H., A. H. Lachenbruch, R. J. Munroe, G. W. Greene, and T. H. Moses, Jr., Heat flow in the western United States, *J. Geophys. Res.*, *76*, 6376–6413, 1971*b*.

Simmons, G., Continuous temperature-logging equipment, *J. Geophys. Res.*, *70*, 1349–1352, 1965.

Slichter, L. B., Crustal structure in the Wisconsin area, *Rep. N9 onr 86200*, Office of Nav. Res., Washington, D. C., 1951.

Steinhart, J. S., and R. P. Meyer, Explosion studies of continental structure, *Carnegie Inst. Washington Publ. 622*, 1–409, 1961.

Thiel, E. C., Correlation of gravity anomalies with the Keweenawan geology of Wisconsin and Minnesota, *Geol. Soc. Amer. Bull.*, *67*, 1079–1100, 1956.

Tourtelot, H. A., Preliminary investigation of the geologic setting and chemical composition of the Pierre shale, Great Plains region, *U.S. Geol. Surv. Prof. Pap. 390*, 1–74, 1962.

Von Herzen, R., and A. E. Maxwell, The measurement of thermal conductivity of deep-sea sediments by a needle probe method, *J. Geophys. Res.*, *64*, 1557–1563, 1959.

Zietz, I., and A. Griscom, Geology and aeromagnetic expression of the midcontinent gravity high, *Geol. Soc. Amer. Spec. Pap. 72*, 1–341, 1964.

Zietz, I., E. R. King, W. Geddes, and E. G. Lidiak, Crustal study of a continental strip from the Atlantic Ocean to the Rocky Mountains, *Geol. Soc. Amer. Bull.*, *77*, 1427–1448, 1966.

(Received November 23, 1971;
revised September 26, 1972.)